Multiple Pathogen Recognition at the *Mla* locus in Barley

Helen Jane Brabham

Thesis submitted to the University of East Anglia for the degree of Doctor of Philosophy

September 2019

Abstract

The majority of NB-LRR-encoding resistance genes recognise single pathogen species; few NB-LRRs have the capacity to recognise multiple pathogens. The *Mla* locus has over 30 described alleles conferring isolate-specific resistance to *Blumeria graminis* f. sp. *hordei* (*Bgh*), contains three NB-LRR encoding gene families (*RGH1*, *RGH2*, and *RGH3*), and is associated with resistance to multiple pathogens including *Puccinia striiformis* f. sp. *hordei* (*QRps1H*) and *Pyricularia oryzae* (*Rmo1*). In addition, sensitivity to the *Bipolaris victoriae* toxin victorin (*Lov1*) is in coupling with *Mla3*. In *Arabidopsis thaliana*, sensitivity to victorin is mediated by an NB-LRR-dependent plant immune response. I performed two high-resolution recombination screens and confirmed the genetic coupling of *Mla3*, *Rmo1*, and *Lov1* in the *Mla3* haplotype, and narrowed the interval for *QRps1H* in the *Mla12* haplotype.

Using sequence capture and RNAseq, copy number variation and high expression levels for *Mla3* (*RGH1;* three copies), with one expressed copy (*Mla3Δ6*) containing a 6 base pair deletion in the LRR region; and presence of a gene fusion between *RGH2* and *Exo70F1* in the *Mla3* haplotype were discovered. Characterisation of diverse barley accessions found substantial allelic variation in *RGH2* including presence/absence of the integrated *Exo70F1*. Across Poaceae species, shared interspecific conservation in the *RGH2-Exo70F1* integration was found. I hypothesise that balancing selection has maintained allelic variation at *Mla* as a *trans*-species polymorphism due to the role of multiple pathogen recognition, preserving interspecific diversity during speciation over 24 My.

Evaluation of stable transgenic barley found that *Mla3* conditions *Bgh* and *P. oryzae* resistance, whereas *Mla3Δ6*, *RGH2*, and *RGH3* do not confer resistance to either pathogen. Resistance to *P. oryzae* is dependent on the copy number of the *Mla3* transgene present. This work suggests that MLA has the potential to recognise multiple plant pathogen effectors—hypothesised due to conserved molecular structures or shared host targets.

Acknowledgements

"You're braver than you believe, stronger than you seem, and smarter than you think."

- *Winnie the Pooh*

I would like to acknowledge and thank everyone involved in the production of this PhD thesis. Foremost, I would like thank Matthew Moscou for first offering this PhD project and position, and for providing opportunities for personal and professional development, teachable moments, and mentoring over these past four years. This research would not be possible without the support of everyone in the group, both past and present. I would like to thank Inma for her wealth of knowledge and expertise—I hope I can be even half as good as you one day; Phon for her patience and management of all things seed, spore, and greenhouse related; Sam for deep chats and essential beverage breaks; Diana, a vital member of team LOV; James for his calmness and realism; Jan, my initial lab mentor who taught me the value in upwards management; and Will, who reminded me to always have fun. I have had the opportunity to supervise excellent students during this time: thank you to Max, Dani, Vicky, and Shanita, I wish you well for the future. I have had the good fortune of working with wonderful collaborators on this project; I would like to thank Tom and Jenny for their warmth and LOV, and Pat for his positivity and love of all things barley. My supervisory committee has played a vital role in my development as a scientist: I would like to thank Simon Griffiths for his support, constructive feedback, and focus; and Yogesh Gupta for his patience, knowledge, and expertise.

TSL has provided opportunities outside research, and I hope my involvement in the Athena Swan initiatives will be a part of shaping the institute for the future. Thank you to the ResNet committee and Steph Allen—you give me hope. To everyone at TSL: it has been inspiring to work with such dedicated and incredible people. The student community is family—T🐍Lytherins forever. Thank you to Janina, Jack, Jeoffrey, Jenna, and Jelle for jovial jubilations in the office. Thank you to Hannah and Josie for being the best housemates and all-round wonderful, inspirational people.

Finally, thank you to my family and Luke: for everything.

Table of Contents

List of Figures

List of Tables

1 Introduction

Often, plants are described as sessile organisms—the definition of permanently attached to a surface. This is presented as a detriment to their survival: an inconvenience that must be overcome, as observed with an anthropomorphic view. Yet, while single individual plants are rooted in a certain area, as species, plants cover great swathes of land through space and time. Populations exist across varied environments as a result of the dispersal of seed, beneficial adaptations, and resistance against abiotic and biotic stresses. For the latter, plants achieve these requirements—as most plants are resistant to the majority of pathogens—so species are maintained and are able to evolve. Pathogen populations are limited by the same means: dependent on the wind, rain, or mechanical dispersal of spores or other reproductive structures. Plant-pathogen interactions are chance encounters, yet these occurrences drive evolutionary adaptations. Novel mutations, recombination, and crossing-over events generate genetic variation in a population that is acted upon by selection. Extant species—and the variation held within them—are, in part, a result of the evolutionary relationship between plants and their pathogens.

Plants are equipped with a highly effective immune system, however pathogens are equally evolved to suppress, manipulate, and overcome host resistance. The change in human populations from hunter-gatherer to permanent settlements through the cultivation of crops has altered plant-pathogen dynamics: extensive monocultures used in agriculture provide ideal conditions for pathogen epidemics. Pathogens are integral components of the agroecosystem. Throughout history, crops have faced pests and disease and references to plant pathogens are found from the Bible, Greek philosophers, and in the presence of Roman gods (Chaves *et al*., 2008). Even in modern systems, an alarming percentage of crop yield is lost to pests and pathogens (Savary *et al*., 2019). When a favourable environment, susceptible plant host, and virulent pathogen coincide, devastating disease epidemics lead to mass famine, human migration, and death (Savary *et al*., 2019; Yoshida *et al*., 2013).

In the early 20th century, the discovery by Sir Rowland Biffen of the Mendelian inheritance of disease resistance provided the foundation for wheat breeding and genetic dissection of resistance (Biffen, 1905). To further this, Flor (1942) articulated the genetic basis of compatible and incompatible plant-pathogens following observations between races of the rust pathogen of flax and varieties of the host plant. Outcomes were defined by the presence of genes in both the plant and the pathogen—gene-for-gene interactions—that have guided the field of plant-microbe interactions (Flor, 1956). The first plant *R* gene was to be cloned almost 40 years later with the description of *Hm1* of maize (*Zea mays*) (Johal and Briggs, 1992). In addition, the development of the small mustard plant *Arabidopsis thaliana* as a model system for plant-pathogen interactions was pivotal to the development and success of plant science research (Meinke *et al*., 1998; Meyerowitz and Somerville, 1994). Since then many plant resistance genes and pathogen elicitors have been characterised which have challenged and expanded our understanding of plant immunity at a molecular level (Kourelis and Van Der Hoorn, 2018). The advent of genomics and the development of new and improved sequencing technologies have allowed scientists to expand research onto a whole genome level: mining wild relatives, utilising whole populations, and monitoring plant and pathogen evolution on a spatial and temporal basis. Combined with biochemical and molecular tools, these data have allowed for the in-depth detailed analysis of plant systems and continue to provide the means to unravel the mechanisms of the plant immune system. Plants around us are far more complex and wonderful than has been historically acknowledged.

1.1 Plant immunity on a molecular level

Plants contain an innate immune system devoid of the adaptive and mobile immune cells of animal systems. The vertebrate immune system contains both an innate and adaptive immune system—the latter incorporating an expanded repertoire of immune cells specialised in their function (Cooper and Alder, 2006; Marshall *et al*., 2018). Similarities between the innate systems of plants and animals arises through convergent evolution of the recognition of the 'non-self' (Yue *et al*., 2012). However, within individual plants this is constrained to immune receptors encoded in the germline. Despite this, the majority of plants are resistant to the majority of pathogens. How they achieve this is the driving force of the field of plant-microbe interactions—

how plant immune receptors function and what are the pathogen molecules being recognised.

Extracellular recognition

The molecular basis of plant immunity has been previously described as a two-fold layered system (Jones and Dangl, 2006). Preformed and inducible barriers form the first layers of the plant defence system, providing resistance to and preventing infection from non-adapted pathogens. Constitutive passive defence mechanisms include the cuticle, cell wall, proteins, peptides and antimicrobial secondary metabolites intended to limit pathogenicity in the first instance. Inducible responses depend on the detection of pathogen-associated molecular patterns (PAMPs), microbe-associated molecular patterns (MAMPs), or identification of the breakdown or modification of cell integrity through danger-associated molecular patterns (DAMPs) (Dodds and Rathjen, 2010). PAMPs and MAMPs are typically species non-specific, conserved microbial epitopes often contributing to fitness—such as fungal chitin or bacterial flagellin. These molecular elicitors are recognised by pattern recognition receptor proteins (PRRs) resulting in the activation of a chain of signalling events and a defence response historically described as pattern-triggered immunity (PTI) (Jones and Dangl, 2006). PRR signalling leads to ion fluxes, calcium influx, oxidative bursts of reactive oxygen species, callose deposition, stomatal closure and the production of defence hormones such as salicylic acid, jasmonic acid and ethylene (Boller and Felix, 2009; Nicaise *et al*., 2009). Examples of PRRs from *A. thaliana* and their PAMP recognition specificity include the membrane-bound receptor kinase FLS2 (FLAGELLIN-SENSING 2) and the flg22 bacterial flagellin epitope (Boller and Felix, 2009; Zipfel *et al*., 2004); EFR (EF-TU RECEPTOR) and the bacterial Elongation factor Tu (EF-Tu) (Zipfel *et al*., 2006); and both CERK1 (Chitin Elicitor Receptor Kinase-1) and LYK5 for fungal chitin (Cao *et al*., 2014; Miya *et al*., 2007). The additional receptor BAK1 (BRI1-associated receptor kinase 1) is required by many PRRs for signalling and for control of PAMP responses, providing central regulation of innate immunity (Chinchilla *et al*., 2007; Heese *et al*., 2007). PRRs can provide resistance to a broad range of pathogens providing PTI is functional (Boller and Felix, 2009; Tena *et al*., 2011; Thomma *et al*., 2011; Zipfel, 2008).

Intracellular recognition

Successful infection occurs when a pathogen has adapted to overcome these preformed, constitutive defences, efficiently suppressing PTI to facilitate lifecycle completion. Such host-adapted pathogens secrete small molecules to manipulate the host environment to sequester nutrients, reprogram host metabolism, and suppress host defence (Dodds and Rathjen, 2010; Jones and Dangl, 2006). These virulence determinants—named effectors—are structurally and evolutionarily diverse, can target diverse processes within the host cell, and are often dispensable as many are encoded in pathogen genomes (Dodds and Rathjen, 2010). Host-pathogen interactions exert strong selection pressure on the plant to evolve recognition capabilities. Host resistance incorporates *R* genes, encoding intracellular receptors that can recognise exogenous molecules of the 'non-self' and monitor the plant cell for modifications of the 'self' (Jones and Dangl, 2006). *R* gene signalling following recognition of effector molecules leads to rapid defence responses broadly termed effector-triggered immunity (ETI) (Dodds *et al*., 2009; Dodds and Rathjen, 2010). Recognised effectors are designated *Avirulence* (*Avr*) genes as their presence in the pathogen determines the lack of virulence of the pathogen. ETI often results in the production of reactive oxygen species, pathogenesis-related proteins, activation of mitogen-activated protein kinases, creation of cell wall appositions, and localised cell-death known as the hypersensitive response. Responses can induce the expression of defence-related genes in distal tissue of the plant known as systemic acquired resistance, priming the plant against secondary pathogen infection (Jones and Dangl, 2006).

The regulation of transcriptional programs following diverse signal perception is controlled through intricate signalling networks, involving multiple transcription factors (TFs), hormones and second messengers (Tsuda and Somssich, 2015). WRKY TFs are key regulators of plant immunity, involved in multiple networks in both PTI and ETI signalling (Eulgem and Somssich, 2007). Resistance can also be developmentally regulated, such as the separation of seedling and adult plant resistance (APR) (Whalen, 2005). Processes such as cell wall appositions and lignin deposition are shared between developmental differentiation and the immune response; overlapping but distinct regulatory networks are crucial for effective control.

The mechanism of the plant immune system is constantly being reviewed and every new identified component improves or challenges existing dichotomy. While general models have been proposed and divisions drawn between pathogen recognition via different receptor classes (Jones and Dangl, 2006), increasingly, distinct categories are blurred, and current models propose that disease resistance occurs as a continuum with overlapping signalling networks and machinery (Thomma *et al*., 2011). Katagiri and Tsuda (2010), propose that previous distinctions of PTI and ETI reflect differences in how the same system is used: occupying 'sectors' of an overall network. Sequential activation of enhanced and stronger defence responses would only be initiated if the current signalling was ineffective, allowing the plant to be conservative in defence and select for the lowest successful response to specific pathogens and effectors. This mitigates potential trade-off between defence and the maintenance of fitness (Cui *et al*., 2015), however clear quantifiable fitness costs of defence have yet to be experimentally validated. The broadest model incorporates all plant-microbe interactions into an 'Invasion Model' (Cook *et al*., 2015). Invasion patterns (IPs) encompassing any host-modified or pathogen-derived molecule results in IP-triggered response—either terminating the parasitic or maintaining the mutualistic symbiotic relationship between the plant and microbe (Cook *et al*., 2015). The generalisation of the IP-triggered response and separation of plant defence responses from immunity importantly encompasses necrotrophic pathogens: classic effector-triggered immune responses such as cell death paradoxically facilitate necrotrophic infection (Wang *et al.*, 2014). What this model has in breadth it is limited by in depth; over-simplification underplays the wealth of evolution of manipulation tactics in the pathogen and of mechanisms of recognition in the plant.

1.2 NB-LRR structure and regulation

R proteins are most commonly intracellular cytoplasmic immune receptors and the largest class of *R* genes encode NB-LRR (or NLR) proteins (Eitas and Dangl, 2010). NB-LRR proteins contain a C-terminal LRR domain involved in recognition specificity, a central nucleotide binding site (NB) or NB-ARC domain and optional variable N-terminal domain (Eitas and Dangl, 2010). NB-ARC protein family

members are involved in immunity, apoptosis and the regulation of transcription. NB-LRRs can further be divided into TIR (Toll/interleukin 1-like receptor) and CC (coiled- coil) classes due to their N-terminal extensions (Takken and Goverse, 2012). TIR NB-LRRs are rare in monocots, suggesting these genes have been greatly reduced or lost since the evolutionary divergence from early land plants (Sarris *et al*., 2016; Tarr and Alexander, 2009).

NB-LRR activation

NB-LRRs are kept inactive but signal competent in the unchallenged cell, requiring additional proteins for correct folding and activation (Takken and Goverse, 2012). The conserved NB-ARC domain mediates nucleotide binding and adenosine triphosphate (ATP) hydrolysis activity (Bernoux *et al*., 2016; Takken *et al*., 2006; Takken and Goverse, 2012). The NB-ARC domain is described as a molecular switch to regulate activation state: binding adenosine dishosphate (ADP) in an inactive "off" state, and ATP when active or switched "on" (Bernoux *et al*., 2016; Tameling *et al*., 2002; Williams *et al*., 2014). The first experimental evidence that an NB-LRR bound ADP in its resting state was provided when MLA27 was shown to bind ADP, rather than ATP (Maekawa *et al*., 2011). Following effector recognition, ATP is bound and NB-LRR conformational changes activate immune signalling via the N-terminal domain however the mechanism of activation and regulation remains unknown (Bernoux *et al*., 2016, 2011; Takken and Goverse, 2012). NB-LRRs are tightly regulated to prevent unwanted immune response and cell death. Intradomain interactions maintain autoinhibition and the highly conserved "MHD" motif of the NB domain is crucial for the regulation of auto-activity (Bernoux *et al*., 2016; Wang *et al*., 2019b). ATP binding of the *A. thaliana* NB-LRR RPS5 is required for activation, as disruptions of the nucleotide-binding site of the NB domain preventing ATP hydrolysis abolish activation and resistance (Ade *et al*., 2007). Domain swaps between related proteins have shown inappropriate interactions lead to auto-activity (Bernoux *et al*., 2016; Wang *et al*., 2015); therefore, the diversity and high sequence polymorphisms observed across NB-LRRs (Meyers *et al*., 2003; Sarris *et al*., 2016) are under tight regulation—engineering NB-LRRs via sequence modification is difficult.

Structural analysis of NB-LRRs has been sparse due to the limited amenability of NB-LRRs to protein purification and crystallisation. Recent work has identified the structure for the activated CC-NB-LRR HOPZ-ACTIVATED RESISTANCE 1 (ZAR1) from *A. thaliana* in complex with the pseudokinase resistance-related kinase 1 (RKS1), and the guarded host kinase PBS1-like protein 2 (PBL2). The resulting complex forms a 'resistosome' structure reminiscent of the NLRC4 inflammasome of mammalian immune receptors (Wang *et al*., 2019a, 2019b). Binding of PBL2, uridylated by the recognised effector AvrAC from the bacterial pathogen *Xanthomonas campestris* pv. *campestris*, induces the release of ADP from ZAR1 in the preformed ZAR1-RKS1 complex. AvrAC, alongside HopZ1a and HopF2 from *Pseudomonas syringae*, are indirectly recognised by ZAR1 (Lewis *et al*., 2013; Wang *et al*., 2015, 2019b, 2019a). The helix bundles of the CC domain form a funnel-shaped structure following oligomerisation of ZAR1. One hypothesis of its purpose is in pore formation in the membrane to facilitate cell death, however this has yet to be experimentally validated. The CC domain of ZAR1 differs from those of Sr33 (Casey *et al*., 2016), Rx (Hao *et al*., 2013), and MLA10 (Casey *et al*., 2016; Maekawa *et al*., 2011) and it is likely that not all CC-NB-LRRs adopt this confirmation (Wang *et al*., 2019a). Alongside ZAR1, the CC domains of RPM1 and Sr33 are also known to contribute to self-association and the hypersensitive response, however the mechanism by which this is achieved may differ between all three proteins (Casey *et al*., 2016; El Kasmi *et al*., 2017; Wang *et al*., 2019a). Furthermore, the CC domain alone is sufficient to trigger cell death in the case of MLA10, Sr33, Sr50 and ZAR1 (Cesari *et al*., 2016; Maekawa *et al*., 2011; Wang *et al*., 2019a) supporting the role of the CC domain in signalling following activation.

The C-terminal LRR domain has been shown to play a regulatory role, prevent inappropriate activation, and is also implicated in recognition specificity in the perception of effectors (Deslandes *et al*., 2003; Dodds *et al*., 2001; Ellis *et al*., 1999; Jia *et al*., 2000; Qi *et al*., 2012; Sela *et al*., 2012; Shen *et al*., 2003); the LRR is key to the autoinhibition of ZAR1 (Wang *et al*., 2019a). In *A. thaliana*, activation of the NB-LRR RPS5 is inhibited via the LRR domain and repression is released on effector perception by the protein complex (Ade *et al*., 2007). The LRR domain shows signatures of diversifying selection (Feuillet *et al*., 2003; Isidore *et al*., 2005; Loutre *et al*., 2009; Sela *et al*., 2012, 2011). Evidence of alternate splicing has been shown

for the *Lr10* leaf rust resistance gene paralogs from wheat (*Triticum aestivum*) and the wild emmer wheat progenitor (*T. dicoccoides*) (Sela *et al*., 2012, 2011) but functional relevance has yet to be elucidated. Truncated LRR domain variants have also been observed in the CC-NB-LRR *JA1tr* of *Phaseolus vulgaris* (Ferrier-Cana *et al*., 2005) and in TIR-NB-LRRs such as and the N gene of tobacco (Takabatake *et al*., 2006; Whitham *et al*., 1994), and presence of splice variants of RPS4 are required for immunity (Zhang and Gassmann, 2003). Shorter LRRs can release the suppression of the LRR domain on NB domain activity (Gassmann, 2008; Jordan *et al*., 2002). Alternatively, spliced mRNA of *Mla* alleles from barley have also been identified (Halterman, 2003). The presence and regulation of splice variants remains unknown.

NB-LRR regulation

Many transcription factor families have been shown to regulate plant immunity; however, the majority of studies have focused on disruptions to innate immunity, phytohormone signalling and PRR-mediated resistance responses (Birkenbihl *et al*., 2017; Tsuda and Somssich, 2015). Nuclear localisation and accumulation of some NB-LRRs is required for function, suggesting their involvement in transcriptional regulation (Bhattacharjee *et al*., 2013). A chaperone complex comprising of the positive regulators HSP90 (Heat shock protein 90 kDa) and (RAR1) (Required for MLA12 Resistance 1), and the positive/negative regulator SGT1 (Suppressor of the G2 allele of SKP1) is required for correct conformation and regulation of NB-LRRs (Elmore *et al*., 2011). In addition, the central regulators *EDS1* (*ENHANCED DISEASE SUSCEPTIBILITY 1*), *NDR1* (*NON-RACE-SPECIFIC DISEASE RESISTANCE1*), *PAD4* (*PHYTOALEXIN DEFICIENT 4*), and *SAG101* (*SENESCENCE ASSOCIATED GENE 101*) are required for NB-LRR-mediated resistance (McDowell *et al*., 1998; Wiermer *et al*., 2005). *EDS1* and *PAD4* have been implicated in transducing redox signals (Rustérucci *et al*., 2001; Wiermer *et al*., 2005). *EDS1* is required for TIR-NB-LRR resistance responses, whereas *NDR1* regulates CC-NB-LRRs (Century, 1995; Elmore *et al*., 2011; Lee and Yeom, 2015). Components of the ubiquitination pathway are also involved in NB-LRR-mediated immunity (Cheng and Li, 2012).

NB-LRRs can induce yield penalties to the host, and incompatible NB-LRR interactions induce costly autoimmune responses (Chae *et al*., 2016, 2014). Altering

regulation of NB-LRRs through mutagenesis or mis-expression via transgenic means can have detrimental effects on the plant: resulting in constitutive defence, stunting, and death (Whalen, 2005). Generally, plants are increasingly resistant to pathogens over their life history; the transition between developmental stages is often associated with the development of resistance (Develey-Rivière and Galiana, 2007). This is distinct from the upregulation of NB-LRRs upon pathogen attack. Correlation between developmental stage and resistance status has been demonstrated for maize (*Zea mays*), where the *Corngrass1* mutant with extended juvenile-vegetative phase displays delayed adult plant resistance to common rust (*Puccinia sorghi*) (Abedon and Tracy, 1996).

The majority of well-characterised age-related identified resistance genes are non-NB-LRRs, such as the receptor-like protein kinase *Xa21* from rice (*Oryza sativa*) (Century *et al*., 1999), however developmental regulation of NB-LRRs has been shown. Tomato *Mi1.2*-mediated resistance against root knot-nematode is present throughout the life-history of the plant, whereas resistance against whitefly and aphid are only present at the adult stage (Fiona L Goggin *et al*., 2004; Martinez de Ilarduya *et al*., 2004). This implicates regulation other than transcriptional, as resistance is not correlated with transcript levels and overexpression of *Mi1.2* does not compensate. Developmental control of co-factors or downstream signalling requirements could be causal. Identifying the regulation of developmental transitions and association with *R* gene regulation remains a major challenge. NB-LRRs also function outside immunity—enhanced expression of *A. thaliana* CC-NB-LRR *ADR1* confers drought tolerance (Grant *et al*., 2003) and mutations in the NB-LRR *UNI* disrupt inflorescence stem growth (Lee and Yeom, 2015; Uchida *et al*., 2011). Tissue specificity also been observed for NB-LRRs. *A. thaliana RPP1* confers resistance to leaf infection by *Hyaloperonospora parasitica* (Hermanns *et al*., 2003). However, *H. parasitica* can also infect via the roots and successful root infection occurs even in the presence of expressed *RPP1* and required downstream signalling components (Hermanns *et al*., 2003). The rice *Pigm* locus contains a cluster of NB-LRRs including *PigmR* conferring broad spectrum resistance to *P. oryzae*, and *PigmS*—a suppressor of *PigmR* resistance. *PigmS* shows pollen-specific expression due to the presence of MITE1 and MITE2 transposable elements, so *PigmR* repression is released in leaves. *PigmR* transgenic lines—without *PigmS*—show a yield penalty of decreased grain weight. Epigenetic

regulation of *PigmS*, through leaf-specific silencing, addresses the trade-offs between defence and development (Cesari and Kroj, 2017; Deng *et al*., 2017). Understanding the regulation of NB-LRR expression, localisation, and activation will be key for effective resistance gene utilisation and deployment.

1.3 NB-LRR recognition

Following the observation of gene-for-gene plant-pathogen interactions and diversifying selection acting on the LRR domains of NB-LRRs, initial hypotheses of *R* gene recognition proposed a direct binding model (Collier and Moffett, 2009; McDowell and Simon, 2006; Van Der Biezen and Jones, 1998). However, increasing examples of NB-LRR genes failed to demonstrate direct interactions and it became clear that additional proteins were sometimes necessary to confer resistance. Since the initial molecular characterisation of *R* genes in the 1990s, over 300 have been cloned and diverse functional mechanisms revealed. Broadly, NB-LRR recognition can be divided into direct and indirect recognition of pathogen products (Kourelis and Van Der Hoorn, 2018).

Direct recognition

Direct recognition between NB-LRRs and pathogen effectors was described for some of the first *R* genes identified. The flax (*Linum usitatissimum*) allelic NB-LRR resistance genes *L5*, *L6*, and *L7* recognise the AvrL567 genes from the flax rust fungus. Recognition is via direct receptor-effector binding; amino acid polymorphisms between AvrL567 variants abolish recognition (Dodds *et al*., 2006, 2004; Ellis *et al*., 2007; Ravensdale *et al*., 2011). In addition, the allelic rice *Pik* NB-LRRs recognise related *AVR-Pik P. oryzae* effectors with different binding and recognition specificity between them (Kanzaki *et al*., 2012). Direct recognition of viral products has also been observed between the *Tobacco Mosaic Virus* helicase domain and the TIR-NB-LRR *N* from tobacco (Ueda *et al*., 2006); and between the oomycete RxLR effector *ATR1* and *A. thaliana* TIR-NB-LRR *RPP1* via the LRR domain (Chou *et al*., 2011; Krasileva *et al*., 2010).

Aside from protein binding, direct recognition also occurs via transcriptional activation. Transcription Activator-like effectors (TALEs) produced by *Xanthomonas* species bind to specific DNA sequences containing specific polymorphic repeats and alter host transcription (Bogdanove *et al*., 2010; Moscou and Bogdanove, 2009; Schornack *et al*., 2006). Alongside altering expression of key susceptibility factors to enhance virulence (Verdier *et al*., 2012), TALEs also can promote the transcription of executor genes—*R* genes that are transcriptionally activated by TALEs (Gu *et al*., 2005; Römer *et al*., 2007; Zhang *et al*., 2015). The addition of TAL effector binding elements to executor genes was shown to broaden TALE specificity by Hummel *et al*., (2012) and Römer *et al*., (2009). Zeng *et al.,* (2015) modified the promoter region of rice TAL effector-dependent resistance gene *Xa10* to allow for recognition of a broader range of TAL effectors from *Xanthomonas oryzae* pv. *oryzae* strains. The identified executor genes encode proteins with a catalytic function (Römer *et al*., 2007) or putative transmembrane domains (Zhang *et al*., 2015), however TALE-mediated NB-LRR induction is also plausible.

NB-LRR allelic series are a common feature of direct recognition mechanisms and are observed in interactions between cereals and host-specific forms—*formae speciales*—of the powdery mildew species *Blumeria graminis* (Eriksson, 1894). The wheat *Pm3* alleles recognise *B. graminis* f. sp. *tritici* (*Bgt*) *AvrPm3* effectors (Bourras *et al*., 2019, 2018) and *Mla* alleles of barley function against *B. graminis* f. sp. *hordei* (*Bgh*) (Jørgensen, 1994; Seeholzer *et al*., 2010). Recent work has shown direct interaction of *Mla* alleles and *Bgh* effectors (Saur *et al*., 2019), and the direct interaction of Pm proteins and *Bgt* effectors is also hypothesised (Bourras *et al*., 2019). The downy mildew (*Hyaloperonospora arabidopsidis*) gene *RPP13* in *A. thaliana* also shows extreme amino acid diversity across alleles (Hall *et al*., 2009; Rose *et al*., 2004), although direct recognition of effectors is yet to be experimentally validated. Outcomes from theoretical models have suggested that direct recognition is likely to lead to rapid evolution of new virulence phenotypes (Van Der Hoorn *et al*., 2002) as direct recognition by NB-LRRs can be overcome through effector loss and sequence diversification to generate new variants with loss of binding affinity. However, this can be mitigated by *R* genes present as diverse allelic series recognising multiple effectors within a pathogen species, and/or if *R* genes recognise conserved pathogen effectors.

Indirect recognition

Indirect recognition occurs either through NB-LRRs 'guarding' a functional host protein under the guard model (Jones and Dangl, 2006), or through surveillance of a mimic or 'decoy' of the target which is 'guarded' by the NB-LRR (Paulus and van der Hoorn, 2018; van der Hoorn and Kamoun, 2008). The 'guard model' proposes that an *R* gene can monitor another protein in the plant and induce ETI when the 'guardee' is perturbed or modified by pathogen *Avr* genes (Chisholm *et al*., 2006; Jones and Dangl, 2006). However, the guardee is evolutionarily unstable, being under opposing selection forces to both maintain host function and yet diversify to evade pathogen recognition. This is exacerbated by variation in *R* gene prevalence in populations; presence selects for increased guardee-effector binding and absence selects against the strength of interaction. Evolution of a 'decoy' separates selection to act in one direction on each protein, allowing the decoy to act as a bait for the effector (Collier and Moffett, 2009; van der Hoorn and Kamoun, 2008).

One of the first *R* genes to be identified, the serine/threonine kinase *Pto* from tomato (*Solanum lycopersicum*) (Martin *et al*., 1993), directly recognises Avr-Pto and Avr-PtoB from *Pseudomonas syringae* and requires the NB-LRR *Prf* for signal transduction and initiation of the hypersensitive cell death resistance response (De Vries *et al*., 2006; Ellis *et al*., 2000; Kim *et al*., 2002; Pedley and Martin, 2003; Wu *et al*., 2004). This example was the foundation for the guard model, providing an initial alternate model to direct recognition (Kourelis and Van Der Hoorn, 2018; Van Der Biezen and Jones, 1998). Indirect recognition and the guarding of host proteins can provide a mechanism for expanded recognition specificities by NB-LRRs. *A. thaliana* RPM1 recognises non-homologous effectors *AvrRpml* and *AvrB* from *Pseudomonas syringae*, via the effector mediated phosphorylation of its guard RIN4 (Grant *et al*., 1995; Mackey *et al*., 2002). In addition, cleavage of RIN4 by pathogen effectors also triggers the NB-LRR RPS2 (Axtell and Staskawicz, 2003; Kim *et al*., 2009; M. G. Kim *et al*., 2005; Mackey *et al*., 2003, 2002). Over 64 effectors from *P. syringae* have been identified, including suppressors of effector recognition. *AvrPphB* is able to suppress recognition of *AvrB* by RPM1—via cleavage of RPM1-interacting protein kinase (RIPK)—however this does not abolish *AvrRpm1* recognition. Different

recognition mechanisms and signalling pathways involving the guarding of RIN4 therefore must be present (Russell *et al*., 2015). RIN4 homologs are conserved across plant species and NB-LRRs recognising pathogen-induced RIN4 modifications are also present outside *A. thaliana* (Toruño *et al*., 2019): soybean *Rpg1b* confers resistance upon *AvrB* mediated modifications of RIN4 (Ashfield *et al*., 2014, 2004; Russell *et al*., 2015). The rice NB-LRR Pii-2 has an integrated domain containing the NOI/RIN4 core motif and interacts with Os-Exo70F3—the exocyst component targeted by the *Pyricularia oryzae* (teleomorph *Magnaporthe oryzae*) effector AVR-Pii (Fujisaki *et al*., 2015). RIN4 and its associated motifs represent a conserved component of the plant immune system and a shared effector target across species.

The *A. thaliana* NB-LRR RPS5 is found in a complex with the protein kinase PBS1 via the RPS5 CC-domain (Ade *et al*., 2007). Cleavage of PBS1 by the bacterial protease AvrPphB produced by *P. syringae* activates RPS5 (Ade *et al*., 2007). Kim *et al.,* (2016) manipulated the cleavage site within PBS1 to alter specificity—using the 'guardee' as an effector bait for engineering resistance. Altered recognition for AvrRpt2, another effector from *P. syringae,* and the NIa protease of *Tobacco Etch Virus* were successful in activating RPS5-mediated resistance (Kim *et al*., 2016). Cleavage sites are clear targets for experimental manipulation. Conserved recognition mechanisms—via conserved guardees or convergent evolution—can be elucidated across species, providing a foundation for engineering resistance.

Integrated domains

To further the guard model, some NB-LRRs contain integrations of additional domains (NB-LRR-IDs)—decoy targets incorporated within or fused to the NB-LRR immune receptor. Such integrated domains are not conserved within the NB-LRR family and show exceptional variation and widespread prevalence throughout many species (Cesari *et al*., 2014; Kroj *et al*., 2016; Sarris *et al*., 2016). Domain integrations have evolved multiple times independently throughout evolutionary history, with examples of recurrent integration as in the case of WRKY transcription factors (Sarris *et al*., 2016). Comprehensive phylogenetic analysis of inter- and intra-specific variation of NB-LRRs identified uneven distribution of NB-LRR-IDs, with the majority residing in few clades—the Major Integration Clades (MICs; MIC1, MIC2,

and MIC3) (Bailey *et al*., 2018). MIC1 contains the majority (30%) and highest diversity of NB-LRR-IDs, whereas the low diversity of MIC2 and MIC3 is thought to represent repeated expansions of ancestral lineages. MIC1 NB-LRR-IDs display inter-specific variation in the domain integrated, suggesting evolution is ongoing (Bailey *et al*., 2018). Integrated domains can highlight pathways and processes targeted by pathogens: as decoys of endogenous proteins subject to effector modification. The *P. oryzae* AVR-Pii effector interacts with rice exocyst complex factor Exo70, specifically OsExo70-F3, to trigger NB-LRR Pii-dependent resistance (Fujisaki *et al*., 2015). NB-LRR-Exo70 fusions have been identified in wheat and barley genomes, while they exist separately in rice in accessions sequenced so far (Sarris *et al*., 2016). Despite evidence as decoys, it cannot be excluded that integrated domains may retain full or partial function as well as 'guardees'. Using Exo70 as an example, domain integration may facilitate NB-LRR localisation to the exocyst complex. Identification of fusions therefore provides cross-species candidate genes for shared effector targets in known interactions, but also speculative targets for yet unknown pathogen interactions (Kroj *et al*., 2016; Nishimura *et al*., 2015).

NB-LRR pairs

Identified NB-LRR-IDs require an additional non-integrated NB-LRR partner to function. Each is functionally specialised; NB-LRR-IDs are 'sensors' recognising pathogen effectors and are paired with 'executors' or 'helpers' for signalling requirement (Cesari *et al*., 2014; Williams *et al*., 2014). MIC1 contains NB-LRR-IDs that require a partner to function, where the non-integrated paired NB-LRRs reside in the C7 clade exclusively. This arrangement suggests an ancient origin, duplication, and subsequent diversification of pairs (Bailey *et al*., 2018). Three well-characterised paired NB-LRRs—*A. thaliana RRS1*/*RPS4*, rice *RGA5*/*RGA4*, and rice *Pik*/*Pik-2*—are in head-to-head orientation and share a bi-directional promoter (Kourelis and Van Der Hoorn, 2018; Okuyama *et al*., 2011). Genetic linkage of NB-LRR pairs limits allele shuffling and unwanted combinations that can lead to hybrid necrosis or autoimmunity. Members of MIC1 are enriched in tandem NB-LRRs irrespective of integrated domain presence (Bailey *et al*., 2018); NB-LRR-IDs with loss of the integrated domain may still require a paired NB-LRR to function due to prior co-evolution and sub-functionalisation of pairs.

The paired *A. thaliana RPS4* and *RRS1* NB-LRRs confer resistance to the fungal pathogen *Colletotrichum higginsianum,* AvrRps4 from *P. syringae* pv. *tomato* and PopP2 from *Ralstonia solanacearum* (Narusaka *et al*., 2013, 2009). RRS1 contains a C-terminal integrated WRKY domain and this has been shown to interact with AvrRps4 and PopP2 (Sarris *et al*., 2015; Williams *et al*., 2014). PopP2 acetylates the C-terminal integrated WRKY transcription factor, disrupts RRS1 DNA association, and activates RPS4-dependent immunity (Le Roux *et al*., 2015). Non-integrated endogenous WRKY transcription factors are also acetylated via the same mechanism, causing loss-of-function and disrupting defence gene expression and disease resistance (Le Roux *et al*., 2015). The integrated WRKY is a bait for pathogen effectors: a decoy of other WRKY transcriptional targets within the host.

In rice, the pairs *RGA4*/*RGA5*, and *Pik-1*/*Pik-2* confer resistance to *P. oryzae*. RGA4/RGA5 recognise the effectors AVR1-CO39 and AVR-Pia via direct binding with the RATX1 (or HMA) domain of RGA5 located at the C-terminus (Cesari *et al*., 2013). RGA4 and RGA5 form complexes via interactions between their CC domains; RGA5 represses RGA4 cell death activation, which is released upon effector recognition via RGA5 (César*i et al*., 2014). Pik-1 also contains an integrated HMA domain but is located between the CC and NB domains as opposed to at the C-terminus. Alleles of Pik-1 have different recognition specificities of *P. oryzae* effectors, driven by the direct recognition and interaction between the HMA domain and AVR proteins (Kanzaki *et al*., 2012; Maqbool *et al*., 2015). The rice *Pi-ta* paired NB-LRR contains a thioredoxin domain (Nishimura *et al*., 2015) which recognises *P. oryzae* AVR-Pita via direct binding (Jia *et al*., 2000). Single amino acid differences in Pi-ta alleles can distinguish resistance specificities, highlighting the importance of specific binding interactions for resistance (Bryan *et al*., 2000). Barley *Rpg5* encodes a NB-LRR with a C-terminal serine threonine protein kinase and provides resistance to rye stem rust (*Puccinia. graminis* f. sp. *secalis*) (Brueggeman *et al*., 2008). *Rpg5* is in head-to-head orientation with the NB-LRR *Rga1* at the *rpg4*-mediated resistance locus (Solanki *et al*., 2019). Recessive resistance to wheat stem rust (*Puccinia graminis* f. sp. *tritici*; *Pgt*) in barley conferred by the *rpg4*-mediated resistance locus is the one of the few effective resistances against the virulent *Pgt* TTKSK (Ug99) race and its lineage (Solanki *et al*., 2019; Wang *et al*., 2013). Mapping of the region found

that the two NB-LRRs *Rpg5* and *Rga1*, and an additional actin depolymerisation factor are required for *rpg4*-mediated resistance (Arora *et al*., 2013; Wang *et al*., 2013). Alleles of *Rpg5* that contain a phosphatase domain in the place of the kinase domain are dominant susceptibility factors (Solanki *et al*., 2019). The mechanism of the actin cytoskeleton involvement has yet to be elucidated.

NB-LRR networks

Single NB-LRRs can also be functional: competent in both pathogen recognition and signalling. Precise intra-specific interactions maintain complex structural confirmation, inhibit auto-immunity, and regulate functionality (Takken and Goverse, 2012). Homo-dimerization of NB-LRRs, crucially N-terminal homodimerization, is vital for signalling and downstream defence responses (Heidrich *et al*., 2012; Williams *et al*., 2014). However, it is likely that specific requirements of domain proximity and timing of dimer formation differs between NB-LRRs (Takken and Goverse, 2012). Paired NB-LRR partners share recognition and signalling requirements, forming hetero-complexes for function. The functional separation and release of selection for both functions—sub-functionalisation—can facilitate the integration of additional domains in the 'sensor' NB-LRR. From the paired example *RPS4*/*RRS1* and *RGA4*/*RGA5*, a functional NB domain is only required in the 'executor' NB-LRR—*RPS4* and *RGA4* respectively. Loss-of-function mutations in the NB domain of the 'sensor' NB-LRR—*RRS1* and *RGA5*—do not abolish resistance function (Césari *et al*., 2014; Sohn *et al*., 2014; Williams *et al*., 2014).

The evolution of paired NB-LRRs is hypothesised to be due to the facilitation of repertoire expansion. Discussed examples show potential for the recognition of multiple effectors, either from the same species or multiple pathogens (Eitas and Dangl, 2010; Nishimura *et al*., 2015). Recent findings have expanded paired NB-LRRs to identify whole networks in *Solanaceae* species. Here, multiple 'sensor' NB-LRRs require core 'helper' NB-LRRs to function (C. H. Wu *et al*., 2017; Wu *et al*., 2018). Perturbation of this system has identified pathogen effectors that are recognised by 'sensor' NB-LRRs, but also effectors that target the core 'helper' signalling NB-LRRs to repress immune responses (Wu *et al*., 2018). It will be interesting to see if

networks are present across other species and if networks are more robust and efficient than individual or paired NB-LRRs.

1.4 Continuum of resistance

Quantitative resistance

Plant pathogen interactions occur on a spectrum from compatibility of host-adapted pathogens to immunity against non-adapted pathogens (Bettgenhaeuser *et al*., 2014). The most well studied *R* genes confer monogenic dominant resistance and have been used extensively in agricultural breeding (St.Clair, 2010). Such resistance is termed qualitative resistance, referring to Mendelian genes that are of large effect, often acting in a gene-for-gene manner with the pathogen. However, continuous variation in resistance phenotypes is also observed; this continuum of resistance extends from complete resistance with lack of symptoms, through to a moderate host defence response with reduction in disease severity and low expressivity of the phenotype, and to complete susceptibility and completion of the pathogen lifecycle. The outcome is dependent on the segregation and presence of causal genes (A. J. Castro *et al*., 2003; St.Clair, 2010). The continuum of resistance can be dependent on the stage at which the pathogen infection is recognised and terminated, or dependent on the expression, localisation, and function of the resistance gene. Quantitative genes can also show epistatic relationships, pleiotropy, or additive effects (Cowger and Brown, 2019; St.Clair, 2010).

Host range

Resistance to non-adapted pathogens is shown by all (or an overwhelming majority of) individuals of a plant species. Basic compatibility between host and pathogen was previously assumed to derive from physical or chemical barriers, inducible defences, and PTI responses (Ayliffe and Sørensen, 2019; da Cunha *et al*., 2006; Thordal-Christensen, 2003). However, it remains unclear if resistance to non-adapted pathogens results from a passive or active response from the plant. Belhaj *et al.,* (2015) showed that infection of *A. thaliana* by the host oomycete pathogen *Albugo laibachii* allows for the subsequent infection by the nonhost *Phytophthora infestans*, usually

limited in its host range to members of the Solanaceae family. *A. laibachii* effectors could be more effective than *P. infestans* at supressing PTI, or such PTI suppression could prevent the response to *P. infestans* recognition. Many pathogen effectors disrupt host processes, so effector incompatibility due to host gene loss or diversification could result in failed infection.

A sub-set of individuals or cultivars within susceptible host-species can show resistance. Heath (2000), hypothesised that cultivar specificity is controlled by specific or combinations of *R* genes and is distinct from resistance to non-adapted pathogens. They suggested this resistance is under complex genetic control with the involvement of multiple factors. This contrasts with host resistance—controlled by single *R* genes conferring genotype-specific resistance in an otherwise susceptible background. In contrast, Tosa (2009), proposed a counter model that resistance to non-adapted but closely-related pathogens is akin to recognition of adapted pathogens. Interactions between plants and pathogens can be divided into plant species specificity and cultivar specificity, the former incorporating resistance to non-adapted pathogens and the latter including resistance to adapted pathogens. Subsequently, several experiments on closely-related pathogen genotypes have confirmed the model of Tosa (2009) for host species adaptation among genotypes of *Pyricularia oryzae* and between *P. oryzae* and its close relative *P. grisea* (Chuma *et al*., 2010; Hyon *et al*., 2012; Nga *et al*., 2012).

Within species, pathogens have differentiated to a sub-set of their host range. Eriksson (1894) introduced taxonomic term *forma specialis* (f. sp.), for pathogen classifications below the species level based on their host. Such adaptation is thought to be the initial step to host specialisation. Genetic analyses of crosses of different but closely-related *B. graminis* ff. spp. and inoculation of appropriate and inappropriate hosts suggests that resistance is dependent on combinations of pathogen effector and plant *R* genes (Tosa, 1989a, 1989b; Tosa et al., 1995; Tosa and Sakai, 1990; Tosa and Tada, 1990) . *B. graminis* ff. spp. do not lack the capability of infection on inappropriate hosts, they carry effectors that are recognised and lead to avirulence (Eriksson, 1894). In addition, the effector gene *AVR1-CO39* corresponding to rice *R* gene *Pi-CO39(t)* was lost during the early evolution of the rice-specific subgroup of *P. oryzae*, allowing it to infect rice (Yukio Tosa *et al*., 2005). Homologs of *AVR1-CO39* present in other *P.*

oryzae ff. spp. were also avirulent on rice (Yukio Tosa *et al*., 2005). The emergence of the wheat infecting lineage of *P. oryzae Triticum* pathotype was due to the sequential loss of specific effectors *PWT3* and *PWT4*. The corresponding wheat *R* genes *Rwt3* and *Rwt4* were responsible for incompatibility of *P. oryzae* during infection; their separation in wheat cultivars facilitated *P. oryzae* step-wise adaptation to become an adapted pathogen of wheat (Inoue *et al*., 2017). However, the subclassification of ff. spp. is based on adaptation to certain hosts, without strict definition as to the defining mechanism of plant resistance to adapted and non-adapted forms (Troch et al., 2014). It is unclear what role specific effector-gene interactions play in the division between ff. spp.

1.5 The *Mla* locus of barley

Barley (*Hordeum vulgare*) is a diploid monocot and is one of the earliest domesticated crop species. The haploid genome of barley is approximately 5 gigabases and consists of 7 chromosomes (Mayer *et al*., 2012); approximately 84% of the genome consists of repetitive or mobile elements (Mayer *et al*., 2012). Clusters of disease resistance genes have been identified across chromosomes, including hotspots for resistances to multiple diseases (Schweizer *et al*., 2011). Such organisation is facilitated through tandem duplications, repetitive elements, and unequal crossing-over during recombination. Subsequent diversifying selection enables the evolution of new resistance specificities which can occur between and within individual genomes—resulting in the generation of allelic series (Leister, 2004; Michelmore and Meyers, 1998).

The *Mla* locus

The *Mla* locus of barley is located on the subteleomeric short arm of chromosome 1H (Wei *et al*., 1999). Allelic variants of the *Mla* CC-NB-LRR gene confer isolate-specific disease resistance against the host pathogen *Bgh* and highly diverse *Mla* homologs are found across barley haplotypes (Halterman *et al*., 2001; Halterman and Wise, 2004; Jørgensen, 1994; Seeholzer *et al*., 2010; Shen *et al*., 2003; Zhou *et al*., 2001). This resistance cluster has been delineated within a 261-kb contig isolated from a bacterial artificial chromosome (BAC) of accession Morex (Wei *et al*., 1999). In this

reference sequence, the *Mla* locus contains eight NB-LRR encoding genes that belong to three distinct families—*RGH1 (Mla)*, *RGH2*, and *RGH3*—and are organised in three gene-rich regions interspersed with transposable elements (Wei *et al*., 2002). The *RGH1* family includes *RGH1a*, *RGH1bcd*, *RGH1e*, and *RGH1f*; *RGH2* family members *RGH2a*, *RGH2b* and the *RGH3* family members *RGH3a* and *RGH3b*. Members within a family show 78-100% amino acid similarity whereas comparisons between families showed less than 43% amino acid similarity (Wei *et al*., 2002). Only *RGH1* members are expressed in Morex, with *RGH1bcd* predicted to be the *Mla* allele (Halterman *et al*., 2001). *RGH1bcd* is non-functional due to the insertion of a solo long terminal repeat from a *BARE-1* retrotransposon element in intron 3, in combination with a 29-bp deletion that results in early termination of the open reading frame (ORF) (Wei *et al*., 2002). The *Mla* locus contains all major classes of transposable elements with *BARE-1* major retrotransposon accounting for ~17% of the sequence of the region. The locus has been subject to multiple insertions, duplications and inversions of genes. Tandem fragments and transposon complexes are still actively evolving and are responsible for drastically increasing the size of the locus (Wei *et al*., 2002). The region experiences suppressed recombination between haplotypes; sequence conservation is limited to the proximal and distal ends of the locus with little conservation in the centre of the locus (Moscou, personal communication).

Over 30 different *Mla* alleles condition race-specific powdery mildew resistance that is conferred by localised cell death at the site of fungal infection. They are hypothesised to have diverged from a common ancestor, due to the presence of shared insertions and deletions, to generate the breadth of the allelic series present today (Wei *et al*., 2002). Alleles share >91% sequence similarity at the protein level (Seeholzer *et al*., 2010). The variable alleles are in repulsion within barley varieties, presenting as a single copy in an allelic series: where *Mla* duplications are observed, usually only one gene copy is expressed (Seeholzer *et al*., 2010). The LRR region of *Mla* determines recognition specificity and shows signatures of positive selection (Seeholzer *et al*., 2010). Shen *et al.*, (2003), determined distinct residues for recognition specificity in the LRRs MLA1 and MLA6 (LRRs 3 to 11 and 9 to 11, respectively). MLA8 and MLA1 are identical in sequence until the 10th LRR suggesting a recombination event created a new allelic variant (Seeholzer *et al*., 2010). Recent work from Saur *et al.*,

(2019), propose a direct recognition mechanism for *Mla* alleles, based on the observation of compatible and incompatible *Mla* and *Bgh* effector interactions: MLA7, MLA9, MLA10, and MLA22 recognise *Bgh* AVR_{a7}, AVR_{a9}, AVR_{a10}, and AVR_{a22} respectively. MLA1 functions in transgenic *A. thaliana*, recognising *Bgh* carrying AVR_{a1}, in a partially immunocompromised background (Maekawa *et al*., 2012). This suggests a conservation in signalling requirements and either a direct recognition mechanism, or conservation in a 'guardee'.

Mla homologs

The *Mla* locus across haplotypes has been associated with resistance to multiple pathogens, other than *Bgh,* including *Puccinia striiformis* f. sp. *tritici* (*Rps7*) (Moscou, personal communication), *Puccinia striiformis* f. sp. *hordei* (Verhoeven *et al*., 2011), *Bipolaris sorokiniana (=Cochliobolus sativus)* (*Rcs6*) (Bilgic *et al*., 2006, 2005) and *P. oryzae* (*Rmo1*) (Inukai *et al*., 2006). In addition, sensitivity to the host-selective toxin victorin (*Lov1*), produced by *Bipolaris victoriae*, has been mapped to the *Mla3* locus (Lorang *et al*., 2010); and susceptibility to the spot blotch fungus *B. sorokiniana* (*Scs6*) to the *Mla* locus in the accession Bowman (Leng *et al*., 2018). Interestingly, the *Pgt* resistance gene *Sr33*, introgressed into wheat from *Aegilops tauschii*, is an ortholog of the barley *Mla*. Other *Pgt* resistance genes *Sr31* and *Sr50* derived from rye (*Secale cereale*), belong to the *Mla* locus and the *RGH1* gene family (Mago *et al*., 2015; Periyannan *et al*., 2013). Sr50 was shown to recognise AvrSr50 from *Pgt* via direct recognition and binding (Chen *et al*., 2017). *Bgh* and *Pgt* are distantly related pathogens—belonging to the Basidiomycota and Ascomycota phyla respectively—implicating MLA homologs with the capability for broad pathogen species recognition.

The *powdery mildew 3* (*Pm3*) resistance locus in wheat also displays exceptional functional diversification and allelic variation (Bhullar *et al*., 2010; Lutz *et al*., 1995). However, *Pm3* is distinct from the wheat *Mla* ortholog, *TaMla*, suggesting parallel evolution of extensive allelic series (Jordan *et al*., 2011; Zhou *et al*., 2001). To date, 17 functional alleles—*Pm3a-g*; *Pm3k-Pm3t*—have been characterised and confer isolate-specific resistance to *Bgt* (Bhullar *et al*., 2010; Stirnweis *et al*., 2014; Yahiaoui *et al*., 2006). *Pm3* alleles are >97% similar yet recognise distinct *Bgt* effectors—

comparable to barley *Mla-Bgh* interactions (Bourras *et al*., 2019, 2018, 2016). In addition, *Bgt* encodes a suppressor of avirulence (*SvrPm3a1/f1*) which is functional against several *AvrPm3-Pm3* specificities (Bourras *et al*., 2019, 2018). *Bgt* effectors recognised by *Pm3* are conserved in other mildew species, showing the potential for *Pm3* alleles in determining host-specificity (Bourras *et al*., 2019). These could represent core effectors of mildew species; *Bgt* has evolved to infect wheat to become an adapted f. spp. similar to the emergence of *P. oryzae Triticum* pathotype (Bourras *et al*., 2019; Inoue *et al*., 2017). This is another example confirming the proposal of NB-LRRs conditioning resistance to adapted and non-adapted pathogens (Tosa, 2009).

Mla-mediated resistance

Mla alleles have been characterised as conditioning either fast-acting (*Mla1*, *Mla6*, *Mla13*) or slow-acting resistance (*Mla7*, *Mla12*), corresponding to the infection stage of *Bgh* arrest (Boyd *et al*., 1995; Caldo *et al*., 2006). Fungal growth is terminated prior to or during haustorium formation via single cell death (Boyd *et al*., 1995; Kruger *et al*., 2003), compared to delayed resistance displaying as the death of multiple cells after *Bgh* haustoria and secondary hyphae formation (Freialdenhoven *et al*., 1996, 1994; Kruger *et al*., 2003). Hyper-accumulation of basal defence transcripts occurs during fast-acting resistance, which are then sustained during incompatible resistant interactions and downregulated in compatible susceptible interactions (Caldo *et al*., 2004). In comparison, hyper-induction of transcripts is followed by suppression, and then re-induction during slow-acting *Mla*-mediated resistance (Caldo *et al*., 2006). Suppression of basal defence may facilitate partial pathogen growth before termination.

Despite sharing sequence similarity, *Mla* alleles have differential requirements for the signalling component *Rar1*: *Mla6*, *Mla10*, *Mla12*, and *Mla13* require *Rar1* and member of the ubiquitin ligase complex, *SGT1*, whereas *Mla1* and *Mla7* do not (Azevedo *et al*., 2002; Halterman *et al*., 2001; Halterman and Wise, 2004; Shirasu *et al*., 1999; Zhou *et al*., 2001). A single amino acid in the LRR domain controls the *Rar1* requirement; single substitutions in *Mla6* and *Mla13* alleviated requirement for *Rar1* yet maintained resistance capabilities (Halterman and Wise, 2004; Shen *et al*., 2003).

Rapid increase in the accumulation of *Mla13*, *Mla6*, and the required *Rar1* and *Sgt1* transcripts post-*Bgh* inoculation is observed only with *Bgh* isolates carrying the corresponding *Avr* gene and recognised effector protein (Halterman *et al*., 2003).

Recognition of corresponding AVR_a proteins results in the translocation of *Mla* NB-LRRs into the nucleus and the initiation of disease resistance signalling (Bai *et al*., 2012; Shen *et al*., 2007). Cytoplasmic cell-death signalling has been shown for MLA10 which is hypothesised to be signal amplification from nuclear initiation or cell-death specific initiation (Bai *et al*., 2012). Many candidate targets of *Mla*-regulated transcriptional cascades have been identified encompassing diverse biological roles, with many induced early during infection and overlapping with genes mediating PTI (Moscou *et al*., 2011). MLA10 has been shown to interfere with and alleviate WRKY-mediated repression of pathogenesis-related gene expression. Barley HvWRKY1 and HvWRKY2 interact with the CC domain of *Mla,* present in all *Mla* variants, and colocalise in the nucleus with MLA10 dependent upon stimulation by AVR_{a10} (Shen *et al*., 2007). Activated MLA10 is also shown to interact with the transcription factor MYB6 through its CC domain, alleviating WRKY1 repression, allowing DNA binding activity and transcriptional activation. The CC domain is conserved through all *Mla* variants, suggesting a role for MYB6 in other *Mla* resistance specificities (Chang *et al*., 2013).

1.6 Pathosystems

Blumeria graminis f. sp. *hordei*

B. graminis, the causal agent of powdery mildew, has been described as the 4th most important fungal pathogen to plant pathology (Dean *et al*., 2012). It exists as an asexual haploid, with a very short diploid sexual stage. Primary and appressorial germ tubes form following germination, and an infection peg penetrates the plant epidermal cell wall. Haustoria form within the plant for nutrient sequestration and additional haustoria form through secondary and tertiary hyphae. Mycelium mats with conidial chains are formed on the leaf surface in susceptible hosts (Boyd *et al*., 1995; Jørgensen, 1994). The genome of *Bgh* has lost genes encoding primary and secondary

metabolism, rendering it an obligate biotrophic pathogen (Frantzeskakis *et al*., 2018; Spanu *et al*., 2010)

Bgh encodes hundreds of effector-like proteins, however few *Bgh* effectors have been characterised. These CSEPs—Candidates for Secreted Effector Proteins—are defined by the presence of a signal peptide and appear unique to the powdery mildews (Pedersen *et al*., 2012). Of these, CSEP families that are structurally similar to RNase-like proteins are further defined as RALPHs—RNase Like Proteins expressed in Haustoria—and comprise the largest set of secreted effector candidates within *Bgh* genomes (Pedersen *et al*., 2012; Pliego *et al*., 2013; Spanu, 2017). Expression of two RALPH-encoding genes is required for full virulence, confirming their effector candidacy (Pliego *et al*., 2013). The majority of RALPHs share a single intron at a relative position; it is hypothesised that they share a single origin from an ancestral RNase-like protein and have undergone duplication and diversification following strong selective pressure to evade recognition (Pedersen *et al*., 2012; Spanu, 2017). A hypothesised role for one candidate CSEP is in the protection of host ribosomal RNA from plant ribosome-inactivating proteins through nucleic acid binding; prevention of ribosomal RNA degradation inhibits host cell death and maintains the living cell for fungal infection (Pennington *et al*., 2019).

Bgh populations display high complexity and variation of effector repertoires (Dreiseitl, 2014; Frantzeskakis *et al*., 2019, 2018; Saur *et al*., 2019). CSEPs experience copy number variation and are locally clustered, but do not reside in preferential regions of the genome (Frantzeskakis *et al*., 2018). Recognised effectors are phylogenetically and sequence unrelated; loss of recognition is due to non-synonymous SNPs and loss of expression (Lu *et al*., 2016; Saur *et al*., 2019). However, sequence unrelated effectors could represent structural homologs: similar conformational folds could facilitate direct binding to the LRR domain of *Mla* alleles. The trade-off between evading recognition and maintaining virulence function constrains effector evolution and limits selective sweeps characteristic of ‘arms race’ plant-pathogen interactions. Expansive diversity of effectors across isolates represents balancing selection in response to the fluctuating allelic repertoires of *R* genes in host plant populations (Frantzeskakis *et al*., 2018).

Pyricularia oryzae

The filamentous ascomycete fungus *Pyricularia oryzae* (teleomorph, *Magnaporthe oryzae*) is the causal agent of rice blast and leaf spot, and infects a wide range of grasses at all development stages (Couch and Kohn, 2002). It has been ranked as the most important fungal pathogen to plant pathology due to causing extensive yield loss of up to 70%. However, its amenability to forward and reverse genetic studies makes it the ideal model system (Dean *et al*., 2012; Liu *et al*., 2014; Wilson and Talbot, 2009). Infection is initiated through conidiospore germination and appresorium formation to penetrate epidermal leaf tissue. During the initial biotrophic infection, secondary metabolites, apoplastic and cytoplasmic effectors are secreted to suppress host PTI. Intracellular NB-LRR receptors can recognise a sub-set of effectors to trigger a stronger immune response to overcome suppression (Talbot, 2003).

P. oryzae contains an approximate 41 Mb nuclear genome, encoding a large diverse set of ~739 predicted secreted proteins (Wilson and Talbot, 2009). Previous phylogenetic analysis and mating experiments have separated rice and grass infecting *P. oryzae* into a distinct species from its previous classification as a f. sp. of *P. grisea*—which is now solely associated with the grass genus Digitaria. These two clades are defined by host associations and show clear sequence divergence, ecological and reproductive isolation (Couch and Kohn, 2002). Both *Pyricularia* species show a tight host specificity conditioned by one or a few dominant genes of the *PWL* multigene family encoding small secreted proteins. *PWL1* and *PWL2* prevent *P. grisea* from infecting the host weeping lovegrass (*Eragrostis curvula*) (Kang *et al*., 1995; Sweigard *et al*., 1995). Tosa *et al.*, (2005), identified a suite of *PWT* genes responsible for *P. oryzae* wheat specificity.

Resistance to *P. oryzae* is either race-specific, complete and controlled by one gene, or partial resistance controlled by QTLs (Liu *et al*., 2014). Diverse QTL regions have been implicated for resistance to different stages of leaf and neck blast progression (Kongprakhon *et al*., 2009; Puri *et al*., 2009). To date, over 100 *R* genes and multiple QTLs in rice have been described to confer resistance to *P. oryzae*, of which only ~21 NB-LRR genes have been cloned (Liu et al., 2014; Sharma et al., 2012). Paralogs of rice resistance gene families, isolated from maize, sorghum, and *Brachypodium* confer

resistance to *P. oryzae* when transformed in rice (Yang *et al*., 2013). As mentioned previously, the rice Exo70 domain OsExo70-F3, is the guardee required for NB-LRR *Pii*-dependent resistance (Fujisaki *et al*., 2015) and could represent a shared effector target across species.

The first reported blast infection of barley was in 1940, and field infections of barley blast were observed in Japan in 1979, and later in 2000 in Thailand (Sato *et al.,* 2001). Yaegashi (1988) identified the dominant blast resistance gene *PHR-1* although this has yet to be replicated or mapped. Basal resistance to *P. oryzae* is observed in barley through the formation of papillae against attempted appressorial penetration, but this is often ineffective and weak. Cell death is triggered after successful appressorium formation to prevent further fungal invasion (Tanaka *et al.,* 2010). *P. oryzae* resistance is highly polymorphic across barley cultivars (Nga *et al.,* 2012). Sato *et al.,* (2001) identified isolate-specific and seedling resistance QTLs, located on 3H, 4H, and 5H. One QTL on 4H co-localised to previously mapped resistances to stem rust (*Puccinia graminis*), scald (*Rhynchosporium secalis*) and net blotch (*Phyrenophora teres*), possibly indicating a region of multiple pathogen resistance. Interestingly, one of the broad-spectrum partial resistance QTLs was donated from a Canadian cultivar—a region where there have been no reports of blast disease. Presumably this functions in resistance to another pathogen for it to be maintained by selection, prior to use in agriculture.

Bipolaris victoriae

Species of *Bipolaris* cause devastating diseases on grasses in the Poaceae family. Recently, multiple species (*Bipolaris, Cochliobolus*, and *Curvularia*) were converged into one genus: *Bipolaris* (Manamgoda *et al*., 2012). The genus contains over 40 species (all necrotrophs with few hemibiotrophs) which are often highly virulent on their hosts (Condon *et al*., 2013). Necrotrophic pathogens thrive on dead plant tissue, often producing phytotoxin secondary metabolites, peptides, and reactive oxygen species to aid tissue degradation (Wang *et al*., 2014). Furthermore, some species secrete toxins toxic only to their host species: non-host species are insensitive to these molecules (Wang *et al*., 2014; Wolpert *et al*., 2002). *Bipolaris* species are able to

evolve novel, virulent races through the production of such host-selective toxins (HSTs) (Condon *et al*., 2013).

Spot blotch, caused by hemibiotroph *Bipolaris sativus*, is one of the most agronomically important diseases of barley (Leng *et al*., 2018). *Bipolaris victoriae* is the causal agent of victoria blight—a disease which arose during the 1940s as a consequence of deployment of oat crown rust (*Puccinia coronata*) resistant oat cultivars (Meehan and Murphy, 1946). Introgression of the *Pc2* resistance gene facilitated the host jump of *B. victoriae* from timothy-grass (*Phleum pratense*) (Meehan and Murphy, 1946). Victorin sensitivity (*Vb*) and oat crown rust resistance (*Pc2*) have not been genetically separated and are assumed to share identity, proposing the idea that an *R* gene can condition both resistance and susceptibility.

B. victoriae pathogenesis is dependent on host sensitivity to the HST victorin: *B. victoriae* mutants defective in victorin production are also non-pathogenic (Walton, 1996; Wolpert *et al*., 2002). Victorin triggers a defence response in the host resulting in localised cell death through hypersensitive response, a form of programmed cell death (Gilbert and Wolpert, 2013). HSTs are described as 'agents of compatibility' that facilitate fungal infection (Walton, 1996); only plants carrying the dominant *Vb* gene are sensitive to victorin and therefore susceptible to *B. victoriae* (Wolpert *et al*., 2002). Victorin has been characterised as a group of cyclised pentapeptides (Wolpert *et al*., 1994, 1985; Wolpert and Macko, 1989) The structures of victorin—victorin B, C, D, E, and victoricine—have been established (Wolpert *et al*., 1994; Wolpert and Macko, 1989) and are routinely used in sensitivity assays (Wolpert and Lorang, 2016).

Puccinia striiformis f. sp. *hordei*

Puccinia striiformis, the causal agent of stripe (yellow) rust is a common and devastating pathogen of grasses and cereals. It is an obligate biotroph, leading a heteroecious life cycle with a telial host in Poaceae and an aecial host in Berberidaceae. Recent adaption to warmer climates has allowed *P. striiformis* to spread to areas without a previous history of the fungus (Hovmøller *et al*., 2011). Regular regional wheat crop losses around 0.1 to 5%, sometimes 25% are observed

due to fungal infection (Singh *et al*., 2016). However, wheat yield losses of 70% or more are possible during an epidemic under favorable conditions (Wellings, 2011).

The most susceptible genera are *Aegilops*, *Agropyron*, *Bromus*, *Elymus*, *Hordeum*, *Secale* and *Triticum* (Stubbs, 1985) and both ff. spp. and cultivar specialisation has been observed within the *P. striiformis* species. Interestingly, Eriksson's (1894), original concept of *formae speciales* arose due to the observation that the ability of *P. striiformis* to infect a given host was dependent on the host species from which it was isolated, and divided *P. striiformis* into five ff. spp.., with respect to the susceptible genera, i.e. f. sp. *agropyri*, *elymi*, *hordei*, *secalis*, and *tritici* (Eriksson, 1894; Liu and Hambleton, 2010). As well as ff. spp.., *P. striiformis* also shows cultivar specificity within the host genus which is conditioned by classic *R-Avr* gene interactions. Biffen (1905) first showed Mendelian inheritance of resistance using stripe rust. Due to the observation of asexual populations in the field, it is hypothesised that recombination during the sexual stage on the alternate host facilitates virulence evolution—but the extent of this is unknown (Hovmøller *et al*., 2011).

The barley specialist *Puccinia striiformis* f. sp. *hordei*, (*Psh*) has spread extensively across the world over the last 40 years since being introduced into South America in 1975 from Europe. *Psh* is found in all major barley-producing areas worldwide (Brown, 2015). Few genes in barley have been found for resistance to *Psh*, compared to over 50 *Yr* (yellow rust) resistance genes identified from wheat (Chen and Line, 1999; Hovmøller *et al*., 2011). Quantitative resistance QTLs have been identified across chromosomes 1H, 4H and 5H, and a QTL on 7H shows qualitative resistance of large effect (A. J. Castro *et al*., 2003; Toojinda *et al*., 2000). Of these, the QTL on 1H—*QRps1H*—encompasses the *Mla12* locus, but the relationship of *QRps1H* and *Mla12* is unknown (Verhoeven *et al*., 2011).

1.7 Summary

B. graminis, *P. oryzae,* and *P. striiformis* are placed within the top 4 fungal plant pathogens, causing devastating yield loss worldwide (Dean *et al*., 2012). While *B. victoriae* does not currently pose as great an economic threat, it is an example of the unexpected consequence of resistance gene deployment and highlights the potential

trade-offs between biotrophic resistance and necrotrophic pathogen susceptibility. The *Mla* locus in barley is a known region conferring recognition to multiple pathogens: *Rmo1* and *Lov1* map to the *Mla3* locus in barley and *QRps1H* encompasses the *Mla12* locus, among other examples. This raises the question: what is the involvement of *Mla* alleles in multiple pathogen recognition? Fine-mapping and characterising candidate genes will give a greater insight into the genetic architecture of the *Mla* locus and the potential for multiple pathogen recognition.

1.9 Dissertation organisation

The first research chapter presented in this thesis details the identification of a *trans*-species polymorphism at *Mla* and is associated with the publication Brabham *et al*., (2018). The second section describes the fine-mapping of *Mla3*, *Rmo1*, and *Lov1*. The third, follows on from the first in characterising *Rmo1* and the barley-*P. oryzae* interaction in the *Mla3* haplotype. The fourth chapter contains the QTL analysis of *QRps1H* for adult plant resistance to *P. striiformis* f. sp. *hordei.*

Chapters*:*

2. This chapter discusses the results and findings presented in the paper, "An ancient integration in a plant NB-LRR is maintained as a *trans*-species polymorphism" (Brabham, 2018). In the characterisation of candidate genes at the *Mla* locus, I identify an integrated Exo70 within the *RGH2* allele in the *Mla3* haplotype. Phylogenetic analysis is then used to identify orthologs of *RGH1*, *RGH2*, and *RGH3 Mla* NB-LRR gene families in other grass species. Interspecific conservation is observed in the *RGH2-Exo70F1* integration, as well as differential integrated domains prior to *Brachypodium* speciation. *RGH2* exists as a *trans*-species polymorphism maintained over 24My, hypothesised to be maintained through balancing selection due to the role of *RGH2-Exo70F1* in multiple pathogen recognition.

3. The research presented in this chapter identifies the fine-mapping of *Mla3*, *Rmo1,* and *Lov1,* and the confirmation of their complete genetic coupling.

4. This chapter confirms the multiple pathogen recognition capability by *Mla3*. Using transformation, Golden Promise + *Mla3* transgenic lines are found to be resistant to both *Bgh* and *P. oryzae* in a copy-number dependent manner.

5. This research chapter contains the delineation of *QRps1H*, a *P. striiformis* f. sp. *hordei* adult plant resistance (APR) QTL in the *Mla12* haplotype. This gene is mapped to a 7.6cM region spanning the *Mla12* locus.

1.10 Contributions to Research

Helen Brabham (HJB), Phon Green (PG), Inmaculada Hernández-Pinzón (IHP), Sam Holden (SH), Matthew Moscou (MM), Jennifer Lorang (JL), Tom Wolpert (TW), Patrick Hayes (PH), Laura Helgerson (LH), Scott Fisk (SF), Hiromasa Saitoh (HS), Motoki Shimizu (MS), Koki Fujisaki (KF), Ryohei Terauchi (RT), Ravi Singh (RS).

A *trans*-species polymorphism at *Mla*

Conception and the design of experiments: HJB, MM.

Experimentation: HJB, IHP, JL.

Data analyses: HJB, SH, MM.

***Mla3, Rmo1* and *Lov1* are in genetic coupling**

Conception and the design of experiments: HJB, MM, TW, JL

Experimentation: HJB, PG, IHP, JL

Data analyses: HJB, MM.

***Mla3* confers resistance to multiple pathogens**

Conception and the design of experiments: HJB, MM, RT, MS.

Experimentation: HJB, PG, IHP, JL, HS, MS.

Data analyses: HJB, MM.

Fine-mapping of *QRps1H*

Conception and the design of experiments: HJB, PH, RS, MM.

Experimentation: HJB, LH, SF, RS, PG, IHP.

Data analyses: HJB, MM.

2 A *trans*-species polymorphism at *Mla*

2.1 Abstract

Plant immune receptors are under constant selective pressure to maintain resistance to plant pathogens. Nucleotide-binding leucine-rich repeat (NB-LRR) proteins are one class of cytoplasmic immune receptors whose genes commonly show signatures of adaptive evolution (Ellis et al., 1999; Mondragón-Palomino et al., 2002; Rose et al., 2004; Seeholzer et al., 2010; Wei et al., 2002). While it is known that balancing selection contributes to maintaining high intraspecific allelic diversity, the evolutionary mechanism that influences the transmission of alleles during speciation remains unclear. The barley *Mla* locus has over 30 described alleles conferring isolate-specific resistance to barley powdery mildew and contains three NB-LRR families (*RGH1*, *RGH2*, and *RGH3*) (Wei *et al*., 2002, 1999). This chapter outlines the discovery (using sequence capture and RNAseq) of the presence of a novel integrated Exo70 domain in RGH2 in the *Mla3* haplotype. Allelic variation across barley accessions includes presence/absence of the integrated domain in RGH2. In addition, interspecific conservation in the RGH2-Exo70 integration is shared across Poaceae species. We hypothesise that balancing selection has maintained allelic variation at *Mla* as a *trans*-species polymorphism over 24 My, thus contributing to and preserving interspecific allelic diversity during speciation.

2.2 Introduction

The plant immune system has been shaped by the interactions with pathogens throughout evolutionary history. Recognition of plant pathogens is mediated by membrane and cytoplasmic immune receptors that recognise pathogen-derived molecules, including effectors (Jones and Dangl, 2006). Cytoplasmic immune receptors recognise secreted pathogen effectors directly, or indirectly through monitoring the molecular status of host proteins targeted by pathogen effectors (Jones *et al*., 2016). At the population level, plant immunity to pathogens is conferred, in part, through the maintenance of diverse allelic variants at immune receptor loci. Pathogen

pressure influences the relative frequency of resistance alleles in plant populations, with selection fluctuating due to pathogen evolution. Mutations that generate novel approaches to manipulate a host by immune suppression or nutrient acquisition, for example, are selected for in the pathogen. Similarly, novel forms of pathogen recognition are selected for in the plant. Despite this, little is known about the origin or maintenance of *R* gene variants in populations.

The current diversity of immune receptors maintained in populations reflects extant pathogen pressure as the majority of *R* genes classified to date occur in a gene-for-gene relationship with their recognised pathogens; individual immune receptors recognise specific pathogen ligands (Dodds and Rathjen, 2010). However, the increasing wealth of genomic resources has revealed complex population dynamics and hidden variation of plant immune receptors driven by diverse evolutionary processes. The majority of plant resistance (*R*) genes are intracellular receptors encoding nucleotide binding, leucine-rich repeat domain-containing proteins (NB-LRRs) and form one of the most diverse and expanded gene families in plants (Sukarta *et al*., 2016).

NB-LRRs contain a central nucleotide domain (NB), C-terminal leucine-rich repeat domain (LRR), and an N-terminal of either coiled-coil (CC) or Toll/interleukin-1 receptor (TIR) domain—defining NB-LRRs further into two major classes (Jones *et al*., 2016). Structural analyses of CC domains indicate the potential for NB-LRR dimerization and NB-LRR-cofactor heterodimerisation, yet it is unclear if this is due to differences in conformational or CC domain function (Casey *et al*., 2016; Hao *et al*., 2013). LRR domains contain signatures of strong diversifying selection pressure reflective of their role in pathogen recognition (Bai et al., 2002; Mondragón-Palomino et al., 2002). The majority of cereal NB-LRRs are non-TIR, with variation presence/absence of an N-terminal CC domain. Structural analysis identified conserved N-terminal nT and P-loop domains, with EDVID motif in CC domains, and presence/absence of variable C-terminal LRR domains of rice (*Oryza sativa*) NB-LRRs (Bai *et al*., 2002; Sukarta *et al*., 2016).

A recent area of intensive research in plant immunity includes the identification of integrated non-canonical domains in NB-LRRs: additional domains which are thought

to serve as baits for pathogen effectors, and thus, facilitate efficient immune responses (Cesari, 2018; Cesari *et al*., 2014; Kroj *et al*., 2016; Sarris *et al*., 2016). Additional domains or protein coding regions are hypothesized to be fusions of interacting partners and contribute to signalling, activation, and pathogen recognition (Kroj *et al*., 2016; Sarris *et al*., 2016; Sukarta *et al*., 2016). In grasses, approximately 10% of NB-LRRs contain additional integrated domains (NB-LRR-IDs). Often residing in Major Integration Clades (MIC), these NB-LRRs have gained the capacity to accommodate additional domain integrations within the protein structure. The MIC1 clade contains diverse integrated domains, whereas MIC2 and MIC3 are hypothesised expansions of single integration events (Bailey *et al*., 2018). NB-LRR-IDs often require a second NB-LRR partner to function, as is the case for *RGA4/RGA5* of rice (Césari *et al*., 2014), these NB-LRR partners reside in clade C7 exclusively (Bailey *et al*., 2018). As integrations are presumed duplications of host proteins, it is hypothesised that integrated domains are released from purifying selection for host function; therefore, they are free to adapt specifically for pathogen recognition (Cesari *et al*., 2014).

Thorough characterisation of the diversity of NB-LRRs within a species has been limited by the extremely polymorphic nature of the gene family. Previous research focus has been on the curation of a representative reference genome of a species, created from a single accession or cultivar. It has become clear that this is a mere fraction of the true intra-specific diversity: extensive presence/absence, sequence, and copy number variation is present as more individuals are sequenced within a species (Bai *et al*., 2002; Bakker *et al*., 2008; Guo *et al*., 2011; Meyers *et al*., 2003; Monteiro and Nishimura, 2018; Van de Weyer *et al*., 2019; Yang *et al*., 2006). Work across seven legume species (Zheng *et al*., 2016), five Brassicaceae genomes (Zhang *et al*., 2016), two Rosid woody perennial species (Yang *et al*., 2008), and two rice genomes (Yang *et al*., 2006) identified signatures of responses to pathogen pressures including patterns of expansion and contraction, species-specific gene loss and duplication events, and differences in the evolutionary rates of the NB-LRR subclasses. Recent publication of a pan-NB-LRRome of *Arabidopsis thaliana* derived from 64 diverse accessions captures a species-wide repertoire of the NB-LRR gene family (Van de Weyer *et al*., 2019). The greatest polymorphisms across accessions were observed in NB-LRRs that provide resistance to adapted biotrophic pathogens of *A. thaliana*. In addition, a single accession contained a fraction of the total diversity of NB-LRR-IDs;

such an expansive collection suggests frequent integration events. NB-LRR-IDs and their partners also showed signatures of co-evolution—where mutations in one NB-LRR would lead to compensatory mutations in the pair. It is clear that the intra-specific variation of NB-LRRs has been previously underestimated. Characterising this intra-specific diversity of plant immune receptors is the first step in understanding the selection pressures acting on NB-LRR repertoires and the driving forces and limitations of NB-LRR evolution.

Population genetic models suggest recurrent selective sweeps with allele fixation (arms race), continuous allele frequency oscillations, and allele maintenance through balancing selection (balanced polymorphisms) can all occur from host-pathogen interactions (Bergelson *et al*., 2001; Rose *et al*., 2007; Tellier *et al*., 2014). Such opposing outcomes are characteristic of frequency-dependent selection and the fast-evolving nature of plant pathogens and their effectors. However, the preservation of allelic pools through speciation events remains unclear. Current understanding of the evolution and maintenance of plant immune receptors has been limited due to lack of population genetic data. However, a few polymorphisms have been observed. Balanced polymorphisms in stress response genes have been reported for *A. thaliana* and *Capsella rubella* (Q. Wu *et al*., 2017), and also at immunity-related loci across *C. rubella* and *C. grandiflora* (Koenig *et al*., 2019). The *A. thaliana Pseudomonas syringae* resistance gene *RPM1* also exists as a presence/absence polymorphism maintained over 9 million years. The entire coding region of *RPM1* is deleted in susceptible individuals; presence of *RPM1* is found to incur a large fitness cost resulting in reduced seed production (Stahl *et al*., 1999; Tian *et al*., 2003). Additional known genes in *A. thaliana—RPP1* (*RESISTANCE* TO *PERONOSPORA PARASITICA1*) (Botella *et al*., 1998; Goritschnig *et al*., 2016; Rehmany *et al*., 2005), *RPS2* (*RESITANCE TO P. SYNRINGAE2*) (Caicedo *et al*., 1999), *RPP4/5* (*RESISTANCE* TO *PERONOSPORA PARASITICA4/5*) (Noël *et al*., 1999; Van Der Biezen *et al*., 2002), and *RPS5* (*RESISTANCE TO PSEUDOMONAS SYRINGAE5*) (Karasov *et al*., 2014)—are present at complex NB-LRR loci and also show extensive sequence or presence/absence polymorphisms between haplotypes. Furthermore, alleles in the *RPP7* (*RESISTANCE* TO *PERONOSPORA PARASITICA7*) NB-LRR cluster, in combination with non-NB-LRR *RPW8* (*RESISTANCE TO POWDERY MILDEW8*) / (*HR*) (*HOMOLOG OF RPW8*) alleles, result in hybrid necrosis for

incompatible interactions (Barragan *et al*., 2019; Chae *et al*., 2014). Such deleterious genetic interactions could contribute to balanced polymorphisms within a population. Identifying the wealth of intra-specific diversity of plant immune receptors is crucial for characterisation of selection pressure and evolutionary history of the plant immune system; data will provide direct evidence to validate evolutionary models.

NB-LRR-encoding loci present a great challenge to genome assembly due to their high complexity, copy number variation, and association with repetitive elements (Cook *et al*., 2012; Muñoz-Amatriaín *et al*., 2013). Genome wide analysis of NB-LRR genes in both *Arabidopsis* and rice identified great diversity of NB-LRRs in the genome—a result of duplication events, rearrangement, and gene conversion (Bai et al., 2002; Meyers et al., 2003; Monosi et al., 2004; Shang et al., 2009; Yang et al., 2006; Zhou et al., 2004). The barley genome has undergone substantial advancement in the last ten years, cumulating in a chromosome conformation capture ordered genome produced by Mascher *et al.*, (2017) yet NB-LRR characterisation remains a challenge.

In this chapter, a RenSeq capture and annotation pipeline for the NB-LRRs of the barley is developed. Substantial intraspecific variation in NB-LRR-ID domain structure is discovered, including presence/absence and structural variation between alleles. Tracing the evolutionary history of an Exo70F1 integration within RGH2 at the *Mla* locus, this integration is dated subsequent to *Brachypodium* speciation and prior to radiation of the Poaeae-Triticeae, forming a *trans*-species polymorphism. This is evidence of balancing selection maintaining an NB-LRR allelic pool through speciation over 24 million years.

2.3 Results

Extensive variation in *RGH* gene families at *Mla*

We set out to understand the intraspecific diversity of the plant immune receptors at the *Mla* locus in barley (*Hordeum vulgare*). The locus contains three NB-LRR encoding gene families—*RGH1*, *RGH2*, and *RGH3*—of which members of the *RGH1* gene family confer resistance to *Blumeria graminis* f. sp. *hordei* (barley powdery mildew), a pandemic disease of barley Wei 2002; Jorgensen 1994; Zhou *et al*. 2001

Plant Cell; Haltermann *et al*. 2001 Plant Journa; Shen, Zhou *et al*. 2003 Plant Cell; Haltermann *et al*. 2004 Plant Journal; Seeholzer *et al*. 2010 MPMI). In a comparison between a limited number of haplotypes, substantial variation has been identified based on sequencing *RGH1* genomic fragments, with alleles sharing >90% protein identity (Seeholzer *et al*., 2010). Based on the assessment of several sequenced genomes and leaf transcriptomes of barley, we found that *de novo* leaf transcriptomes can be used to assess the presence or absence of the three *RGH* gene families. We performed RNAseq on leaf tissue derived from 40 diverse barley accessions that include domesticated and wild barley. Sequence variation and presence/absence variation in expression of *RGH1*, *RGH2* and *RGH3* were identified across accessions (Figure 2-1A). All three genes families showed considerable sequence variation between allelic variants. *RGH1* was the most prevalent of all *RGH* gene families with variation including intact open reading frames (ORF), pseudogenised genes, and in two cases, absence at the expression level. In contrast, *RGH2* and *RGH3* were found in the minority of haplotypes. For all haplotypes sequenced, *RGH2* was always present with *RGH3*. Presence of *RGH3* without *RGH2* was seen in four accessions, and only in those also containing a pseudogenised *Mla* allele. Evaluation of the coding sequence of *RGH2* alleles, five haplotypes (accessions Baronesse, Duplex, Finniss, HOR 1428, and Maritime) were found to have a gene fusion with *Exo70*, encoding a component of the exocyst complex. Allelic variants of RGH2 in other accessions contain a coiled coil integrated domain derived from RGH1 or an in-frame full length RGH1 family member. To test whether the RGH2-Exo70 fusion was not an artefact of *de novo* transcriptome assembly, we used sequence capture designed on the entire *Mla* locus and PacBio circular consensus sequencing to assemble the physical sequence encompassing *RGH2* (Witek *et al*., 2016). Using the barley cultivar Baronesse, we found a single genomic contig that contained integrated *RGH2-Exo70* (Figure 2-1B, C). *RGH2-Exo70* and *RGH3* in Baronesse were found in close proximity and were arranged in head-to-head orientation (Figure2-1B). In summary, *Mla* alleles of barley have presence/absence variation in *RGH1*, *RGH2*, and *RGH3*, as well as different gene fusions, including *Exo70*.

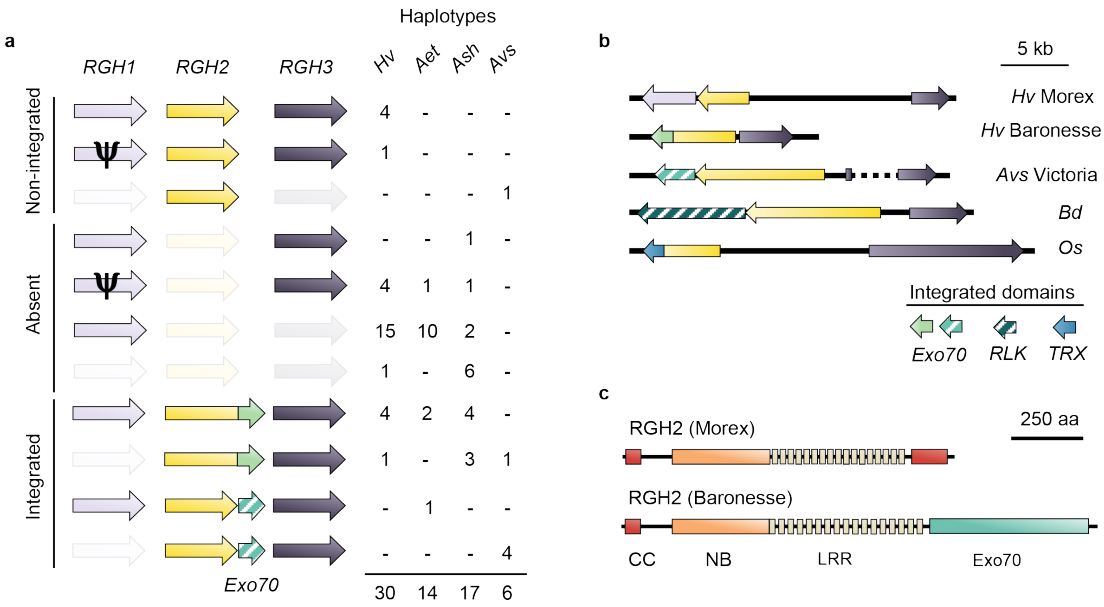

Figure 2-1. Intra- and inter-specific variation in *RGH1*, *RGH2*, and *RGH3*.

RGH1, *RGH2*, and *RGH3* family members are shown in coloured arrows (light purple, yellow, and dark purple, respectively). (a) Haplotype variation in leaf expression of *RGH1*, *RGH2*, and *RGH3* within barley (*Hordeum vulgare*; *Hv*), *Aegilops tauschii* (*Aet*), *Aegilops sharonensis (Ash*), and oat (*Avena sativa*; *Avs*). Presence of a complete coding sequence of each gene family is shown with coloured arrows in each column (*RGH1*, *RGH2*, and *RGH3*), and absence with faded arrows. Each combination of expressed gene families is represented in rows, classified as Non-integrated, Absent, and Integrated as defined by the status of the RGH2 family member. Pseudogenised *RGH1* is indicated with the symbol ψ. Integrated RGH2-Exo70 forms are represented through green arrows alongside the yellow arrows, with out-of-frame integrated Exo70 shown with hatched shaded turquoise arrows. Haplotypes is defined as the number of haplotypes containing different RGH gene combinations in each row. *Aet* includes RGH2 from TaD genome of wheat. (b) Genomic structure of the region encompassing *RGH2* and *RGH3* across Poaceae species showing conserved head-to-head orientation of *RGH2* and *RGH3*. Variation is observed in RGH2 integrated domains with barley accessions Morex (*mla*) (Wei *et al*., 2002) and Baronesse (*Mla3*/*Rmo1*) (Inukai *et al*., 2006; Seeholzer *et al*., 2010) containing *RGH2-Exo70* (yellow-turquoise arrow), oat accession Victoria containing *RGH2-Exo70* (yellow-turquoise arrow), *Brachypodium distachyon* (*Bd*) containing *RGH2-Receptor-like-kinase* (yellow-teal arrow), and rice (*Oryza sativa*; *Os*) containing *RGH2-Thioredoxin* (yellow-light blue arrow). *A. sativa* accession Victoria and *B. distachyon* integrated *Exo70* are out-of-frame with *RGH2*, indicated with the hatched shaded arrows. (c) Protein model of non-integrated RGH2 and integrated RGH2-Exo70. Individual domains include coiled coil (CC; red), nucleotide-binding (NB; orange), leucine-rich repeats (LRR; cream), and Exo70 (turquoise).

The Origin of Integrated Exo70 within RGH2 is Exo70F1

To identify the source of the integrated Exo70, we identified and curated the Exo70 protein families from several sequenced grass species including *Brachypodium distachyon*, barley, *Oryza sativa* (rice), *Oropetium thomaeum*, *Sorghum bicolor*, *Setaria italica*, and *Zea mays* (maize). Based on protein alignment and maximum likelihood phylogenetic analysis, we found that the Exo70F and Exo70FX clades were found to be greatly expanded within these grasses compared to *Arabidopsis thaliana* (Figure 2-2A) (Cvrčková *et al*., 2012). The integrated Exo70 was found to originate from Exo70F1. Alignment and phylogenetic analysis of the Exo70F family showed that Exo70F1 is a single copy family for the majority of Poaceae (Figure 2-2B). The 5' region of *Exo70F1* was truncated after integration in *RGH2*, with approximately 87% of the coding sequence of *Exo70F1* present. Non-integrated *Exo70F1* and *RGH2* integrated *Exo70F1* are highly divergent at the nucleotide and protein level, with 67% and 62% identity, respectively. This degree of divergence suggests that an ancient duplication and fusion event led to the formation of *RGH2-Exo70F1*.

Interspecific Conservation in the *RGH2-Exo70F1* Gene Fusion

Based on the observation of highly divergent non-integrated *Exo70F1* and *RGH2* integrated *Exo70F1*, we hypothesized that other species may contain this gene fusion. Using BLAST on NCBI, we found an identical integration of *Exo70F1* in *RGH2* in *Aegilops tauschii* (Periyannan *et al*., 2013) and *Triticum urartu* (Ling *et al*., 2013). In barley, we observed that *RGH2-Exo70F1* is only present in a minority of *Mla* haplotypes (Figure 2-1A). To determine if *RGH2-Exo70F1* exists as a presence/absence polymorphism in *Aegilops tauschii*, we analysed the genome of accession AL8/78 (Luo *et al*., 2017) and 15 leaf transcriptomes of diverse accessions (Nishijima *et al*., 2016). We observed presence of *RGH2-Exo70F1* and *RGH3* in 7 accessions but were not detected in 11 other accessions, suggesting they may be absent from these genomes (Figure 2-1A). In contrast to barley, we did not identify in *Ae. tauschii* an allele of *RGH2* without the *Exo70F1* integration. Barley and *Ae. tauschii RGH2-Exo70F1* have 88% identity at the nucleotide level. Together, these results indicate that *RGH2-Exo70F1* is a *trans*-species polymorphism between barley and *Ae. tauschii* (Klein *et al*., 1998).

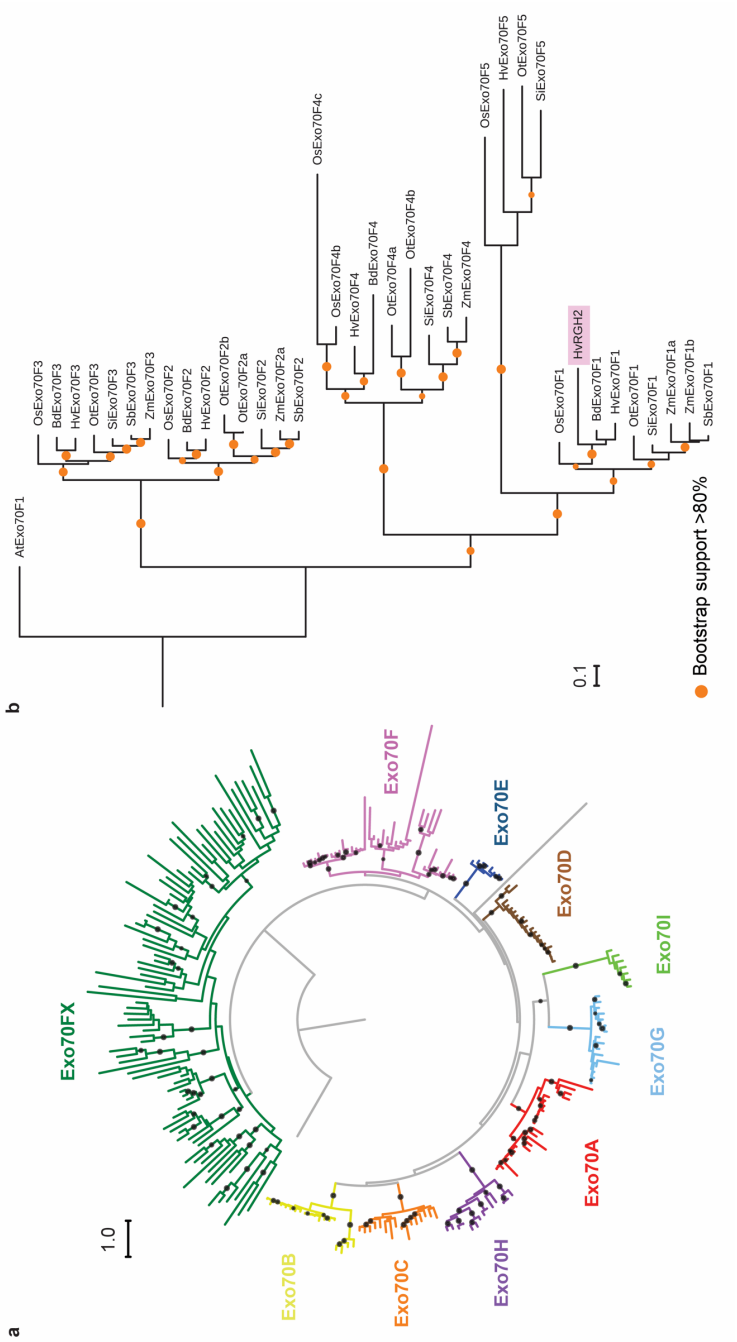

Figure 2-2. *Exo70F1* is the donor of the *Exo70* integration in *RGH2*.

(a) Maximum likelihood phylogenetic tree of Exo70 proteins from seven grass species, including barley *RGH2* integrated *Exo70* denoted HvRGH2. *Saccharomyces cerevisiae* Exo70 gene (YJL085W) was used as an outgroup. Black dots represent bootstrap support greater than 80% based on 1,000 bootstraps. (b) Maximum likelihood phylogenetic tree of Exo70F proteins from seven grass species (see below). The origin of the integrated Exo70 in RGH2 is Exo70F1 family (highlighted in pink). *Arabidopsis thaliana* Exo70 gene (AT5G50380; AtExo70F1) was used as an outgroup. Orange dots represent bootstrap support greater than 80% based on 1,000 bootstraps. Species included in the analysis were: *B. distachyon* (*Bd*), barley (*Hv*), rice (*Os*), *Oropetium thomaeum* (*Ot*), *Sorghum bicolor* (*Sb*), *Setaria italica* (*Si*), maize (*Zea mays*; *Zm*).

We expanded our search to include all Pooideae species with sequenced genomes or publicly available leaf RNAseq data. In total, we evaluated 14 sequenced genomes and 126 transcriptomes from 63 species. Sequence analysis found allelic variation and interspecific conservation in the *RGH2-Exo70F1* integration across diverse Poaceae species (Figure 2-1A). Non-integrated alleles of *RGH2* are present in both Triticeae (barley) and Poeae (*Poa supina* and *Avena sativa* (oat)) species, indicating that multiple alleles of *RGH2* have been maintained in these lineages. Based on the conservation of *RGH2-Exo70F1* and *RGH3*, we hypothesized that the head-to-head orientation of *RGH2* and *RGH3* is preserved between Triticeae and Poeae species. We used sequence capture designed on oat NB-LRR encoding genes, including *RGH2* and *RGH3*, and performed PacBio circular consensus sequencing to assemble the physical sequence encompassing *RGH2-Exo70F1* and *RGH3* from the oat cultivar Victoria. An identical structural arrangement was observed, with *RGH2-Exo70F1* and *RGH3* in head-to-head orientation (Figure 2-1B). Within oat, several accessions had interrupted *RGH2-Exo70F1* open reading frames either through an early stop codon (Hanzou2, Hanyou5, and Mongolia) or InDel (Victoria) (Figure 2-1A). The oat accession Kanota was the only accession identified with an intact *RGH2-Exo70F1* open reading frame (Figure 2-1A). A similar observation was made for the allele *RGH2-Exo70F1* found in the *Ae. tauschii*-derived D genome of wheat. This suggests that while *RGH2-Exo70F1* is maintained, it may experience pseudogenisation in multiple species.

RGH2-Exo70F1 Gene Fusion Occurred Prior to Poeae-Triticeae Radiation

To date the origin of the gene fusion event, we performed maximum likelihood phylogenetic analysis using non-integrated and integrated *Exo70F1*. We found that integrated *Exo70F1* derived from Triticeae and Poeae species form a distinct clade from non-integrated *Exo70F1* (Figure 2-3). *B. distachyon* and *B. stacei* form the outgroup of this integrated clade, suggesting that integration of *Exo70F1* in *RGH2* occurred after speciation of Brachypodieae but prior to radiation of the Poeae and Triticeae. The *RGH2* ortholog in *B. distachyon* encodes an NB-LRR with a C-terminal integrated receptor-like kinase with intact transmembrane and extracellular lectin domains. The observation of both integrated and non-integrated forms of *RGH2* in species of Triticeae and Poeae is characteristic of a *trans*-species polymorphism (Figure 2-4). This *Exo70F1* integration occurred after Brachypodieae speciation, but

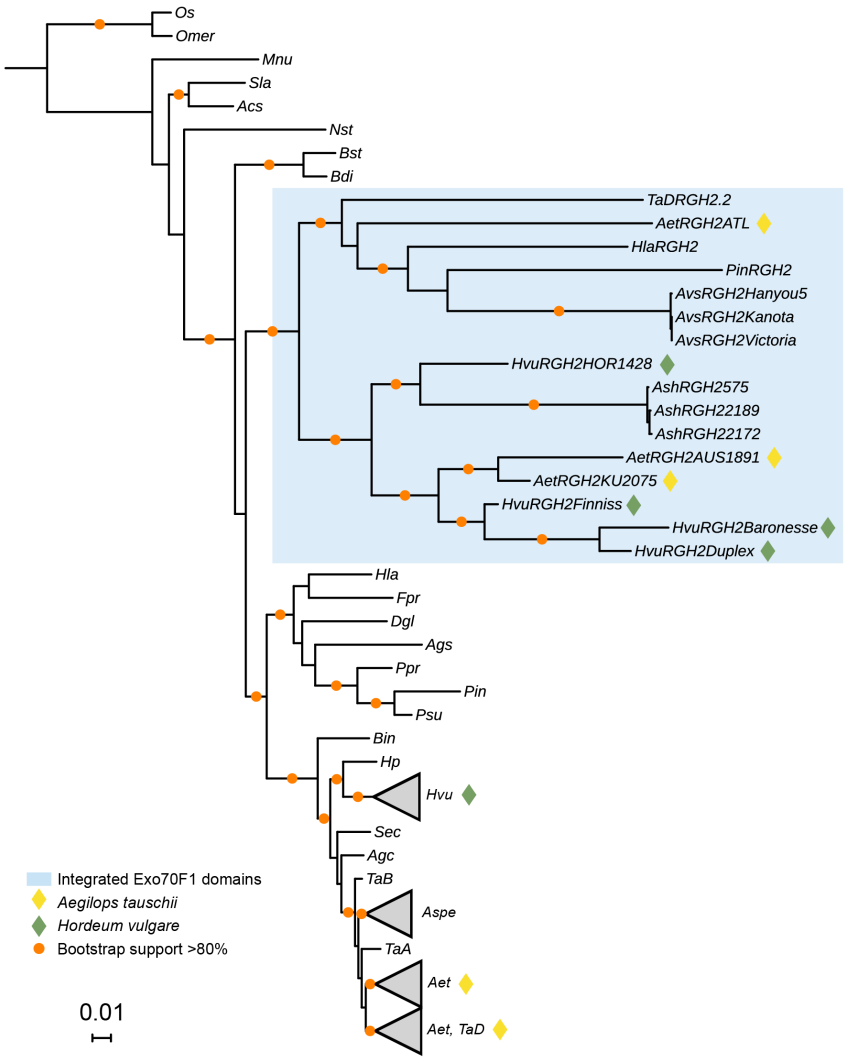

Figure 2-3. *Exo70F1* integration in *RGH2* occurred prior to the Poeae-Triticeae radiation.

Maximum likelihood phylogenetic tree was performed on codon aligned *Exo70F1* genes from 19 grass species. Integrated *Exo70F1* highlighted in blue. Branch support was generated using 1,000 bootstraps, with orange dots designating support greater than 80%. Rice *Exo70F1* (*OsExo70F1*; *Os01g69230.1*) and *O. meridionalis* Exo70F1 were used as outgroups. Scale bar shows nucleotide substitutions per site. Species included in the analysis were: *Achnatherum splendens* (*Acs*), *Ae. tauschii* (*Aet*), *Agropyron cristatum* (*Agc*), *Agrostis stolonifera* (*Ags*), *Aegilops sharonensis (Ash*), *A. sativa* (*Avs*), *B. distachyon* (*Bd*), *Bromus inermis* (*Bin*), *Dactylis glomerata* (*Dgl*), *Festuca pratensis* (*Fpr*), *Holcus lanatus* (*Hla*), *H. pubiflorum* (*Hp*), barley (*Hvu*), *Melica nutans* (*Mnu*), *Nardus stricta* (*Nst*), rice (*Os*), *O. meridionalis* (*Omer*), *Poa inermis* (*Pin*), *Poa pratensis* (*Ppr*), *Poa supina* (*Psu*), *Secale cereale* (*Sec*), *Stipa lagascae* (*Sla*), *Triticum aestivum* (*TaA*, *TaB*, *TaD* subgenomes), maize (*Z. mays*; *Zm*). Clusters were formed due to 100% identical sequence and are listed in Appendix Table 7-2. Collapsed nodes represent non-integrated Exo70F1 derived from designated species and are shown in full in Figure 2-5.

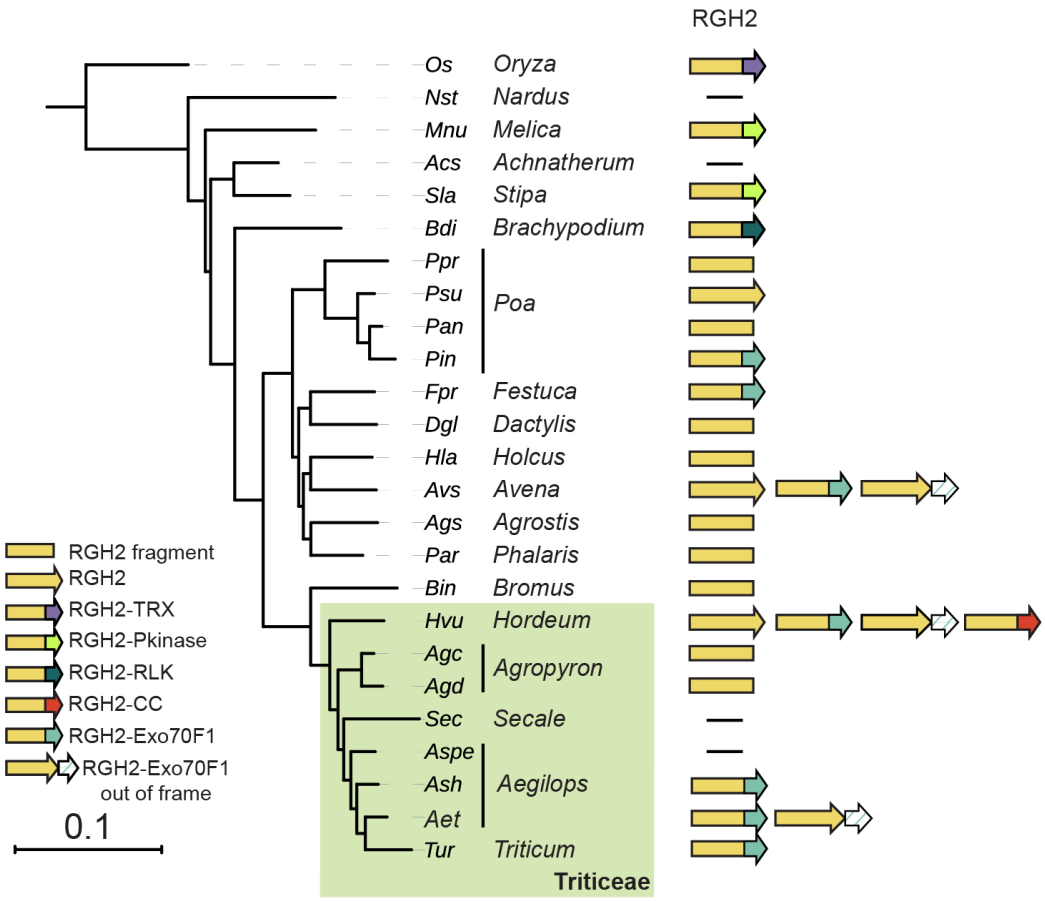

Figure 2-4. Integrated and non-integrated alleles of RGH2 are maintained in Triticeae and Poeae species.

The species maximum likelihood phylogenetic tree was generated using 1,263 universal single copy orthologs identified during BUSCO assessment of genome and transcriptome assembly, using rice as an outgroup species. The shaded green box indicates members of the Triticeae tribe. On the *right-hand side*, identified allelic variants of RGH2 in integrated domain status are shown as arrows with thioredoxin (TRX; purple), protein kinase (Pkinase; green), and receptor-like kinase (RLK; teal) integrations in non-Triticeae/Poeae species, and Exo70F1 (turquoise) and CC/ NB-LRR (red) integrations in Triticeae/Poeae species. Non-integrated RGH2 is shown as a solid yellow arrow, whereas fragmented RGH2 (unable to classify integration status) is shown as a rectangle. Out of frame Exo70F1 are shown as hashed arrows that are disjoint from RGH2.

prior to Poeae-Triticeae radiation dates this event at 24 Mya (CI: 18.4 to 29.8 Mya) (Leaché, 2009).

We hypothesized that after integration of *Exo70F1* into *RGH2*, integrated *Exo70F1* would subfunctionalize, in concert with *RGH2*, for pathogen recognition. Under this model, integrated *Exo70F1* would experience relaxed purifying selection compared to its non-integrated *Exo70F1* counterpart. To understand the degree of selection acting on all *Exo70* gene families, we estimated the ratio of nonsynonymous to synonymous mutations (d_N/d_S) for *Exo70* gene families from sequenced grass species. All grass *Exo70* gene families are under strong purifying selection (Appendix Table 7-3). d_N/d_S values (ω) ranged from 0.07 for *Exo70A1* and *Exo70D2* gene families to 0.55 for the *Exo70A4* gene family. To understand the impact on the molecular evolution of non-integrated and integrated *Exo70F1*, we performed branch-specific tests allowing for variable levels of selective pressure. Evidence of relaxed purifying selection was observed for the integrated *Exo70F1* clade (ω_a = 0.413; p<0.001), compared to stronger purifying selection for non-integrated domains of *Exo70F1* (ω_0 = 0.092) (Appendix Table 7-4, Figure 2-5). Evidence of relaxation in selective constraints supports the hypothesis that integration of *Exo70F1* releases this gene from strong purifying selection, whereas selection is preserved on endogenous *Exo70F1* (Cesari *et al*., 2014).

Integrated *Exo70F1* Evolves Independently of *RGH2*

We hypothesized that *RGH2* alleles have an altered evolutionary history following *Exo70F1* integration compared to non-integrated *RGH2* alleles. To investigate the potential co-evolution of *RGH2* and the integrated *Exo70F1*, we compared the topologies of *RGH1*, *RGH2*, and *RGH3* gene families and *Exo70F1* phylogenetic trees. All *RGH* gene families predominantly exhibit species specific grouping (Figure 2-6, Figure 2-7, Figure 2-8). Variation is seen in the domain structure of RGH2 homologs: the majority contain an Exo70F1 integration, however other domains such as coiled coil, receptor-like kinase (with lectin domains), thioredoxin and protein kinase are observed in orthologs outside of the Triticeae and Poeae tribes (Figure 2-4, Figure 2-7). The only exception was barley, where allelic variants include a CC and full-length NB-LRR from the *RGH1* gene family in place of *Exo70F1* (Figure 2-4;

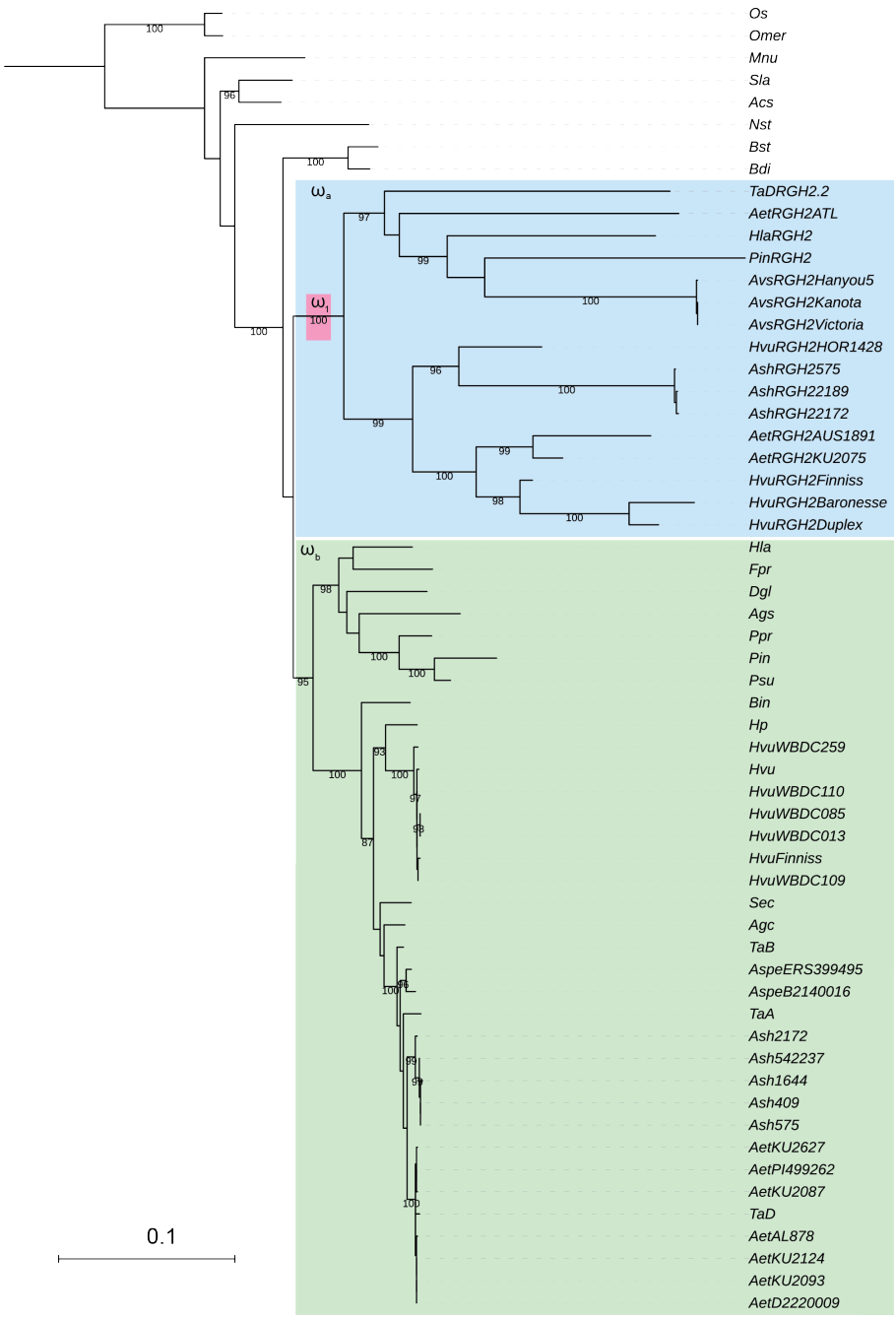

Figure 2-5. *Exo70F1* maximum likelihood phylogenetic tree used for molecular evolutionary analyses.

Branch and clade-based estimation of ω (d_N/d_S) are highlighted: ω_1 in pink, ω_a in blue, and ω_b in green (Appendix Table 7-4). Unit of distance is nucleotide substitutions per evaluated sites. Species abbreviations listed in Figure 2-3. *HvuRGH2Maritime* clusters with *HvuRGH2Baronesse* due to 100% similarity. Rice (*Os*; *LOC_Os01g69230.1*) and *O. meridionalis Exo70F1* were used as outgroup species.

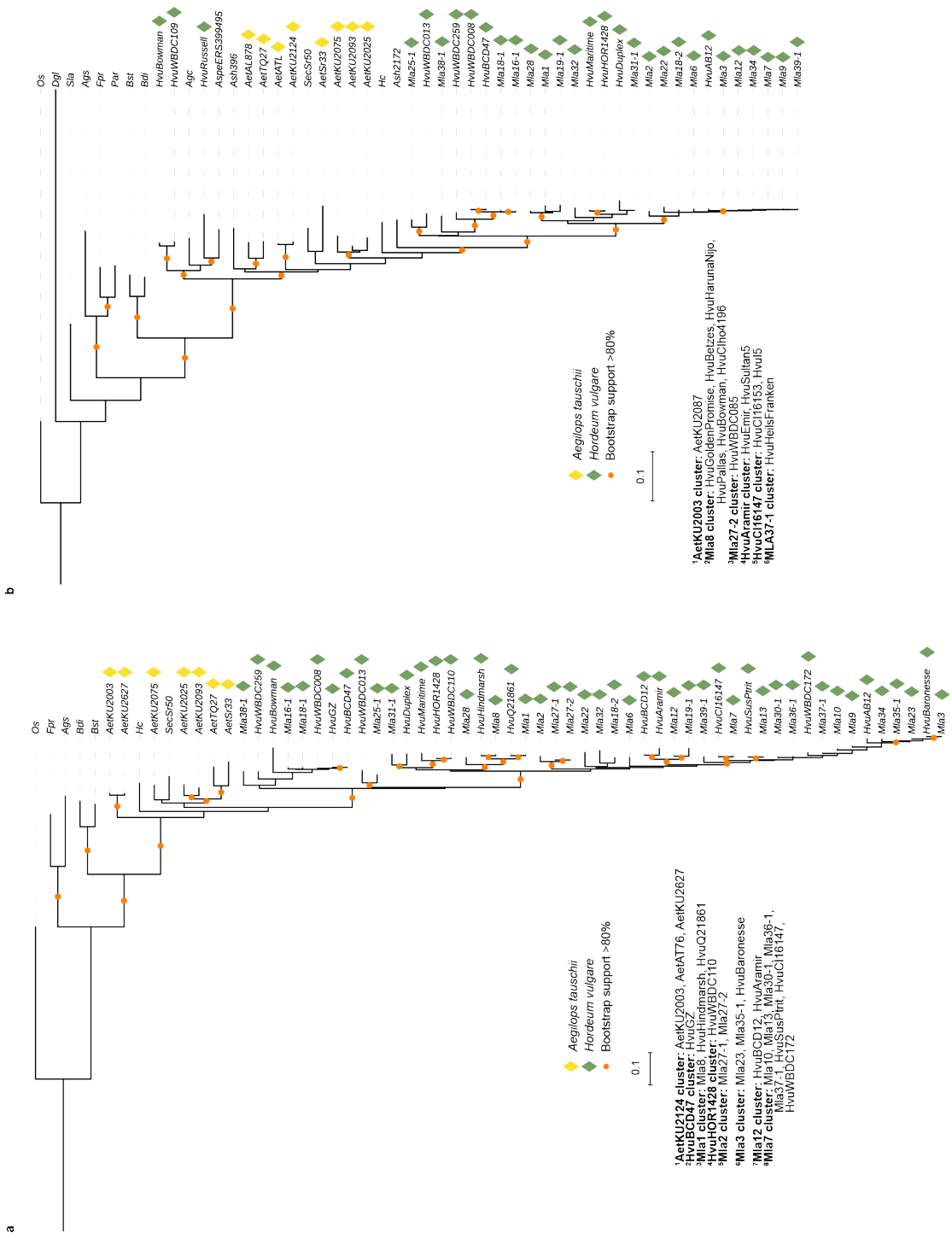

Figure 2-6. Maximum likelihood phylogenetic tree of *RGH1* homologs across the Poaceae.

Alignments and phylogenetic trees of full length (a) and NB domain analyses (b) were performed. Clusters of identical sequence are indicated by superscript numbers and indicated in the legend. Branch support was generated using 1,000 bootstraps for both phylogenetic trees, with orange dots designating support from 80-100%. Species abbreviations listed in Figure 2-3 and Appendix Table 7-1. Rice (*Os*; *LOC_Os11g43700.1*) used as an outgroup.

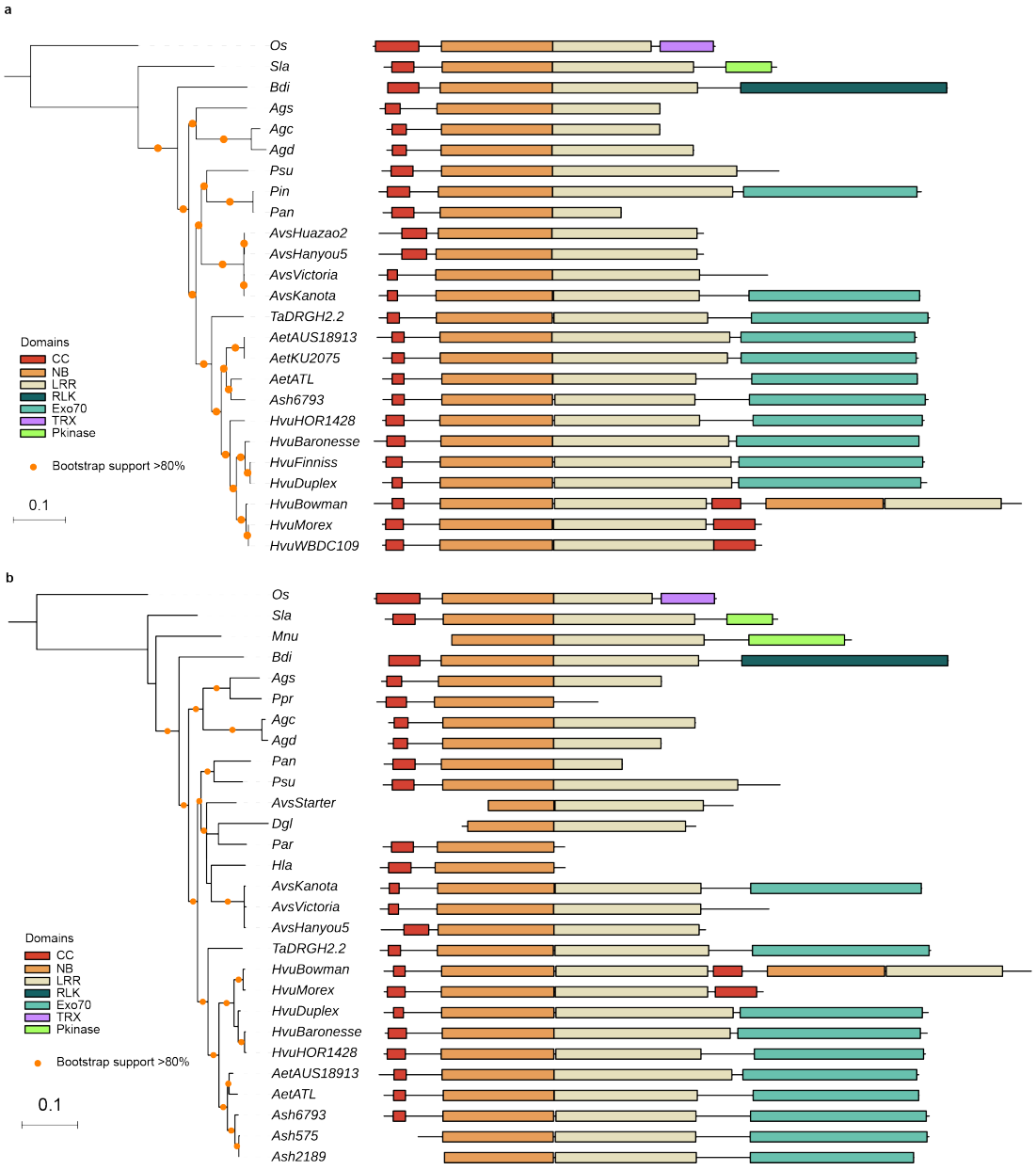

Figure 2-7. Maximum likelihood phylogenetic tree and domain structure of RGH2 homologs across the Poaceae.

Alignments and phylogenetic trees of full length (a) and NB domain analyses (b) were performed. RGH2 domain structure represented on the right. RGH2 from *Ae. tauschii* and *H. vulgare* indicated with yellow and green, respectively. *Avs*Victoria, *Avs*Huazao2, and *Avs*Hanyou5 integrated Exo70F1 are absent from domain structure due to early stop codons and frame-shift relative to RGH2. In addition to canonical domains (CC; red, NB; orange, LRR; cream), additional C-terminal integrated domains are observed in RGH2 alleles and include thioredoxin (TRX; purple), protein kinase (Pkinase; light green), lectin (teal) and Exo70 (cyan). Dashed lines represent fragmented ORFs (only observed for *Hla* RGH2). Branch support was generated using 1,000 bootstraps, with orange dots designating support from 80-100%. Species abbreviations listed in Figure 2-3 and Appendix Table 7-1. Rice (Os; AK071926 (=LOC_Os12g18360.2)) used as an outgroup.

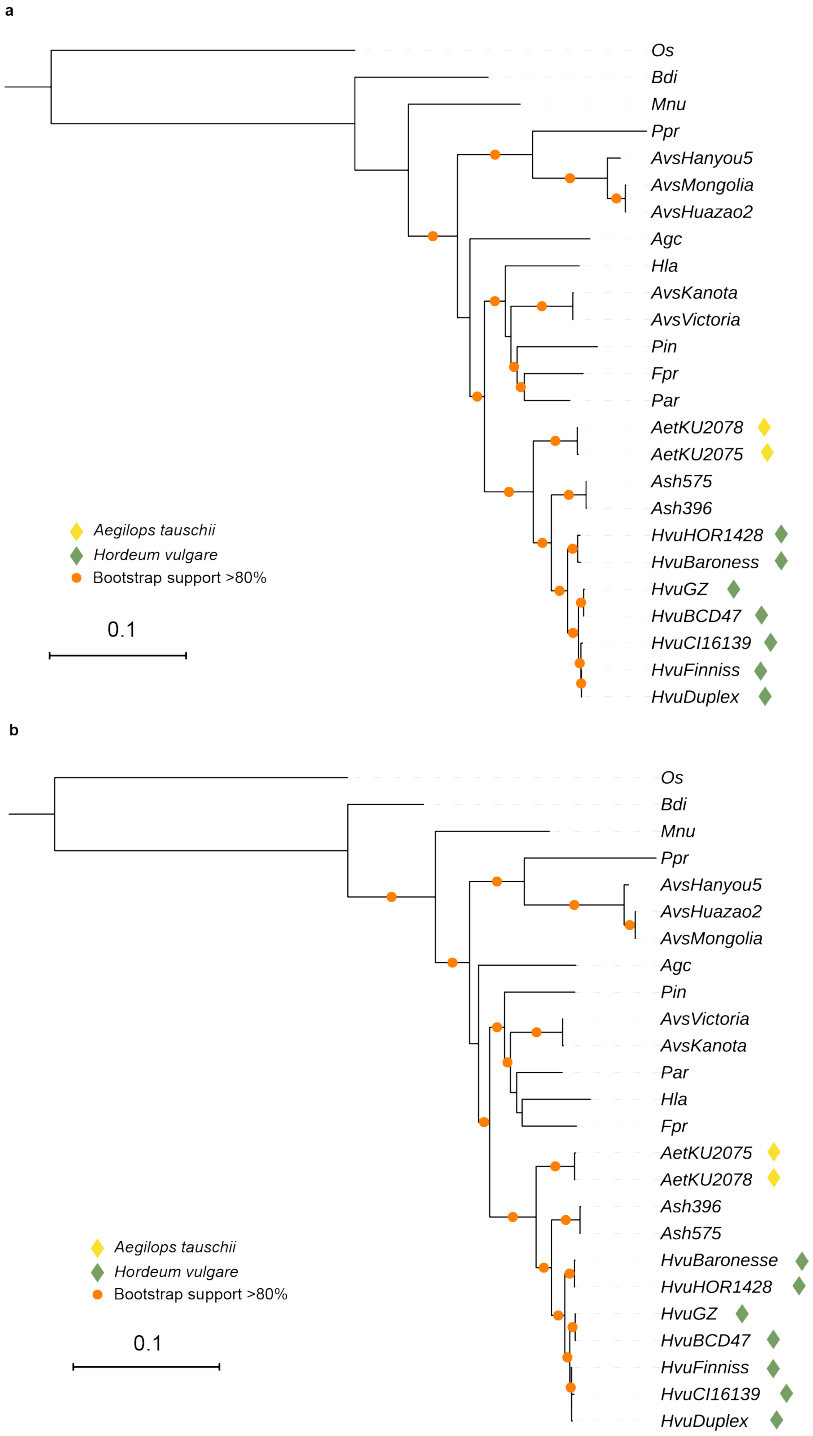

Figure 2-8. Maximum likelihood phylogenetic tree of RGH3 homologs across the Poaceae.

Alignments and phylogenetic trees of full length (a) and NB domain analyses (b) were performed. *RGH3* from *Ae. tauschii* and *H. vulgare* indicated with yellow and green highlighting respectively. Branch support was generated using 3,000 and 10,000 bootstraps for *RGH3* full length and NB domain, respectively, with orange dots designating support from 80-100%. Species abbreviations listed in Figure 2-3 and Appendix Table 7-1. Rice (*Os*; *LOC_Os12g18374.1*) used as an outgroup.

Figure 2-7). *RGH2* belongs to the NB-LRR clade MIC1 whose members are known to contain diverse integrated domains (Bailey *et al*., 2018). Our results suggest that MIC1 clade members identified without integrated domains in sequenced species may have intraspecific variants with integrated domains, such as *RGH2*.

Integrated *Exo70F1* have a distinct evolutionary history compared to their non-integrated counterparts. The integrated *Exo70F1* clade follows the species phylogeny, with two major subclades containing the *Aegilops* and barley alleles, and the other comprising wheat, *Phalaris arundinacea, Holcus lanatus*, and oat (Figure 2-3). Exceptions include alleles derived from accessions *AetATL, HvuHOR1428,* and *TaD*, the latter derived from the D subgenome of wheat (Figure 2-3). This observation suggests that either multiple alleles of *RGH2-Exo70F1* are preserved during speciation events or convergent processes constrain the evolvability of integrated *Exo70F1*. In contrast, integrated and non-integrated forms of *RGH2* do not show the same clade distinction; therefore, integrated status has not substantially altered the evolutionary trajectory of *RGH2*, nor has significant co-evolution occurred (Figure 2-7).

2.4 Discussion

The majority of genetic diversity is neutral or slightly deleterious; yet within populations, certain polymorphisms are maintained where selection favours advantageous genetic variation. During speciation events, these loci can be preserved when balancing selection conserves diverse allelic variants. Such balanced polymorphisms are only maintained if selection can prevent allele fixation and overcome genetic drift or selective sweeps. Extant species can contain allelic variation which transcends the lifetime of the species and is shared with sister taxa and evolutionary ancestors: creating *trans*-species polymorphisms. Classic well-studied examples include the major histocompatibility locus (MHC) in vertebrates (Klein *et al*., 2007), histo-blood groups in primates (Ségurel *et al*., 2013), mating compatibility of filamentous fungi (Brown and Casselton, 2001; Glass and Kaneko, 2003; Wu *et al*., 1998), and plant self-incompatibility (SI) systems (Nasrallah, 2017, 2002). These known loci are involved in self and non-self recognition mechanisms, which are pivotal to life processes such as sexual reproduction and immunity. While self-recognition systems such as SI loci are limited by single receptor-ligand binding

models, genes involved in non-self recognition systems with multiple-receptor ligands and multiple-ligand receptors experience diversifying selection and intraspecific polymorphisms. Plant resistance genes are known to experience high levels of allelic diversity, yet our understanding of deep evolutionary history has been limited.

Recognition of plant pathogens is mediated by membrane and cytoplasmic immune receptors that recognise pathogen-derived molecules, including effectors (Jones and Dangl, 2006). Cytoplasmic immune receptors recognise secreted pathogen effectors directly, or indirectly through monitoring the molecular status of host proteins targeted by pathogen effectors (Jones *et al*., 2016). At the population level, plant immunity to pathogens is conferred, in part, through the maintenance of diverse allelic variants at immune receptor loci. Pathogen pressure influences the relative frequency of resistance alleles in plant populations, with selection fluctuating due to pathogen evolution. Mutations that generate novel approaches to manipulate a host by immune suppression or nutrient acquisition, for example, are selected for in the pathogen. Similarly, novel forms of pathogen recognition are selected for in the plant. A recent area of intensive research in plant immunity includes the identification of integrated non-canonical domains in NB-LRRs, which are thought to serve as baits for pathogen effectors, and thus, facilitate efficient immune responses (Cesari, 2018; Kroj *et al*., 2016; Sarris *et al*., 2016). It is hypothesised that integrated domains are released from purifying selection for host function and are free to adapt specifically for pathogen recognition (Cesari, 2018).

Here, we observe the integration of *Exo70F1* within the NB-LRR encoding gene *RGH2* at the *Mla* locus in barley has been maintained as a *trans*-species polymorphism in the Triticeae and Poeae tribes for over 24 million years. Exo70 is one of the eight subunits comprising the exocyst complex, a crucial component of the exocytosis pathway which mediates the active transport of molecules out of the cell. The exocyst complex is involved in the tethering of post-Golgi secretory vesicles to the plasma membrane prior to SNARE complex-mediated membrane fusion (He *et al*., 2007; Heider and Munson, 2012; Synek *et al*., 2006). In plant genomes, the core exocyst subunits of Sec3, Sec5, Sec6, Sec8 and Sec10 are retained in few or single copies, whereas Exo70 has experienced dramatic proliferation into multiple gene families (Cvrčková *et al*., 2012). Diversification is characteristic of sub-functionalization or

neo-functionalization (Lynch and Conery, 2000) and Exo70 genes are involved in diverse roles in morphogenesis (Heider and Munson, 2012), development (Sekereš *et al*., 2017), and immunity (Gu *et al*., 2017). Cvrčková *et al.* (2012) comprehensively described members of the exocyst complex throughout land plants using representative species from both monocots and dicots and observed considerable expansion of the grass Exo70F and FX clades (Cvrčková *et al*., 2012), similar to findings reported here. Members of *Exo70F* and *Exo70FX* gene families are known to have a role in immunity: barley *EXO70F-like* (*ExoFX11b.a*) is essential for full penetration resistance to *B. graminis* f. sp. *hordei* (Ostertag *et al*., 2013), and rice Exo70F3 binds the *Pyricularia oryzae* effector AVR-Pii; this interaction is essential for *Pii* (NB-LRR) mediated resistance (Fujisaki *et al*., 2015). The integration of *Exo70F1* in *RGH2* suggests a potential role in immunity either through localisation of the NB-LRR or as a decoy for effector recognition.

Until now, it was unclear how selective forces in the plant-pathogen interaction influence the preservation of diverse alleles through plant speciation events because previous evolutionary analyses were limited by high rates of intraspecific and interspecific variation of NB-LRRs. In plants, previous work established time scales of long-term maintenance of polymorphic sites in stress response genes between *A. thaliana* and *Capsella rubella* (Q. Wu *et al*., 2017) over 5 Mya, in immunity genes in *Capsella* species (Koenig *et al*., 2019), and presence/absence polymorphisms in *RPS5* in *A. thaliana* due to long-term balancing selection (Karasov *et al*., 2014) over 2 Mya. Here, we have used the integrated *Exo70F1* domain within *RGH2* as an evolutionary footprint to track the history of the *Mla* locus through speciation of the grasses. We observed both integrated and non-integrated forms of *RGH2*, as well as absence of *RGH2*, in species of Triticeae and Poeae. This establishes a *trans*-species polymorphism originating 24 Mya (Leaché, 2009) and maintained to present day (Figure 2-4). Long-lasting *trans*-species polymorphisms are maintained through balancing selection, as in its absence, mutations within a population are either lost, achieve fixation, or exist in a frequency-dependent manner (Klein *et al*., 1998). Based on the allelic diversity we observe today in extant species, we can infer the evolutionary history of *RGH2-Exo70F1* (Figure 2-9). We hypothesise that an ancient

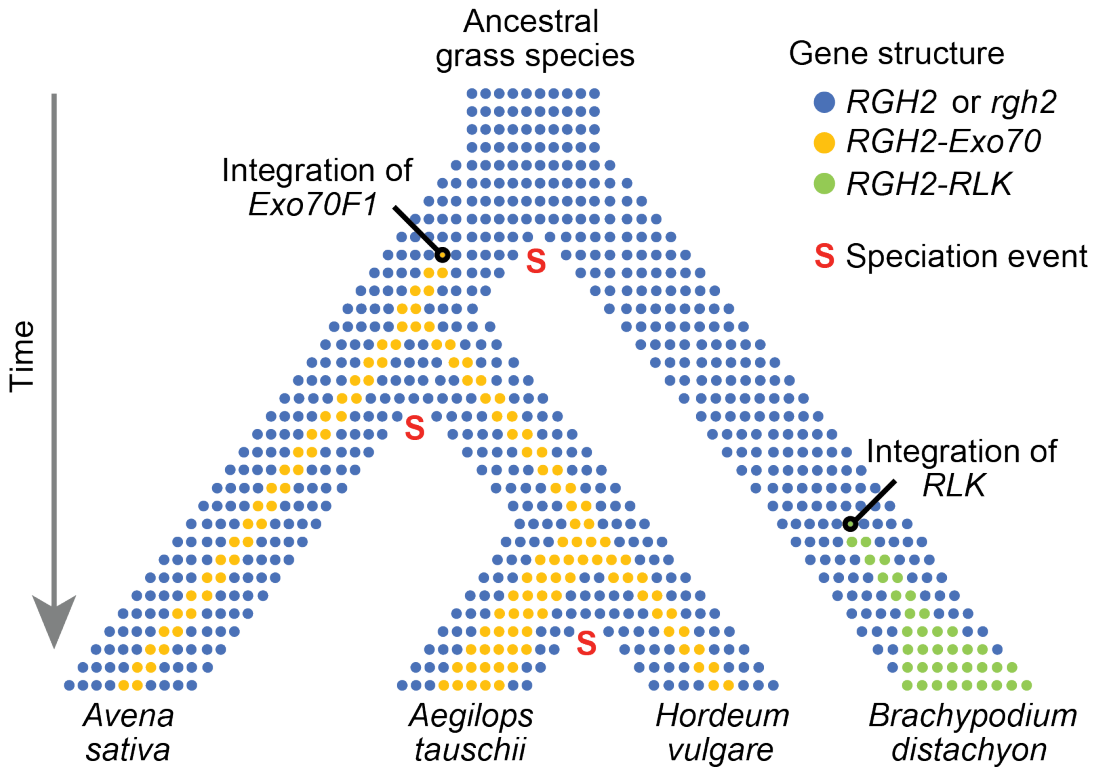

Figure 2-9. Evolutionary model of *RGH2*.

Reconstitution of the evolutionary history of the *RGH2* alleles through time. Allelic pools of *RGH2* within a population indicated by the horizontal row of dots. Alleles of *RGH2* include the non-integrated *RGH2* or *rgh2* (blue) and integrated forms: *RGH2-Exo70F1* (yellow) and *RGH2-RLK* (green). Speciation events (red S) give rise to distinct populations and *RGH2* allelic pools. Evolutionary time indicated by the grey arrow on the *left-hand side* with modern extant species indicated at the *bottom* of the model (*A. sativa, A. tauschii, H. vulgare, B. distachyon*).

gene fusion event of an *RGH2* allele with the non-integrated *Exo70F1* was subsequently retained in an ancestral grass population (Figure 2-9). The diverse *RGH2* allelic pool was maintained during the evolution of the grasses and through speciation events, as balancing selection favoured immune receptor variation beneficial against both extinct and extant pathogen species. In oat, we observed integrated *RGH2-Exo70F1* and several alleles with interrupted open reading frames of *RGH2* and *Exo70F1*. This indicates that selection is required to maintain the *RGH2-Exo70F1* gene fusion. The diversity of *RGH2* alleles identified in barley was likely due to substantial sampling (40 accessions). Sequencing of more accessions in other species would likely reveal a similar observation. Using genomes and transcriptomes from species across the Poaceae, we have unravelled the evolutionary history of a shared integrated NB-LRR within the grasses and shown that allelic diversity is present as a *trans*-species polymorphism at *Mla*. The association of the *Mla* locus with multiple pathogen recognition (Inukai *et al*., 2006) emphasises the impact of diverse pathogen populations on the evolutionary forces shaping immune receptor diversity in the Poaceae.

2.5 Materials and methods

Plant material

A full inventory of plant species and acronyms used in this study are available in (Appendix Table 7-1).

RNAseq and de novo *assembly*

First and second leaf tissue was harvested at 10 days after sowing of barley and oat accessions grown in the greenhouse. Tissue was flash frozen in liquid nitrogen and stored at -80 °C. Tissue were homogenized into a fine powder in liquid nitrogen-chilled pestle and mortars. RNA was extracted, purified, and quality assessed as described by Dawson *et al.* (2016) (Dawson *et al*., 2016). RNA libraries were constructed using Illumina TruSeq RNA library preparation (Illumina; RS-122-2001). Barcoded libraries were sequenced using either 100 or 150 bp paired-end reads. Library preparation and sequencing was performed at either the Earlham Institute (Norwich, United Kingdom) or BGI (Shenzhen, China). Quality of all RNAseq data was assessed using FastQC (Andrews, 2010) (0.11.5). Trinity (Grabherr *et al*., 2011) (2.4.0) was used to assemble *de novo* transcriptomes using default parameters and Trimmomatic (Bolger *et al*., 2014) for read trimming. *Exo70F1*, *RGH1*, *RGH2*, and *RGH3* were identified in *de novo* assemblies using BLAST+ (v2.2.9) (Camacho *et al*., 2009).

Development of the barley and oat sequence capture

The barley capture library TSLMMHV1 is composed of 99,421 100 mer baits with 2x coverage over the target space. Targeted sequences include repeat masked *Mla* locus from Morex (Wei *et al*., 2002), all cloned alleles of *Mla* (Halterman *et al*., 2001; Halterman and Wise, 2004; Seeholzer *et al*., 2010; Shen *et al*., 2003; Zhou *et al*., 2001), the *Mlo* locus (Büschges *et al*., 1997), the *Rpg1* locus (Brueggeman *et al*., 2002), and the *rpg4*/*Rpg5* locus (Brueggeman *et al*., 2008). In addition, the capture library targets the barley NB-LRR gene space identified in genomic sequence from barley accessions Barke, Bowman, and Morex, full length cDNA derived from barley accession Haruna Nijo, and transcriptomes of barley accessions Abed Binder 12, Baronesse, CI 16153, CIho 4196, Manchuria, Pallas, Russell, and SusPtrit. The capture library TSLMMAS1 is composed of 29,672 100 mer baits with 2x coverage

over the target space. Targeted sequences include NB-LRR containing contigs from *de novo* assembled transcriptomes of oat accessions Kanota and Victoria.

For both libraries, NB-LRR gene space was identified using the following approach. For transcriptomes, TransDecoder (Haas *et al*., 2013) (v4.1.0) was used to identify and translate ORFs. Using a similar strategy as Jupe *et al*. (2012) (Jupe *et al*., 2013), we developed a motif set using MEME (Bailey *et al*., 2009) trained on a random randomized proportional sample of NB-LRR (J. Li *et al*., 2010; Tan and Wu, 2012) from rice (N=35) and *B. distachyon* (N=17). The MEME motifs spanned the CC domain (motifs 4, 11, 13, and 15), NB domain (motifs 1, 2, 3, 5, 6, 7, 8, 10, 12, and 14), and the LRR domain (motifs 19, 9, 20, 16, 17, and 18) . All the identified motifs in the NB are similar to those previously defined by Meyers *et al*. (2003) (Meyers *et al*., 2003) in *A. thaliana*. A MAST significance threshold of 1e-20 was selected based on its ability to identify all annotated NB-LRRs within *B. distachyon* and rice. For barley whole genome shotgun assemblies, all six ORFs were translated for each contig and concatenated into a single peptide sequence for the forward and reverse strand. Translated genomic contigs were scanned using FIMO, which assesses all twenty MEME-generated motifs independently. Contigs were included in the capture if one of two conditions were met: (1) at least one CC and two NB motifs were present or (2) at least two NB and one LRR motifs are present in the translated sequence strand.

Next, redundancy within the sequence capture template was removed. We fragmented the input data set into 100 bp fragments with a scanning window of 25 bp and performed BLASTn onto the entire data set. Any sequence found to have identity of 95% or higher was considered redundant other than the original site. The first occurrence of the sequence would be retained and the others were masked. While this approach removes redundancy in the data set, the inclusion of extensive genomic sequence will introduce repetitive sequence that can produce competition in the sequence capture due to the high copy number of repetitive sequence in the barley genome. Therefore, two approaches were used to remove repetitive sequence in the sequence capture design. All loci were repeat masked based using RepeatMasker (Smit *et al*., 2013-2015) (v4.0.5) using default and Triticeae-specific repeat databases. As repeat databases are not complete, we applied genomic masking of the capture design. To do so, we fragmented the input data set into 100 bp fragments with a

scanning window of 50 bp and performed BLAST onto the barley Morex WGS assembly. A threshold of eight or fewer copies was found selected to balance between copy number variation within NB-LRRs and avoiding the inclusion of repetitive sequence.

DNA extraction and sequencing library preparation

Total genomic DNA was extracted from leaf tissue according to a CTAB method (Stewart and Via, 1993). In brief, 3 g of leaf tissue were ground on liquid N_2 and homogenized with 20 mL of CTAB extraction buffer (2% CTAB, 100 mM Tris-HCl pH8.0, 20 mM EDTA pH8.0, 1.4 M NaCl, 1% β-Mercaptoethanol). Samples were incubated for 30 min at 65°C followed by two chloroform extractions and ethanol precipitation. DNA was then resuspended in 1x TE, 50 µg/mL RNase A solution and incubated for 1 h at 37°C. DNA was subsequently precipitated with 2.5 volumes of ice-cold 95% ethanol and resuspended in 1x TE. Quantification of DNA samples was performed using a Nanodrop spectrophotometer (Thermo Scientific) and the Qubit dsDNA HS Assay Kit (Molecular Probes, Life Technologies). DNA samples were normalized to 3 µg and sheared to an average length of 3-4 kb using a Covaris S2 sonicator with the following settings: Duty Cycle 20%, Intensity 1, Cycle Burst 1000, Time 600 s, Sample volume 200 µL. After sonication, a small aliquot was assayed by gel electrophoresis and additional size selection was carried out using 0.4x Agencourt AMPure XP beads (Beckman Coulter Genomics). Samples were then end repaired followed by 3'dA addition using the NEBNext Ultra DNA Library Prep Kit for Illumina (New England Biolabs). Illumina sequencing adapters were ligated onto the ends and following purification with AMPure XP beads, the DNA was PCR amplified (8 cycles) using indexed PCR primers (NEBNext Multiplex Oligos for Illumina, New England Biolabs) and the Illumina PE1.0 PCR primer. After purification using AMPure XP beads, quality assays were performed with a Bioanalyzer DNA 1000 chip (Agilent) and the Qubit dsDNA assay to determine the average fragment sizes and concentrations.

Target enrichment and sequencing

Enrichment and sequencing was carried out as described by Witek *et al.* (2016) (Witek *et al*., 2016). Briefly, DNA sequencing libraries was enriched according to the

MYbaits protocol (MYbaits User Manual version 2.3.1) and using MYbaits reagents (MYcroarray). Briefly, 500 ng of the prepped library was hybridized in hybridization buffer (10x SSPE, 10X Denhardt's solution, 10 mM EDTA, 0.2% SDS) to the biotinylated RNA baits for 20 h at 65°C on a thermocycler. After hybridization bound DNA was recovered using magnetic streptavidin-coated beads as follows: the hybridization mix was added to 30 µL Dynabeads MyOne Streptavidin C1 (Invitrogen, Life Technologies) that had been washed 3 times and resuspended in binding buffer (1 M NaCl; 10 mM Tris-HCl, pH 7.5; 1 mM EDTA). After 30 m at 65°C, beads were pulled down and washed three times at 65°C for 10 m with 0.02% SSC/0.1% SDS followed by resuspension in 30 µL of nuclease-free water. Library was then PCR amplified (26 cycles) using Kapa HiFi HotStart Ready Mix (Kapa Biosystems) and Illumina P5 and P7 primers. The amplified library was size fractionated with the Sage Scientific Electrophoretic Lateral Fractionator (SageELF, Sage Science) using a 0.75% SageELF agarose gel cassette. Fractions with size distribution between 3 and 4 kb were pooled and purified with AMPure PB beads (Pacific Biosciences). Then, library was assembled for PacBio sequencing using the SMRTbell Template Prep Kit 1.0 (Pacific Biosciences) according the 2-kb Template Preparation and Sequencing protocol (www.pacificbiosciences.com/support/pubmap/documentation.html). PacBio RSII sequencing using C4-P6 chemistry was performed at the Earlham Institute (Norwich, UK), using four SMRT cells for each barley accession Baronesse and oat accession Victoria.

PacBio assembly

PacBio circular consensus reads with at least three passes were used for genome assembly. Reads were trimmed to remove the adapter sequence (first and last 70 bp) and size selected to reads less than 4kb. We used Geneious (Kearse *et al*., 2012) (v10.2.3) De Novo Assembly with the following Custom Sensitivity parameters for assembly: don't merge variants with coverage over approximately 6, merge homopolymer variants, allow gaps up to a maximum of 15% gaps per read, word length of 14, minimum overlap of 250 bp, ignore words repeated more than 200 times, 5% maximum mismatches per read, maximum gap size of 2, minimum overlap identity of 90%, index word length 12, reanalyze threshold of 8, and maximum ambiguity of 4.

Phylogenetic analyses

Exo70 coding and protein sequences were accessed from Department of Energy-Joint Genome Institute Phytozome database (https://phytozome.jgi.doe.gov), *A. thaliana* gene sequence was accessed from TAIR (www.arabidopsis.org), and barley *Exo70* gene families from the recently updated 2017 genome (Mascher *et al*., 2017). Substantial curation of the barley *Exo70* gene family was required and incorporated gene models from the 2012 genome (IBGSC *et al*., 2012). Outgroups for complete Exo70, Exo70F, and *Exo70F1* phylogenetic trees were *Saccharomyces cerevisiae* Exo70 protein (YJL085W), *A. thaliana* Exo70F1 protein (AT5G50380), and *O. sativa Exo70F1* (*Os01g69230.1*), respectively. MUSCLE (Edgar, 2004) (v3.8.31) and PRANK (Löytynoja, 2014) (v.140603) were used for protein and codon-based sequence alignment using default parameters, respectively. Curation of the multiple sequence alignment for complete Exo70 and Exo70F gene family was used to remove sequences with less than 40% of the breadth of the alignment and to remove positions with more than 60% missing data. Gene families were identified based on bootstrap support in the phylogenetic tree (Figure 2-2A), incorporating a previous annotation performed on the *Exo70* gene family (Cvrčková *et al*., 2012) (Appendix Table 7-5). We required that 90% sequence coverage for inclusion in the *Exo70F1* phylogenetic tree. RAxML (Stamatakis *et al*., 2005) (v8.2.9) was used for phylogenetic tree construction using the PROTGAMMAJTT and GTRCAT models for protein and coding sequence alignment, respectively. Bootstrap support was determined for all phylogenetic trees, using a convergence test to confirm sufficient sampling.

Exo70F1 homologs were identified from diverse Poales species (McKain *et al*., 2016) using BLAST+ (Appendix Table 7-1 Table 7-5, Brabham *et al*., 2018). The only species found without a non-integrated *Exo70F1* was *H. lanatus*. Alignment of *H. lanatus* RNAseq reads to *Dactylis glomerata Exo70F1* and *de novo* assembly using Geneious was used to reconstruct *H. lanatus Exo70F1*. Multiple sequence alignment and phylogenetic analysis of *Exo70F* gene families was used to establish *Exo70F1* orthology (Appendix Figure 7-1). The site of sequence conservation between integrated and non-integrated *Exo70F1* was determined based on codon-based sequence alignment.

The species phylogenetic tree was generated using universal single copy orthologs identified during BUSCO assessment of genome and transcriptome assembly (Simão *et al*., 2015; Waterhouse *et al*., 2018). A total of 1,263 genes were identified, aligned using PRANK (v.140603) with codon-based sequence alignment using default parameters. Genes were concatenated and subjected to maximum likelihood phylogenetic tree construction. The bioinformatic pipeline can be found on the GitHub repository https://github.com/matthewmoscou/QKbusco (v1.0).

Molecular evolutionary analyses

Molecular evolutionary analyses were performed with PAML (Yang, 2007) (v4.8) *codeml*. The F3x4 codon frequency model was used for all analyses. Codon-based sequence alignment using PRANK, phylogenetic analysis using RAxML, and codeml were used to estimate ω (d_N/d_S) for all Exo70 gene families (Appendix Table 7-3). For molecular evolutionary analyses of the non-integrated and integrated *Exo70F1* gene family, four hypotheses were tested: H_0: a single rate of ω_0 across the entire tree, H_1: a different rate of ω_1 for the initial branch of the integrated *Exo70F1*, H_2: a different rate of ω_a for integrated *Exo70F1* compared to non-integrated *Exo70F1* (ω_0), and H_3: three different rates of ω: ω_0, non-integrated *Exo70F1* outside of the Poeae and Triticeae, ω_a, integrated Exo70F1, and ω_b, non-integrated *Exo70F1* from the Poeae and Triticeae (Figure 2-5, Appendix Table 7-4).

Data

All high-throughput sequencing data, *de novo* transcriptome assemblies, and *de novo* assembly of the NB-LRR gene space of barley and oat are deposited in the NCBI BioProject PRJNA378334, PRJNA378723, PRJNA422803, and PRJNA422986. *De novo* transcriptome assemblies for publically available RNAseq data, multiple sequence alignments, and phylogenetic trees in Newick format are available from figshare (https://figshare.com). Scripts, analysis pipeline, and details associated with *Exo70* gene family curation can be found on the GitHub repository https://github.com/matthewmoscou/Exo70 (v1.0).

2.6 Author Contributions

Conceived and designed the experiments: H.J.B., J.L., and M.J.M. Performed transcriptome sequencing and sequence capture: I.H-P. Performed bioinformatic analyses: H.J.B., S.H., and M.J.M. Analysed the data: H.J.B., S.H., J.L., and M.J.M.

3 *Mla3*, *Rmo1*, and *Lov1* are in complete genetic coupling

3.1 Abstract

The ability to resolve the potential for multiple-pathogen recognition specificities is severely limited when disease resistance QTLs overlap in the genome. This requires fine-mapping at the desired locus associated with disease phenotype. The *Mla* locus has over 30 described alleles conferring isolate-specific resistance to *Blumeria graminis* f. sp. *hordei* (powdery mildew), contains three NB-LRR encoding gene families (*RGH1*, *RGH2*, and *RGH3*), and is associated with resistance to multiple pathogens including *Puccinia striiformis* f. sp. *tritici* (wheat stripe rust; *Rps7*) and *Pyricularia oryzae* (rice blast; *Rmo1*). In addition, sensitivity to the *B. victoriae* toxin victorin (*Lov1*) has been mapped near the *Mla* locus. We performed a high-resolution recombination screen and found *Mla3* and *Rmo1* to be in complete coupling. Furthermore, *Lov1* was also found to be in complete genetic coupling with *Mla3* and *Rmo1*. Using sequence capture and RNAseq, we discovered that all three NB-LRR gene families—*RGH1* (*Mla*), *RGH2-Exo70F1*, *RGH3*—are expressed and are all potential candidate genes. Taking advantage of existing genetic resources of an *Mla* introgression panel and association genetics, we identify *Mla3* as the primary candidate for *Rmo1* and *Lov1*.

3.2 Introduction

The majority of plant *R* genes operate in a gene-for-gene manner recognising a single effector gene in the pathogen—or even more specifically a single effector gene in a single isolate of a pathogen. Few *R* genes have been shown to recognise multiple plant pathogens. The largest class of *R* genes encode nucleotide-binding, leucine-rich repeat (NB-LRR) proteins which initiate a defence response upon recognition of pathogen infection (Jones *et al*., 2016; Jones and Dangl, 2006). Direct recognition of pathogen effectors is hypothesised to limit the potential for multiple-pathogen recognition, due

to the reliance on conserved effectors or shared structural features. As plant genomes encode a finite number of immune receptors, maintaining resistance to the majority of pathogens is challenging. Indirect recognition by *R* genes, or the guarding of plant proteins, has the potential to expand recognition capacity and distances the requirement to sustain recognition of fast-evolving pathogen effectors.

The clustering of plant resistance genes is well known (Michelmore and Meyers, 1998; van Wersch and Li, 2019) and has been observed in rice (Wisser *et al*., 2005), barley (Bailey *et al*., 2018; Muñoz-Amatriaín *et al*., 2013; Schweizer *et al*., 2011), and *Arabidopsis thaliana* (Meyers *et al*., 2003). The observation of overlapping QTL in the genome highlight potential 'hotspots' of *R* gene loci. However, use of different mapping populations and haplotype-specific markers limit the resolution of these regions and their potential contribution to multiple pathogen recognition specificities. The short arm of chromosome 1H of barley has been associated with resistance to multiple pathogens, with multiple co-localising genes and QTLs against *Blumeria graminis* f. sp. *hordei* (*Bgh*)*, Puccinia striiformis* f. sp*. hordei*, *B. sativus*, *Puccinia striiformis* f. sp. *tritici* (Leng et al., 2018; Roy et al., 2010; Schweizer et al., 2011). This region includes the *Mla* locus of barley which is known to contain three coiled-coil NB-LRR (CC-NB-LRR) gene families (Wei *et al*., 2002, 1999). Allelic variants of the *Mla* CC-NB-LRR gene (*RGH1*) confer isolate-specific immunity against the host pathogen barley powdery mildew *Bgh* (Halterman *et al*., 2001; Halterman and Wise, 2004; Seeholzer *et al*., 2010; Shen *et al*., 2003; Zhou *et al*., 2001). While other loci have been mapped that confer resistance to powdery mildew, only the *Mla* locus displays extreme functional diversification present as an allelic series across diverse barley haplotypes (Jørgensen, 1994; Seeholzer *et al*., 2010).

Resistance to *Pyricularia oryzae* (teleomorph *Magnaporthe oryzae*) in barley (*Rmo1*; *Resistance to* Magnaporthe oryzae*1*) has been mapped to the *Mla* locus (Inukai *et al*., 2006). *Rmo1* was resolved to 3.0 cM within the 95% confidence interval (Inukai *et al*., 2006). *P. oryzae* is the causal agent of the rice blast and, despite the disease being named after the most common host, *P. oryzae* is known to infect over 50 cultivated and wild monocot plant species (Gladieux *et al*., 2018). Blast epidemics in barley have been previously reported in Japan and northern Thailand (Kawai *et al*., 1979; Matsumoto and Mogi, 1979; Sato *et al*., 2001), and isolates collected on barley and

rice form a monophyletic clade (Gladieux *et al*., 2018). Resistance to *P. oryzae* is highly polymorphic across barley accessions (Nga *et al*., 2012). Previous isolate-specific and partial seedling resistance QTLs have been mapped across chromosomes 3H, 4H, and 5H, with the 4H QTL co-localising with previously mapped loci conferring resistance to stem rust (*Puccinia graminis*), scald (*Rhynchosporium secalis*), and net blotch (*Phyrenophora teres*) (Sato *et al*., 2001). Resistance QTLs were donated from barley cv. TR306: a Canadian accession from a region devoid of blast disease (Sato *et al*., 2001). With recent epidemics of wheat blast in Bangladesh (Islam *et al*., 2016), and historical and recent evidence of host jumps through loss of effector genes (Inoue *et al*., 2017), understanding resistance that limits host range across grasses is crucial.

Despite extensive use in breeding for resistance to biotrophic pathogens, NB-LRRs are also targets of necrotrophic effectors and can act as susceptibility factors. Necrotrophic pathogens thrive on host dead tissue, actively secreting phytotoxic secondary metabolites, peptides, and reactive oxygen species (ROS) to induce host tissue degradation. Necrotrophic pathogens can have a broad host range, such as the moulds *Botrytis cinerea*, *Monilinia fructicola*, and *Sclerotinia sclerotiorum* and leaf spot *Alternaria brassicicola* (Glazebrook, 2005; Horbach *et al*., 2011; van Kan, 2006; Wang *et al*., 2014); whereas others have narrow host range, requiring the production and secretion of a host-selective toxin (HST) for virulence. Necrotrophic effectors and HSTs can be proteinaceous or small metabolites and are defined as HSTs if host sensitivity to toxin production defines the host range of these pathogens (Friesen *et al*., 2008; Wang *et al*., 2014; Wolpert *et al*., 2002).

During the 1940s, breeding of "Victoria-type" oats (*Avena sativa*) for oat crown rust (*Puccinia coronata*) resistance unwittingly facilitated a host jump of the necrotrophic pathogen *B. victoriae* and the corresponding Victoria blight disease from timothy-grass (*Phleum pratense*) (Meehan and Murphy, 1946). *B. victoriae* is a nectrotroph and its pathogenesis is dependent on host sensitivity to the HST victorin (Wolpert *et al*., 2002; Walton 1996). The newly introgressed *Pc2* oat crown rust resistance also introgressed sensitivity to victorin (*Vb*). Insensitive mutants of *Vb* also exhibit susceptibility to *P. coronata* (Mayama *et al*., 1995). Sweat *et al*., (2008), identified natural variation for sensitivity to victorin in *Arabidopsis thaliana*, and several plant

species exhibit degrees of victorin sensitivity including oat, rice, *Brachypodium*, common bean (*Phaseolus vulgaris*), and barley (Lorang *et al*., 2018). *Pc2* and *Vb* have never been genetically separated in oat, raising the hypothesis that they might be the same gene. Work in A. *thaliana* identified *LOV1* (*LOCUS ORCHESTRATING VICTORIN EFFECTS1*), a CC-NB-LRR conditioning victorin sensitivity (Lorang *et al*., 2007). *LOV1* is conserved in *A. thaliana*, which suggests it is maintained due to selection for functional resistance to an as yet unidentified pathogen (Sweat *et al*., 2008). Mutagenesis of *LOV1*-containing lines identified *LIV1* (*LOCUS OF INSENSITIVITY TO VICTORIN1*), a second gene required for victorin sensitivity (Sweat and Wolpert, 2007). *LIV1* encodes a thioredoxin h5, a member of the thioredoxin family involved in redox homeostasis (Sweat and Wolpert, 2007). Victorin binding to thioredoxin h5 activates LOV1 initiating a defence response and subsequent cell death: characteristic of the guard model of NB-LRR mediated defence. Lorang *et al*., (2010) mapped sensitivity to the host-selective toxin victorin produced by *B. victoriae* in barley (*Lov1*) to a QTL on the short arm of 1H, encompassing the *Mla3* locus. An NB-LRR in this region is a prime candidate for *Lov1* if the mechanism of victorin sensitivity is conserved.

The barley accession Baronesse—*Mla3* haplotype—displays race-specific resistance to *P. oryzae* isolate KEN54-20 (Inukai *et al*., 2006), *Bgh* isolates carrying AVR_{a3} (Jørgensen, 1992), and is sensitive to the host selective toxin victorin produced by *B. victoriae* (Lorang *et al*., 2010). The barley accession BCD47 displays opposing phenotypes to each pathogen. The BCD47 *Mla* resistance specificity is uncharacterised and is most closely related to *Mla16* and *Mla18* (Figure 3-8) (A. J. Castro *et al*., 2003). Mapping of *Rmo1* and *Lov1* was performed in a doubled-haploid (DH) population derived from the cross of barley accessions Baronesse and BCD47 (Inukai *et al*., 2006; Lorang *et al*., 2010). The coupling of *Mla*, *Rmo1*, and *Lov1* is limited to the resolution available in the DH population, therefore the generation of additional recombinant individuals is crucial to resolve the genetic relationship of these three genes. Here, the fine-mapping and candidate gene identification of *Rmo1* and *Lov1* on the *Mla3* locus is outlined.

3.3 Results

Confirming the mapping of *Mla3*/*Rmo1*/*Lov1* using the DH population

Previous work used low resolution simple sequence repeat (SSR) markers to develop a genetic map for the Baronesse x BCD47 DH population. The population was genotyped with a selection of KASP (Kompetitive Allele Specific PCR) markers derived from polymorphic OPA markers (Close *et al*., 2009). Markers were chosen in equidistant positions based on the consensus genetic map at intervals of 20 cM (Muñoz-Amatriaín *et al*., 2011). Seventeen additional markers were chosen, improving the genetic map considerably (Figure 3-1A). The resolution of the 1H chromosome was improved to an 11 cM region covered by 12 non-redundant markers which encompasses the *Mla3* locus. Suppressed recombination is still observed across the locus. Re-evaluation of the original victorin sensitivity data found victorin sensitivity to be in genetic coupling with the *Mla3* locus (Figure 3-1B).

High resolution recombination screen at *Mla*

To elucidate the genetic basis of *Mla3*, *Rmo1*, and *Lov1*, a high resolution recombination screen using Baronesse x BCD47 F_2 individuals (N=2,304 gametes) was performed and 173 recombinants in a 22.9 cM region were identified (Figure 3-2). Of these, 82 individuals contained a recombination event between the two flanking markers of the *Mla* locus as defined by K_963924_115 and K_206D11_281. A genetic map of the 1H chromosome of the Baronesse x BCD47 population was developed using 12 KASP markers (Figure 3-2). A wide genetic interval from markers K_3_0933 to K_4261 was selected to ensure the capture of the entire *Mla* locus. Homozygous recombinants were identified for 56 unique $F_{2:3}$ families, with 95 recombinants in the target interval. Twenty-four additional KASP markers were generated by identifying single nucleotide polymorphisms (SNPs) between Baronesse and BCD47 from PCR amplification of the *Mla* locus. Suppressed recombination was observed at the *Mla3* locus, with 18 markers in complete genetic coupling with K_Mla_RGH1_2920

A.

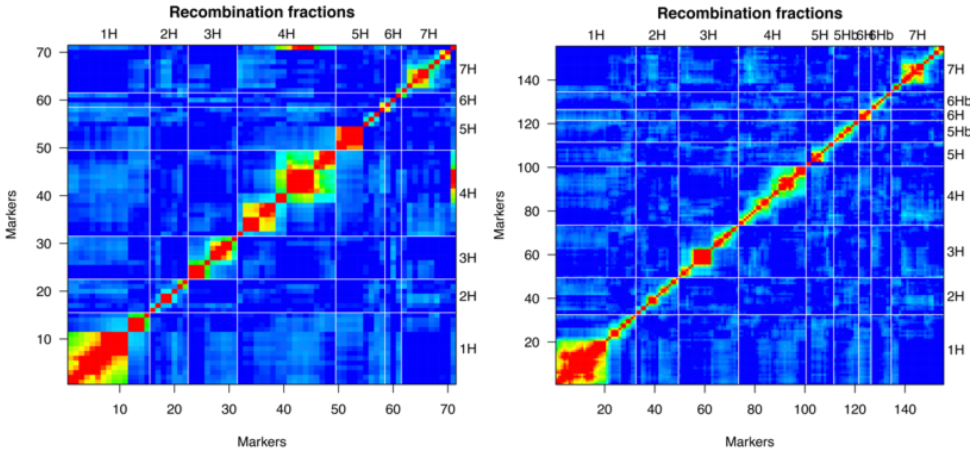

B.

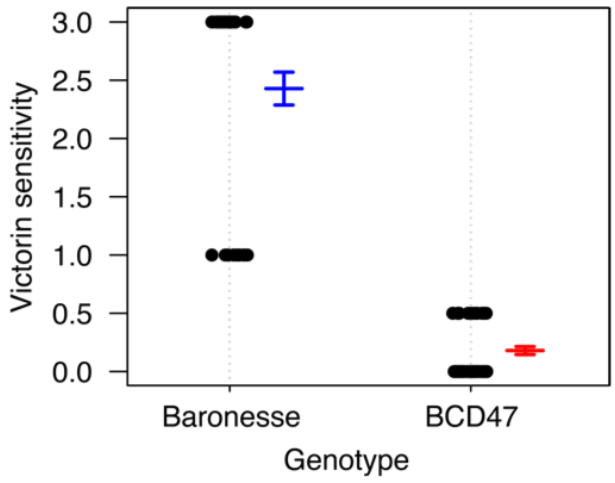

Figure 3-1. Improved Baronesse x BDC47 genetic map and confirmation of *Lov1* at the *Mla* locus.

A) Recombination fractions of the previous genetic map and the updated genetic map. The updated genetic map is improved with lower recombination fractions between distant markers, and the loss of association between markers on 4H and 7H as observed in the first plot.
B) Phenotype by Genotype plot of the ORO (Baronesse x BCD47) DH population phenotyped for victorin sensitivity on a scale where 0 = completely insensitive and 3 = completely sensitive. Victorin sensitivity is in complete genetic coupling at the *Mla* locus.

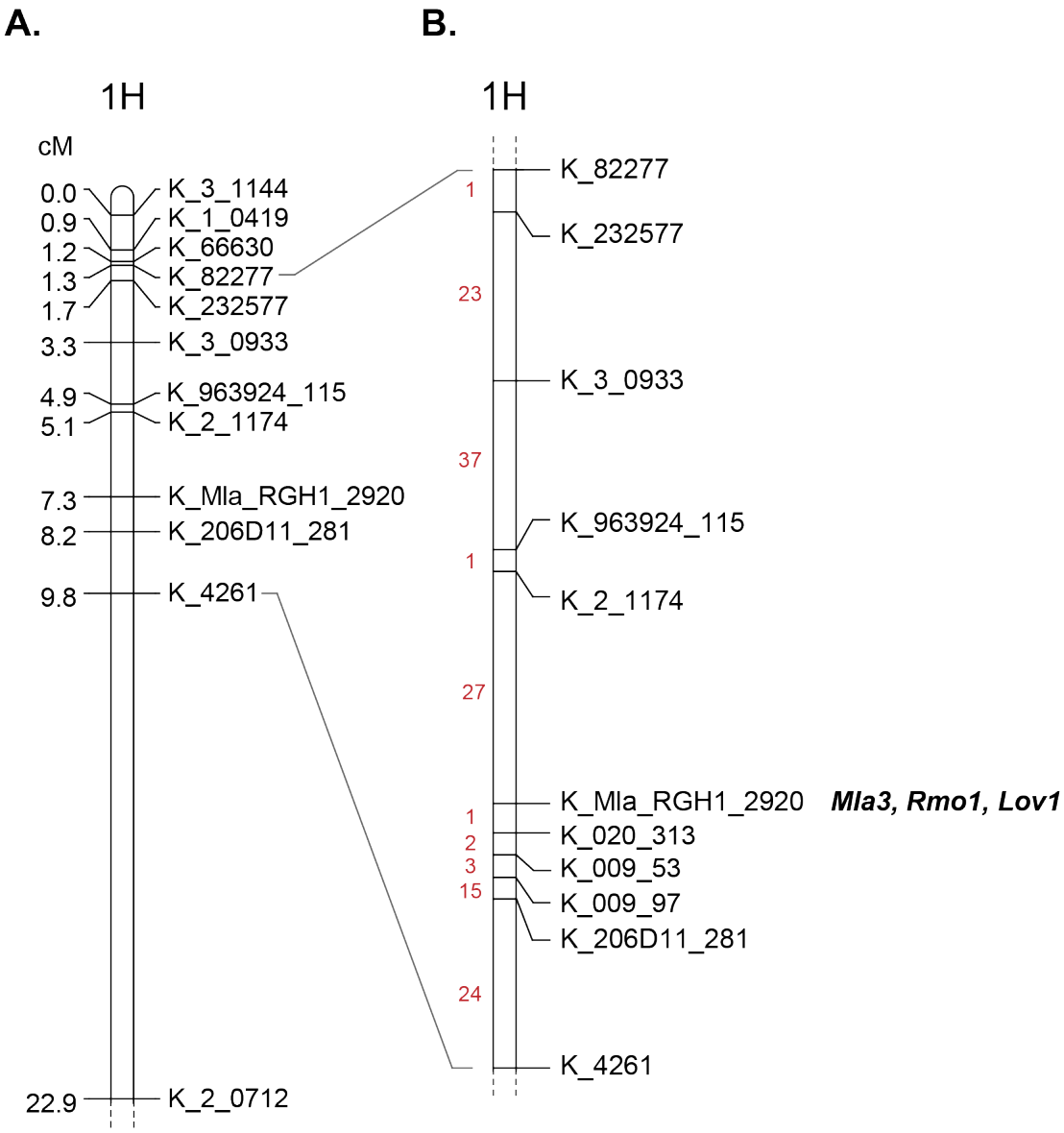

Figure 3-2. *Rmo1* and *Lov1* are in genetic coupling with *Mla3*.

A) The distal end of the short arm of chromosome 1H based on non-redundant KASP markers in the Baronesse x BCD47 population. Numbers of the *left-hand side* correspond to the cM distance with marker names on the *right-hand side*. **B)** High-resolution genetic map based on a recombination screen including N=2,304 gametes. Numbers on the *left-hand side* correspond to the number of recombination events between markers, with KASP markers on the *right-hand side*. Twenty additional markers (not shown) are in complete genetic coupling with K_Mla_RGH1_2920 at the *Mla* locus. *Mla3*, *Rmo1*, and *Lov1* are in complete genetic coupling with K_Mla_RGH1_2920 at the Mla locus.

despite spanning a ~240 kb physical region in the reference sequence cv. Morex. The physical size, sequence, and gene content of the *Mla3* locus remains unknown.

Mla alleles have been extensively characterised therefore the mapping of *Bgh* resistance can be used to confirm the mapping position of the *Mla* locus. Marker K_Mla_RGH1_2920 corresponds to the physical sequence of the *RGH1 Mla3* coding sequence and is a physical reference for the *Mla* locus. In total, 165 $F_{2:3}$ families were phenotyped with *Bgh* isolate CC148 (AVR_{a3}) to confirm the co-segregation for disease resistance. Resistance to *Bgh* isolate CC148 is in complete genetic coupling with marker K_Mla_RGH1_2920 (Figure 3-2).

Critical recombinants were screened with victorin to confirm previous mapping to the *Mla3* locus. *Lov1* was found to be in complete genetic coupling with *Mla3*, underlying K_Mla_RGH1_2920 (Figure 3-2). Flanking markers to K_RGH1, distal K_2_1174 and proximal K_206D11 denoted the gain of function interval for *Lov1* and flank the *Mla* locus.

Rmo1 and *Lov1* are in genetic coupling with *Mla3*

Baronesse and BCD47 show clear differential phenotypes upon inoculation with the *P. oryzae* isolate KEN54-20 carrying *AVR-Rmo1* (Figure 3-3). To map *Rmo1*, 86 homozygous F_4 recombinants, from 48 unique $F_{2:4}$ families, were inoculated with *P. oryzae* isolate KEN54-20 using whole plant spray inoculation and further repeated with leaf-spot inoculation for confirmation. At least 3 biological replicates were included of each F_4 recombinant and critical recombinants were screened with 2 phenotyping replicates. Phenotypes were scored on a semi-quantitative scale ranging from complete resistance to complete susceptibility, with scores of 2 and above classified as susceptible (Figure 3-4). This classification was based on the presence of lesions and completion of the *P. oryzae* life cycle. *Rmo1* is in complete genetic coupling with *Mla3*, where presence of the *Mla3* locus is indicative of *Rmo1* resistance (Figure 3-5).

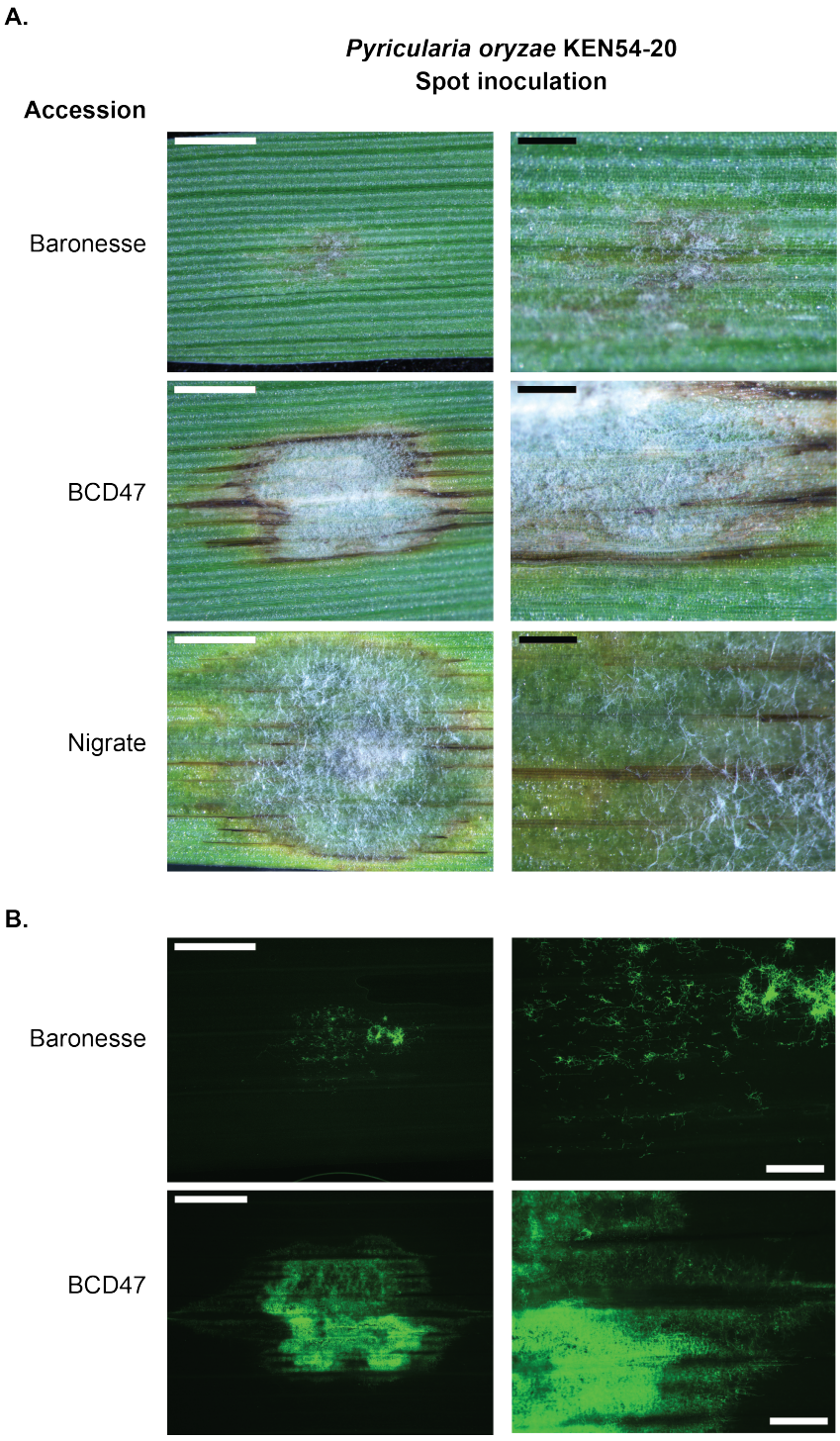

Figure 3-3. Macroscopic and microscopic phenotypes of *P. oryzae* inoculation.

A) Macroscopic phenotypes of spot inoculated leaves with *P. oryzae* isolate KEN54-20 showing resistant phenotype on Baronesse, characteristic susceptible eyespot lesion on BCD47, and hyper-susceptibility on Nigrate. White scale bars in the *left-hand* images indicate 2mm and black scale bars in the *right-hand* images indicate 500 µm. **B)** Microscopic phenotypes of spot inoculated leaves with *P. oryzae* isolate KEN54-20 stained with WGA-FITC chitin stain. *P. oryzae* falsely coloured with green. Scale bars in the *top left-hand* corner on the *left-hand* images indicate 2mm and scale bars in the bottom *right-hand* corner the *right-hand* images indicate 500 µm.

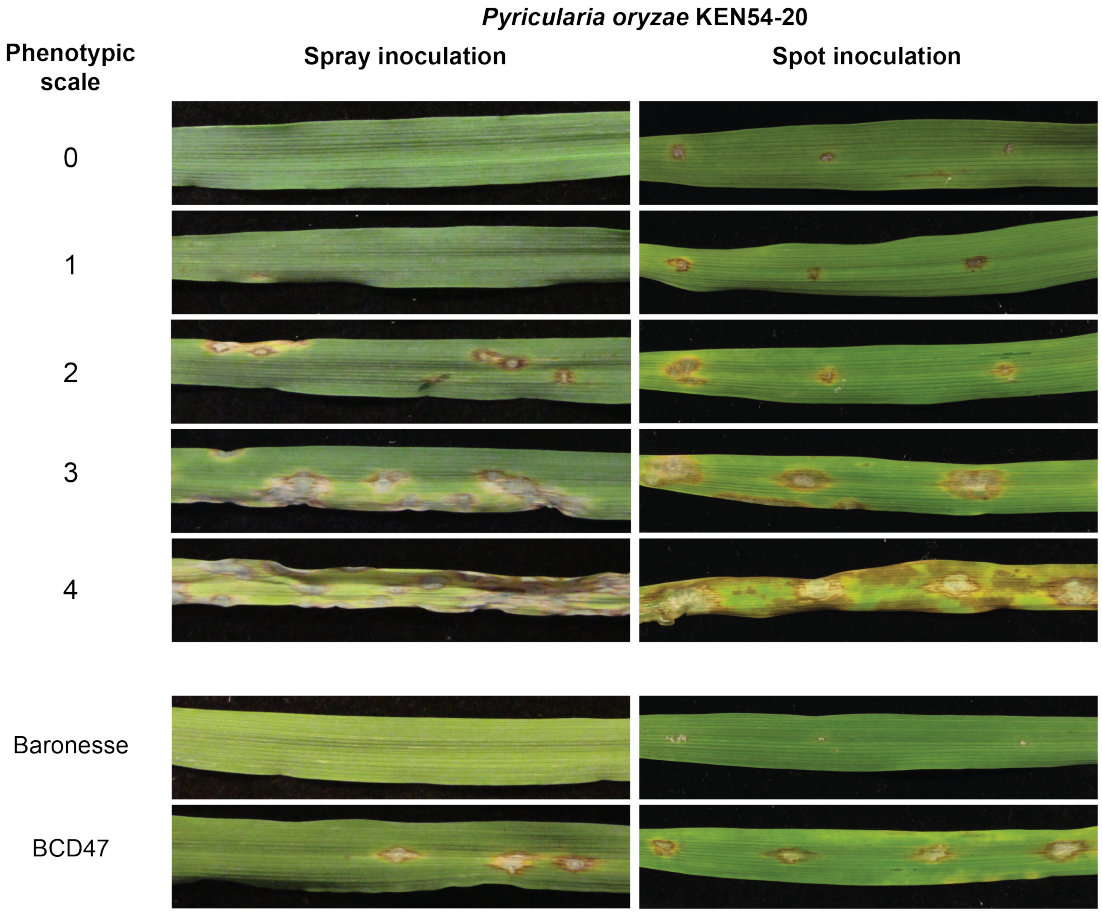

Figure 3-4. Phenotypic scales for scoring *P. oryzae* spot and spray inoculations.

Healthy resistant leaf = 0; resistant small brown lesions = 1; larger eyespot lesions = 2; larger spreading lesions = 3; hyper-susceptibility and leaf collapse = 4. Parental lines Baronesse and BCD47 included for comparison.

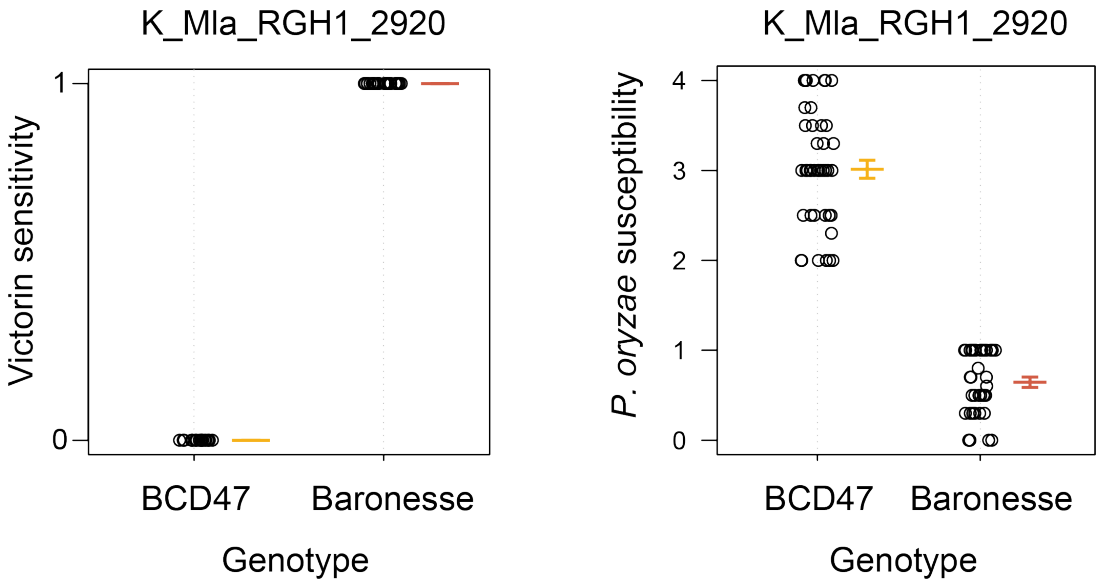

Figure 3-5. *Rmo1* and *Lov1* are in complete genetic coupling with the marker at *Mla3*.

Phenotyping of $F_{3:4}$ homozygous critical recombinants with *P. oryzae* and HST victorin showing complete genetic coupling with the marker K_Mla_RGH1_2920 and the *Mla3* locus. **A)** Phenotype by genotype plot showing *P. oryzae* susceptibly from the spray-based inoculation, where scores 0 and 1 = resistant and 2 to 4 = susceptible (Figure 3-4). **B)** Phenotype by genotype plot of victorin sensitivity, where 0 indicates victorin insensitivity and 1 indicates victorin sensitivity.

Three expressed NB-LRR families are at the *Mla* locus; *RGH1*, *RGH2*, and *RGH3*

Despite *Rmo1* and *Lov1* shown to be in genetic coupling at the *Mla3* locus, the physical size, structure and the gene content the *Mla3* locus is unknown. The *Mla* locus of the reference genome (accession Morex) was derived from BAC-sequencing data (Wei *et al*., 1999). The locus fails to assemble using data from long read sequencing technology due to high repetitive content and presence of large duplications. In Morex, the *Mla* locus encompasses multiple members of three NB-LRR gene families—*RGH1*, *RGH2*, and *RGH3*—of which all three are present within a 40kb tandem duplication. Using RenSeq-PacBio (Witek *et al*., 2016) and RNAseq, *RGH1*, *RGH2*, and *RGH3* gene family members were found to be present in the genome and transcriptome of barley accession Baronesse. The expressed *RGH1* gene family member was identical to *Mla3*. We hypothesized that additional gene family members may be expressed but collapsed on the assembled cDNA contig. To identify additional genes, we performed self-alignment of RNAseq data onto all three cDNA contigs. No variation was observed in *RGH2* and *RGH3*, whereas we identified multiple copies of *Mla3*, including evidence that at least one copy has a 6 base-pair deletion in the LRR region—designated *Mla3Δ6*. The presence of this additional copy was confirmed with PCR using cDNA, molecular cloning of fragments, and sequencing. As described in Chapter 2, the *RGH2* family member contains an integrated *Exo70F1*, and is in head-to-head orientation with *RGH3*. *RGH2* and *RGH3* belong to the Major Integration Clade 1 (MIC1) and C7 clades of NB-LRRs respectively (Bailey *et al*., 2018). Other members of the MIC1 clade include *Rpg5* from barley (Wang *et al*., 2013) and *RGA5* from rice (César *et al*., 2014), which require additional NB-LRRs to function as a pair. Their respective partners, *RGA1* (Wang *et al*., 2013) and *RGA4* (César *et al*., 2014) also reside in the C7 clade. Following this observation, we hypothesise *RGH2-Exo70F1* and *RGH3* also function as paired NB-LRRs. Therefore, candidate genes for conferring *Rmo1* resistance and *Lov1* sensitivity are *Mla3*, *Mla3Δ6*, and *RGH2-Exo70F1*/*RGH3*.

An Exo70 in rice, OsExo70F3, is the target of the *P. oryzae* effector AVR-Pii, and this interaction is guarded by the resistance gene pair *Pii* and *Pii-2* (Fujisaki *et al*., 2015). Therefore, we hypothesised that Exo70s could be a conserved effector target between rice and barley and *RGH2-Exo70F1* (and the *RGH3* partner) became a prime candidate for *Rmo1*. Barley haplotypes contain extensive variation at the *Mla* locus and we can utilise this natural variation to identify lines expressing identical copies of *RGH2-Exo70F1* and *RGH3*. Using RNAseq data from a panel of over 40 diverse barley accessions, we identified multiple accessions containing diverse allelic variants of *RGH2-Exo70F1* and *RGH3* (as described in Chapter 2). Of these, the accession Maritime contains identical copies of *RGH2-Exo70F1* and *RGH3* as the accession Baronesse. The diversity panel was screened with *P. oryzae* isolate KEN54-20 carrying *AVR-Rmo1* using both a spray- and spot-based inoculation (Figure 3-6). All accessions, aside from Baronesse, were susceptible. Therefore, *RGH2-Exo70F1* and *RGH3* can be excluded as candidate genes for conferring *Rmo1*-mediated resistance.

To assess *RGH1* candidacy for *Rmo1* resistance, we took advantage of an introgression panel containing diverse mildew resistance loci. Multiple donor accessions were crossed with the recurrent parent Siri (*Mla8*) and each line underwent multiple rounds of backcrossing and selection using *Bgh* isolates to generate a panel of near-isogenic lines (Kølster and Stølen, 1987). This panel contains the 13 mildew loci, including 11 *Mla* specificities, in isogenic background of Siri including *Mla1*, *Mla3*, *Mla6*, *Mla7* (Nordal), *Mla7* (Moseman), *Mla9*, *Mla10*, *Mla12*, *Mla13*, *Ml22*, *Mla23*, *Ml-(Ru2)*, and *Mlk* (Appendix Table 7-7). The panel was inoculated with the *P. oryzae* isolate KEN54-20 using a spray- and a spot-based inoculation each with 4 biological replicates within 3 replicates of inoculation. As expected, the line S02 containing the *Mla3* resistance specificity was resistant to KEN54-20. However, in addition, the line S13 containing the *Mla23* specificity was also resistant (Figure 3-7). *Mla23* is the most closely related *Mla* allele to *Mla3* (Figure 3-8) and they share 98% sequence similarity at the DNA and protein level, with variation limited to the

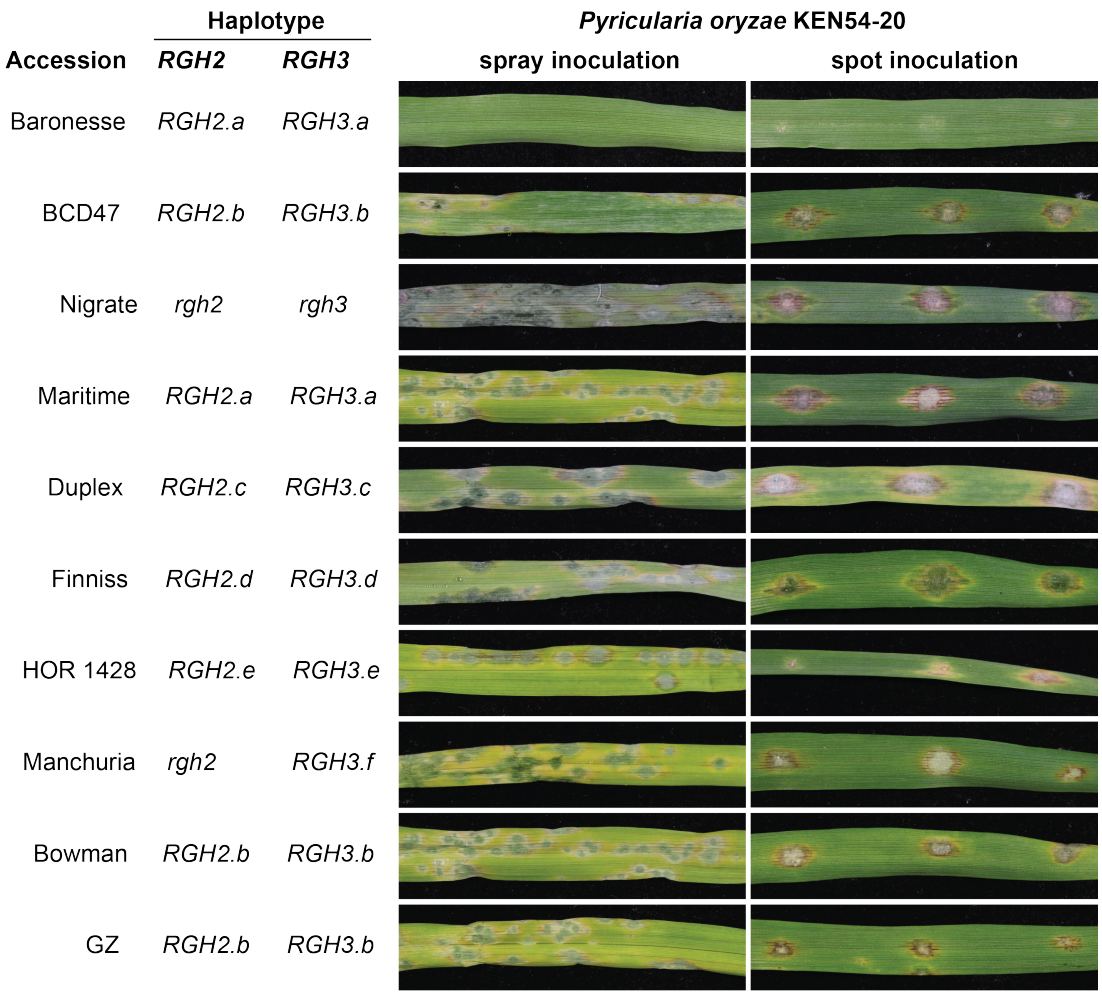

Figure 3-6. *RGH2-Exo70F1* and *RGH3* do not confer *Rmo1*-mediated resistance to KEN54-20.

RGH2-Exo70F1 diversity panel inoculated with KEN54-20 using both the spot and spray inoculation protocol. The *left-hand* side shows *RGH2* and *RGH3* haplotype of each accession. Three replicates were performed with 4 biological replicates in each. Phenotypes from third replicate of inoculations.

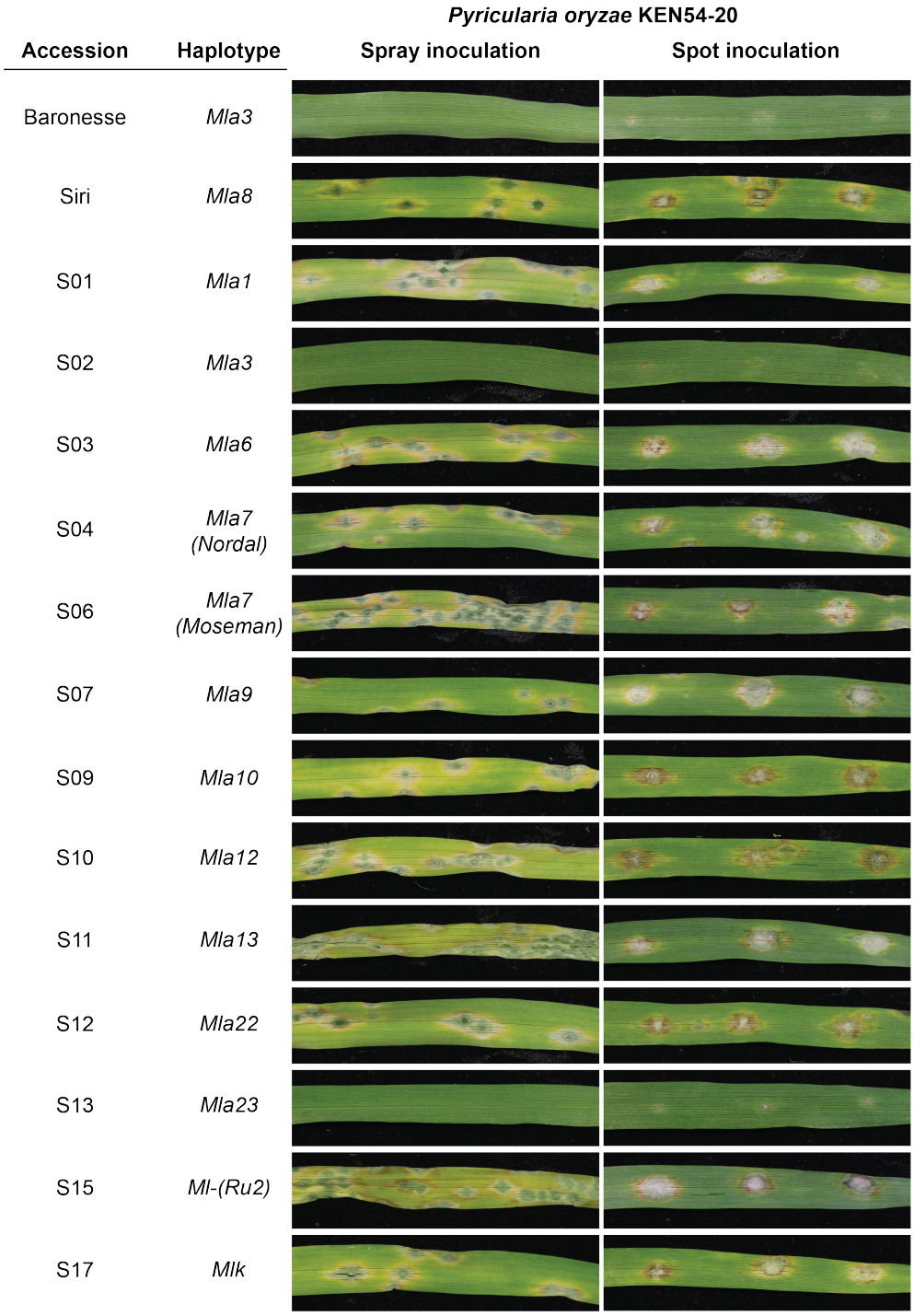

Figure 3-7. *Mla3* and *Mla23* haplotypes confer *Rmo1* mediated resistance to KEN54-20.

Siri introgression panel inoculated with KEN54-20 using both the spot and spray method. Control includes resistant cv. Baronesse, susceptible parent BCD47, and hyper-susceptible Nigrate same as included in Figure 3-6. Siri introgression line and corresponding introgressed *Mildew loci* indicated on the *left-hand* side. Three replicates were performed with 4 biological replicates in each. Phenotypes from third replicate of experiment.

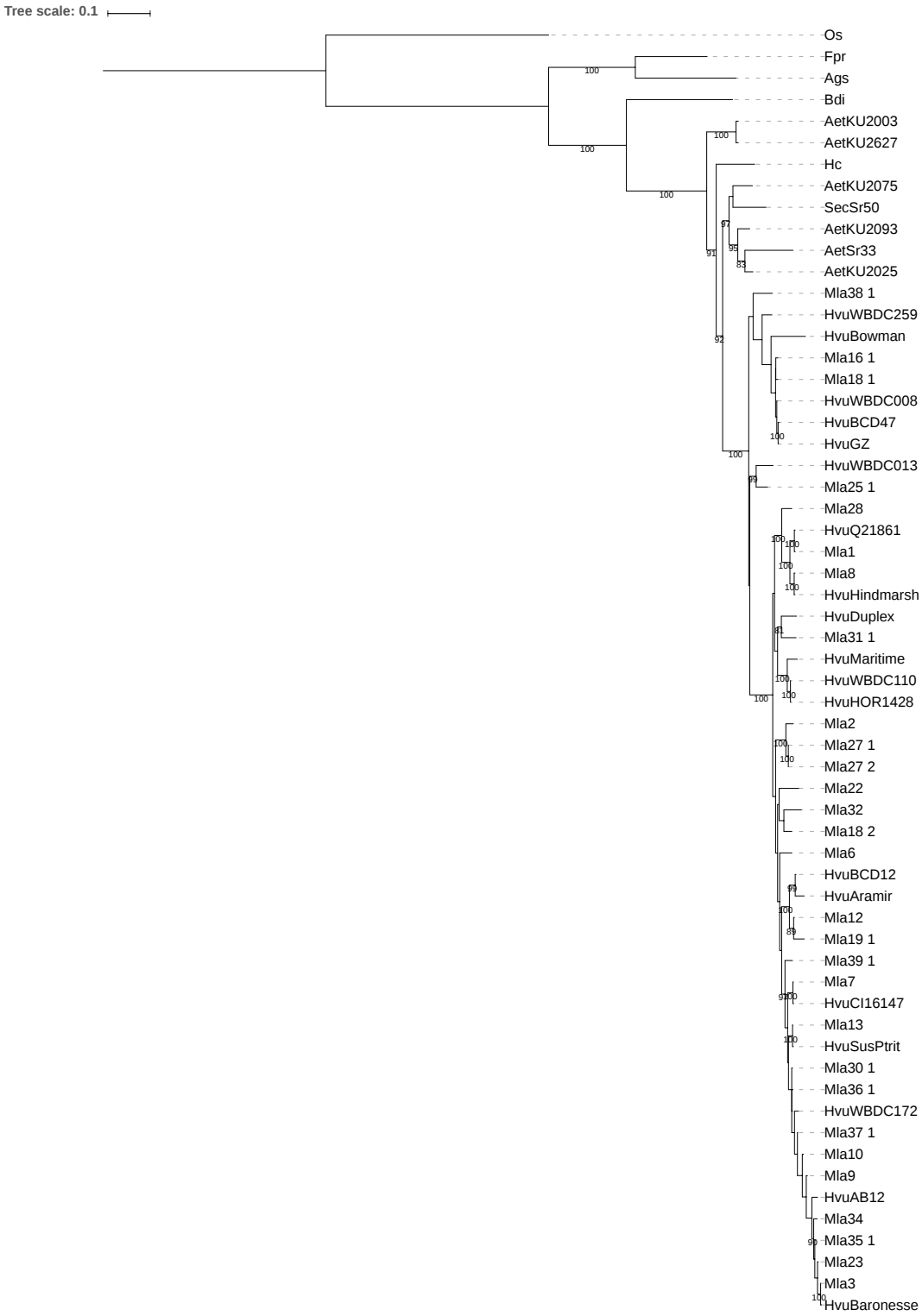

Figure 3-8. *Mla3* and *Mla23* are closely related *RGH1* (*Mla*) alleles.

Maximum likelihood phylogenetic tree of *RGH1* (*Mla*) alleles. Bootstrap support indicated by the number representing support greater than 80% based on 1,000 bootstraps.

C-terminal region of the LRR (Figure 3-9, Figure 3-10). *RGH2* and *RGH3* are not present in this haplotype based on assessment of RNAseq data. Furthermore, the close phylogenetic relationship between *Mla3* and *Mla23* provide strong evidence that *Mla3* is a clear candidate for *Rmo1.* Interestingly, S13 showed an intermediate resistance phenotype to the *Bgh* isolate CC148 carrying AVR_{a3} with presence of few small colonies, whereas S02 was completely resistant. Sequence comparison and generation of chimaeric constructs between *Mla3* and *Mla23* could be used to differentiate the requirement for *AVR-Rmo1* and AVR_{a3} recognition, however further phenotypic quantification is required.

To investigate the role of *RGH1*, *RGH2*, and *RGH3* in conditioning *Lov1* sensitivity, the key control accessions containing the candidate genes—Maritime (*RGH2-Exo70F1*/*RGH3*), S02 (*Mla3*), and S13 (*Mla23*)—were screened with victorin at the laboratory of Thomas Wolpert. Maritime was insensitive to victorin, therefore excluding *RGH2-Exo70F1* and *RGH3* as candidates. Both S02 (*Mla3*) and S13 (*Mla23*) were sensitive to victorin confirming *Mla3* as the candidate for *Lov1* (Figure 3-11).

3.4 Discussion

This chapter outlines the fine mapping of *Mla3*, *Rmo1* and *Lov1*. Fine-mapping in the Baronesse (*Mla3*, *Rmo1*, *Lov1*) x BCD47 (*MlaBCD47, rmo1*, *lov1*) population provided a high-resolution genetic map of the *Mla3* locus. Screening of segregating $F_{2:3}$ families and homozygous $F_{3:4}$ recombinant families with *P. oryzae*, *Bgh*, and the HST victorin show their complete genetic coupling at the *Mla3* locus. The *Mla3* haplotype contains the *RGH1* family members *Mla3* and *Mla3Δ6*, and *RGH2-Exo70F1*/*RGH3* that are hypothesised to function as a pair. A diversity panel of barley accessions containing these candidate genes was screened and phenotyping data confirms the *RGH1* family member *Mla3* as the prime candidate for conferring *Rmo1* resistance and *Lov1* sensitivity.

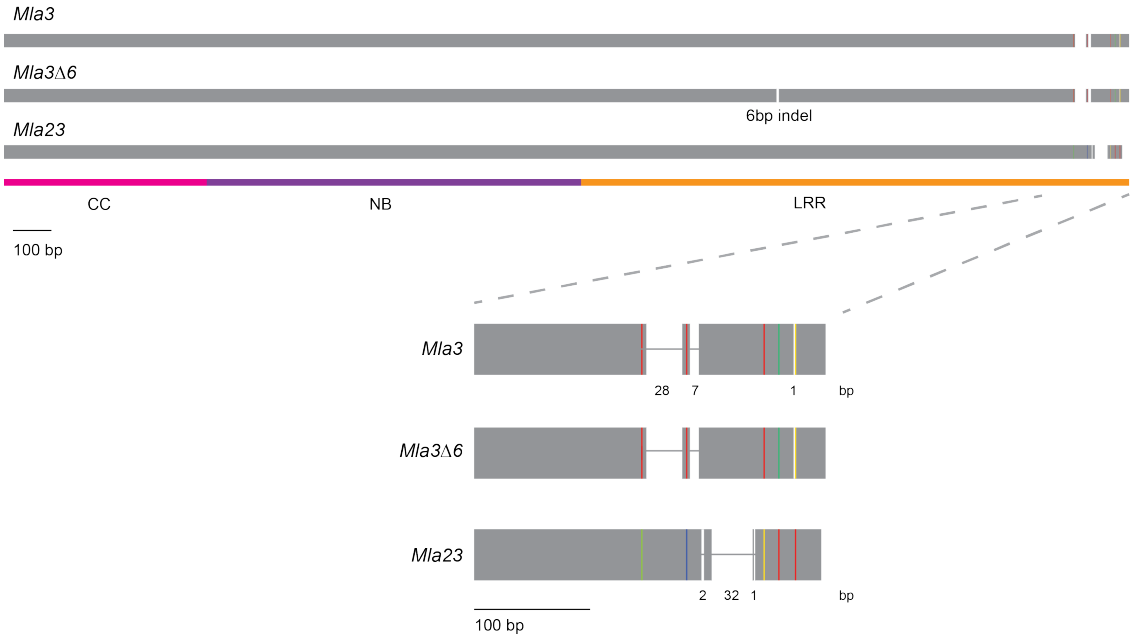

Figure 3-9. DNA sequence comparison of *Mla3*, *Mla3Δ6*, and *Mla23*.

Indels between *Mla3*, *Mla3Δ6,* and *Mla23* sequences indicated with white space for deletions, size of indels (basepairs; bp) indicated with integers beneath the white space. SNPs indicated with coloured lines where red = A, green = T, yellow = G, and blue = C. Scale bar indicates 100 bp. Encoded protein domains are annotated by coloured lines under the sequence comparison, coiled-coil (CC; pink), nucleotide-binding (NB; purple), and leucine-rich-repeat (LRR; orange).

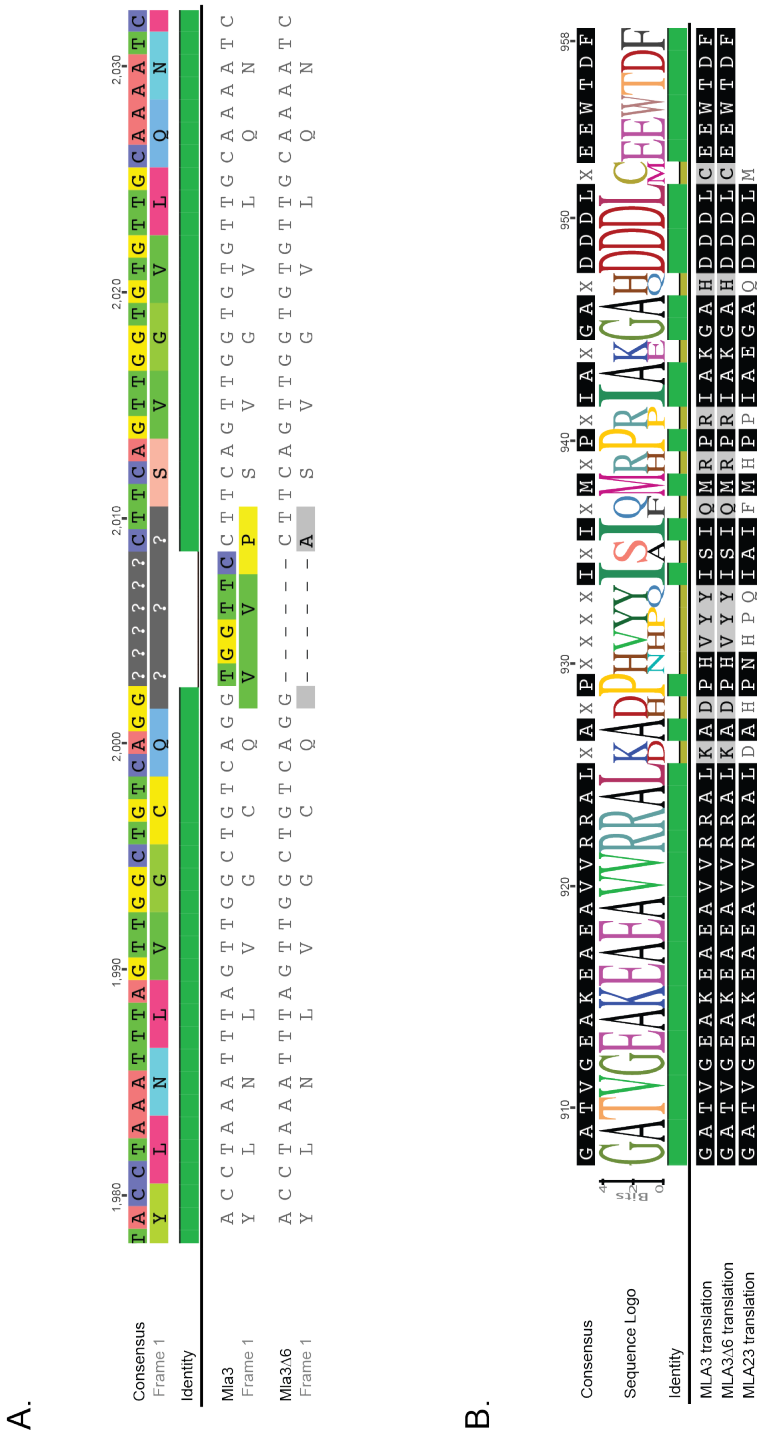

Figure 3-10. Sequence comparison of *Mla3*, *Mla3Δ6*, and *Mla23*.

A) Sequence comparison of *Mla3* and *Mla3Δ6* at the DNA and amino acid level. DNA sequence of *Mla3* and *Mla3Δ6* with translation. The 6 bp indel causes a loss of two amino acids and an amino acid change in *Mla3Δ6*. Sequence comparison exported from Geneious. **B)** Amino acid sequence comparison of *Mla3*, *Mla3Δ6,* and *Mla23* of the C-terminus of the leucine-rich repeat. Sequence comparison exported from Geneious.

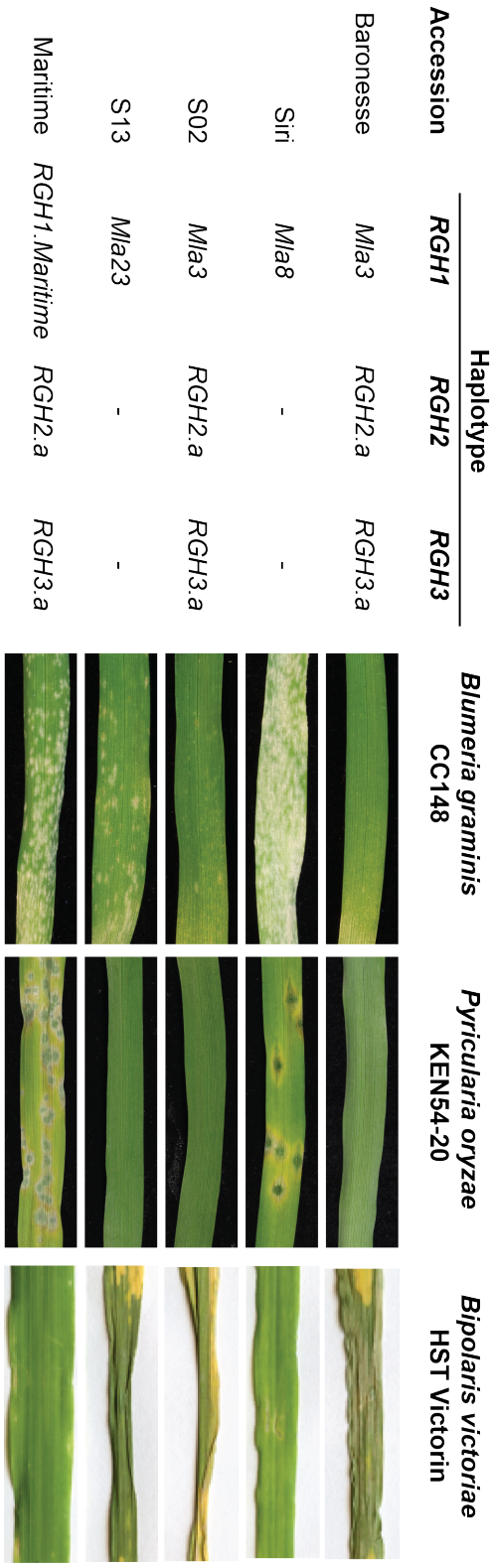

Figure 3-11. Recognition of *Bgh* CC148, *P. oryzae* KEN54-20, and victorin sensitivity is coupled with the presence of *Mla3*/*Mla23*.

Accessions carrying candidate genes *RGH1*, *RGH2-Exo70F1* and *RGH3* inoculated with *Bgh* isolate CC148, *P. oryzae* isolate KEN54-20, and HST victorin from *B. victoriae*.

Mascher *et al*., (2017) found distal telomeric regions of barley chromosomes to be enriched with genes involved in defence and the presence of transposable elements. The *Mla* locus on the short arm of chromosome 1H is a resistance gene complex showing extreme intraspecific diversity between barley haplotypes (Jørgensen, 1994; Seeholzer *et al*., 2010). Previous characterisation of the *Mla* locus in the reference genome Morex identified a region of high complexity containing three gene-rich regions flanked by repetitive and mobile elements. Genetic linkage of gene families facilitates recombination events between them; unequal crossing over and gene conversion generate new combinations and sequence variants. Duplication events provide additional copies of genes—which either leads to pseudogenisation or the production of allelic variants through the action of diversifying selection (Hulbert *et al*., 2001; Leister, 2004; Michelmore and Meyers, 1998). This is evident in the reference sequence Morex which contains 8 NB-LRRs from the three *RGH* gene families: 3 of which result from a 40kb tandem duplication encompassing each *RGH* family member (Wei *et al*., 2002, 1999). The *Mla* locus has been associated with recognition of multiple pathogens. While the structure of region promotes the production of diverse NB-LRRs, the genetic and molecular basis of this linked resistance is unknown. Here, we confirm the genetic coupling of *Mla3*, *Rmo1*, and *Lov1*.

The mapping of multiple resistance specificities to adjacent regions of the genome is not uncommon; overlapping resistance QTLs are present on all chromosomes of barley (Schweizer *et al*., 2011). However, the majority of the underlying causal genes have yet to be identified. The main question remains: does this represent resistance gene clusters, or are single genes conferring multiple pathogen recognition? The identification of *Mla3*, *Rmo1*, and *Lov1* in genetic coupling does little to further the answer, as the resolution here is of the entire *Mla3* locus (Figure 3-2, Figure 3-5). Candidate NB-LRR genes from known *RGH* family members within the locus were identified from RNAseq and RenSeq-PacBio sequencing: *RGH1* (*Mla3* and *Mla3Δ6*), *RGH2-Exo70F1* and *RGH3*—with *RGH2* and *RGH3* hypothesised to function as a pair as they belong to the MIC1 and C7 clades, respectively (Bailey *et al*., 2018). Using a diversity panel containing different *RGH* alleles and *Mla* introgression lines we were able to confirm *Mla3* as a candidate for *Rmo1* (Figure 3-6, Figure 3-7). In

addition, *Mla23* also displays resistance to KEN54-20 and these alleles are 98% similar at the DNA and protein level (Figure 3-9, Figure 3-10). We hypothesise that *Mla23* is also recognising *AVR-Rmo1*, however the presence of an additional recognised effector cannot be excluded. *RGH2-Exo70F1* and *RGH3* were excluded as candidates for *Rmo1* and *Lov1* as the accession Maritime was susceptible to KEN54-20 and insensitive to victorin; Maritime contains the same alleles of these genes as Baronesse (Figure 3-11). The generation of transgenic barley and systematic isolation of *RGH1* alleles is required to investigate the potential for multiple pathogen recognition by *Mla3*.

The capability of multiple pathogen recognition has been shown for a limited number of NB-LRRs. The *A. thaliana* paired NB-LRRs RPS4 and RRS1 are the most well characterised of these and directly recognise the effectors *AvrRps4* from *P. syringae* pv. *tomato*, *PopP2* from *Ralstonia solanacearum*, and an unidentified effector from the fungal pathogen *Colletotrichum higginsianum* (Narusaka *et al*., 2013, 2009). RRS1 contains a C-terminal fusion of a WRKY domain—an integrated decoy—that interacts with *AvrRps4* and *PopP2*. Acetylation of the WRKY domain by *PopP2* and hypothesised direct binding with *AvrRps4* triggers RPS4-mediated resistance (Le Roux *et al*., 2015; Saucet *et al*., 2015; Williams *et al*., 2014). The NB-LRR *Mi-1.2* from tomato confers resistance to root-knot nematodes of the genus *Meloidogyne*, the potato aphid (*Macrosiphum euphorbiae*), and sweet potato whiteflies in the genus *Bemisia* (Nombela *et al*., 2003; Vos *et al*., 1998). Extended recognition of NB-LRRs can be achieved via the guarding of host proteins; multiple pathogen effectors from across species can modify or bind the same plant protein. RIN4 is a known example, its perturbation is guarded by two NB-LRRs in *A. thaliana* (Axtell and Staskawicz, 2003; H.-S. Kim *et al*., 2005; Kim *et al*., 2009; Mackey *et al*., 2003, 2002; Russell *et al*., 2015), and by alleles of *RPG1* in soybean (*Glycine max*) (Ashfield *et al*., 2014; Whitham *et al*., 2016). RIN4 is a conserved component of the plant immune system; thus, other as yet uncharacterised guard-guardee interactions are also hypothesised across species (Toruño *et al*., 2019).

The presence of *Mla* alleles in an expanded allelic series is suggestive of a direct recognition mechanism between MLA receptors and *Bgh* effectors (Bourras *et al*., 2019; Saur *et al*., 2019). The *Mla* family member Sr50 from rye (*Secale cereale*)

confers resistance to (*Puccinia graminis* f. sp. *tritici*; *Pgt*), and also when introgressed into wheat, and was recently shown to directly bind the *Pgt* effector AvrSr50 (Chen *et al*., 2017). This work not only provides evidence for direct recognition by *Mla* family members but shows that recognition by this family is not limited to *Bgh*; diverse orthologs have the potential to recognise different pathogen species. Evaluation of candidate NB-LRRs in the region—*Mla3* and *Mla3Δ6*—for *Rmo1*-mediated resistance and *Lov1*-mediated susceptibly will confirm the potential for multiple pathogen recognition specificity by an *Mla* allele.

Crop breeding has historically focused on the introgression of large-effect *R* genes into susceptible commercial cultivars to provide resistance to biotrophic pathogens. One of the most famous examples of unexpected consequences of resistance breeding is "Victoria-type" oats (*Avena sativa*) bred for oat crown rust (*Puccinia coronata*) *Pc2* resistance. Introgression of the *Pc2* resistance gene facilitated the epidemic of victoria blight during the 1940s, allowing for a host jump of the necrotrophic pathogen *B. victoriae* (Meehan & Murphy, 1946). *B. victoriae* produces the HST victorin to aid infection. Due to the considerable size and complexity of the oat genome, *Pc2* and victorin sensitivity (*Vb*) have never been genetically separated or identified and are presumed to share identity—a single oat *R* gene conferring resistance to oat crown rust yet providing susceptibility to *B. victoriae*.

Following the observation of the similarity between the victorin sensitivity response and the plant defence response (Wolpert *et al*., 2002), the notion that *R* genes could also enable disease susceptibility was confirmed with the identification of the NB-LRR *LOV1* in *A. thaliana*. *LOV1* encodes a NB-LRR and confers sensitivity to the HST victorin, and subsequent susceptibility to *B. victoriae* (Lorang *et al*., 2007, 2004; Sweat and Wolpert, 2007; Wolpert and Lorang, 2016). *LOV1* guards thioredoxin h5, in a mechanism familiar to biotrophic pathogen resistance. In *A. thaliana*, six groups of thioredoxins are expressed and localised in different subcellular compartments (Reichheld *et al*., 2002). Thioredoxin h5 is induced by abiotic and biotic stress conditions, appearing unique in the thioredoxin h group, and provides specificity to plant signalling through selectively reversing *S*-nitrosothiols formed during SA-dependent immune signalling (Kneeshaw *et al*., 2014; Sweat and Wolpert, 2007). As

key modifier of the defence signalling pathway, thioredoxin h5 is vulnerable to pathogen effector disruption, leading to the evolution of its guardee, *LOV1*. Biotrophic pathogen effectors and necrotrophic HSTs and effectors are under opposing evolutionary forces, despite often converging at the same outcome (Wang *et al*., 2014). Upon triggering a defence reaction leading to pathogen avirulence, biotrophic effectors would be under selection to lose recognition—either through effector gene loss or sequence diversification. However, for necrotrophic pathogens, effectors or HSTs that trigger a defence reaction that facilitates infection can be under positive selection. This difference is reflected in the plant immune response: necrotrophic pathogen defence is suggested to be predominantly mediated by jasmonic acid and ethylene signalling, compared to salicylic acid as for biotrophic pathogens (Glazebrook, 2005). Such regulation could have evolved due to selection to separate resistance and susceptibility factors (Glazebrook, 2005; Walters *et al*., 2014). The evolution of *LOV1* to guard modification of thioredoxin h5 is hypothesised to have arisen in response to biotrophic pathogens: due to pathogen suppression or interference of thioredoxin h5 (Lorang *et al*., 2012; Wolpert and Lorang, 2016). The co-option of this system by necrotrophic pathogens to confer susceptibly would lead to selection against *LOV1* function; *LOV1* retention must be due to stronger selection for biotrophic pathogen resistance than against necrotrophic pathogen susceptibility (Wolpert and Lorang, 2016). The majority of *A. thaliana* ecotypes assessed are sensitive to victorin; *LOV1* shows little variation between *A. thaliana* accessions and evaluation of alleles found no evidence that *LOV1* was under balancing selection (Sweat *et al*., 2008).

In this work, a member of the *RGH1* family at the *Mla* locus is hypothesised to be conditioning victorin sensitivity in a mechanism similar to as shown in *A. thaliana* (Lorang *et al*., 2012). Lorang *et al*., (2010) identified a single significant QTL for victorin sensitivity in barley. However, *Lov1* could be guarding the interactor of victorin, similar to thioredoxin h5 in *A. thaliana* (Sweat and Wolpert, 2007). Further work to identify a guardee, such as the initiation of a mutagenesis screen, is required: a conserved guardee with no variation in the parental accessions would be missed in the original mapping population. If *Mla3* is *Lov1*, a guard-guardee mechanism challenges the hypothesis of direct recognition of MLA alleles presented by Saur *et al*., (2019). Furthermore, if *Lov1* requires the barley thioredoxin h5 guardee, then

thioredoxins are revealed as a conserved component of the defence signalling machinery and shared pathogen target. Integrated thioredoxin domains within NB-LRRs have also been reported (Bailey *et al*., 2018; Bryan *et al*., 2000; Costanzo and Jia, 2009) providing evidence for their role as a target by pathogen effectors. However, victorin sensitivity in barley could be conditioned in a manner independent to *A. thaliana*, through the direct binding of victorin to MLA3.

Victorin sensitivity is highly conserved, being present in oat (Meehan and Murphy, 1946), *Arabidopsis* (Lorang *et al*., 2004), common bean (*Phaseolus vulgaris*) (Lorang *et al*., 2018), *Brachypodium*, rice (Wolpert, personal communication) and barley (Lorang *et al*., 2010). However, despite displaying sensitivity to isolated victorin, natural infection of *B. victoriae* has not been observed outside of oat. Pathogens cause devastating losses to barley production worldwide (Newton *et al*., 2011) and examples with necrotrophic growth phases include *Pyrenophora teres* f. *teres* causing net blotch (Liu *et al*., 2015), *Fusarium* species causing fusarium head blight (Brown *et al*., 2017; Salas *et al*., 1999; Steffenson, 2003; Wegulo *et al*., 2015), *Rhynchosporium secalis* causing leaf scald (Able, 2003; Zhan *et al*., 2008), and *Ramularia collo-cygni* causing *Ramularia* leaf spot (Havis *et al*., 2015; Walters *et al*., 2008). In these examples, limited resistance has been observed with the majority of accessions only displaying partial resistance. The destructive nature of necrotrophic pathogen invasion drives selection in plants to evade HSTs and constrain initial necrosis (Laluk and Mengiste, 2010; Stukenbrock and McDonald, 2009). Victorin sensitivity in barley was also found to be age dependent (Lorang *et al*., 2010); developmental regulation of NB-LRRs could be selection against necrotrophic pathogens—*B. victoriae* or otherwise. The maintenance of hypothesised NB-LRR mediated victorin susceptibility across diverse species suggests a strong selection for retention of biotrophic resistance. Such opposing selective pressures may contribute to the evolutionary outcome of NB-LRR gene frequency and specificity in plant populations. Caution must be taken with the wide-scale deployment of NB-LRR genes, especially of alleles with low frequency in populations, to prevent unexpected susceptibility to other pathogens. With a changing climate and increased pathogen mobility through globalisation, fine-tuned NB-LRR gene repertoires could be broken down, with more pathogen host-jumps and necrotrophic pathogen epidemics to be seen in the future.

3.5 Materials and methods

Plant materials and growth conditions

Barley accessions were obtained from United States Department of Agriculture Germplasm Resource Information Network (Aberdeen, ID, USA), Oregon State University (Corvallis, OR, USA), John Innes Centre (JIC; Norwich, UK), and CSIRO (Canberra, Australia). All plants underwent single seed descent before performing pathogen assays with the exception of the *Mla3* diversity panel. Plant materials are detailed in Appendix Table 7-6.

For the Baronesse x BCD47 population, seedlings were germinated in John Innes Peat & Sand Mix (85% Fine Peat, 15% Grit, 2.7kg/m³ Osmocote 3-4 months, Wetting Agent, 4kg/m³ Maglime, 1kg PG Mix). Leaves were sampled at second leaf emergence, DNA extracted, and individuals genotyped for recombination events. Recombinants were transferred to FP9 pots in John Innes Cereal Mix (40% Medium Grade Peat, 40% Sterilised Soil, 20% Horticultural Grit, 1.3kg/m³ PG Mix 14-16-18 + Te Base Fertiliser, 1kg/m³ Osmocote Mini 16-8-11 2mg + Te 0.02% B, Wetting Agent, 3kg/m³ Maglime, 300g/m³ Exemptor) and grown in a greenhouse under natural conditions.

For *P. oryzae* inoculation, seedlings were germinated in John Innes Cereal Mix (40% Medium Grade Peat, 40% Sterilised Soil, 20% Horticultural Grit, 1.3kg/m³ PG Mix 14-16-18 + Te Base Fertiliser, 1kg/m³ Osmocote Mini 16-8-11 2mg + Te 0.02% B, Wetting Agent, 3kg/m³ Maglime, 300g/m³ Exemptor). Seedlings were germinated and grown in a controlled environment at 25°C under a 16-h light and dark cycle. For *B. graminis* inoculation, seedlings were germinated in John Innes Cereal Mix at 18°C under a 16-h light and dark cycle. Seedlings were transferred to a containment greenhouse under natural conditions prior to inoculation.

Baronesse x BCD47 population and genetic map development

The *H. vulgare* accessions Baronesse and BCD47 were crossed and allowed to self-pollinate to generate a founder F_2 population. The population, N=2,304 gametes, was evaluated for recombination events across the *Mla3* locus. Following single-seed descent, DNA was extracted from leaf tissue of F_2 and F_3 recombinants using a CTAB gDNA extraction protocol modified for 96-well plate-based extraction (Dawson *et al*., 2016; Stewart and Via, 1993).

Genetic markers designed for the barley oligonucleotide pool assay (BOPA1) panel were converted to Kompetitive allele specific PCR (KASP) markers, which are also SNP based (Close *et al*., 2009). KASP markers are listed in Appendix Table 7-8. Briefly, KASP SNP genotyping utilises two competitive, allele-specific forward primers and one common reverse primer for allele-specific oligo extension, amplification, and fluorescence output. Genotyping was performed by the Genotyping service at the JIC, Norwich, UK. Parental lines of mapping populations were genotyped to identify polymorphic markers. Additional markers were generated across the *Mla* locus by amplify sequence from parental lines using primers designed from the *Mla* locus accession Morex (Wei *et al*., 1999). SNPs were identified between parental accessions and KASP markers generated.

Genetic maps were created using JoinMap v4 was used using default parameters (van Ooijen, 2006). Genetic distances were estimated using the Kosambi mapping function. Integrity of the genetic map was evaluated through comparison with the current OPA consensus genetic map of barley (Muñoz- Amatriaín *et al*. 2011). The genetic map was evaluated using Rstudio (Version 1.1.463) and the R/qtl package (Version 1.44.9) (Broman *et al*., 2003).

Pyricularia oryzae isolates and culture

P. oryzae isolates KEN54-20 and Sasa2 were obtained from the group of Ryohei Terauchi (Iwate Biotechnology Research Centre, Kitakami, Iwate, Japan). Protocols for culturing and inoculation were similar as described by Jia *et al*., (2003) and Parker *et al*., (2008). Isolates were maintained on Potato Dextrose Agar media at 24°C and as frozen stocks of dried mycelia on Whatman filter paper (GE Healthcare Whatman™

Qualitative Filter Paper: Grade 1 Circles, Fisher Scientific UK) at -20°C. Hyphal tips were transferred to oatmeal agar (20 g oatmeal, 10 g agar, 2.5 g sucrose, addition of ddH20 to 500 ml) plates (deep petri dish 100 x 20 mm) for the production of spores and incubated for 10-15 days at 24°C. To increase spore production some plates were used for a second time after washing and a further 10-15 day incubation.

Pyricularia oryzae conidal suspension

Conidia were collected by the addition of 8ml dH20 to the oatmeal agar plates and gentle scraping with the tip of a 1.5ml Eppendorf. Suspension was poured and filtered through Miracloth (Merck Chemicals, Ref.: 475855-1r) and collected in a 50 ml Corning tube. Spore concentration was counted via haemocytometer and adjusted to 1 x 10^5 spores per ml. Tween 20 (Merck Chemicals, CAS Number: 9005-64-5) was added to a final concentration of 0.01%.

Pyricularia oryzae spot inoculations

Spot inoculations were carried out on detached leaves in boxes (Display Box with Push Fit Lid, 126 x 82 x 22mm, azpack.co.uk) on agar (2.5g Agar-agar (Fisher, CAS 9002-18-0); 50ml benzimidazole (1g/1L H_2O stock soltution); 450ml H_2O). Barley was germinated at 25°C under a 16-h light and dark cycle and 1-week old seedlings were used for inoculation at emergence of second leaf. The first leaf was cut and placed on agar inside the boxes. Each leaf was inoculated with 3 to 4 drops of 5µl of conidal suspension. Boxes were placed at 25°C in a Sanyo growth cabinet and maintained under continuous light for the first 24 hours. After 24hrs droplets were removed from the leaves using sterile Miracloth and boxes returned to 25°C in a 16-h light and dark cycle. Detached leaves were monitored for development of lesions and phenotyped 7 days post inoculation (dpi), however phenotypes could be observed from 5dpi. Phenotypes were scored as resistant on a scale of 0 = complete resistance; 1 = small brown resistant spots; 2 = susceptible larger eyespot lesions; 3 = larger spreading lesions; 4 = hyper susceptibility (Figure 3-4).

Pyricularia oryzae spray inoculations

Spray inoculations were carried out on whole 1-week old seedlings at emergence of second leaf. Barley was germinated 25°C under a 16-h light and dark cycle with 9 seeds placed in an FP9 pot, with 8 pots in a tray. Each tray was sprayed with ~5ml of conidal suspension using a 20 mm atomiser spray bottle (Ampulla; Ref.: X9031CL/C1118W50). Trays were placed in polythene autoclave bags tied with tape and placed inside a Sanyo cabinet at at 25°C under a 16-h light and dark cycle. Bags remained covering the plants until phenotyping due to containment requirements. First leaves were phenotyped 7 dpi and scored on a similar scale to spot inoculations.

Victorin sensitivity assays

Victorin sensitivity assays were carried out by Tom Wolpert and Jennifer Lorang at Oregon State University using the protocol as described in Lorang *et al*., 2010. Briefly, the second and third leaves of 4-week old plants were incubated in 20µg/ml victorin and scored over a 48hr period as 0 = insensitive or 1 = sensitive.

Microscopy

For macroscopic phenotyping, infected leaves were imaged 7 dpi using a stereo microscope using the 1x objective. For fluorescence microscopy phenotyping, leaves were cleared 7dpi in a 1.0 M KOH solution, neutralised by washing in 50 mM Tris at ph 7.5, and stained with a chitin-specific fluorophore (20 µg/mL WGA-FITC (Sigma–Aldrich; L4895- 10MG) in 50 mM Tris at pH 7.5), as described in Dawson *et al*., (2016) and adapted from Ayliffe *et al*., (2013, 2011). *P. oryzae* growth within leaves was visualised under blue excitation on a fluorescence microscope with a GFP filter using a 10x, and 20x objective. Images were observed and taken via the Leica Application Suite software and scale bars added using the Fiji distribution of ImageJ (Version 2.0.0-rc-69/1.52p) (Schindelin *et al*., 2012) using the Bio-formats plugin (Linkert *et al*., 2010).

Isolation of genomic DNA

DNA from all structured populations was extracted from leaf tissue following a CTAB- based protocol (Stewart and Via, 1993). In brief, 3 g of leaf tissue were ground on liquid N_2 and homogenized with 20 mL of CTAB extraction buffer (2% CTAB, 100 mM Tris-HCl pH8.0, 20 mM EDTA pH8.0, 1.4 M NaCl, 1% β-Mercaptoethanol). Samples were incubated for 30 min at 65°C followed by two chloroform extractions and ethanol precipitation. DNA was then resuspended in 1x TE, 50 µg/mL RNase A solution and incubated for 1 h at 37°C. DNA was subsequently precipitated with 2.5 volumes of ice-cold 95% ethanol and resuspended in 1x TE. Quantification of DNA samples was performed using a Nanodrop spectrophotometer (Thermo Scientific) and the Qubit dsDNA HS Assay Kit (Molecular Probes, Life Technologies).

RNAseq and *de novo* assembly

First and second leaf tissue was harvested at 10 days after sowing of barley and oat accessions grown in the greenhouse. Tissue was flash frozen in liquid nitrogen and stored at -80 °C. Tissue were homogenized into a fine powder in liquid nitrogen-chilled pestle and mortars. RNA was extracted, purified, and quality assessed as described by Dawson *et al*. (2016). RNA libraries were constructed using Illumina TruSeq RNA library preparation (Illumina; RS-122-2001). Barcoded libraries were sequenced using either 100 or 150 bp paired-end reads. Library preparation and sequencing was performed at either the Earlham Institute (Norwich, United Kingdom) or BGI (Shenzhen, China). Quality of all RNAseq data was assessed using FastQC (0.11.5) (Andrews, 2010). Trinity (2.4.0) (Grabherr *et al*., 2011)was used to assemble *de novo* transcriptomes using default parameters and Trimmomatic (Bolger *et al*., 2014) for read trimming. Genes of interest were identified in *de novo* assemblies using BLAST+ (v2.2.9) (Camacho *et al*., 2009).

Phylogenetic tree construction

Phylogenetic tree construction was carried out as outlined in Chapter 2, following multiple alignment using the full-length DNA sequence of *Mla* alleles.

4 *Mla3* confers resistance to multiple pathogens

4.1 Abstract

The majority of NB-LRR-encoding disease resistance genes recognise single pathogen species; few NB-LRRs are known to have the capacity to recognise multiple pathogens. Following fine-mapping of *Mla3*, *Rmo1*, and *Lov1* outlined in the previous chapter, this chapter continues with molecular cloning, transformation, and phenotypic analysis of candidate genes. Using sequence capture and RNAseq, we discovered copy number variation for *Mla3* (*RGH1*; 3 copies), with one expressed copy containing a 6 bp deletion in the LRR region—*Mla3Δ6*. The *RGH2* family member contains an integrated *Exo70F1*, and this is in head-to-head orientation with *RGH3*. The stable transgenic barley found that *Mla3* conditions powdery mildew and rice blast resistance, whereas *Mla3Δ6*, *RGH2-Exo70F1*, and *RGH3* do not confer resistance to either pathogen. Assessment of a diversity panel of barley accessions containing the candidate genes suggests the role of *Mla3* in victorin sensitivity. This work, coupled with the recent discovery of direct interaction of MLA and AVR_a effectors (Saur *et al*., 2019), suggests that MLA3 has the capacity to recognize molecular structures conserved among plant pathogen effectors. Identification of *AVR-Rmo1* from *P. oryzae* and *AVR_{a3}* from *B. graminis* in combination with victorin toxin will provide a means to unravel the underlying mechanism of multiple pathogen recognition by *Mla3*.

4.2 Introduction

A major characteristic of known disease resistance genes encoding nucleotide-binding domain leucine-rice repeat proteins (NB-LRRs) is their ability to recognise a single pathogen, or a subset of isolates within a species. Flor's (1971) seminal work in flax and flax rust established the gene-for-gene hypothesis, postulating that single plant resistance (*R*) gene and avirulence gene of a pathogen determine the outcome of their interactions. When a plant *R* gene recognises a pathogen effector an immune response

is activated. Recognised effectors are subsequently determined avirulence genes for they specify the virulence profile of the pathogen. Direct interactions between *R* genes and effectors were first demonstrated for the tomato serine-threonine protein kinase Pto and *Pseudomonas syringae* AvrPto proteins (Pedley and Martin, 2003; Scofield *et al*., 1996; Tang *et al*., 1996) and for rice NB-LRR Pi-ta and the *Pyricularia oryzae* AVR-Pita proteins (Bryan *et al*., 2000; Jia *et al*., 2000).

Few identified NB-LRRs have the capacity to recognise multiple pathogens (Kourelis and Van Der Hoorn, 2018). The tomato NB-LRR *Mi-1.2* confers race-specific resistance to three species of root-knot nematodes of the genus *Meloidogyne*, the potato aphid (*Macrosiphum euphorbiae*), and sweet potato whiteflies in the genus *Bemisia* (Casteel *et al*., 2006; Milligan *et al*., 1998; Nombela *et al*., 2003; Vos *et al*., 1998). All three species are phloem feeders and *Mi-1.2* is associated with reduced reproduction and abundance of the pests (Casteel *et al*., 2006; Guo *et al*., 2016). Aphid and white fly resistance manifests in the adult plant, whereas root-knot nematode resistance is maintained throughout the life history of the plant (Fiona L Goggin *et al*., 2004; Martinez de Ilarduya *et al*., 2004). In addition, expression of *Mi-1.2* in eggplant (*Solanum melongena*) only provided nematode resistance, suggesting additional components necessary for multiple pathogen resistance (Fiona L. Goggin *et al*., 2004). However, the mechanism of *Mi-1.2*-mediated resistance remains unknown.

The paired *RPS4* and *RRS1* NB-LRRs from *Arabidopsis thaliana* confer resistance to the fungal pathogen *Colletotrichum higginsianum,* and direct-recognition of the effectors *AvrRps4* from *P. syringae* pv. *tomato* and *PopP2* from *Ralstonia solanacearum* (Narusaka *et al*., 2013, 2009). The WRKY-domain of RRS1 C-terminal fusion has been shown to interact with and recognise AvrRps4, and acetylation of the WRKY domain by PopP2 triggers an RPS4-mediated defence response (Sarris *et al.,* 2015; Williams *et al.,* 2014). Mutations and truncations of the RRS1-R allele abolish PopP2—but not AvrRps4—recognition by the NB-LRR pair (Ma *et al*., 2018). In addition, the linked paralogous pair *RRS1-B*/*RPS4-B* only recognises AvrRps4 and not PopP2 (Ma *et al*., 2018; Saucet *et al*., 2015). There are distinct genetic requirements of *RPS4* and *RRS1* for response to *AvrRps4* and *PopP2*; multiple recognition by *RPS4*/*RRS1* occurs via different mechanisms and recognition capacity is varied

between alleles—new alleles may have the capability for additional expanded recognition specificities.

Pathogens have an expanded repertoire of effectors, evolved to disrupt and manipulate multiple different host targets. Pathogens can evade recognition by gene loss or sequence diversification of an effector. Due to this, direct recognition by NB-LRRs without an integrated domain is thought to limit the potential for multiple pathogen recognition. This can be mitigated by NB-LRRs present as diverse allelic series at the population level, and/or if NB-LRRs recognise conserved pathogen effectors. In addition, an indirect mechanism for NB-LRR recognition—such as guarding the modifications of host proteins—buffers against rapidly evolving effectors. For example, RIN4 is the target of diverse effectors of *Pseudomonas* and its cleavage, depletion, or phosphorylation is recognized by both RPS2 and RPM1 NB-LRRs in *A. thaliana* (H.-S. Kim *et al*., 2005; Kim *et al*., 2009; M. G. Kim *et al*., 2005; Liu *et al*., 2011).

Non-NB-LRR resistance mechanisms have also been shown to confer resistance against multiple pathogens. Typically, non-NB-LRR mediated resistance is thought to occur via modifications of the host environment to limit pathogen growth. The wheat *Lr34* gene encodes an ATP binding cassette (ABC) transporter and confers resistance to the three rusts; leaf rust (*Puccinia triticina)*, stripe rust (*P. striiformis),* stem rust (*P. graminis* f. sp. *tritici*); and powdery mildew (*Blumeria graminis*) in adult plants (Chauhan *et al*., 2015; Ellis *et al*., 2014; Krattinger *et al*., 2015, 2009). Lr34 belongs to the same protein family as *A. thaliana* PEN3—an ATP binding cassette transporter involved in penetration resistance—suggesting its role in general plant immunity; PEN3 also confers resistance to non-adapted pathogens (Stein *et al*., 2006). *Lr34* expressed in barley activates multiple defence pathways and provides resistance to *P. triticina* f. sp. *hordei* and *B. graminis* f. sp. *hordei* (*Bgh*)—pathogens of barley which do not normally infect wheat (Chauhan *et al*., 2015; Risk *et al*., 2013). In addition, transgenic rice plants expressing *Lr34* showed increased resistance against multiple isolates of the pathogen *P. oryzae* (Krattinger *et al.,* 2015). These observations across multiple grass species suggest a shared mechanism of resistance against a broad-spectrum of pathogens.

Similar to *Lr34*, the wheat *Lr67* hexose-proton transporter confers quantitative resistance to multiple pathogens of rust and mildew (Ellis *et al*., 2014; Herrera-Foessel *et al*., 2014; Moore *et al*., 2015). *Lr67*-mediated resistance can be transferred to barley, retaining the capability to recognise multiple pathogens (Milne *et al*., 2019). Lr67res, the resistant allele of Lr67, differs by two amino acids compared to the susceptible allele, which render it incapable of transporting glucose (Moore *et al*., 2015). The resistance mechanism is hypothesised to be due to the limitation of sucrose for nutrients or signalling (Milne *et al*., 2019). Both *Lr34* and *Lr67* function in the adult plant, providing partial resistance or slowed pathogen growth. Generally, identified adult plant resistance does not require specific recognition of pathogen effector molecules, differing from the NB-LRR-mediated resistance mechanism which often terminates in the hypersensitive response and cell death (Ellis *et al*., 2014; Milne *et al*., 2019).

While NB-LRRs are associated with resistance to biotrophic pathogens, necrotrophic pathogens exploit these immune receptors: byactivating an immune response to their benefit. Necrotrophic host-selective toxins (HSTs) can act in a similar manner to biotrophic effectors: both function to facilitate infection of host tissue by the pathogen. However, biotrophic pathogens exploit the host whilst maintaining viability, as they require living tissue to complete their life-cycle, whereas necrotrophic pathogens benefit from host cell death (Friesen *et al*., 2008; Lewis, 1973; Wang *et al*., 2014). Biotrophic effectors are under selection to evade recognition, driving complex co-evolutionary relationships between host and pathogen. Necrotrophic effectors actively destroy host tissue through the secretion of broad-acting toxic metabolites and proteins, and through the action of HSTs (Laluk and Mengiste, 2010). Described as inverse gene-for-gene interactions, HSTs only function on hosts with the corresponding susceptibility or sensitivity gene. The NB-LRR *Tsn1* from wheat mediates susceptibility to ToxA produced by the necrotrophic pathogens *Stagonospora nodorum* and *Pyrenophora tritici-repentis* (Faris *et al*., 2010). In *Sorghum bicolor*, the *Pc* locus conditions sensitivity to a HST produced by the fungal pathogen *Periconia circinata* (Nagy and Bennetzen, 2008). Natural resistant alleles, *pc,* harbour rearrangement of a tandemly duplicated NB-LRR family at the locus and arise via unequal crossing over (Nagy *et al*., 2007; Nagy and Bennetzen, 2008). Selection for maintenance of biotrophic resistance must outweigh selection pressure

to lose necrotrophic susceptibility in order to maintain these NB-LRRs in the genome; however, to what degree this is the case is not entirely clear. Of NB-LRRs recognising HSTs characterised to date, biotrophic resistance has yet to be identified (Wang *et al*., 2014).

Sensitivity to the HST victorin produced by *B. victoriae* in barley was mapped to the *Mla3* locus. Genetic coupling of *Mla3, Rmo1*, and *Lov1* was outlined in the previous chapter. Here, *Agrobacterium*-based transformation and phenotypic assessment of three candidate genes—*Mla3*, *Mla3Δ6*, and the paired *RGH2-Exo70F1/RGH3*—is described. We confirm *Mla3* confers resistance to *Bgh* and *P. oryzae*; characterisation of victorin sensitivity is ongoing. Based on the recent work by Saur *et al*., (2019) that suggests direct recognition of effectors from *Bgh* and the comparison with *LOV1*-mediated susceptibility in *A. thaliana*, we propose the two hypotheses for *Mla3* recogntion: a direct mechanism of recognition of multiple pathogens and an indirect recognition mechanism via a guardee—a proposed thioredoxin h family member.

4.3 Results

Candidate *RGH* family members cloned from the *Mla3* locus

As outlined in the previous chapter, *Mla3*, *Rmo1*, and *Lov1* were in complete genetic coupling at the *Mla3* locus. Three NB-LRR gene families are present at the *Mla* locus, *RGH1* (*Mla*), *RGH2*, and *RGH3* (Wei *et al*., 2002, 1999). Using RNAseq and RenSeq-PacBio sequencing, we identified these alleles from barley accession Baronesse. The *RGH1* family member, *Mla3* was found to have at least two copies: a full-length sequence identical to the previously published allele (Seeholzer *et al*., 2010), and an additional copy with a 6 bp deletion in the LRR region (*Mla3Δ6*). From RNAseq data, we estimate there are at least three copies of *Mla3*—two full length, and one *Mla3Δ6* based on the ratio of *Mla3Δ6* transcripts to reads from *Mla3.* The *RGH2* family member has an integrated *Exo70F1* and is hypothesised to function as a pair with *RGH3* due to their head-to-head orientation in the genome and phylogenetic relationship (Bailey *et al*., 2018). Based on screening of a genetic diversity panel in

the previous chapter, *RGH2-Exo70F1* and *RGH3* have been excluded as candidates for *Rmo1* and *Lov1* and were retained as negative controls.

All four candidate genes were cloned via PCR amplification—*Mla3* and *Mla3Δ6* from cDNA, and *RGH2-Exo70F1* and *RGH3* from gDNA. *Mla3* and *Mla3Δ6* were placed in an expression construct containing the *Mla6* promoter and terminator, with *RGH2-Exo70F1* and *RGH3* maintained in the native form and head-to-head orientation. The construct includes ~1.5 kb of *RGH2-Exo70F1* terminator and ~1.1 kb of *RGH3* terminator; the promoters are embedded within the coding sequence of the partner, with ~300 bp sequence between them (Figure 4-1). *RGH2* and *RGH3* have an embedded bi-directional promoter therefore the native promoter and terminator system was used. The *Mla6* promoter/terminator system was selected due to insufficient promoter/terminator regions for *Mla3*, despite the use of RenSeq-PacBio. Use of the *Mla6* expression construct also allows for direct comparison of *Mla6* and *Mla3Δ6* coding sequence by eliminating native promoter variation.

The transformable accession Golden Promise is susceptible to KEN54-20

All constructs were transformed into the barley accession Golden Promise via *Agrobacterium* mediated transformation of immature embryos. Golden Promise is susceptible to *Bgh* and the *P. oryzae* isolate KEN54-20 (*+AVR-Rmo1*) (Figure 4-2). At 24 hours post-inoculation, *P. oryzae* appressoria are clearly visible however no difference is observed between the response of Baronesse and Golden Promise. At 48 hours post-inoculation, cell death is observed in Baronesse with dead cells stained blue through Trypan blue staining (Figure 4-2). Cell death is specific to cells penetrated by *P. oryzae*, as appressoria are present above dead cells and initial short intracellular hyphae are visible; cell death prevents further colonisation by the fungus. In contrast, Golden Promise supports growth of *P. oryzae* and intracellular hyphae are present within cells. No resistance response or cell death is evident in Golden Promise (Figure 4-2).

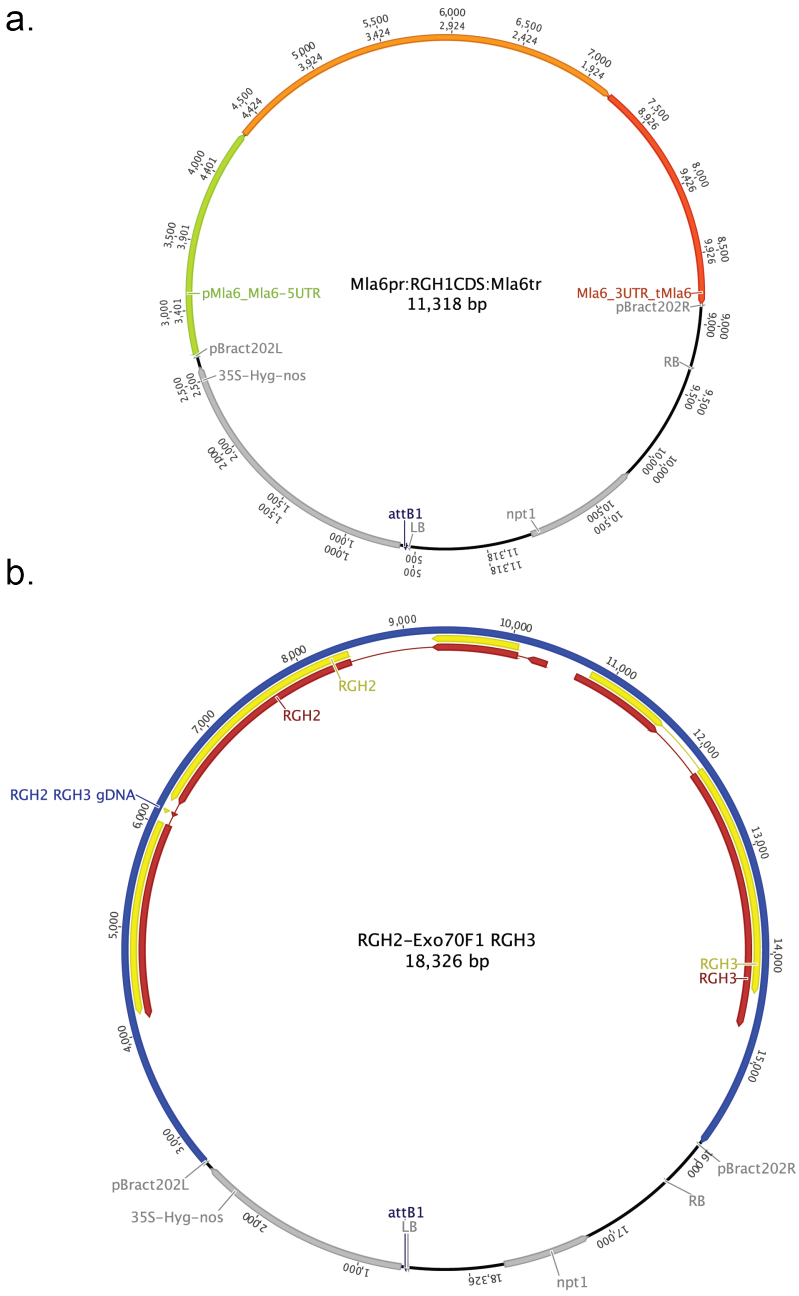

Figure 4-1. Construct maps for *RGH1* and *RGH2-Exo70F1-RGH3* candidate genes.

Generate of constructs of candidate genes, *Mla3*, *Mla3Δ6*, and *RGH2-Exo70F1-RGH3* from cv. Baronesse for *Agrobacterium*-mediated transformation in pBRACT202 vector containing hygromycin plant selectable marker (35S-Hyg-nos; grey) and neomycin phosphotransferase (npt1; grey) conferring kanamycin resistance for bacterial selection. **A)** Construct design using *RGH1* coding sequence (CDS; orange) with *Mla6* promoter (green) and terminator (red) in the pBRACT202 backbone vector. The same construct design was used for *Mla3* and *Mla3Δ6.* **B)** Native RGH2-Exo70F1 and RGH3 construct design in the pBRACT202 backbone vector, including annotations for the mRNA (red) and CDS (yellow).

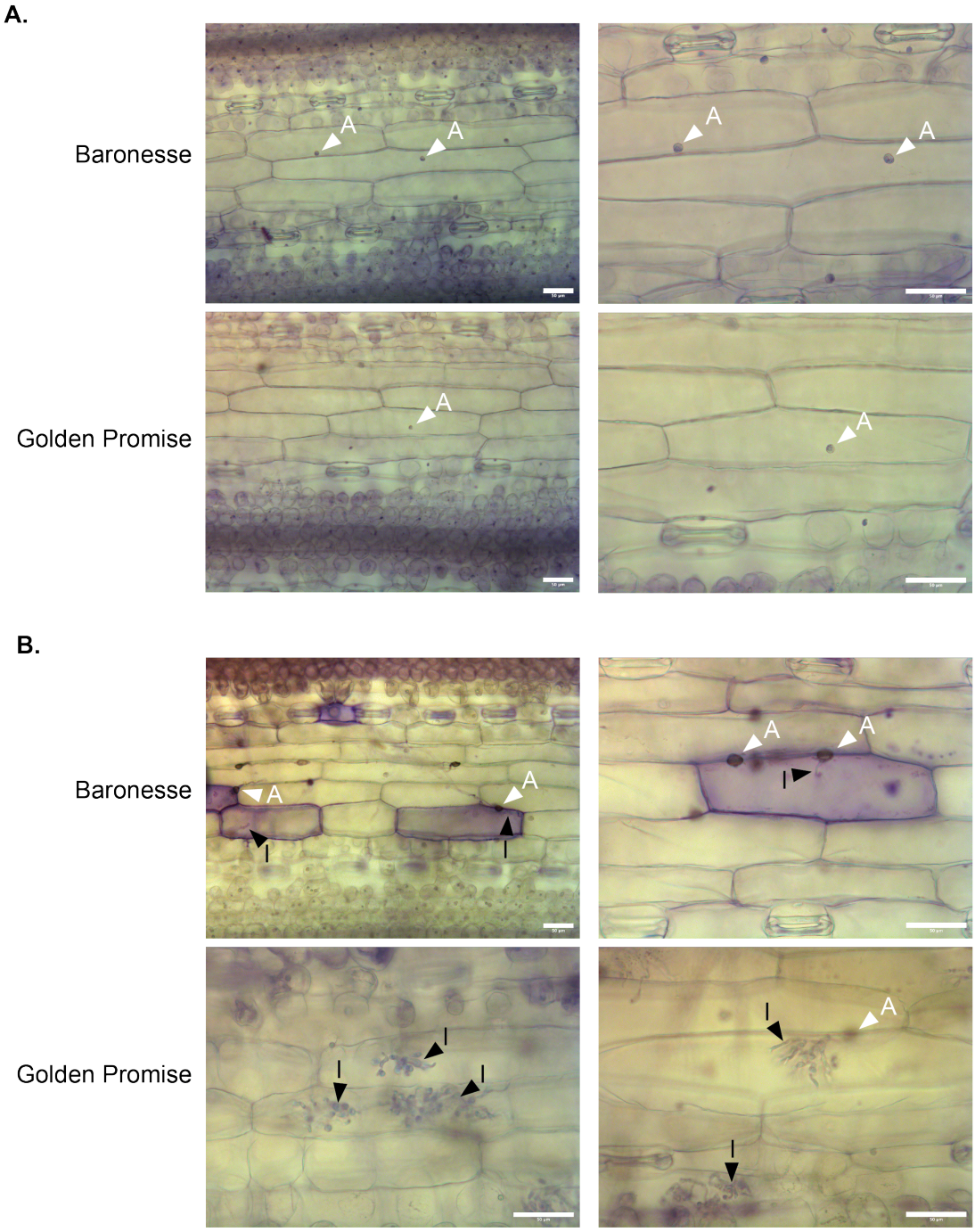

Figure 4-2. Trypan blue staining of *P. oryzae* inoculated Baronesse and Golden Promise.

White scale bars at the *bottom right-hand* of the images indicate 50 µm. Appressoria labelled with white arrows and the letter A; and inter-cellular hyphae labelled with black arrows and the letter I. Accessions Baronesse (resistant) and Golden Promise (susceptible) indicated at the *left-hand side* of the panels. **A)** Twenty-four hours post inoculation. **B)** Forty-eight hours post inoculation.

Mla3 confers resistance to *Bgh*

Mla3, *Mla3*Δ6, and *RGH2-Exo70F1-RGH3* transgenic Golden Promise T_1 families were tested with the *Bgh* isolate CC148 (AVR_{a1}, AVR_{a3}, avr_{a6}). Eight seed from two spikes were evaluated per family. Eight T_1 families were evaluated for *Mla3* (HVT_0665, HVT_0667, HVT_0668, HVT_0669, HVT_0670, HVT_0673, HVT_0674, and HVT_0675); six T_1 families were evaluated for *Mla3*Δ6 (HVT_0266, HVT_0267, HVT_0268, HVT_0269, HVT_0272, and HVT_0275); and eight T_1 families for *RGH2-Exo70F1-RGH3* (HVT_0615, HVT_0620, HVT_0623, HVT_0626, HVT_0634, HVT_0639, HVT_0641, and HVT_0643).

Only full-length *Mla3* was shown to confer resistance to *Bgh* CC148, with all transgenic *Mla3Δ6* lines displaying susceptibility (Figure 4-3). Copy number analysis was performed on the individual lines using qPCR on the selectable marker (hygromycin). For the *Mla3* T_1 families the number of copies ranged from 0 to 6. For the *Mla3Δ6* T_0 lines, the number of copies of the transgenic insert varied from 1 to 4. All *RGH2-Exo70F1-RGH3* transgenic barley lines were susceptible to *Bgh*. Copy number analysis of the *RGH2-Exo70F1-RGH3* T_0 lines varied from 0 to 4 copies. All positive *Mla3* individuals were resistant and all *Mla3*Δ6 and *RGH2-Exo70F1-RGH3* individuals were susceptible, regardless of copy number.

Mla3 confers resistance to *P. oryzae* isolate KEN54-20

Rmo1 confers dominant, race-specific resistance to *P. oryzae* isolate KEN54-20 (Inukai *et al*., 2006). *Mla3*, *Mla3Δ6*, and *RGH2-Exo70F1-RGH3* transgenic T_1 families were screened with *P. oryzae* KEN54-20 using spot inoculation on detached leaves. *Mla3* transgenic lines showed resistance to *P. oryzae* KEN54-20, recapitulating the wild-type phenotype. Analysis of segregating *Mla3* transgenic T_1

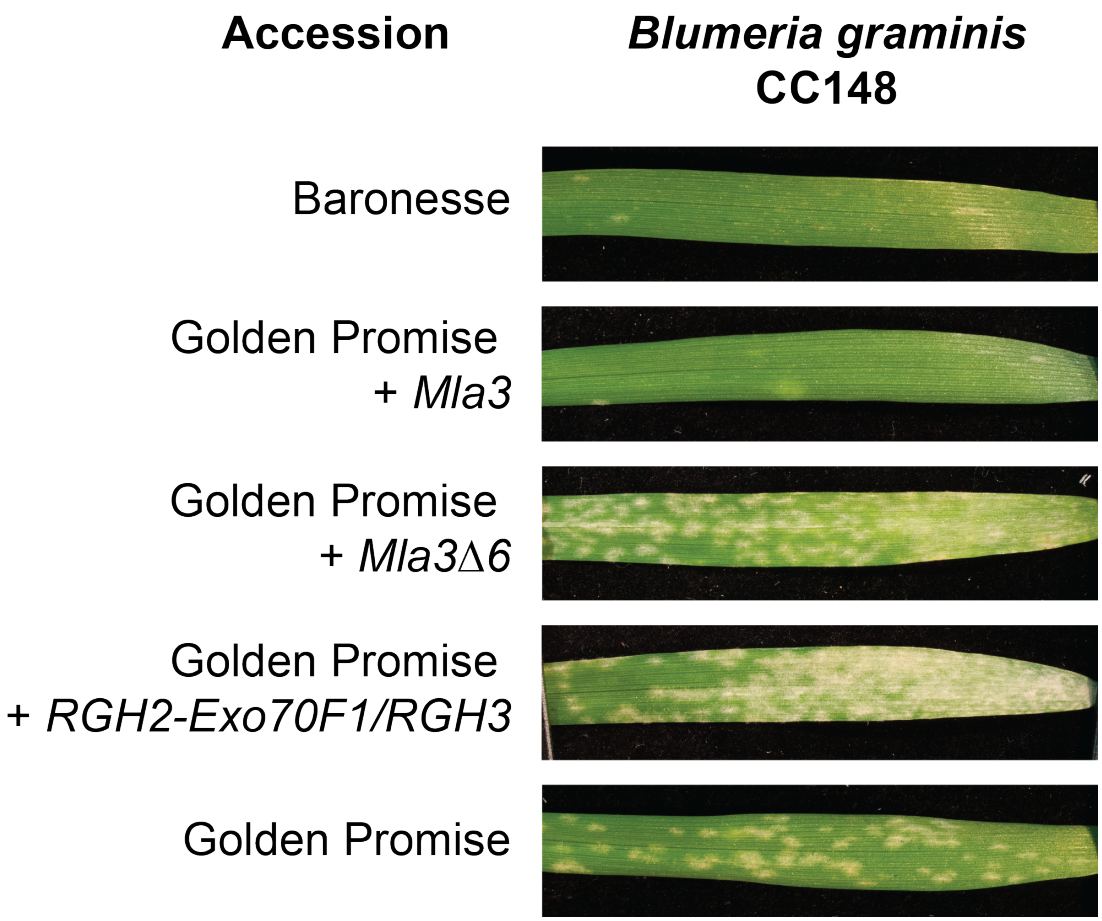

Figure 4-3. *Mla3* confers resistance to *Bgh* isolate CC148.

Transgenic lines of *Mla3*, *Mla3*Δ6, and *RGH2-Exo70F1/RGH3* inoculated with *Bgh* isolate CC148 carrying AVR_{a3}. Controls include resistant wild-type Baronesse and susceptible wild-type Golden Promise used for transformation. Complete resistance shown by Baronesse and transgenic line Golden Promise + *Mla3* (T_1 family HVT_0667), whereas wild-type Golden Promise and transgenic lines Golden Promise + *Mla3Δ6* (T_1 family HVT_0275) and + *RGH2-Exo70F1/RGH3* (T_1 family HVT_0634) are susceptible. Phenotypes are representative of inoculated T_1 families.

families showed phenotypic variation, with some families displaying partial or no resistance. *Mla3*Δ6, and *RGH2-Exo70F1-RGH3* transgenic individuals were fully susceptible (Figure 4-4).

Based on the observation of variable expression in resistance to *P. oryzae* KEN54-20 in contrast to the complete resistance shown for *Bgh* CC148, I hypothesised that sufficient expression of *Mla3* is required to confer resistance. Copy number variation of the individual transgenic lines was evaluated, under the assumption copy number of the insert is correlated with expression. An inverse linear correlation was observed between the number of copies and the *P. oryzae* phenotypic score: multiple copies of *Mla3* were required to complement the wild-type phenotype and confer complete resistance to KEN54-20 (Figure 4-5A). Except for one individual, complete resistance was only observed in individuals carrying two or more copies of the insert; a single copy was insufficient for complementation. Data were collated from the individual lines of the resistant T_1 families and family HVT_0667 contained the highest number of resistant lines due to the segregation of higher insert copy number (Figure 4-5B). Two additional families HVT_0679 and HVT_0680 contained resistant lines with 4 insert copies, showing a resistant phenotype of 1.5. However, complete resistance—a phenotypic score of 0—was only observed for the HVT_0667 family (Figure 4-5B). The transgene is driven by an *Mla6* promoter and is assumed to be comparable to the native *Mla3* promoter. Copy number variation is observed in wild-type Baronesse with an estimated three copies in the haploid genome—two *Mla3*, and one *Mla3*Δ6—resulting in four hypothesised full-length *Mla3* copies in the diploid plant.

MLA3 specifically recognises AVR-Rmo1

Due to the requirement of high copy number (and assumed high expression) being required for complementation in the transgenic lines, we were concerned that the observed resistance could be due to auto-activity of the transgene. Overexpression of NB-LRRs has been shown to cause constitutive defence activation and broad-spectrum disease resistance to multiple pathogens (Lai and Eulgem, 2018; Li *et al*., 2019). To evaluate this, resistant *Mla3* transgenic lines need to be tested with a

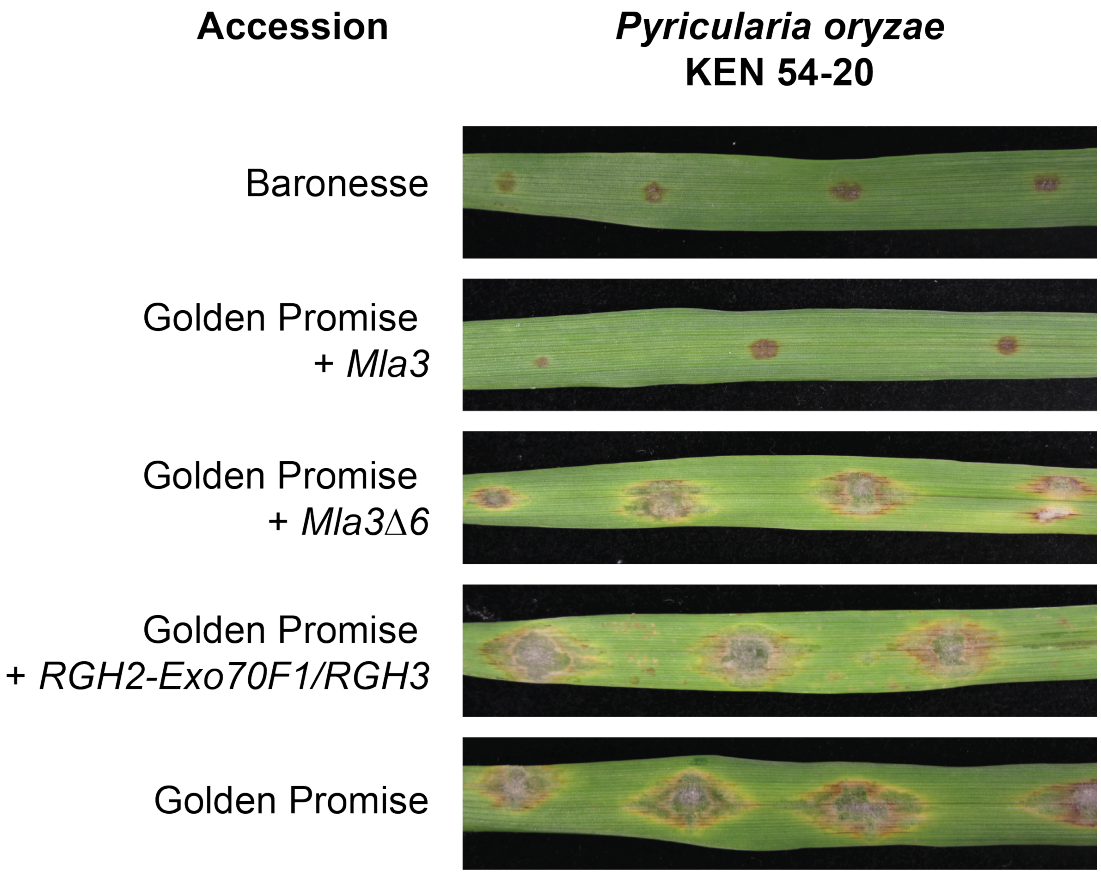

Figure 4-4. *Mla3* confers resistance to *P. oryzae* isolate KEN54-20.

Transgenic lines of *Mla3*, *Mla3*Δ6, and *RGH2-Exo70F1/RGH3* inoculated with *P. oryzae* isolate KEN54-20 containing *AVR-Rmo1*, including controls of WT Baronesse and Golden Promise. Complete resistance shown by WT Baronesse and transgenic line Golden Promise + *Mla3* (HVT_0667), whereas WT Golden Promise and transgenic lines Golden Promise + *Mla3Δ6* (HVT_0522) and + *RGH2-Exo70F1/RGH3* (HVT_0626) are susceptible.

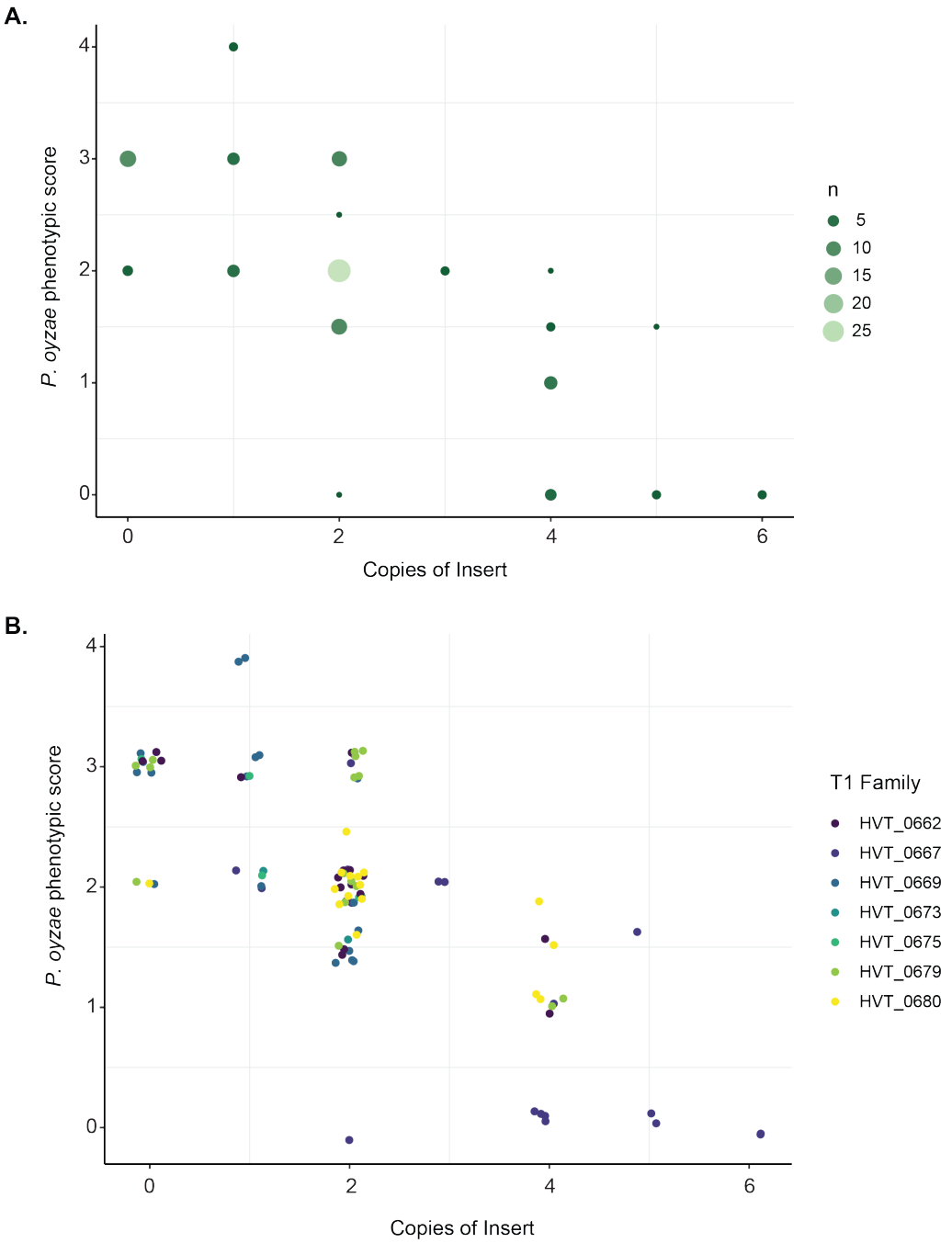

Figure 4-5. *Mla3* transgenic lines carrying multiple copies of the *Mla3* transgene construct are resistant to *P. oryzae* isolate KEN54-20.

T_1 families of Golden Promise + *Mla3* showing resistance with varying copy number (0 to 6) inoculated with *P. oryzae* isolate KEN54-20. Phenotypic scores 0 and 1 = resistant; 2 to 4 = susceptible. A score of 1.5 was given to individuals with resistant lesions with evidence of a very small eyespot, and a score of 2.5 was given to an individual with a mixture of small and large lesions. Data from one replicate with 3 biological replicates. **A)** Number of individual lines from T_1 families with insert copy number for each phenotypic score. Circle size and colour gradient indicate number of individuals at each plot point (small dark green circles = >5 through to large light green circles = 25). **B)** Separation of data shown in A) based on T_1 family.

P. oryzae isolate that is virulent on wild-type Baronesse carrying *Mla3*. Baronesse is susceptible to the *P. oryzae* isolate Sasa2, which lacks *AVR-Rmo1*. Transgenic *Mla3* lines with high copy number, that previously displayed resistance to KEN54-20, were spot inoculated with both KEN54-20 and Sasa2 in single spots in both proximal and distal positions to the leaf base. *Mla3* shows specific recognition of KEN54-20 similar to wild-type Baronesse and fails to provide resistance to Sasa2, with clear susceptible lesions seen (Figure 4-6). Both Golden Promise and Nigrate are susceptible to KEN54-20 and Sasa2. Specific resistance to KEN54-20 was maintained regardless of spot inoculation position on the leaf (Figure 4-7A).

Mla3 confers a specific and clear resistance phenotype to KEN54-20. This can be used for screening of KEN54-20 mutants for a gain-of-virulence or loss of *AVR-Rmo1* function in order to identify *AVR-Rmo1*. Mutants of *P. oryzae* isolate KEN54-20 were generated using UV mutagenesis and isolated from susceptible lesions on wild-type Baronesse following a spray-based inoculation of irradiated spores. Loss of *AVR-Rmo1* function was confirmed following re-inoculation on Baronesse using a spot-based method—currently a single mutant KEN54-20 M1 has been confirmed. Spot inoculations using KEN54-20 and the mutant KEN54-20 M1 were repeated on the resistant transgenic lines as described previously for the isolate Sasa2. Barley accession Golden Promise carrying *Mla3* confers specific resistance through recognition of *P. oryzae* isolate KEN54-20, as the mutant KEN54-20 M1 was virulent in both proximal and distal positions on the leaf (Figure 4-7B).

AVR-Rmo1 is present in multiple isolates

The presence of *AVR-Rmo1* determines the compatibility of *P. oryzae* isolates on barley lines carrying *Mla3*. Despite *AVR-Rmo1* remaining unknown, different *P. oryzae* isolates can be evaluated for the prevalence of *AVR-Rmo1* within the population. A diversity panel of 20 Japanese *P. oryzae* isolates were inoculated on Baronesse. Inoculations were performed using a spot inoculation of the first leaf on whole plants in the laboratory of Professor Ryohei Terauchi. Of the diversity panel, 9 isolates were avirulent and are presumed to carry *AVR-Rmo1* (Table 4-1). Additional

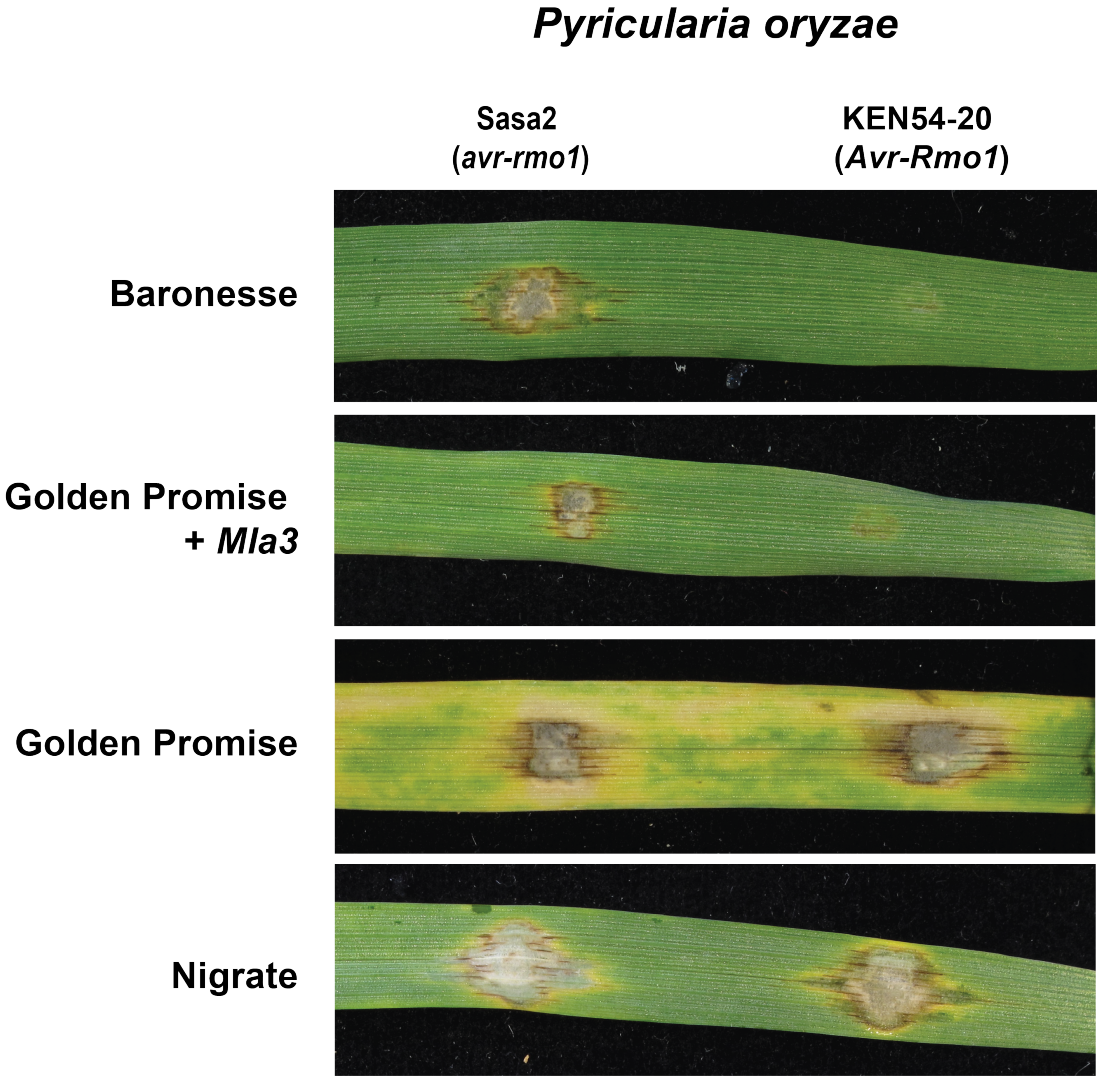

Figure 4-6. *Mla3* specifically recognises AVR-Rmo1.

Transgenic Golden Promise + *Mla3* (HVT_0934) spot inoculated with *P. oryzae* isolates KEN54-20 (+*AVR-Rmo1*) and Sasa2 (-*AVR-Rmo1*). *Mla3* confers resistance to only isolates carrying *AVR-Rmo1*. Transgenic line Golden Promise +*Mla3* HVT_0934 T_2 used, from T_1 family HVT_0667. Controls Golden Promise used for transformation and hyper-susceptible Nigrate are susceptible to both Sasa2 and KEN54-20.

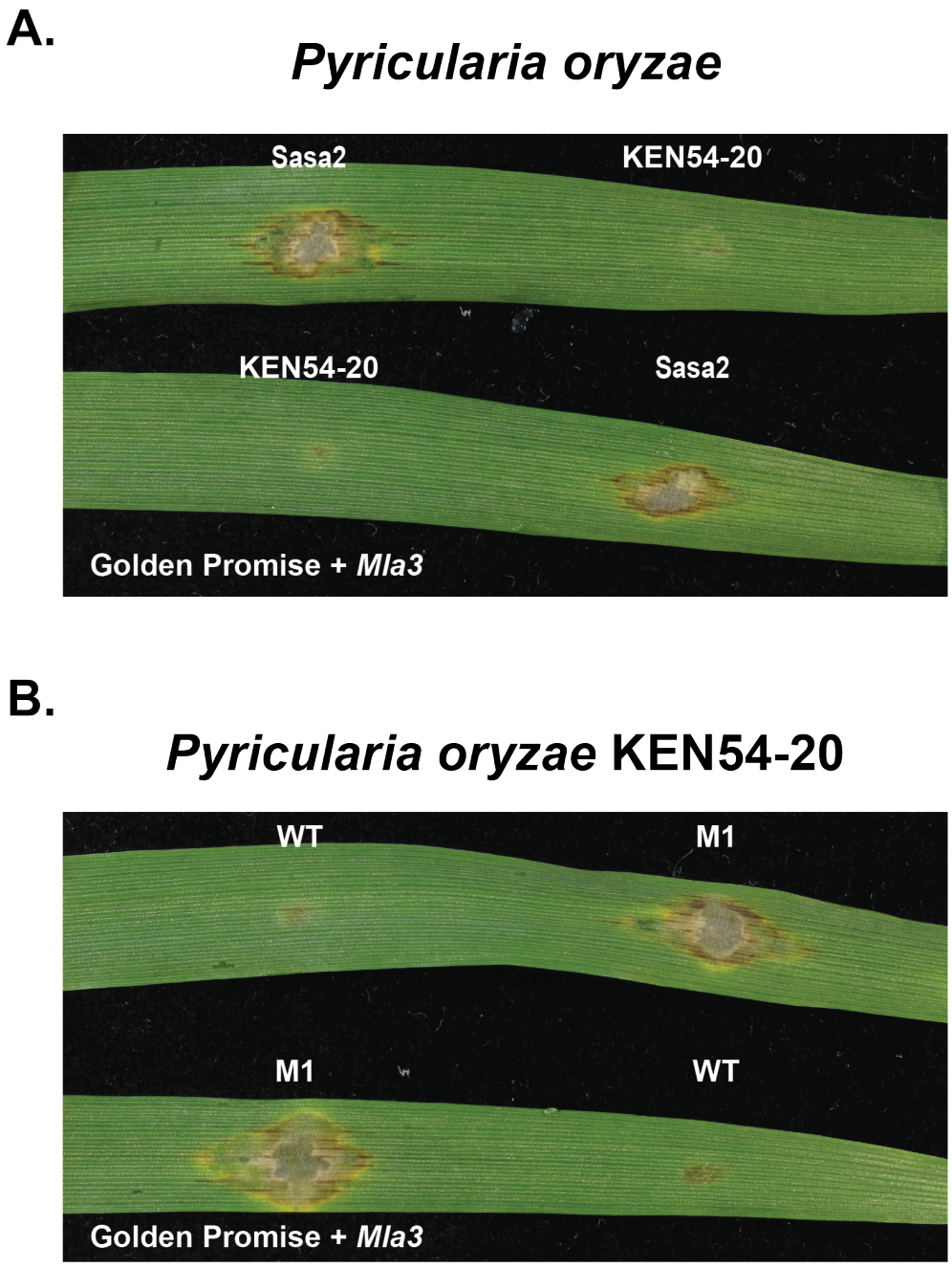

Figure 4-7. *Mla3* specifically recognises AVR-Rmo1.

Transgenic line Golden Promise +*Mla3* HVT_0934 T_2 used, from T_1 family HVT_0667. **A)** Transgenic Golden Promise + *Mla3* spot inoculated with *P. oryzae* isolates KEN54-20 (+*AVR-Rmo1*) and Sasa2 (-*AVR-Rmo1*). *Mla3* confers resistance to only isolates carrying *AVR-Rmo1* regardless of localisation of spot inoculation on leaf. **B)** Transgenic Golden Promise + *Mla3* spot inoculated with *P. oryzae* isolate KEN54-20 (+*AVR-Rmo1*) and a loss-of-*AVR-Rmo1* recognition mutant KEN54-20 M1. *Mla3* confers resistance to only KEN54-20 carrying *AVR-Rmo1* regardless of localisation of spot inoculation on leaf.

Table 4-1. Diversity panel of 20 *P. oryzae* isolates inoculated on barley accession Baronesse (*Mla3*/*Rmo1*/*Lov1*).

P. oryzae isolate	HB_0243	HB_0245
Ina168 WT	-	S
Naga69-150 (30733)	-	R
2403-1	S	S
2012-1	R	R
24-22-1-1	-	S
85-141	S	S
Ina87T-56A	R	R
83R-131B	-	S
SL91-48D	R	S
H98-315-1	R	S
Sasamori121	-	S
0423-1	R	S
Ao92-06-02	R	S
TH68-126	-	R
TH68-140	-	R
TH68-141	-	R
Sasa2	S	S
Ina85-182 #E	R	-
Ken 54-20	R	R

Phenotypes from two experiments where R = resistant, S = susceptible. Hyphen indicates isolate not used in the experiment.

replicates will be performed using spot inoculations on detached leaves to confirm phenotypes. Association genetics on these isolates and sequencing of mutagenized KEN54-20 isolate will provide powerful tools in the identification of *AVR-Rmo1*.

4.4 Discussion

Following the confirmation of the genetic coupling of *Mla3*, *Rmo1*, and *Lov1* outlined in the previous chapter, this chapter details the characterisation of candidate genes at the *Mla3* locus. The *Mla* locus is a resistance gene cluster containing three NB-LRR gene families. This region experiences suppressed recombination between haplotypes due to the presence of multiple repetitive regions, mobile elements, and different duplication events (Wei *et al*., 1999). Due to this, the *Mla* locus is unable to be assembled using current long read sequencing technologies and characterisation of the locus across barley haplotypes has been limited. RNA sequencing on 40 barley accessions found presence/absence, sequence, and copy number variation of the three NB-LRR gene families—*RGH1*, *RGH2*, and *RGH3*—including the integrated *Exo70F1* within *RGH2* alleles (Chapter 2).

Here, the *RGH1* family experiences copy number variation and within the accession Baronesse (*Mla3*/*Rmo1*/*Lov1*), full length *Mla3* and *Mla3Δ6* with a 6 bp deletion in the LRR are present. The *RGH2-Exo70F1* and *RGH3* alleles present are hypothesised to work as a pair due to their phylogenetic relationship and head-to-head orientation in the genome. The candidate genes were cloned via PCR, assembled into expression constructs, and transformed into susceptible barley accession Golden Promise. Screening of a diversity panel of accessions harbouring the same alleles of *RGH1*, *RGH2*, and *RGH3* as Baronesse in the previous chapter, *RGH2-Exo70F1* and *RGH3* were excluded for conferring *Rmo1*-mediated resistance and *Lov1*-mediated susceptibility. Therefore, complementation was used to assess *Mla3* and *Mla3Δ6* function. Due to copy number variation of *RGH1* family members and the small 6 bp polymorphism between alleles a silencing approach (such as using *Barley Stripe Mosaic Virus*) would be unreliable. Baronesse is also unable to be transformed so Cas9-mediated knock out was unfeasible.

Mla3 was shown to confer resistance to both *Bgh* and *P. oryzae*, recognising both AVR_{a3} and *AVR-Rmo1* respectively. Neither *Mla3Δ6* or *RGH2-Exo70F1-RGH3* conferred resistance to either pathogen. Resistance to *P. oryzae* was shown to require multiple copies of *Mla3*, whereas a single copy was sufficient for *Bgh* resistance. Furthermore, resistance to *P. oryzae* was specific to isolates carrying *AVR-Rmo1* as Sasa2 (-*AVR-Rmo1*) and a mutant of KEN54-20 M1 with loss-of-*AVR-Rmo1* function were virulent on resistant transgenics. Characterisation of transgenic lines for victorin sensitivity is ongoing. *Mla3* is a single NB-LRR that is able to recognise two distinct pathogens; the hypothesis for *Mla3* also conferring sensitivity to a necrotrophic HST is currently being tested.

Although the majority of single NB-LRRs are pathogen species- or isolate-specific, a broader recognition specificity in a species can be maintained via allelic series within populations (Brown and Tellier, 2011; Dangl and Jones, 2001). Such polymorphisms are maintained through frequency dependent selection and balancing selection, as discussed in previous chapters. *Mla* alleles have been well characterised for conferring isolate-specific resistance to *Bgh* via functional divergence of alleles (Jørgensen, 1994; Saur *et al*., 2019), yet their potential for multiple pathogen recognition is only now being realised (Moscou personal communication). Homologs of *Mla*, *Sr33* in wheat (*Triticum aestivum*) and *Sr50* in rye (*Secale cereale*), confer disease resistance to diverse races of stem rust pathogen *Puccinia graminis* f. sp. *tritici*, including virulent isolate TTKSK (Chen *et al*., 2017; Periyannan *et al*., 2013). *Mla*, *Sr33*, and *Sr50* highlight the potential for orthologous genes to evolve new and different pathogen specificities.

Saur *et al*., (2019) described a direct recognition mechanism of *Bgh* effectors, AVR_{a7}, AVR_{a9}, AVR_{a10}, and $AVR_{a22,}$ by *Mla* alleles, MLA7, MLA9, MLA10, and MLA22 respectively. These *Bgh* effectors are sequence unrelated, apart from the allelic AVR_{a10}, and $AVR_{a22,}$ highlighting the capability of *Mla* alleles to recognise diverse pathogen proteins. Similarly, the wheat *Pm3* NB-LRR alleles control isolate-specific resistance to wheat powdery mildew (*Blumeria graminis* f. sp. *tritici*), interacting through specific allele-effector combinations (Bourras *et al*., 2019, 2016, 2015). Sequence and functional diversity in alleles of the *Arabidopsis* NB-LRR *RPP13*

confer specificity of resistance to the oomycete pathogen *Peronospora parasitica* in a comparable manner (Allen *et al*., 2004; Ding *et al*., 2007a; Hall *et al*., 2009; Rose *et al*., 2004).

Alleles of NB-LRRs can also provide resistance to very different pathogens. The Arabidopsis *RPP8* gene family encodes NB-LRRs with diverse resistance specificities, with alleles conferring resistance to the oomycete *H. arabidopsidis* (*RPP8*); *Turnip crinkle virus* (*HRT*), and *Cucumber mosaic virus* (*RCY1*) (Cooley *et al*., 2000; Kuang *et al*., 2008; McDowell *et al*., 1998; Takahashi *et al*., 2002). Unequal crossing over that generates chimaeras between alleles is thought to be a driving force for new *RPP8* specificities (Ding *et al*., 2007b; McDowell *et al*., 1998).

Few single genes have been identified that confer resistance to multiple pathogens. Of these, even fewer encode NB-LRRs. The paired NB-LRRs *RPS4*/*RRS1* confer complete resistance through the direct recognition of pathogen effector molecules (Ma *et al*., 2018; Narusaka *et al*., 2017). Tomato NB-LRR *Mi-1.2* reduces pathogen abundance and life cycle completion through an as yet unknown mechanism (Goggin *et al*., 2006), in comparison to the defence-initiated cell death shown by *RPS4/RRS1*. This opens the potential for new mechanisms of immune defence regulated by NB-LRRs, not only terminating in cell death and the hypersensitive response. *Mla3*-mediated resistance results in cell death for *P. oryzae* (Figure 4-2) and *Bgh*, and is hypothesised upon recognition of victorin. These observations would suggest a shared downstream signalling cascade and immune response in all three interactions; however, each pathogen may require a different threshold level of immune response in order for resistance.

Multiple copies of *Mla3* are required to confer resistance to *P. oryzae* (Figure 4-5), yet a single copy was sufficient for resistance to *Bgh*. This could be due to a difference in requirement for expression level—assuming copy number correlates with expression and *Mla6* and *Mla3* promoters are comparable. Multiple copies of *Mla3* are present in wild-type Baronesse (*Mla3/Rmo1/Lov1*); if a single copy is sufficient for *Bgh* resistance, is recognition of *P. oryzae* or another unknown pathogen driving an increase in expression? *Mla* is an intracellular immune receptor; differential requirements could be due to variation between pathogens in effector expression or

presence within in cell. The threshold requirement for effector recognition could also be different between pathogens due to effector protein abundance, signalling initiation, overcoming immune suppression by the pathogen, or additional unknown factors. Only a single isolate of *Bgh* was used in this study and inoculating with diverse *Bgh* isolates carrying AVR_{a3} would test if a single copy of *Mla3* is sufficient for resistance in all cases. More virulent isolates, or the presence of suppressors of recognition, may require a higher copy number of *Mla3* to show the same level of resistance. In constrast, *P. oryzae* isolate KEN54-20 may also secrete suppressors of resistance or recognition. Identifying less virulent isolates carrying *AVR-Rmo1* or transforming *AVR-Rmo1* into less virulent isolates for inoculation of the *Mla3* transgenic panel may result in a lower copy number being sufficient for resistance.

Increased expression level required for function could be driving duplication and copy number variation observed between *Mla* alleles. NB-LRRs are under tight regulation to prevent auto-activity and unwanted cell death; gene duplications are hypothesised to be an easier evolutionary route to increased expression rather than promoter mutations that could lead to deleterious consequences (Lai and Eulgem, 2018). The mechanism for increased resistance following higher expression, and the potential for newly acquired recognition to multiple pathogens is as yet unknown.

Following NB-LRR duplication, there is opportunity for diversification and the evolution of new recognition specificities, however, the majority of duplicated *R* genes undergo pseudogenisation (Michelmore and Meyers, 1998). Copy number variation at the *Rgh1* locus in soybean modulates resistance to soybean cyst nematode; the resistant *Rgh1-b* haplotype contains 10 tandem copies of the required three genes for resistance. Susceptible cultivars have only one copy present per haploid genome (Cook *et al*., 2012; Lee *et al*., 2015). Resistance can be recapitulated through overexpression of the three required genes in the locus that encode an amino acid transporter, an α-SNAP protein, and a WI12 (wound-inducible domain) protein, supporting the hypothesis that gene expression dosage is causal (Cook *et al*., 2012). Although this region does not contain NB-LRR genes, this dose dependency is consistent with previous observations of a required threshold of *R* genes for effective resistance (Bieri *et al*., 2004; Holt *et al*., 2005; Lai and Eulgem, 2018). Here, gene

duplications would lead to selection against sequence divergence of paralogs in order to retain recognition specificity. Copy number variation in *Mla3* alleles could be a result of relaxed purifying selection on additional *Mla3* copies above the required expression threshold. *Mla3Δ6* could be an example of a new unknown recognition specificity. It is important to note the distinction of copy number variation from overexpression and auto-activity (Lee and Yeom, 2015) as specificity of *Mla3* to *AVR-Rmo1* is retained (Figure 4-6, Figure 4-7).

The direct recognition of *Mla* alleles (and homologs of *Mla*) is supported through yeast-two-hybrid assay and *Nicotiana benthamiana* infiltration assay, where co-expression of MLA and *Bgh* AVRs is sufficient to trigger cell death (Chen *et al*., 2017; Saur *et al*., 2019). However, crystal structures of direct binding have not been solved, so the presence of additional proteins in complex or as additional recognition requirements cannot be excluded. The direct recognition of two different pathogens by *Mla3* could be achieved via a shared structural conformation of AVR_{a3} and AVR-Rmo1, effector-mediated protein modifications of *Mla3* leading to immune activation, or the presence of an additional proteins conserved across species.

Direct binding of MLA3 and AVR_{a3} has not yet been demonstrated. It is possible that *Mla* alleles could mediate recognition via different mechanisms, as different requirements for the signalling component *Rar1* has demonstrated between alleles (Halterman and Wise, 2004; Shen *et al*., 2003). A simpler model for multiple pathogen recognition is via the guard model—where an NB-LRR monitors a host protein for pathogen-mediated modification. Multiple pathogens can target the same host protein, thought to be 'hubs' for immune receptor signalling or shared susceptibility targets. RIN4 is a known example, its perturbation is guarded by two NB-LRRs in *A. thaliana* (Axtell and Staskawicz, 2003; H.-S. Kim *et al*., 2005; Kim *et al*., 2009; M. G. Kim *et al*., 2005; Mackey *et al*., 2003, 2002; Russell *et al*., 2015), and by alleles of *RPG1* in soybean (*Glycine max*) (Ashfield *et al*., 2014; Whitham *et al*., 2016). The guarding of RIN4 has evolved convergently as soybean *RPG1* is not an ortholog of *A. thaliana RPM1* (McDowell, 2004). The hypothesis of *Mla3* conferring sensitivity to the HST victorin also challenges this direct recognition model. The mechanism of victorin sensitivity in *A. thaliana* is mediated through *LOV1*, an NB-LRR, guarding a

thioredoxin h5. Victorin binding to the thioredoxin h5 triggers *LOV1*, resulting in cell death and sensitivity (Lorang *et al*., 2012; Wolpert and Lorang, 2016). Thioredoxins are highly conserved across species and regulate redox-mediated immune signalling pathways: thioredoxin h5 mediates specificity and reversibility during salicylic acid-dependent plant immunity (Kneeshaw *et al*., 2014; Mata-Pérez and Spoel, 2019). As thioredoxins are also present in yeast, the assays used to evaluate the direct binding of MLA and *Bgh* AVRs are not independent of thioredoxins (Gan, 1991). Once AVR_{a3} and *AVR-Rmo1* have been identified, this hypothesis can be investigated.

Clear hypotheses for the mechanism of *Mla3*-mediated multiple pathogen recognition are limited by a dearth of similar examples. *A. thaliana RPS4*/*RRS1* remain the best characterised NB-LRRs conferring recognition of multiple pathogens and RIN4 the best described guardee across species (Kourelis and Van Der Hoorn, 2018). In comparison, knowledge of necrotrophic pathogen interactions is even more sparse: only *A. thaliana RLM3* (TIR-NB class protein) has been associated with resistance to necrotrophic pathogens (Mengiste, 2012; Staal *et al*., 2008) and few NB-LRRs have been identified as sensitivity or susceptibility genes. Wheat *Tsn1*, an NB-LRR with an integrated serine/threonine protein kinase domain, confers sensitivity to the HST ToxA produced by both *Stagonospora nodorum* and *Pyrenophora tritici-repentis* (Chu *et al*., 2010; Faris *et al*., 2010; Friesen *et al*., 2008; Liu *et al*., 2017, 2006). In addition, in sorghum, the NB-LRR *Pc* mediates sensitivity to the PC toxin produced by *Periconia circinata* (Nagy and Bennetzen, 2008). While the NB-LRR-mediated immune response is effective against biotrophic pathogens, it remains as a susceptibility factor for necrotrophic pathogens.

Comparing the structure and binding interfaces of victorin with effector candidates from *Bgh* and *P. oryzae* would provide an initial step in effector identification. Recognised *Bgh* alleles are sequence un-related yet hypothesised to share a conserved structural fold; this could represent a core structure of pathogen effectors shared across species. Resolving the structure of AVR_{a3} and AVR-Rmo1 will allow for the identification of new specificities for *Mla* alleles, with the opportunity for engineering resistance against multiple pathogens. Characterisation of *Bgh* and *P. oryzae* recognition by *Mla3* provides the second example of a single NB-LRR conferring

multiple pathogen recognition. Following confirmation of victorin, *Mla3* could provide the first NB-LRR sensitivity gene with known biotrophic resistance function.

4.5 Materials and methods

Oligonucleotides (primers)

Primers were designed and were assessed for GC content (~50%) and secondary structures using mfold (Zuker, 2003). Primers were synthesised from Integrated DNA Technologies and Sigma-Aldrich using a standard desalting purification method at a stock concentration of 100 μM and stored at -20°C. Working solutions were diluted to 10 μM. Primers used for polymerase chain reaction (PCR) for gene amplification and construct development are listed in Appendix Table 7-9.

Polymerase chain reaction (PCR) and *E. coli* transformation

Polymerase chain reactions (PCRs) were carried out to amplify regions of DNA for molecular cloning and to confirm the presence of target plasmids in transformed bacterial colonies—referred to as colony PCRs. *E. coli* colonies were touched with a pipette tip and diluted directly into the PCR reaction mix for colony PCRs. PCR reactions were performed using GoTaq G2 Flexi DNA polymerase (Promega; Catalogue number M7805), Phusion High Fidelity DNA polymerase (New England Biolabs Ltd; Catalogue number M0530S) and GoTaq Long PCR Master Mix (Promega; Catalogue number M4020). Reaction mixes were set up as per manufacturing instructions and reactions performed in a G-STORM and Bio-Rad thermal cycler. cDNA was used as the template for cloning of the *RGH1* candidate genes, and gDNA the template for the *RGH2-Exo70F1* and *RGH3* construct. Annealing temperatures and elongation times were optimised for reaction based on primer combination.

Example PCR program for Phusion PCR:

PCR step	Temperature (ºC)	Time (seconds)	Number of cycles
Priming	95		1
Denaturing	95	30	30/32
Annealing	Variable	15	
Extension	72	30s/1kb	
Final extension	72	1min/1kb	1
Hold	16	∞	1

Example PCR program for colony PCR:

PCR step	Temperature (ºC)	Time	Number of cycles
Initial denaturation	95	7 min	1
Denaturing	95	30 sec	
Annealing	Variable	30 sec	
Extension	72	1 min/1kb	
Final extension	72	5 min	1
Hold	16	∞	1

PCR reactions were run on a 1% agarose gel in TBE buffer, longer fragments were run in a TAE buffer for cleaner band separation. Gel extraction of fragments was performed with the QIAquick gel extraction kit (Qiagen; Cat No.: 28704) according to the manufacturer's instructions. Excised and cleaned fragments were A-tailed via incubation at 72ºC for 20 mins using GoTaq polymerase and dATPs. A-tailed fragments were cloned via the TOPO XL PCR Cloning Kit (Invitrogen; K7030-20) according to manufacturer's instructions and transformed into DH5α *E. coli* competent cells (1 – 2 µl reaction into 50 µl cells). Transformations were kept on ice for 30 mins, heat-shocked at 42 ºC for 90 secs, then ice for 2 mins; recovered in 500 µl L media via shaking at 37 ºC for 1 hour; and plated on L media plates in varying dilutions with appropriate selection for overnight growth at 37 ºC . Positive clones were identified using colony PCR as described previously using specific primers for amplification of the insert. Plasmids were extracted from positive colonies using 5 ml liquid cultures with the NucleoSpin Plasmid Purification kit (Macherey-Nagel; Ref.: 11932392) and Sanger sequenced (GATC; 80 - 100 ng/ plasmid DNA, 5 µM primer). Plasmids were also confirmed through digestion with the restriction enzyme *EcoRI* (New England Biolabs; Ref.: R3101S) according to the manufacturer's instructions.

Presence of *Mla3Δ6* and differentiation between *Mla3* was assessed via digestion with *BspLI* (Thermo Scientific; Cat No.: ER1151) which cuts on the 6bp indel.

Construct development

Constructs were assembled via multiple PCR fragments into the pBract202 vector backbone. pBract202 was generated by the Crop Transformation (BRACT) team at the John Innes Centre, Norwich, UK (Smedley and Harwood, 2015). The backbone contains the npt1 Kanamycin resistance gene for bacterial selection and the left border contains the 35S hygromycin selectable marker used for plant transformation.

Primers for Gibson Assembly consisted of 20bp fusion from both fragments to be assembled (40bp total) and were assessed for GC content (~50%) and secondary structures using mfold (Zuker, 2003) (Appendix Table 7-9). Constructs were assembled via using Gibson Assembly (Gibson *et al*., 2008) with a Gibson Assembly master mix (New England Biolabs; Ref.: E2611). Gibson Assembly is used for the assembly of large DNA constructs in a single tube isothermal reaction. Briefly, multiple overlapping gene fragments are designed and amplified via PCR; appropriate overlaps are unique ~18bp overhangs. Overlaps were added using the high fidelity Phusion polymerase. PCR products were digested with DpnI (New England Biolabs; Ref.: R0176S) to remove circular DNA. Fragments were resolved with gel electrophoresis (1% agarose in 1x TAE buffer) and excised using the Zymoclean Gel DNA Recovery Kit (Zymo Research; Ref.: D4008) for elution of high-concentration ultra-pure DNA. Fragments were added to the reaction tube in appropriate dilutions and ratios according to molecular weight, as outlined in the manufacturer's instructions. The reaction tube was incubated at 50°C for 1 hour – fragments trimmed by an exonuclease creating single-stranded 3' overhangs that anneal with their complementary counterparts, DNA polymerase extends 3' ends of annealed fragments, and sealed with a DNA ligase. Competent *E. coli* DH5α cells were transformed with the successful construct as outlined above. Construct visualisation, primer development, and assessment was performed using the software Geneious (Version 9.0.5). Sequencing was performed by the company GATC using the Sanger sequencing method.

The *Mla3* and *Mla3Δ6* coding sequences (CDS) were amplified from cDNA isolated from barley accession Baronesse. The CDS was cloned into the pBract202 vector backbone containing the *Mla6* promoter and terminator sequence.

The native *RGH2-Exo70F1-RGH3* construct was amplified from gDNA from barley accession Baronesse using primers designed on the contig identified via Renseq PacBio sequencing. The final construct contains the CDS of RGH2-Exo70F1 and RGH3 in native head-to-head orientation with 2 kb of native promoter and terminator sequence into the pBract202 vector backbone.

Generation of transgenic barley

Constructs were transformed into *Agrobacterium tumefaciens* AGL1 containing pSoup via electroporation (~100 ng plasmid into 50 µl cells), recovered in 500 µl L medium via shaking at 28°C for 2 hours, and grown on L media plates with appropriate selection for three days. Barley accession Golden Promise was transformed with via *Agrobacterium*-mediated transformation via the transformation team at TSL.

Copy number assessment of transgenics

Assessment of insert copy number of transgenic lines was performed via iDna Genetics Ltd (Norwich, UK) using a TaqMan Assay. Samples were analysed for copy number using real-time PCR using hygromycin gene sequence primers present on the transformed construct.

Pyricularia oryzae assays and mutagenesis

P. oryzae isolates were maintained, prepared, and inoculated as outlined in the previous chapter. Phenotypic assessment and copy number of insert was performed using Rstudio (Version 1.1.463) and the ggplot2 package (Version 3.1.0) (Wickham, 2016).

Mutagenesis of *P. oryzae* isolate KEN54-20 was performed on the conidal suspension using ultraviolet light (UV). Spore concentration was adjusted to 1 x 10^5 spores per ml and placed inside a petri dish until the solution was just covering the entire base of the dish – a shallow depth is required to ensure even UV light penetration. The open petri dish was placed inside a UV Stratalinker 2400 (Stratagene) and exposed to set UV light. A dosage curve was generated to assess the UV dose at which spore death was at 50%, for KEN54-20 this was 20 seconds. The UV light exposed conidal suspension was then used for a spray-based inoculation as outlined in the previous chapter. Wild-type Baronesse was used for the isolation of KEN54-20 gain-of-virulence mutants. Lesions were isolated from leaves 7 dpi, sterilised in ethanol for 30 seconds, and placed on Potato Dextrose Agar (10g PDA, 6.25g agar per litre of H_20). *P. oryzae* growth was sampled from each lesion, cultured, and re-inoculated onto Baronesse to confirm gain-of-virulence.

Trypan blue staining

The excised plant tissues were placed inside a 15ml Corning tube and immersed in trypan blue staining solution (2.5 mg ml–1 trypan blue in lactophenol (lactic acid, glycerol, liquid phenol and H2O in a ratio of 1:1:1:1)). Samples were boiled in a water bath in a fume hood for 1-2 minutes. Trypan blue staining solution was removed and replaced with chloral hydrate (Sigma Aldrich; CAS Number 302-17-0) at a concentration of 2.5 g/ml. Samples were placed in a rotator mixer for 24 hours with replacement of fresh chloral hydrate solution. Samples were maintained in 50 mM Tris at ph 7.5 prior to mounting for microscopy.

Blumeria graminis assay

Bgh isolate CC148 was obtained from James Brown (John Innes Centre) maintained on detached leaves on agar media. *Bgh* inoculations were carried out on seedlings at emergence of the second leaf. *Bgh* inoculum was maintained on susceptible barley varieties. Inoculation was carried out by laying pots on their side and gently shaking infected leaves over both sides.

5 Fine mapping of *QRps1H* conferring APR to *Puccinia*

5.1 Abstract

Resistance to plant pathogens is developmentally regulated; expression can occur during the seedling, adult, or all stages of the plant lifecycle. Previous work by Castro *et al*., (2003) identified an adult plant resistance QTL—*QRps1H*—that encompasses the *Mla* locus and developed a near-isogenic line containing this locus in a Baronesse genetic background (Verhoeven *et al*., 2011). This chapter outlines the fine-mapping of *QRps1H* through the development homozygous recombinant lines, marker saturation at the *QRps1H* locus, and field-based assessment of resistance contributed by this locus.

5.2 Introduction

Humans have been selectively breeding grass species such as wheat, barley and maize for traits such as flavour, ease of processing, and large grains throughout history to create the domesticated cereals we know today. The ability to resist disease was an important factor in crop selection as our ancestors were routinely plagued by pathogens causing mildew, blight, and rust. Modern agriculture relies heavily on large swathes of monocultures—a practice conducive to disease outbreaks and epidemics. With increasing globalisation, one of the major challenges facing agriculture today is increasing food production in the face of emerging virulent pathogens. Disease epidemics can occur following the introduction of new pathogen strains with increased virulence, or after existing field resistance has been defeated. Understanding the diversity in plant immune genes and identifying novel sources of resistance are key for breeding resistant crop varieties in preparation for prevention of future disease outbreaks.

The most well studied *R* genes confer monogenic, dominant or semi-dominant resistance and have been used extensively in agricultural breeding (St.Clair, 2010). Such resistance is termed qualitative resistance, referring to Mendelian genes that are of large effect, often acting in a gene-for-gene manner and exhibiting race-specificity (A. J. Castro *et al*., 2003; St.Clair, 2010). At the other end of the spectrum, multiple genes of small phenotypic effect often underlie quantitative disease resistance, with quantitative traits showing continuous variation in phenotype often outside Mendelian segregation ratios (Ariel J Castro *et al*., 2003). This continuum of resistance extends from complete resistance, to a moderate host defence response and reduction in disease severity with low expressivity of the phenotype and is dependent on the segregation and presence of causal genes. Quantitative genes can also show epistatic relationships, pleiotropy, or additive effects (St.Clair, 2010). Classical breeding using phenotypic and DNA marker assisted selection, with markers on or in linkage disequilibrium with the gene of interest, has been successful in mapping qualitative resistance (St. Clair, 2010). The "boom-and-bust" cycle of defeated major *R* genes overcome by pathogen adaptation is a major threat to plant resistance breeding; partial or quantitative resistance is increasingly being sought to lower pathogen selection pressure in the field (Burdon *et al.,* 2014).

The use of race-specific resistant cultivars is the most effective and environmentally-benign method of disease control (Singh *et al.,* 2011). Deployed in 1942, the *Puccinia graminis* f. sp. *tritici* (*Pgt*) resistance gene *Rpg1* of barley has provided durable qualitative stem rust resistance (Brueggeman *et al.,* 2002). However, virulence to deployed *R* genes is increasingly common. The TTKSK, or Ug99 strain, of *Pgt* was first detected in Uganda in 1998 and has since spread worldwide. New lineages of TTKSK have overcome the majority of *R* genes used in wheat (*Triticum aestivum*), including *Sr31* derived from rye (*Secale cereale*), making TTKSK and its variants a threat to wheat production worldwide (Pretorius *et al*., 2000; Singh *et al*., 2016, 2015). A concerted research effort in the wake of TTKSK diagnosis has resulted in the identification of new quantitative trait loci and adult plant resistance (APR) genes for use in breeding for *Pgt* resistance (Bhavani *et al*., 2019). This pathosystem reveals how vulnerable agriculture can be to emerging pathogens; effective gene stewardship is crucial to ensure the limitation of future epidemics (Singh *et al*., 2016, 2011).

Puccinia striiformis, the causal agent of stripe rust is a common and devastating pathogen of grasses. Recent adaption to warmer climates has allowed *P. striiformis* to spread to areas without a previous history of the fungus (Hovmøller *et al*., 2011; Singh *et al*., 2016). Regular regional wheat crop losses around 0.1 to 5%, sometimes 25% are observed due to fungal infection (Savary *et al*., 2019, 2012). However, wheat yield losses of 70% or more are possible during an epidemic under favourable conditions (Wellings, 2011). Recent adaption to warmer climates has allowed *P. striiformis* to spread to areas without a previous history of the fungus (Hovmøller *et al*., 2011). The barley specialist *Puccinia striiformis* f. sp. *hordei*, (*Psh*) has spread extensively across the world over the last 40 years since being introduced into South America in 1975 from Europe. Today, *Psh* is found in all major barley producing areas worldwide with the exception of Australia, which remains an untouched island for *Psh* (Brown, 2015). Only *P. striiformis* f. sp. *pseudo-hordei* is present on naturalised barley-grass and can only infect a small number of Australian barley cultivars (Wellings, 2011; Wellings *et al*., 2000). Isolates first discovered in America we thought to have originated from European isolate 24, but now have diversified to over 31 different *Psh* races within the US (Chen and Line, 2002). In wheat, the emergent virulent 'Warrior' race of *Puccina striiformis* f. sp. *tritici* (*Pst*) quickly spread throughout Europe from 2011, dramatically altering the population structure by replacing previously present isolates (Hovmøller *et al*., 2016; Hubbard *et al*., 2015). The evolution of races with increased virulence, incursion of new exotic isolates, or the re-emergence of virulent strains in a new geographic area can all cause epidemics (Hovmøller *et al*., 2016; Hubbard *et al*., 2015). The rapid spread of genetically diverse *Pst* lineages highlights the need for the maintenance of genetic diversity within accessions and active surveillance of pathogen populations on a global scale (Hubbard *et al*., 2015; Wellings, 2011).

Resistance in barley to *Psh* can be classified into two developmental categories: all stages or adult plant resistance (APR). Few genes in barley have been found for resistance to *Psh*, compared to over 70 *Yr* (yellow rust) resistance genes identified from wheat (Chen and Line, 1999; Hovmøller *et al*., 2011; Losert *et al*., 2017). A major qualitative resistance gene (*Rpsx*) has been mapped to the long arm of chromosome 7H and several quantitative trait loci (QTL) have been identified (A. J. Castro *et al*., 2003). Moseman and Reid (1961), identified the first barley *Psh* qualitative resistance gene denoted *Yr4*—later renamed *Rps4*—located close to the

Mla locus on chromosome 1H (Brown *et al*., 2001). Since the discovery of this gene multiple QTL have been mapped, but no underlying causal genes have been identified as yet. Chen *et al.,* (1994) mapped a major effect *Psh* resistance gene on 5H and a minor effect 4H QTL accounting for 57% and 10% of the variation in adult plant disease severity, respectively. Chen and Line (1999) identified at least 20 genes involved in *Psh* resistance across 18 cultivars, present singularly and polygenically, suggesting a complex genetic architecture of quantitative resistance to *Psh*. Toojinda *et al.,* (2000) identified QTLs on chromosomes 1H, 2H, 3H, and 6H as principal determinants of resistance to *Psh*. Due to the presence of resistance alleles in the susceptible parent, Toojinda *et al*., (2000) hypothesised unique combinations of multiple alleles may underlie stripe rust resistance. The quantification of seedling and APR has been more difficult to characterise with previously identified 'dual' resistance QTL on 4H separating into 4Ha and 4Hb, for APR and seedling resistance respectively, favouring the hypothesis of differential gene control through developmental stages (Castro *et al*., 2002). In further work using a DH population, Castro *et al*., (2002) showed seedling resistance localised to 5H and 6H QTLs and to regions already implicated to be involved in APR. As seedling resistance against *Psh* is limited across all adult-plant stages (Gyawali *et al*., 2017), breeding efforts have shifted to utilising quantitative resistance.

The basis of this resistance and potential separation of adult and seedling resistance will only be elucidated through fine mapping, cloning, and confirmation of candidate genes within significant QTLs. Quantitative resistance could be a result of differential control of different aspects of the defence signalling pathway, or resistance at varying points of the pathogen infection and life cycle. This has been shown for three *R* genes in barley cv. Golden Promise that confer resistance to *Pst*. *Rps7* and *Rps6* prevent colonization and *Rps8* prevents *Pst* pustule formation. *Rps7* colocalises with *Mla*, providing another example to of multiple pathogen recognition at the *Mla* locus (Moscou *et al*., unpublished).

The barley near-isogenic (BISON) lines were developed to dissect the quantitative, more complex, polygenic inheritance of adult plant resistance to barley stripe rust (Richardson *et al*., 2006; Verhoeven *et al*., 2011). Using marker assisted selection, *Psh* resistance loci were introgressed into the susceptible genetic background of

Baronesse individually and in all combinatorial allele introgressions. The donors of the resistance alleles were cv. BCD47 (4H and 5H) and BCD12 (1H), developed from double haploid lines created by (A. J. Castro *et al*., 2003; Ariel J Castro *et al*., 2003). Two control lines were also created: BISON 0-QTL, selected for the susceptible Baronesse alleles at all QTL locations, and resistant line BISON 7H containing a qualitative major gene on chromosome 7H, derived from the experimental line D3-6/B23 (Ariel J Castro *et al*., 2003). The separation of resistance QTLs into different experimental lines is a valuable tool in the characterisation of quantitative resistance in the barley-*Psh* model pathosystem (Vales *et al.,* 2005).

The recurrent parent Baronesse used in the BISON lines is susceptible to *Psh* (Verhoeven *et al*., 2011). In this chapter, the mapping population of BISON 1H x Baronesse has been used in a recombination screen to delineate *QRps1H* and investigate the relationship to *Mla*. Homozygous recombinants have been used in field trials to fine-map *QRps1H* and introgression of *QRps1H* into elite barley cultivars has been initiated.

5.3 Results

QRps1H encompasses the Mla12 locus

QRps1H has previously been identified on the short arm of chromosome 1H and has been introgressed into a near-isogenic line BISON 1H (Verhoeven *et al*., 2011). A recombination screen using BISON 1H (*QRps1H*) x Baronesse (*qrps1H*) F_2 identified 346 recombinants based on N = 1,510 gametes across a 24 cM spanning the QTL introgression (Figure 5-1). A genetic map of the 1H chromosome of the BISON 1H x Baronesse population was developed using nine KASP (Kompetitive Allele Specific PCR) markers (Figure 5-1). The linkage map was 24.4 cM, where cM was calculated using the Kosambi mapping function. A further recombination screen identified 144 homozygous recombinants, from 67 unique $F_{2:3}$ families, spanning the QTL (Figure 5-1). Homozygous recombinants were generated to ensure that regions encompassing critical recombinants will be fixed in material analysed in the field.

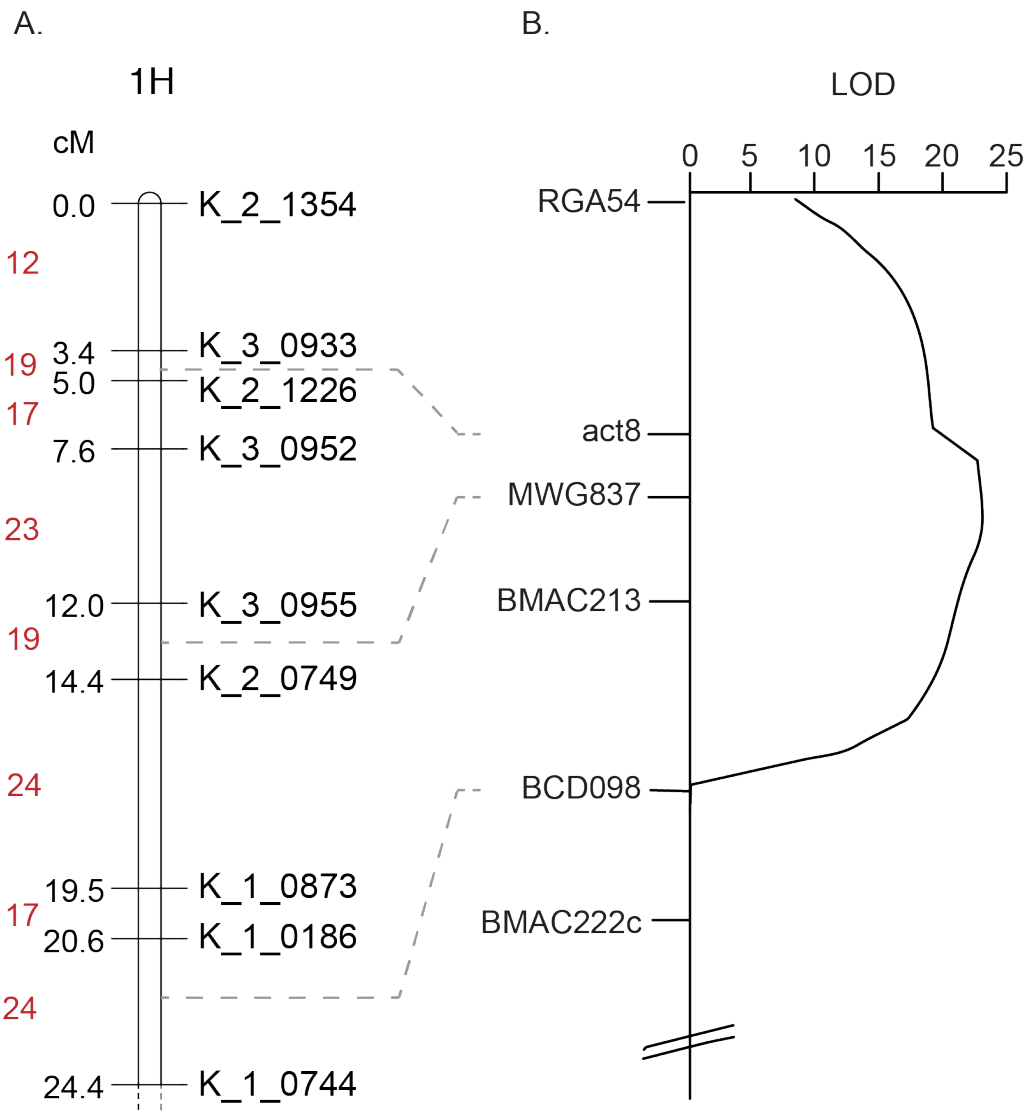

Figure 5-1. Genetic map of the short arm of chromosome 1H encompassing QRps1H in the BISON 1H x Baronesse population.

The distal end of the short arm of chromosome 1H based on non-redundant KASP markers based on a recombination screen including N = 1,510 gametes. **A)** Black numbers of the *left-hand side* correspond to the cM distance with marker names on the *right-hand side*. Red numbers on the *left-hand side* correspond to the number of recombination events between markers. **B)** Log-likelihood (LOD) of the location of *QRps1H* with inferred marker positions on the genetic map (dashed grey lines) based on comparison to the barley SNP consensus map as identified by Verhoeven *et al*., (2011).

The population was evaluated for *Psh* resistance in three environments spanning three years, including the 2019 field season which is ongoing at the time of completion of this thesis (Table 5-1). Forty-two homozygous $F_{2:3}$ families were sent to Patrick Hayes at Oregon State University for field trials in 2017 using a randomised complete block design with two replicates. Seed was bulked in the field for use in 2018 field trials. Seventy F_3 lines were sent to Ravi Singh at CIMMYT, Mexico, of which 63 were unique $F_{2:3}$ families.

Field trials in 2017 and 2018 at Church Farm, JIC experienced no disease pressure as infection failed despite field inoculation of bulked spores, susceptible spreader rows, and the transplanting of inoculated seedlings into the field. Yellow pustules characteristic of *Psh* were not observed on material in the field. In addition, the trial in Oregon during 2017 failed to have sufficient establishment of *Psh* infection—despite the observation of initial infection. Field trials at Oregon and CIMMYT (Mexico) in 2018 were successful and experienced a maximum disease pressure of 80% and 100%, respectively.

Using data from the 2018 OSU field trial scored as percent severity (scale from 0 to 100%), *QRps1H* was mapped using interval mapping (Figure 5-2). *QRps1H* was narrowed to an interval under the peak marker K_3_0933 at 3.84 cM with a LOD score of 4.96 (Figure 5-2). The average of the two replicates gave a significant peak of 4.96 compared to the peak of 3.31 for replicate 1 and 2.4 for replicate two, all of which are above the experiment-wise threshold (Figure 5-2). The phenotype by genotype plot at the peak marker (K_3_0933) shows slight separation of the BISON 1H (resistant; BCD12 donor of *QRps1H*) and Baronesse (susceptible) genotypes, but *QRps1H* is not yet mendelised in this population (Figure 5-3).

Field trails in Mexico were phenotyped three times over a 17-day period and scored as percent severity and reaction type for each plot. The coefficient index (CI) was

Table 5-1. Summary of field trials.

Year	Site + GPS coordinates	Sowing Date	Phenotyping date	Design	Disease pressure
2017	Church Farm, JIC, UK	13 Mar 2017	NA	RCBD, two replicates	0
2017	OSU, Oregon, USA	31 Jan 2017	22 Jun 2017	RCBD, two replicates	0
2018	Church Farm, JIC, UK	26 Mar 2018	NA	RCBD, two replicates	0
2018	OSU, Oregon, USA	17 Oct 2017	23 May 2018	RCBD, two replicates	0-80%
2018	CIMMYT, Mexico	May 2018	13 Aug 2018 23 Aug 2018 30 Aug 2018	RCBD, two replicates	0-100%
2019	CIMMYT, Mexico	06 Jun 2019	ongoing	RCBD, two replicates	ongoing

JIC: John Innes Centre; UK: United Kingdom; OSU: Oregon State Univeristy; USA: United States of America; CIMMYT: International Maize and Wheat Improvement Center; RCBD: Randomised Complete Block Design.

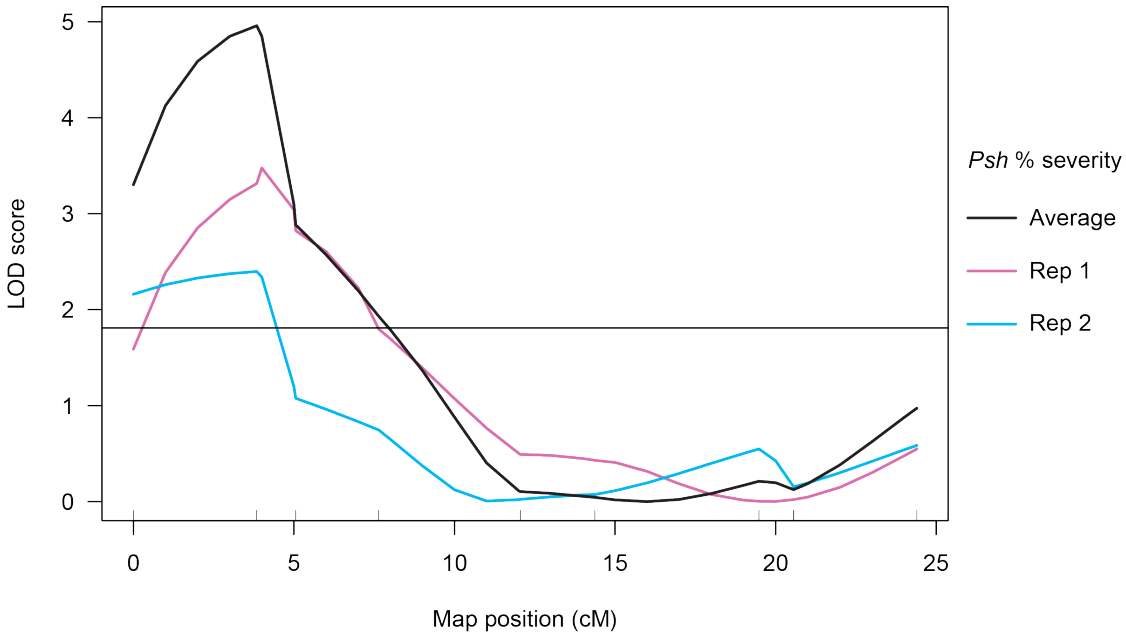

Figure 5-2. Interval mapping on the BISON1H x Baronesse $F_{2:5}$ mapping population using *Psh* 2018 field trails at Oregon State University.

LOD scan of *QRps1H* for *Psh* percent severity including each individual replicate and the average of both replicates. The black horizontal line represents the maximum experiment-wise threshold across replicates and average based on 1,000 permutations.

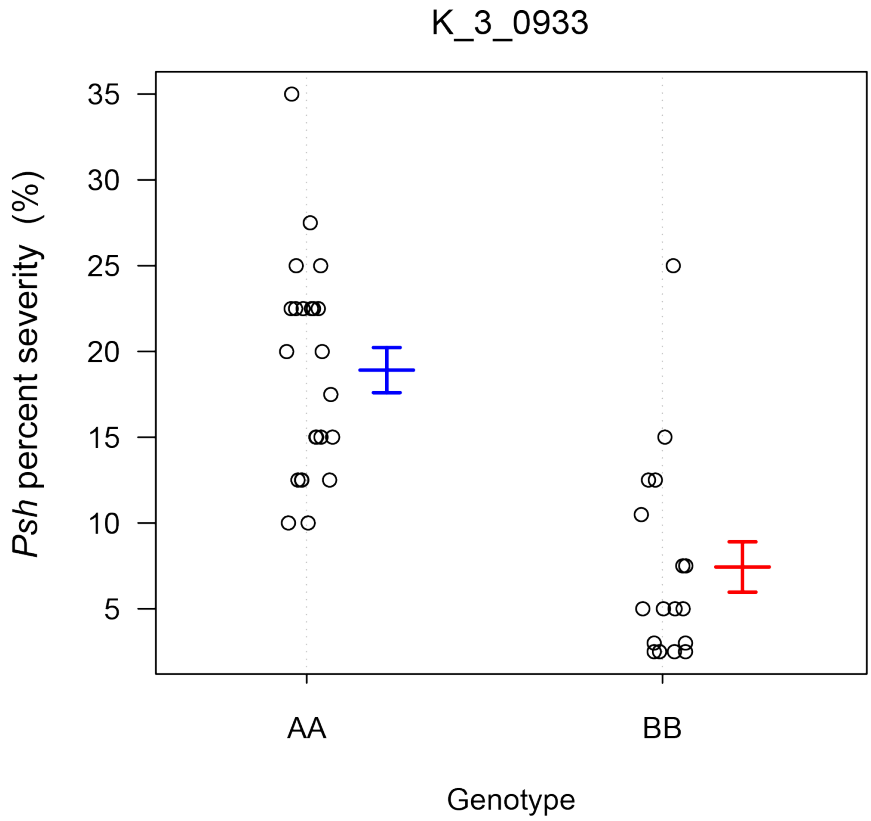

Figure 5-3. Phenotype by genotype plot of the marker K_3_0933 located at the peak of *QRps1H* from phenotypic data from 2018 field trails at Oregon State University.

Genotype A = susceptible parent Baronesse, B = resistant parent BISON 1H (BCD12 donor of *QRps1H*).

calculated from these two values using a weighted average for reaction type (Results Table 5-2). Data from Mexico showed higher significance and improved fine-mapping of *QRps1H* compared to Oregon. *Psh* infection showed increasing severity over time, with the highest LOD score under the peak marker (K_3_0933) of 12.5 from the average of replicates from the final phenotyping date (Figure 5-4A). The first phenotyping date had a LOD score of 1.16 below the maximum experiment-wise threshold (Figure 5-4A). The peak LOD score from the second phenotyping date was 10.8 and the overall average of the phenotyping scores gave a peak of 11.5 both above maximum experiment-wise threshold (Figure 5-4A).

Using the CI gave similar LOD peaks under the marker K_3_0933 to the percent severity phenotypes (Figure 5-4B): incorporating the reaction type with the percent severity into the CI did not substantially improve the peak LOD score (Figure 5-4B). The CI data gave a slightly lower LOD peak of 11.5 for the highest phenotyping date and 10.6 for the overall average. The LOD peak of the second phenotyping date 9.34 was also above the maximum experiment-wise threshold. The first phenotyping date gave a LOD score of 1.1 for the peak marker which fell below the experiment-wise threshold.

The phenotype by genotype plot using the peak marker K_3_0933 and phenotypic data using the average from the last phenotyping date of the Mexico field trial showed increased separation between the BISON 1H resistant genotype and the Baronesse susceptible genotype—which displays near complete separation of *QRps1H* and *qrps1H* in the population (Figure 5-5). Increased resolution through the generation of new genetic markers and phenotypic data from further years of field trials over multiple locations are required in the delineation of *QRps1H*.

BISON lines confer varying resistance to *Psh*

The panel of BISON lines were included in the Mexico field trials, alongside the donor lines BCD12 and BCD47 (Verhoeven *et al*., 2011). BCD12 is the donor of the 1H QTL and showed high levels of resistance with a maximum of 15% *Psh* severity

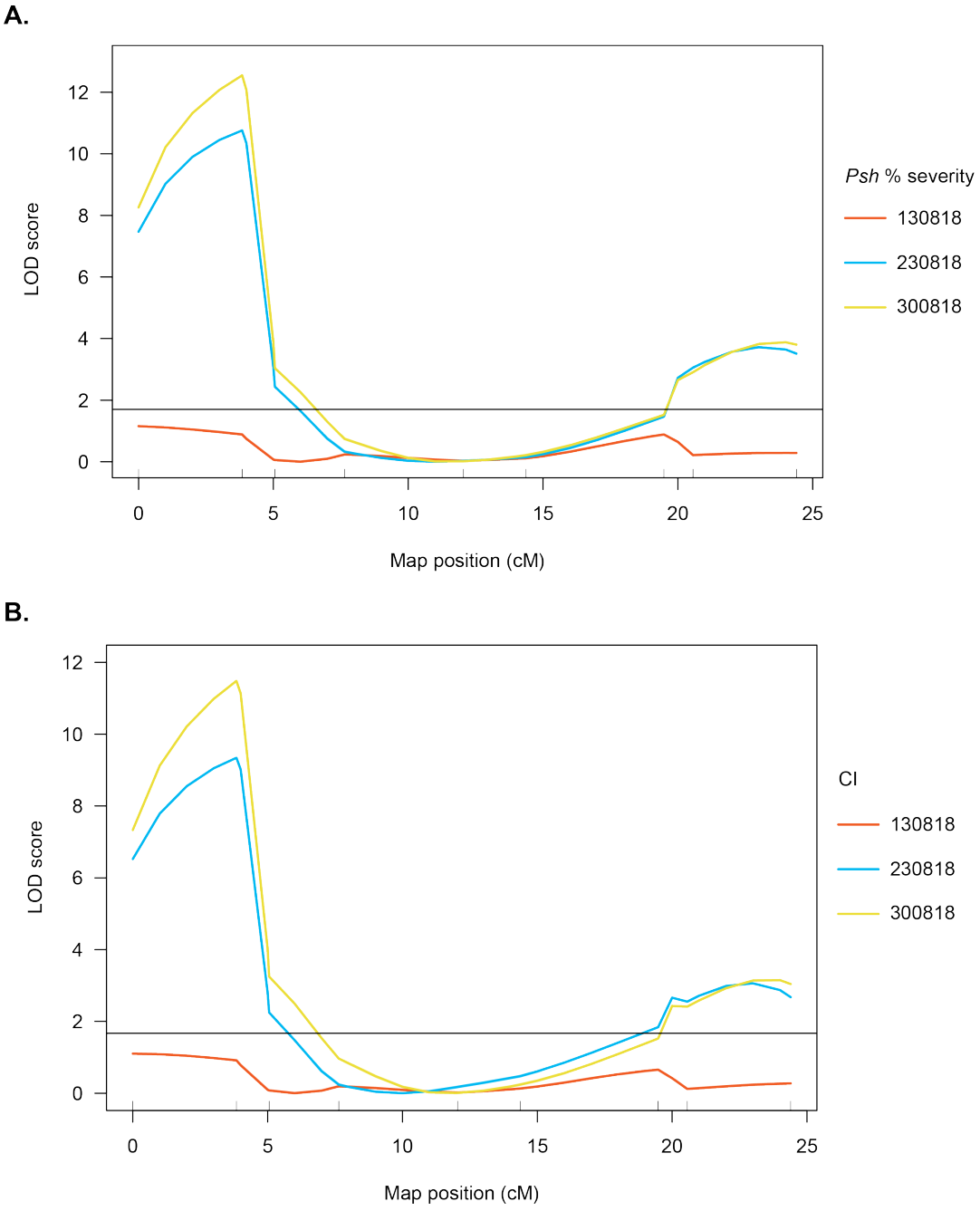

Figure 5-4. QTL analysis of *QRps1H* in the BISON1H x Baronesse $F_{3:4}$ mapping population using phenotypic data from 2018 field trials at CIMMYT, Mexico.

LOD scan of *QRps1H* including the average of two replicates at three phenotyping dates. Phenotyping dates include 13th August 2018 (orange; 130818), 23rd August 2018 (blue; 230818), 30th August 2018 (yellow; 300818), and the overall average (black). The black horizontal line represents the maximum experiment-wise threshold across replicates and average based on 1,000 permutations. **A)** LOD scan of *QRps1H* including the average of two replicates at three phenotyping dates. **B)** Coefficient Index (CI) including the average of the coefficient index of the two replicates at the three phenotyping dates.

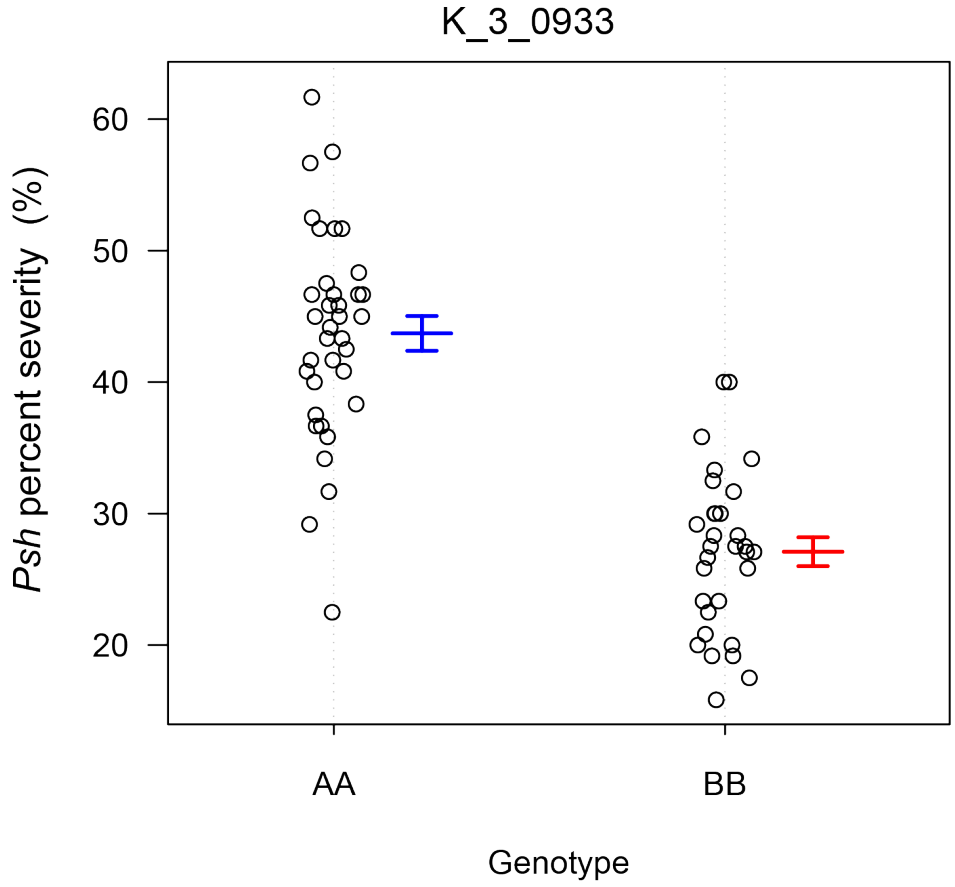

Figure 5-5. Phenotype by genotype plot of the marker K_3_0933 located at the peak of *QRps1H* from phenotypic data from 2018 field trials at CIMMYT, Mexico.

Genotype A = susceptible parent Baronesse, B = resistant parent BISON 1H (BCD12 donor of *QRps1H*).

scored (Figure 5-6). BISON 1H fails to recapitulate the donor resistance with a higher maximum 40% *Psh* severity under the highest disease pressure at the third phenotyping date (Figure 5-6). BCD47, the donor of the 4H and 5H resistance QTLs shows almost complete resistance to *Psh*, having a maximum 5% severity (Figure 5-6). Introgression of both QTL in BISON 4H and 5H also fails to complement to the wild-type resistance levels, showing similar percent infection severity as the single introgression of the 4H QTL. The 5H resistance QTL is very weak, reaching 100% infection severity at the final phenotyping date (Figure 5-6). The combination of the 1H, 4H, and 5H QTLs in the BISON 1H + 4H + 5H line showed almost complete resistance with a maximum 5% infection severity across the phenotyping dates suggesting an additive effect of the QTLs (Figure 5-6). This resistance was slightly stronger than the introgression of the 7H qualitative resistance gene *Rpsx* (A. J. Castro *et al*., 2003; Verhoeven *et al*., 2011) which showed a maximum of 10% severity during the field trial (Figure 5-6).

Mla12 does not confer APR to *Psh*

The *Mla* locus has been associated with resistance to multiple pathogens, and *Mla3* shown to confer multiple pathogen recognition (Chapter 4). *QRps1H* encompasses the *Mla12* locus so *Mla12* is a candidate gene for conferring APR to *Psh*. The barley mutant lines *mla12-m66*, *rar1-m82*, and *rar1-m100* derived from barley cv. Sultan5 (*Mla12*) are deficient in *Mla12*-mediated hypersensitive resistance to *Blumeria graminis* f. sp. *hordei* (Torp and Jørgensen, 1986). The line *mla12-m66* carries a mutation in *Mla12;* and *rar1-m82* and *rar1-m100* carry mutations in *Rar1* which is required for the *Mla12* dependent disease response (Hückelhoven *et al*., 2000; Torp and Jørgensen, 1986). These mutant lines and the wild-type Sultan5 were included in the field trials in Mexico to evaluate the role of *Mla12* in *Psh* resistance. The line Manchuria was used as a susceptible control. The greatest disease pressure was observed at the third phenotyping date; however, no difference was observed between the mutant lines and the wild-type Sultan5 as both showed similar levels of infection across all the phenotyping dates (Figure 5-7). These data suggest *Mla12* is not the causal gene underlying *QRps1H*.

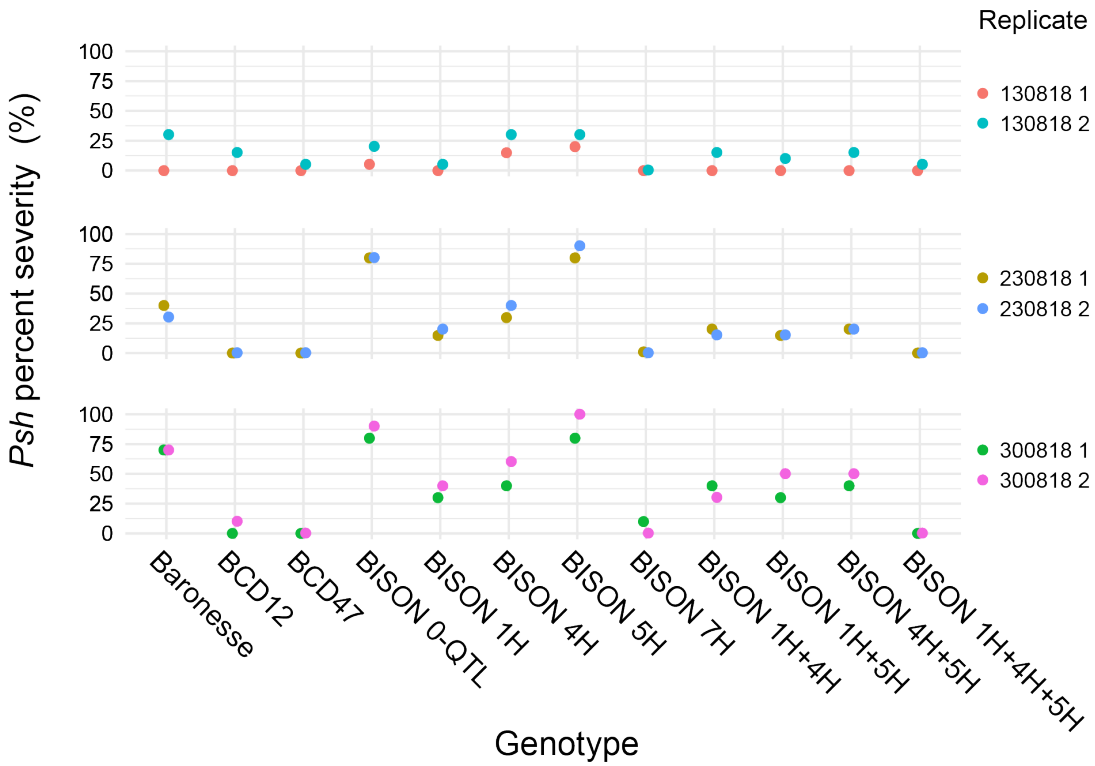

Figure 5-6. *Psh* percent severity of BISON introgression lines from 2018 field trials at CIMMYT, Mexico.

BISON lines include the null control line BISON 0-QTL, BISON 1H, BISON 4H, BISON 5H, BISON 7H, BISON 1H + 4H, BISON 1H + 5H, BISON 4H + 5H, and BISON 1H + 4H + 5H. Control lines include susceptible parent Baronesse, the donor of the 1H QTL BCD12, and the donor of the 4H and 5H QTLs BCD47 (Verhoeven *et al*., 2011). Top panel shows data from phenotyping date 13th August 2018 (130818) from replicate 1 (orange) and replicate 2 (blueish green); middle panel shows phenotyping data from 23rd August 2018 (230818) of replicate 1 (brown) and replicate 2 (blue); and bottom panel shows phenotyping data from 30th August 2018 (300818) of replicate 1 (green) and replicate 2 (pink).

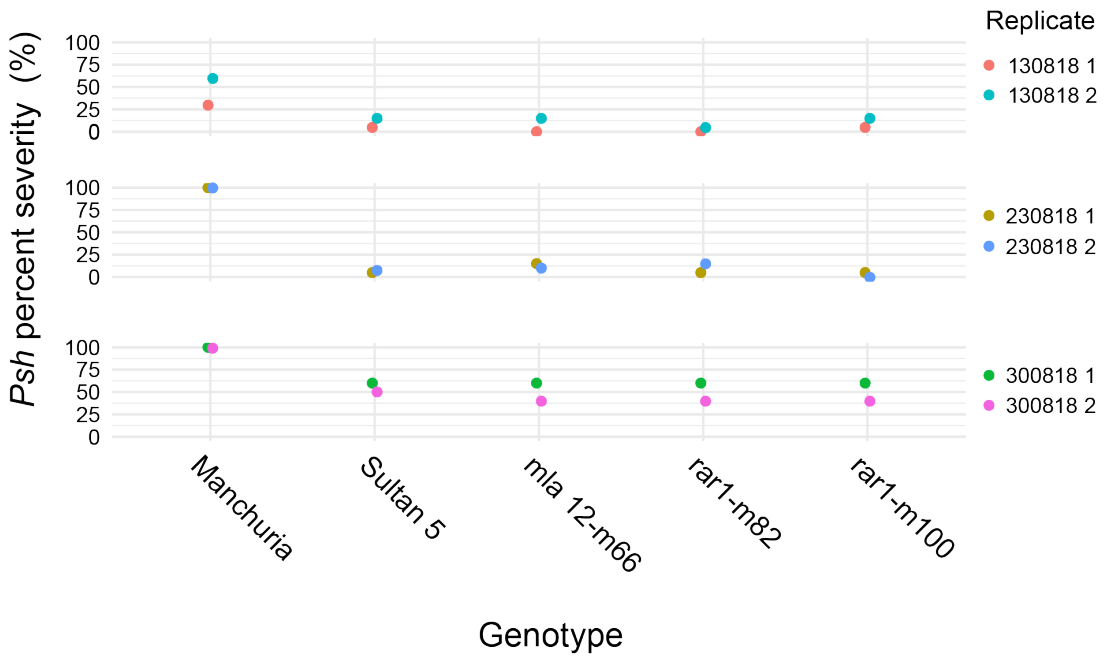

Figure 5-7. *Psh* percent severity of *Mla12* and *Rar1* mutants from 2018 field trials at CIMMYT, Mexico.

Mutants include *mla12-m66*, *rar1-m82*, *rar1-m100* and wild-type Sultan 5. Manchuria is the susceptible control. Top panel shows data from phenotyping date 13th August 2018 (130818) from replicate 1 (orange) and replicate 2 (blueish green); middle panel shows phenotyping data from 23rd August 2018 (230818) of replicate 1 (brown) and replicate 2 (blue); and bottom panel shows phenotyping data from 30th August 2018 (300818) of replicate 1 (green) and replicate 2 (pink).

Mildew resistance loci confer little resistance to *Psh*

The Siri introgression panel contains mildew loci introgressed into recurrent parent Siri background (Kølster and Stølen, 1987). This panel was included in the field trial to assess if known mildew resistance loci would confer resistance to *Psh*. Wild-type Siri was moderately resistant to *Psh*, showing a maximum 60% infection severity under the highest disease pressure (Figure 5-8). The 12 introgression lines S01, S02, S03, S04, S06, S07, S09, S10, S12, S13, and S17 showed varying degrees of resistance to *Psh* (Figure 5-8). The lines S03 (*Mla6*), S10 (*Mla12*), and S17 (*Mlk*) showed increased resistance than the wild-type, with other lines showing a greater degree of susceptibility (Figure 5-8). S06 (*Mla7* (Moseman)) and S09 (*Mla10*) were variable across the replicates in comparison to the wild-type (Figure 5-8). As other lines showed a higher percent severity compared to the recurrent parent Siri, susceptibility genes could have been introgressed from the donor lines, or resistance genes lost or disrupted from the wild-type background. However, these data are generated from one year of field trials: while trends can be observed, additional replicates over multiple years are required for conclusive conclusions.

Introgression of the *Mla12* locus in line S10 confers moderate resistance to *Psh*, comparable to the BISON 1H containing *QRps1H*. The *Mla12* locus in S10 originates from the donor line Emir (Kølster and Stølen, 1987), whereas *QRps1H* in BISON 1H originates from Shyri (Toojinda *et al*., 2000; Verhoeven *et al*., 2011). Shyri is a two-rowed feed barley developed by ICARDA/CIMMYT (GSHO 2430, Lignee 640//Kober/Teran 78) and released in Ecuador (USDA GRIN; NordGen) and Emir (CIho 13541; PI 321787) is a two-row line originating from Germany with a Delta//Agio/3/Kenia/Arabische pedigree (Chen and Line, 2002; Díaz-Perales *et al*., 2003; USDA GRIN)—they are unlikely to have a shared heritage. *Mla12* may be involved in the *Psh* resistance response, or an additional linked gene at the locus is causal.

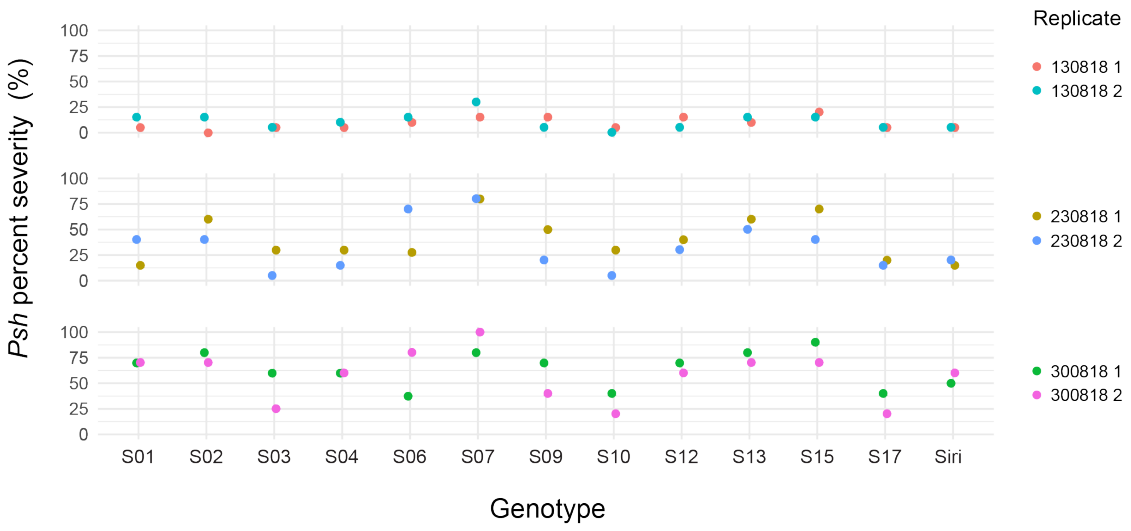

Figure 5-8. *Psh* percent severity of Siri introgression panel from 2018 field trials at CIMMYT, Mexico.

Wild-type recurrent parent Siri and introgression lines of mildew loci. Top panel shows data from phenotyping date 13th August 2018 (130818) from replicate 1 (orange) and replicate 2 (blueish green); middle panel shows phenotyping data from 23rd August 2018 (230818) of replicate 1 (brown) and replicate 2 (blue); and bottom panel shows phenotyping data from 30th August 2018 (300818) of replicate 1 (green) and replicate 2 (pink).

Current elite spring barley cultivars used in the UK harbour varying levels of resistance to yellow rust, (AHDB, 2019). Elite UK barley cultivars were obtained from Limagrain and include LG Diablo spring malting variety, LG Tomahawk spring feed variety, LG Casting spring variety, and LG Mountain and LG Flynn winter two-row feed varieties. LG Tomahawk has shown high resistance to stripe rust (AHDB, 2019) however additional introgression of *QRps1H* would only aid in the mitigation of future susceptibility. All cultivars were recently released from 2018 so have yet to experience varying *Psh* disease pressure. Crosses for the introgression of *QRps1H* into elite UK cultivars were initiated in spring 2018, and F_1 were advanced in winter 2019. These crosses will be used in future marker-assisted backcrossing to generate introgression lines. Evaluation of introgressions under field conditions will establish the resistance potential of *QRps1H* in these backgrounds.

5.4 Discussion

The barley near-isogenic (BISON) lines were created aid in the dissection of quantitative, more complex, polygenic inheritance (Richardson *et al*., 2006; Verhoeven *et al*., 2011) and the introgression of quantitative resistance into breeding through marker assisted selection (A. J. Castro *et al*., 2003). Pyramiding quantitative and qualitative resistance genes aims to provide protection against the emergence of races virulent on large effect *R* genes (A. J. Castro *et al*., 2003). A resistance QTL (*QRps1H*) conferring APR to *Psh* was previously mapped to the short arm of chromosome 1H (Toojinda *et al*., 2000) and was introgressed into the near-isogenic line BISON 1H, in the recurrent parent Baronesse (Verhoeven *et al*., 2011). *QRps1H* encompasses the *Mla12* locus and a mapping population of BISON 1H x Baronesse was used to fine-map *QRps1H* to investigate the relationship to *Mla12*. Critical homozygous recombinants across the *Mla12* locus were used in successful field trials at Oregon State University, USA, and CIMMYT, Mexico. Disease pressure and infection was highest in Mexico, where phenotyping data were taken over three timepoints with increasing percent severity recorded (Table 5-2). *QRps1H* was narrowed to 5 cM, encompassing the *Mla12* locus; additional marker saturation and

further years of field trials are necessary to delineate this region further. This peak was maintained across both field sites: *QRps1H* is robust against disease pressure from different *Psh* populations. *QRps1H* is not yet mendelised in this population (Figure 5-3, Figure 5-5), additional genetic markers and map saturation alongside further phenotypic data is required.

BISON 1H is a useful donor of the 1H resistance allele, however it displays undesirable agronomical characteristics such as semi-dwarf height and poor kernel plumpness (Verhoeven *et al*., 2011). Introgression of *QRps1H* into elite cultivars is necessary: in doing so, the resistance capabilities of these lines will be increased to protect against future epidemics. The initial cross and one round of marker-assisted backcrossing has been performed to date of *QRps1H* into LG Diablo, LG Tomahawk, LG Casting, LG Mountain, and LG Flynn produced by Limagrain. Although introgression of a single QTL conferring partial resistance may not provide effective protection, the additional resistance QTL identified on 4H, 5H, and 7H (*Rpsx*) (Ariel J Castro *et al*., 2003) provide additional loci for pyramiding in future.

Based on observations of the multiple pathogen recognition capabilities of *Mla* alleles, it cannot be excluded that *Mla12* could be the causal *Psh* resistance gene underlying *QRps1H*. However, the power of the BISON 1H x Baronesse population to fine-map *QRps1H* may be limited due to suppressed recombination observed across the *Mla* locus. The Siri panel line S10 containing introgression of the *Mla12* locus showed increased resistance and a lower percent severity than the wild-type recurrent parent (Figure 5-8). Considering mutants in the *Mla12*-dependent resistance response failed to show increased susceptibility compared to the wild-type (Figure 5-7), *Psh* resistance could be due to a tightly linked gene at the locus rather than *Mla12* itself. *Mla* loci contain considerable variation in the *RGH1*, *RGH2*, and *RGH3* alleles present (Chapter 2) with haplotype divergence contributing to suppressed recombination. Therefore, sequencing and complementation of candidate genes from the resistant *Mla12* haplotype is required for characterisation. As considerable variation was observed in the percent severity of *Psh* infection and disease pressure across phenotyping dates during the field trial, *Psh* inoculations in a controlled environment may reveal more consistent or subtle differences in resistance and allow for finer characterisation of candidate genes. *Mla* alleles are known to function effectively at

the seedling and adult level. *Mla12* is a 'slow acting' resistance gene permitting the growth of haustoria and more elongating secondary hyphae of *Blumeria graminis* f. sp. *hordei* (*Bgh)*. Overexpression of *Mla12* converted to the fast-acting type suggesting the protein accumulation or complexes are rate limiting (Boyd *et al*., 1995; Shen *et al*., 2003). Developmental regulation could also affect the expression of *Mla12*. The field trial at CIMMYT included mutants in *Mla12* and *Rar1* – the required chaperone for some *Mla* alleles (Hückelhoven *et al*., 2000; Shen *et al*., 2003) – however phenotypic results were variable across replicates and timepoints. Phenotyping in controlled environments and more field data is required to confirm this.

P. striiformis is a devastating fungal pathogen of grasses. It is increasingly found in warmer regions as the pathogen adapts to higher temperatures and with a greater ability to cause disease (Hovmøller *et al*., 2011). The aggressive 'Warrior' race of *Pst* highlights the potential danger of the emergence of increased virulence, were *Psh* to follow the same trajectory. The use of resistant cultivars is the best approach to disease control, especially with interest in reducing fungicide use, however resistance in barley is limited to few QTL (Brown *et al*., 2001; Yan and Chen, 2008). The majority of barley malting cultivars grown in the United States display a degree of susceptibility to *Psh* (Yan and Chen, 2008). In 2000, the cultivar Bancroft was released as a new resistant cultivar yet was found infected with *Psh* soon after release (Wesenberg *et al*., 2001). Phenotypic characterisation showed cv. Bancroft to have high-temperature APR to *Psh* alongside isolate-specific all-stage resistance (Chen and Moore, 2003; Yan and Chen, 2008). However, the all stage resistance present in Bancroft is ineffective against the current population of *Psh* present in the United States (Yan and Chen, 2008). *Psh* in North and South America exhibits more heterogeneity than European populations (Brown *et al*., 2001); current germplasm is ineffective protection for future incursions and evolution of increased *Psh* virulence.

Partial, quantitative resistance is associated with a long latency period, a low infection frequency, a decreased spore production, and a short infectious period of pathogen infection (Sandoval-Islas *et al*., 2007; Singh *et al*., 2015; St.Clair, 2010). It is thought to reduce the selection pressure on the pathogen by permitting limited life-cycle competition. In the cereal-rust pathosystem, phenotyping has often been described as

a score of disease severity at a given time-point of development, such as flag-leaf latency period which is highly correlated with partial resistance in the field (Sandoval-Islas *et al*., 2007). Effective resistance against multiple rust pathogens at the adult stage has been shown in wheat for *Lr34* (McIntosh, 1992; Spielmeyer *et al*., 2005), *Lr46* (Kolmer *et al*., 2015; Lillemo *et al*., 2008, 2007), and *Lr67* (Herrera-Foessel *et al*., 2014, 2011; Hiebert *et al*., 2010). *Lr34* encodes an ABC transporter (Krattinger *et al*., 2015, 2009), *Lr67* encodes a hexose sugar transporter (Milne *et al*., 2019), and *Lr46* remains unknown. *Lr34res*—the resistant allele of *Lr34*—confers resistance only at the adult stage in wheat, whereas expression of *Lr34res* in barley also functions at the seedling stage (Risk *et al*., 2013). *Lr34res* induces various defence pathways in barley and is thought to enhance basal resistance through increased lignification (Chauhan *et al*., 2015; Krattinger *et al*., 2019). To date, effective APR resistance is mediated by mechanisms other than NB-LRRs (Jafary *et al*., 2006). When resistance is described as 'durable', it is often in comparison to short-lived large effect resistance—often NB-LRR mediated—which is overcome rapidly by pathogen evolution following deployment in the field. The most cited example of 'durable' resistance is *mlo* of barley—a loss of function mutation that confers broad-spectrum resistance to the adapted pathogen *Bgh* (Acevedo-Garcia *et al*., 2014; Büschges *et al*., 1997; Jørgensen, 1992). While the mechanism of *mlo* resistance remains unknown, it has remained effective for over 30 years in the field (Kusch and Panstruga, 2017; Lyngkjær *et al*., 2000). In contrast, the *Mla* locus is a known resistance gene complex containing multiple NB-LRR families (Wei *et al*., 2002, 1999). Elucidating the relationship of *QRps1H* with the *Mla* locus will reveal the potential involvement NB-LRR resistance genes in conferring APR, and further the breadth of multiple pathogen recognition specificities at *Mla*.

5.5 Materials and methods

BISON 1H x Baronesse population and genetic map construction

The *H. vulgare* accessions BISON 1H and Baronesse were crossed and allowed to self-pollinate to generate a founder F_2 population. The population, N = 1,510 gametes from 6 selfed F_1 individuals, was evaluated for recombination events across *QRps1H*. Following single-seed descent, DNA was extracted from leaf tissue of F_2 and F_3 recombinants using a CTAB gDNA extraction protocol modified for 96-well plate-based extraction (Dawson *et al*., 2016; Stewart and Via, 1993).

Genetic maps were created using JoinMap v4 with default parameters (van Ooijen, 2006). Genetic distances were estimated using the Kosambi mapping function. Integrity of the genetic map was evaluated through comparison with the current OPA consensus genetic map of barley (Muñoz- Amatriaín *et al*. 2011). The genetic map was evaluated using Rstudio (Version 1.1.463) and the R/qtl package (Version 1.44.9) (Broman *et al*., 2003).

Plant growth

Seedlings were germinated in John Innes Peat & Sand Mix (85% Fine Peat, 15% Grit, 2.7kg/m³ Osmocote 3-4 months, Wetting Agent, 4kg/m³ Maglime, 1kg PG Mix). Leaves were sampled at second leaf emergence, DNA extracted, and individuals genotyped for recombination events. Recombinants were transferred to FP9 pots in John Innes Cereal Mix (40% Medium Grade Peat, 40% Sterilised Soil, 20% Horticultural Grit, 1.3kg/m³ PG Mix 14-16-18 + Te Base Fertiliser, 1kg/m³ Osmocote Mini 16-8-11 2mg + Te 0.02% B, Wetting Agent, 3kg/m³ Maglime, 300g/m³ Exemptor) and grown in a greenhouse under natural conditions.

Puccinia striiformis f. sp. *hordei* (*Psh*) assays

Psh isolate B01/2 was collected from the United Kingdom in 2001 and maintained at the National Institute of Agricultural Botany (NIAB) in Cambridge, UK on susceptible

barley cultivars. Ureodineospores were stored at 6°C after collection. At The Sainsbury Laboratory, ureodineospores were bulked from susceptible cultivars and stored at -80°C prior to phenotyping. For field trials in Oregon State University (OSU), Oregon, USA and CIMMYT, Mexico natural inoculum was used.

Barley accessions used in field trials are listed in Appendix Table 7-6. For phenotyping data collected at OSU, *Psh* infection was scored as a percent severity across each plot. For data collected at CIMMYT, Mexico, infection phenotypes were collected as a percentage score of infection severity and a reaction score (Stubbs *et al*., 1986). Reaction score was converted to a constant value according to Stubbs (1986), for mixed reaction score a weighted average was calculated. A coefficient of infection was calculated through the multiplication of the percent severity and reaction score.

Table 5-2. field reaction and corresponding constant value.

Reaction	Symbol	Constant value
Resistant	R	0.2
Moderately Resistant	MR	0.4
Intermediate or M	M	0.6
Moderately susceptible	MS	0.8
Susceptible	S	1.0

QTL and phenotypic analysis

Files and data were prepared using the QKcartographer scripts (https://github.com/matthewmoscou/QKcartographer) and analysed with RStudio (Version 1.1.463) using the R/qtl package (Version 1.44.9) (Broman *et al*., 2003). QTL genotype probabilities were calculated using the calc.genoprob() function using default parameters and a step-size of 1 cM. Interval mapping was performed using the scanone() function using default parameters (maximum likelihood via the EM algorithm) and a genotyping error rate of 0.01. Statistical significance for QTLs was determined by performing 1,000 permutations and controlled at $\alpha = 0.05$ (Doerge and Churchill, 1996). The experiment-wise threshold was taken from the maximum 5% LOD threshold calculated from the average of each replicate and the overall average.

The function lodint() was used to calculate the 2 LOD support interval for each of the field trials.

Phenotyping data from control lines included in the Mexico field trials were analysed with RStudio (Version 1.1.463) and plotted using the ggplot2 package (Version 3.1.0) (Wickham, 2016).

6 Discussion

> *"Therefore, it appears likely that several of the defence mechanisms against powdery mildew also are effective against many other factors that may damage barley plants."*
>
> — (Jørgensen, 1994)

The *Mla* locus provides an excellent genetic resource for the study of NB-LRR gene evolution. A wealth of phenotypic, genetic, and genomic resources have been accrued over decades of research, beginning with the investigation of the barley and *Bgh* interaction in the early 20th century (Jørgensen, 1994). This thesis is the cumulation of observations, curiosities, and investigations of the *Mla* locus; molecular biology and sequencing technology only now provide the tools in which to confirm prior hypotheses.

6.1 The evolution of the *Mla* locus

The *Mla* locus is a known resistance gene cluster with a wealth of haplotype and allelic diversity of *Mla* NB-LRRs conferring isolate-specific resistance to *Bgh* (Halterman *et al*., 2001; Halterman and Wise, 2004; Jørgensen, 1994; Seeholzer *et al*., 2010; Shen *et al*., 2003; Zhou *et al*., 2001) The majority of *Mla* alleles are in repulsion (Jørgensen, 1994) and evidence of suppressed recombination across the *Mla* locus suggests a mechanism for maintaining haplotype diversity (Wei *et al*., 1999). While additional *RGH* families of *RGH2* and *RGH3* are known to be present at the locus (Wei *et al*., 1999), investigations of these NB-LRRs pales in comparison to *RGH1* (*Mla*). Here, we found extensive presence/absence and sequence diversity of alleles, including presence/absence of an integrated *Exo70F1* domain at the C-terminus of *RGH2*. This forms a *trans*-species polymorphism maintained through multiple speciation events over 24 million years.

Many plant-pathogen interactions are described as gene-for-gene interactions. At the *Mla* locus it is clear there are extensive allelic series and polymorphisms of the *RGH* families, reflecting the diversity of the *RGH1* family in conferring isolate-specific

resistance to *Bgh*. *RGH* families at *Mla* form a stable polymorphism maintained through speciation and may represent NB-LRRs that recognise conserved pathogens of grasses, or effector conformations common to conserved pathogens of grasses. However, the recognised effectors by *RGH1* are sequence-unrelated (Lu *et al*., 2016; Saur *et al*., 2019) suggesting that allelism does not reflect co-evolution of NB-LRR-effector interactions; effector polymorphisms can also be generated through presence/absence variation and may extend across multiple pathogen species. A high level of genetic variation exists in recognised effectors within *Bgh* populations (Saur *et al*., 2019) and *Bgh* populations can rapidly change virulence gene frequencies in the field (Hovmøller, 1993). In response, balancing selection acts to maintain diverse alleles of *RGH1* in the population.

Observations of the genetic architecture of species reveals the evolutionary processes acting on them. Stable polymorphisms are present under certain conditions: the maintenance of this *trans*-species polymorphism predicts alleles are long-lived and genetic variation is detectable in natural populations; balancing selection can then act to sustain allele frequencies (Brown and Tellier, 2011). The gene-for-gene model and the coupling of plant and pathogen life cycles is an unstable equilibrium that drives an arms race between host and pathogen (Brown, 2015; Tellier *et al*., 2014). The addition of ecological parameters such as spore dispersal and environmental conditions alleviates such a tight interaction and generates direct frequency-dependent selection: where the fitness effect of an allele declines as its frequency in the population increases (Brown, 2015; Cowger and Brown, 2019). The advantage of—and selection for—virulence is highest when host resistance is also high. Increased virulence in the pathogen population decreases the advantage of resistance: defeated *R* genes are no longer selected for. A cost of virulence prevents the continuing evolution of aggressive pathogen species, however experimental examples are sparse (Brown, 2015). In theory, extreme virulence can be capped due to antagonistic or lethal effector combinations; restrictions in mutations to evade recognition, or the presence of an *R* gene that recognises an indispensable core pathogen component (in the absence of suppressors of recognition/immune response). Pathogen populations are not isogenic: accumulation of effectors and virulence components is not a viable method of evolution.

The diversity of *RGH1*, *RGH2*, and *RGH3* alleles at the *Mla* locus is thought to be due to the fluctuating selection from variable pathogen pressures. From the work outlined in this thesis describing the multiple pathogen recognition capabilities by *Mla3*, selection on this allele over evolutionary history comes from not only *Bgh* populations, but also those of *P. oryzae*. In other haplotypes, additional pathogen species may also contribute to selection for multiple pathogen recognition at the locus: spot blotch (Bilgic *et al*., 2006; Leng *et al*., 2018) and *Psh* (A. J. Castro *et al*., 2003; Verhoeven *et al*., 2011) among others also mapped to the region. Balancing selection also increases diversity at closely-linked neutral sites, as recombination events rarely occur between them (Charlesworth, 2006); it is possible that balancing selection acting on *Mla* alleles is inadvertently leading to maintenance of *RGH2* and *RGH3* allelic pools. Coupled with diversifying selection and supressed recombination over the whole *Mla* locus, extreme haplotype variation is present of all three *RGH* families. The recognition specificities of *RGH2* and *RGH3* alleles is unknown: allelic variation may be an artefact of *RGH1* selection rather than of functional relevance.

True alleles rarely exist in combination—only one allele is present in the same genomic location. Where multiple *Mla* specificities are present, often silencing of one copy occurs (Seeholzer *et al*., 2010). This suggests additional mechanisms are present to maintain polymorphism outside of suppressed recombination. Incompatible interactions of NB-LRRs can give rise to hybrid necrosis: an uncontrolled hypersensitive response that results in stunting and death of the plant (Barragan *et al*., 2019; Bomblies, 2009; Chae *et al*., 2016). The population dynamics of hybrid necrosis suggests this would lead to loss of detrimental alleles and fixation of non-detrimental alleles in the population through purifying selection. The maintenance of diverse alleles through the action of diversifying or balancing selection must counteract such stabilising selection. For paired NB-LRRs, the genetic linkage of pairs—observed through their head-to-head orientation and embedded promoters—limits the potential for recombination events leading to loss of pairs.

Identified long-lived polymorphisms predominately exist in presence/absence variation: examples from *A. thaliana* include *RPM1* (Stahl *et al*., 1999; Tian *et al*., 2003), *RPP1* (Botella *et al*., 1998; Goritschnig *et al*., 2016; Rehmany *et al*., 2005), *RPS2* (Caicedo *et al*., 1999), and *RPS5* (Karasov *et al*., 2014). Allelic variants of NB-

LRRs are present in *A. thaliana*, but the expansive diversity observed also arises from paralogs. *RPP13* of *A. thaliana* exists in copy number variation and paralogs are also present at different loci (Hall *et al*., 2009; Rose *et al*., 2004). Alleles of *RPP13* were also found to evolve at different rates, forming different clades independent of geographic origin (Ding *et al*., 2007a). Expansive allelic series at a single locus such as *Mla* are few—only *Pm* alleles of wheat are comparable (Bourras *et al*., 2019, 2015). Characterising the frequency of each *Mla* allele within the population would be the first step in assessing the evolutionary dynamics of the *RGH1* family.

The *RGH2-Exo70F1* integration exists as presence/absence, including frameshifts between *RGH2* and *Exo70F1* resulting in non-integrated forms. This suggests that once integrated, *RGH2-Exo70F1* is not fixed: this could be an indication of balancing selection of RGH2 alleles. In barley, an integrated CC domain was found in one allele of RGH2—domain integrations within this gene family may be pervasive. It is possible that variable integrated domains exist; the sequencing of multiple individuals within a species from different populations is necessary to assess this hypothesis. However, the repeated identification of an integrated *Exo70F1* across species is greater than expected from chance suggesting *RGH2-Exo70F1* has been maintained through selection. Exo70 proteins are involved in the tethering of vesicles to the plasma membrane and may also provide tissue or spatial specificity of localisation (He *et al*., 2007; Žárský *et al*., 2009). There are two hypotheses for Exo70 integration: that the Exo70 is involved in the intracellular localisation of the NB-LRR-ID or Exo70 is a decoy involved in effector binding. The involvement of Exo70 in plant immunity is increasingly being elucidated, especially for Exo70F and FX clades (Fujisaki *et al*., 2015; Ostertag *et al*., 2013; Stegmann *et al*., 2014). Functions of integrated domains outside of effector recognition have yet to be demonstrated.

The duplication of resistance genes observed at the *Mla* locus is a mechanism for the birth of *R* genes: allowing for neofunctionalization of new specificities (Michelmore and Meyers, 1998). Gene duplication provides potential for unequal crossing over and recombination of sequence similar *Mla* alleles (e.g. *Mla3* and *Mla23*)—permitting recombination in the locus. Such events could account for the different RGH allele combinations: the same *RGH2-Exo70F1*/*RGH3* alleles are present in the accessions Baronesse and Maritime, y*et al*ongside quite different *RGH1* (*Mla*) alleles. New

paralogs either undergo pseudogenisation or diversification and neofunctionalization into new resistance specificities (Michelmore and Meyers, 1998). The identification of copy number variation of *Mla3* alleles challenges this binary outcome; selection has maintained identical copies of *Mla3* within the genome. The inability to assemble the locus via long-read sequencing technologies is a limitation of assessing the genetic architecture of the *Mla3* locus: the number of copies of *Mla3* remains unconfirmed. Chromosome flow-sorting and conformation capture (Belton *et al*., 2012) of chromosome 1H from Baronesse has been initiated—the reduction of undesired sequencing and proximity labelling may aid the assembly of the region. Of course, the generation and sequencing of a BAC library for the *Mla3* haplotype—as performed for the reference sequence—is another method in which to assemble the locus but the cost is prohibitive.

Evidence presented in this thesis drives the hypothesis of copy number variation for increased recognition specificity: a higher number of gene copies are required for *P. oryzae* recognition. However, RNA sequencing needs to be performed on transgenic lines to confirm the correlation of copy number and expression of the transgene. The panel of increasing copy number, if indeed it is correlated to expression, provides an opportunity to investigate intermediate phenotypes. Requirements for resistance could be elucidated through the quantification and molecular characterisation of phenotypes; arrest of *P. oryzae* growth may be terminated at an earlier and crucial timepoint with higher copy number. NB-LRR expression and regulation is tightly controlled via epigenetic factors, transcription factors, and small RNAs (Bhattacharjee *et al*., 2013; Elmore *et al*., 2011; Kong *et al*., 2018; Lee and Yeom, 2015; Zhai *et al*., 2011); it is unclear how increasing expression of *Mla3* via increasing copy number is affected by such regulation. Combinatory pathogen inoculations would also show if any inter-specific interactions or variation is present in the resistance response.

Mla alleles are known to be highly expressed (Halterman *et al*., 2001). The generation of *Mla3* overexpression lines driven, for example, by the ubiquitin promoter would be useful for comparison (and also would alleviate potential *trans*-silencing effects of multiple copies of the *Mla3* transgenic insert). Overexpression lines of *Mla3* would provide a resource with which to investigate the potential costs of the high expression of NB-LRR genes. The majority of *A. thaliana* NB-LRRs are expressed at low level

and show tissue specificity in expression patterns (Tan *et al*., 2007). Increased NB-LRR expression is thought to confer fitness costs to the plant—tight regulation has evolved to prevent detrimental effects (Brown, 2015; Y. Li *et al*., 2010). However, few examples have been shown experimentally. Presence of the NB-LRR *RPM1* from *A. thaliana* confers a fitness cost of reduced seed set under field conditions (Tian *et al*., 2003) and tissue specificity through epigenetic regulation of the rice *Pigm* NB-LRR gene cluster prevents a yield detriment (Deng *et al*., 2017). Overexpression of NB-LRRs via transgenic means is known to result in constitutive activation of defence which can lead to growth defects and stunting of plants (Lai and Eulgem, 2018; Li *et al*., 2019; Oldroyd and Staskawicz, 1998). It is curious then how *Mla* alleles can be expressed at such high levels without detrimental effects? Preliminary work from the lab suggests *Mla* is expressed highly and constitutively: *Mla* alleles can be identified from RNAseq data from uninfected leaves. Quantification of *Mla3* expression, including at developmental timepoints, tissue specificity, and following pathogen inoculation, would be the first step in investigating this question.

The *Mla* locus has been associated with multiple pathogen recognition and it was hypothesised that this could be driving the maintenance of diverse haplotypes: increasing the recognition specificities within a population. The identification of the multiple pathogen recognition capabilities of *Mla3* provides evidence for this hypothesis. It is possible that this phenomenon is conserved between alleles, this could be elucidated through the cloning of additional *Mla* specificities from haplotypes where multiple recognition specificities map to the *Mla* locus. How *Mla* alleles—especially as singleton NB-LRRs—have this capability remains unknown.

6.2 Mechanism of multiple pathogen recognition by *Mla3*

Major questions remain: what is the mechanism of *Mla3* recognition and how does this facilitate recognition of multiple pathogens? There are two competing hypotheses for this: direct recognition by *Mla3* or indirect recognition via an *Mla3* guardee. While direct recognition has been all but shown via crystal structure for a subset of *Mla* alleles (Lu *et al*., 2016; Saur *et al*., 2019), indirect recognition cannot be excluded.

Identification of AVR_{a3} and *AVR-Rmo1* is crucial for unravelling the recognition mechanism and establishing protein interactions. Few AVR genes from *Bgh* have been characterised to date. Cloned effectors from *Bgh* encode CSEPs (candidate secreted effector proteins) or RALPHs (RNase-like proteins expressed in haustoria) and many more are encoded in the genome (Lu *et al*., 2016; Saur *et al*., 2019; Spanu, 2017). In comparison, the majority of *P. oryzae* effectors are small secreted proteins that lack homology to known proteins (Valent and Khang, 2010; Yoshida *et al*., 2009; Zhang and Xu, 2014). *P. oryzae* MAX (*Magnaporthe* avirulence proteins and ToxB-like) effectors are sequence-unrelated, sharing less than 25% sequence similarity, and are grouped only via their shared structural fold (de Guillen *et al*., 2015; Franceschetti *et al*., 2017). The direct recognition of two effectors can be explained via a structural similarity; *Bgh* and *P. oryzae* appear not to be limited by species-specific sequence-related effector proteins so similarities may occur.

Mutagenesis of *P. oryzae* isolate KEN54-20 was successful in generating a confirmed gain-of-virulence mutant on *Mla3*—KEN54-20 M1. Additional putative mutants have been isolated and are waiting re-inoculation for confirmation, and further rounds of mutagenesis could be undertaken to generate additional virulent isolates. Sequencing of KEN54-20 M1 is ongoing and the addition of further mutants will provide more sequencing data and power for comparative analyses in the identification of *AVR-Rmo1*. SNPs or indels present in the coding sequences of predicted effector candidates will be prioritised, however mutations in regulatory elements or genes required for *AVR-Rmo1* function could also be causal for the gain-of-virulence phenotype. From initial inoculations, the mutant KEN54-20 M1 appears not to be compromised in growth and virulence, with only functional *AVR-Rmo1* disrupted. This suggests that only *AVR-Rmo1* function is mutated and this effector is not essential for virulence. Competition experiments against the wild-type KEN54-20 on a susceptible line will assess the virulence capabilities of the two isolates and confirm this observation. Existing isolates with knock-out and complementation of known effectors can also be screened on wild-type Baronesse and resistant transgenic lines, in a reverse-genetic approach for effector confirmation. *Bgh* is less amenable to experimental manipulation as *P. oryzae*. Many candidate CSEPs have been identified following genome sequencing, and mapping populations have been generated, that could be screened

against *Mla3*. Once *AVR-Rmo1* has been confirmed, the predicted structure can be used to screen *Bgh* candidates that share structural similarities.

Genetic evidence implicates *Mla3* as also conditioning *Lov1* sensitivity. The structure of HST victorin produced by *B. victoriae* is known. Victorin exists as a group of closely-related cyclized pentapeptides with victorin C the predominant form: composed of glyoxylic acid and a cyclic combination of five amino acids (Wolpert *et al*., 2002; Wolpert and Lorang, 2016). Victorin binds to thioredoxin h5 in *A. thaliana* via the active-site cysteine 39 and this interaction triggers AtLOV1-mediated sensitivity (Lorang *et al*., 2012). Victorin sensitivity is present across species and a conserved mechanism for sensitivity has been proposed, as thioredoxins are essential components of plants (Wolpert and Lorang, 2016). Recognition via a guard model does not alleviate the necessity for a shared structure of effectors; however, perturbation of a guardee can occur in multiple ways. RIN4 of *A. thaliana* is a clear example; effector-mediated modification of RIN4—through a multitude of ways—is guarded by numerous NB-LRRs (H.-S. Kim *et al*., 2005; Kim *et al*., 2009; M. G. Kim *et al*., 2005; Liu *et al*., 2011; Russell *et al*., 2015). Barley thioredoxin h5 will certainly be included in interaction experiments with AVR_{a3} and AVR-Rmo1.

Mla3-mediated victorin sensitivity and subsequent susceptibility to *B. victoriae* provides an opposing selection pressure against that of its resistance function. A susceptibility gene to *B. sorokiniana*—the causal agent of spot blotch—is present in the cultivar Bowman at the *Mla* locus (Leng *et al*., 2018). As efficient immune receptors, *Mla* alleles may also provide effective susceptibility factors. The trade-offs between biotrophic resistance and necrotrophic susceptibility contribute to the frequency-dependent selection of *Mla* alleles. Other sensitivity or susceptibility genes identified that recognise necrotrophic pathogen effectors and HSTs have yet to demonstrate a resistance function—although this is hypothesised (Faris *et al*., 2010; Wang *et al*., 2014). The *Mla3* (alongside other candidate gene) transgenic lines are currently being tested for victorin sensitivity with Thomas Wolpert and Jennifer Lorang. If confirmed, *Mla3* would represent the first sensitivity gene with a known resistance function and provide a direct cost of resistance.

Not only proteinaceous effectors are recognised from *P. oryzae*. A secondary metabolite produced by some isolates of *P. oryzae,* is synthesised by the ACE1 gene cluster and is recognised by *Pi33* from resistant rice cultivars (Ballini *et al*., 2006; Collemare *et al*., 2008; Fox and Howlett, 2008). ACE1 differs from other known effectors as it encodes a polyketide synthase (PKS) fused to a nonribosomal peptide synthetase (NRPS). Polyketides are major fungal secondary metabolites involved in diverse biological activities with important roles in pathogenicity (Collemare *et al*., 2008). The *Pi33* locus contains LRR-Kinases and NB-LRR encoding genes, but the causal *Pi33* gene has yet to be identified (Ballini *et al*., 2007; Berruyer *et al*., 2003). ACE1 expression is coupled to the onset of appressorium-mediated penetration of the host cuticle (Collemare *et al*., 2008; Fudal *et al*., 2007); this fits the timepoint for *Mla3*-mediated resistance (Figure 4-2). Characterising the product of ACE1 synthesis has proven difficult: the recognised ACE1 avirulence determinant remains unknown (Song *et al*., 2015). Assessing the genome of *P. oryzae* KEN54-20 for an intact *ACE1* as candidate for *AVR-Rmo1* is a high priority; the product of *ACE1* may share a recognition mechanism with victorin.

Comparing these observations between systems, there lacks a clear common mechanism to explain the multiple pathogen recognition shown by *Mla3*. The most tempting hypothesis is that of the guard model, with *Mla3* activated on perturbation of another host protein by each pathogen. This model is established for AtLOV1 recognition of victorin (Sweat and Wolpert, 2007) and other biotrophic effectors (Dodds *et al*., 2009). However, this is difficult to reconcile with the recent experimental evidence for direct recognition by *Mla* alleles by Saur *et al.,* (2019). Direct recognition of sequence-unrelated effectors—even of both proteinaceous and metabolite—may be facilitated by the adoption of a similar structural fold. The direct recognition via an LRR domain is limited by the rapid diversification of effectors and the strong selection pressure they are under to evade recognition; it is not an intrinsic limitation of the protein structure. Structural insights of *Mla3* and the corresponding effectors or interacting partners, in the case of indirect recognition, will provide clues to the mechanism of multiple pathogen interaction, or yield a mechanism for direct perception of multiple effectors and a HST.

6.3 Engineering resistance

Increasing interest has focused on the potential for engineering NB-LRRs for expanded or novel recognition. Prior attempts at modifications of coding regions or domain swaps led to constitutive activation, autoimmunity, and rendered NB-LRRs non-functional; inter-domain interactions crucial for regulation and function are easily disrupted. A challenge remains of understanding the NB-LRR structure: only recently has a crystal structure of an NB-LRR been defined (Wang *et al*., 2019a). The defined NB-LRR ZAR1 recognises effector-mediated modification of PBS1-like protein 2 (PBL2) kinase in complex with resistance-related kinase 1 (RKS1) (Wang *et al*., 2019b). Due to the variation of NB-LRRs (Bailey *et al*., 2018; Kourelis and Van Der Hoorn, 2018), it is likely that other examples adopt distinct confirmations and interact with pathogen products in different ways—the application of the ZAR1 system to other NB-LRRs is thought to be limited. The LRR domain hypothesised to directly bind effectors is incredibly diverse and appears to bear little correlation to the effectors recognised: no patterns or correlations have been observed in this region that could provide predictions for binding interfaces amenable to modification. Interacting partners and even the effectors recognised remain unknown for many NB-LRRs (Kourelis and Van Der Hoorn, 2018); without this knowledge engineering is almost futile. Exceptions exist with the engineering of known interaction sites such as through the modification of cleavage sites within NB-LRRs (Kim *et al*., 2016) and TALE binding sites in the promoters of executor genes (Hummel *et al*., 2012; Zeng *et al*., 2015).

The discovery of functional integrated domains (Cesari *et al*., 2014; Césari *et al*., 2014; Kroj *et al*., 2016; Sarris *et al*., 2016) provides a foundation for engineering. While large domain swaps with divergent proteins is hypothesised to disrupt conformational structure and inter-domain interactions, domain modification or substitution with closely related domains from the same protein family may provide a feasible approach. It has not escaped attention that *RGH2-Exo70F1* provides an opportunity for engineering. Assuming *RGH2-Exo70F1* (and *RGH3* partner) is a functional NB-LRR, this provides a base for targeted modification. Swapping the *Exo70F1* domain for the rice *OsExo70F3* and *OsExo70F2* proteins which bind *AVR-Pii* from *P. oryzae* (Fujisaki *et al*., 2015) would be an initial target. If effector binding

is sufficient for NB-LRR activation, then the *OsExo70F3* chimaera would recapitulate the resistance shown in rice, and the *OsExo70F2* chimaera would provide a novel mechanism for *AVR-Pii* resistance—*Pii*-mediated resistance in rice is only via *OsExo70F3* (Fujisaki *et al*., 2015). Crystal structures of Exo70s bound to effectors would reveal the sites of interaction; targeted amino acid swaps or the generation of chimaeric domains of these regions may prove less disruptive to function than whole domain modification. However, whether *RGH2-Exo70F1* is functional and what pathogen it is recognising has yet to be shown.

Genome editing has accelerated resistance breeding: allowing the transfer of NB-LRRs across species in a rapid and efficient manner and providing targeted and efficient gene modifications (Krenek *et al*., 2015; Yin *et al*., 2017). Although translation into agriculture remains restricted due to regulation and lack of societal acceptance (Araki and Ishii, 2015). Unexpected consequences of transformation have arisen: the APR resistance of *Lr34* has been shown to confer seedling resistance in transgenic tetraploid durum wheat (*Triticum turgidum*) blurring the developmental divide (Rinaldo *et al*., 2017). In addition, the transfer of *Lr34* into barley provides resistance to addition pathogens and results in the constitutive activation of multiple defence pathways (Chauhan *et al*., 2015; Risk *et al*., 2013). Distinctions could be due to endogenous regulation and expression of genes during development; the transfer to other species via transgenic means disrupts this regulation. Once identified, transformation and/or modification of the underlying causal gene of *QRps1H* may provide seedling resistance to *Psh*—and potentially multiple pathogens.

P. oryzae is a devastating disease of rice, and recent emergence of wheat blast highlights the persistent threat that this pathogen has on modern cereal production (Islam *et al*., 2016; Maciel *et al*., 2014; Wilson and Talbot, 2009). Epidemics of blast on barley have occurred in Japan and northern Thailand and barley accessions are known to be susceptible to *P. oryzae* (Inukai *et al*., 2006; Kawai *et al*., 1979; Matsumoto and Mogi, 1979; Sato *et al*., 2001). The major factor limiting the impact of *P. oryzae* is the current location and climate of barley growing areas. Identification of new sources of resistance are beneficial for agricultural breeding to mitigate future epidemics. As seen by the recent incursion of wheat blast into Bangladesh, agricultural production can quickly be decimated by the favourable combination of a virulent

isolate, amenable climate, and susceptible varieties. Identification of *Mla3* conferring resistance to *P. oryzae* isolates carrying *AVR-Rmo1* provides potential for control of this pathogen—testing wheat blast isolates against *Mla3* is a priority. Sequencing data from isolates can be mined for the presence of *AVR-Rmo1*, once it has been identified, and *Mla3* deployed to confer resistance. Transformation of *Mla3* into wheat and rice is also paramount for resistance breeding in these species. *Mla* alleles could also provide resistance against other effectors from *P. oryzae*, assuming multiple pathogen recognition capabilities are shared.

6.4 Future perspectives

Human civilisation has changed the dynamics of plant-pathogen interactions: migration and globalisation has led to the acceleration of plant and inadvertent pathogen movement. Evolutionary curated dynamics have been disrupted—introducing novel species into areas previously uncolonized. The distribution of NB-LRR genes in agricultural systems imposes local selection on neighbouring pathogen populations and can provide reservoirs for pathogens: the 'Oases in the desert' model of pathogen evolution occurs with the presence of swathes of susceptible agricultural monocultures; the long-distance dispersal of spores allows pathogens to move between them (Brown, 2015) and epidemics are born. Rapid pathogen evolution allows for adaptation to new environments and hosts; however, new interactions have the potential to reveal plant *R* genes with multiple pathogen recognition capabilities—for both resistance and sensitivity.

Since the first cloning of a plant resistance gene, a lot has changed in our understanding of the plant immune system. Presumed simple gene-for-gene interactions have expanded to a wealth of NB-LRR recognition mechanisms, pathogen effector-mediated modifications of host proteins, and sheer diversity of NB-LRRs. With the advent of new sequencing technologies and molecular tools, NB-LRR repertoires can be characterised. Population dynamics including inter- and intra-specific diversity can be assessed through the increasing number of individuals sequenced—revealing complex selection pressures and evolutionary history of the plant immune system. Wild relatives of modern crop species can be mined for *R* gene variation and novel recognition specificities for use in breeding.

Now, the major challenge remains of the translation of research into effective deployment in agriculture. Modern agriculture is reliant on high-yielding crop varieties, chemical control, and improved farming practice. However, food insecurity is an increasing threat—and an existing crisis for many people. Future agriculture will be increasingly reliant on resistance breeding due to improving environmental stewardship, climate change, and increasing genetic technology (Kettles and Luna, 2019; Savary *et al*., 2019). For this, understanding plant-microbe interactions not only on a molecular scale but also in an evolutionary context will be crucial. Science will have to provide the knowledge and tools to face the upcoming challenges of climate change and the increasing demand for food with a scarcity of resources. However, the fear is that the future of agriculture lies not in scientific understanding, but in human cooperation on a local and global scale—a monumental undertaking unparalleled in human history.

7 Appendices

Figure 7-1. Maximum likelihood phylogenetic tree of Exo70F family members from diverse Poales species.

Branch support was generated using 1,000 bootstraps, with orange dots designating support from 80-100%. Species abbreviations listed in Appendix Table 7-1. *A. thaliana* (*At*; *AT5G50380.1*) used as an outgroup.

Table 7-1. Species acronyms.

Species	Acronym
Achnatherum splendens	*Acs*
Aegilops sharonesis	*Ash*
Aegilops speltoides	*Aspe*
Aegilops tauschii	*Aet*
Agropyron cristatum	*Agc*
Agropyron desertorum	*Agd*
Agrostis stolonifera	*Ags*
Aphelia sp.	*Asp*
Arabidopsis thaliana	*At*
Avena sativa	*Avs*
Brachypodium distachyon	*Bdi*
Brachypodium stacei	*Bst*
Bromus inermis	*Bin*
Centrolepis monogyna	*Cmo*
Cyperus alternifolius	*Cal*
Dactylis glomerata	*Dgl*
Ecdeiocolea monostachya	*Emo*
Elegia fenestrata	*Efe*
Eleocharis dulcis	*Edu*
Festuca pratensis	*Fpr*
Flagellaria indica	*Fin*
Holcus lanatus	*Hla*
Hordeum pubiflorum	*Hp*
Hordeum vulgare	*Hvu*
Joinvillea ascendens	*Jas*
Juncus effusus	*Jef*
Lachnocaulon anceps	*Lan*
Leersia perrieri	*Lpe*
Mayaca fluviatilis	*Mfl*
Melica nutans	*Mnu*
Nardus stricta	*Nst*
Neoregelia carolinae	*Nca*
Oropetium thomaeum	*Ot*
Oryza australiensis	*Oau*
Oryza barthii	*Oba*
Oryza coarctata	*Oco*
Oryza glaberrima	*Ogla*
Oryza glumipatula	*Oglu*
Oryza meridionalis	*Omer*
Oryza meyeriana	*Omey*
Oryza minuta	*Omi*
Oryza nivara	*Oni*
Oryza officinalis	*Oof*
Oryza punctata	*Opu*
Oryza rufipogon	*Oru*
Oryza sativa	*Os*
Phalaris arundinacea	*Par*
Phyllostachys edulis	*Ped*
Poa annua	*Pan*
Poa infirma	*Pin*
Poa pratensis	*Ppr*
Poa supina	*Psu*
Secale cereale	*Sc*
Setaria italica	*Si*
Sorghum bicolor	*Sb*
Stegolepis ferruginea	*Sfe*
Stipa lagascae	*Sla*
Streptochaeta angustifolia	*San*
Triticum aestivum	*TaA*
Triticum aestivum	*TaB*
Triticum aestivum	*TaD*
Triticum urartu	*Tur*
Typha latifolia	*Tla*
Xyris jupicai	*Xju*
Zea mays	*Zm*

Table 7-2. Identical gene clusters in *Exo70F1* phylogenetic analysis.

Cluster	Members
HvuRGH2Baronesse	*HvuRGH2Baronesse, HvuRGH2Martime*
Hvu	*Hvu, HvuAB12*, *HvuAramir*, *HvuBarke*, *HvuBaronesse*, *HvuBCD12*, *HvuBCD47*, *HvuCI16139*, *HvuCI16147*, *HvuCI16153*, *HvuCIho4196*, *HvuDuplex*, *HvuEmir*, *HvuFongTien*, *HvuGZ*, *HvuHarunaNijo*, *HvuHeilsFranken*, *HvuHindmarsh*, *HvuHOR1428*, *HvuIgri*, *HvuManchuria*, *HvuMaritime*, *HvuMorex*, *HvuRussell*, *HvuSultan5*, *HvuWBDC172*
HvuWBDC110	*HvuWBDC110, HvuI5*, *HvuSusPtrit*, *HvuWBDC008*
HvuFinniss	*HvuFinniss, HvuBetzes*, *HvuBowman*, *HvuCommander*, *HvuGoldenPromise*, *HvuPallas*, *HvuQ21861*
AetPI499262	*AetPI499262*, *AetAT76*, *AetKU20252*
AetKU2093	*AetKU2093, AetERS399496*
AetKU2087	*AetKU2087*, *AetKU2003*
AetKU2124	*AetKU2075, AetKU2078, AetKU2124, Aet2220007, AetATL, AetTQ27*
AetRGH2D2220009	*AetRGH2AUS1891, AetRGH2D2220009*
Ash409	*Ash396, Ash409, Ash546, Ash548, Ash1998, Ash2020, Ash2205, Ash6793, Ash6856*
AshRGH22172	*AshRGH22172, AshRGH22233, AshRGH26793*
AshRGH2575	*AshRGH2396, AshRGH2575*
AvsRGH2Hanyou5	*AvsRGH2Huazao2, AvsRGH2Hanyou5, AvsRGH2Mongolia*

Table 7-3. Parameter estimates of dN/dS (ω) in different *Exo70* gene families.

Gene family	Species	Genes	Codons	κ	ω
Exo70A1	7	7	407	1.87	0.07
Exo70A2	4	4	355	2.22	0.48
Exo70A3	6	6	309	2.63	0.08
Exo70A4	5	5	420	2.16	0.55
Exo70B1	7	7	362	2.59	0.09
Exo70B2	4	4	345	4.01	0.30
Exo70B3	7	8	434	1.88	0.10
Exo70C1	7	8	382	1.94	0.08
Exo70C2	7	8	313	2.56	0.08
Exo70D1	7	8	428	2.08	0.12
Exo70D2	7	9	352	2.63	0.07
Exo70E1	7	8	470	2.67	0.24
Exo70F1	6	7	443	2.32	0.15
Exo70F2	7	8	232	2.04	0.10
Exo70F3	7	7	440	1.57	0.11
Exo70F4	7	8	369	2.23	0.11
Exo70F5	4	4	167	2.53	0.43
Exo70G1	7	8	444	3.69	0.10
Exo70G2	7	7	519	1.85	0.16
Exo70H1	7	9	359	2.41	0.13
Exo70I1	7	7	426	2.97	0.08

Codons, number of codons used to estimate ω; κ, transition:transversion ratio; ω, d_N/d_S ratio.

Table 7-4. Parameter and log likelihood estimates of dN/dS (ω) in non-integrated and integrated *Exo70F1* homologs.

Model	κ	ω_0	ω_1	ω_a	ω_b	lnL
H_0 (one ω)	2.418	0.217	= ω_0	= ω_0	= ω_0	-13005.2
H_1 (two ω; ω_0 and ω_1)	2.418	0.220	0.078	= ω_0	= ω_0	-13003.5
H_2 (two ω; ω_0 and ω_a)	2.437	0.092	= ω_a	0.413	= ω_0	-12871.9
H_3 (three ω; ω_0, ω_a, ω_b)	2.435	0.075	= ω_a	0.413	0.118	-12867.4

Significant differences in ω were observed for H_0 vs. H_2 (p<0.001) and H_2 vs. H_3 (p=0.003). Variables: κ, transition:transversion ratio, ω d_N/d_S ratio, lnL, log-likelihood. All likelihood ratio tests had degrees of freedom of 1.

Table 7-5. Gene identifiers for *Exo70* gene family.

Identifier	Gene
AT5G03540.1	AtExo70A1
AT5G52340.1	AtExo70A2
AT5G52350.1	AtExo70A3
AT5G58430.1	AtExo70B1
AT1G07000.1	AtExo70B2
AT5G13150.1	AtExo70C1
AT5G13990.1	AtExo70C2
AT1G72470.1	AtExo70D1
AT1G54090.1	AtExo70D2
AT3G14090.1	AtExo70D3
AT3G29400.1	AtExo70E1
AT5G61010.1	AtExo70E2
AT5G50380.1	AtExo70F1
AT4G31540.1	AtExo70G1
AT1G51640.1	AtExo70G2
AT3G55150.1	AtExo70H1
AT2G39380.1	AtExo70H2
AT3G09530.1	AtExo70H3
AT3G09520.1	AtExo70H4
AT2G28640.1	AtExo70H5
AT1G07725.1	AtExo70H6
AT5G59730.1	AtExo70H7
AT2G28650.1	AtExo70H8
Bradi5g26580.1.p	BdExo70A1
Bradi5g26587.6.p	BdExo70A2
Bradi4g24960.1.p	BdExo70A3
Bradi4g41980.2.p	BdExo70A4
Bradi2g53820.1.p	BdExo70B1
Bradi2g22490.1.p	BdExo70B3
Bradi4g41750.1.p	BdExo70C1
Bradi4g24680.3.p	BdExo70C2
Bradi4g31270.1.p	BdExo70D1
Bradi3g37580.1.p	BdExo70D2
Bradi2g50730.2.p	BdExo70E1
Bradi2g59057.1.p	BdExo70F1
Bradi3g43960.2.p	BdExo70F2
Bradi5g07740.2.p	BdExo70F3
Bradi3g41160.1.p	BdExo70F4
Bradi5g04622.2.p	BdExo70FX1
Bradi2g50515.1.p	BdExo70FX10
Bradi5g25512.2.p	BdExo70FX11a
Bradi5g25531.1.p	BdExo70FX11b
Bradi5g01926.1.p	BdExo70FX2a
Bradi5g01930.1.p	BdExo70FX2b
Bradi3g32640.2.p	BdExo70FX3
Bradi3g03860.1.p	BdExo70G1
Bradi1g33940.1.p	BdExo70G2
Bradi5g06870.2.p	BdExo70H1
Bradi3g40510.1.p	BdExo70I1
HORVU2Hr1G123320.1	HvExo70A1
HORVU2Hr1G123350.m1	HvExo70A2
HORVU4Hr1G021040.1	HvExo70A3
HORVU5Hr1G040140.3	HvExo70A4
HORVU3Hr1G088110.3	HvExo70B1
HORVU1Hr1G070390.1	HvExo70B3
HORVU5Hr1G039240.1	HvExo70C1
HORVU4Hr1G020050.1	HvExo70C2

Identifier	Gene
HORVU5Hr1G062200.3	HvExo70D1
MLOC_19124.1	HvExo70D2
HORVU3Hr1G073850.1	HvExo70E1a
HORVU3Hr1G073910.1	HvExo70E1b
HORVU3Hr1G094570.3	HvExo70F1
HORVU7Hr1G028060.3	HvExo70F2
MLOC_59065.1	HvExo70F3
HORVU7Hr1G054020.2	HvExo70F4
HORVU2Hr1G116970.2	HvExo70F5
HORVU7Hr1G030080.3	HvExo70FX1
HORVU2Hr1G118460.1_1_377	HvExo70FX11a
HORVU2Hr1G118520.1	HvExo70FX11b.a
HORVU2Hr1G118500.1	HvExo70FX11c
HORVU2Hr1G118450.1	HvExo70FX11d
HORVU2Hr1G118510.1	HvExo70FX11e
HORVU2Hr1G118490.1	HvExo70FX11f
HORVU4Hr1G079440.1	HvExo70FX12a
HORVU2Hr1G003540.3_1213_1543	HvExo70FX2
HORVU7Hr1G082050.1	HvExo70FX3a
HORVU0Hr1G021500.1_32_517	HvExo70FX3b
MLOC_11137.3	HvExo70FX4
HORVU6Hr1G021690.1	HvExo70G1
HORVU7Hr1G098020.1	HvExo70G2
MLOC_56456.1	HvExo70H1
HORVU7Hr1G052100.1	HvExo70I1
HvRGH2_1025_1637	HvRGH2
LOC_Os04g58880.1	OsExo70A1
LOC_Os04g58870.1	OsExo70A2
LOC_Os11g05880.1	OsExo70A3
LOC_Os01g61180.1	OsExo70B1
LOC_Os01g61190.1	OsExo70B2
LOC_Os05g39610.1	OsExo70B3
LOC_Os12g06840.1	OsExo70C1
LOC_Os11g06700.1	OsExo70C2
LOC_Os09g26820.1	OsExo70D1
LOC_Os08g35470.1	OsExo70D2
LOC_Os01g55799.1	OsExo70E1
LOC_Os01g69230.1	OsExo70F1
LOC_Os02g30230.1	OsExo70F2
LOC_Os04g31330.1	OsExo70F3
LOC_Os01g05580.1	OsExo70F4a
LOC_Os08g41820.1	OsExo70F4b
LOC_Os10g33850.1	OsExo70F4c
LOC_Os06g14450.1	OsExo70F5
LOC_Os01g56210.1	OsExo70FX10
LOC_Os06g08460.1	OsExo70FX1a
LOC_Os01g49460.1_57_151	OsExo70FX1b
LOC_Os12g24620.1_57_141	OsExo70FX1c
LOC_Os04g02070.1	OsExo70FX2
LOC_Os07g10920.1	OsExo70FX3a
LOC_Os07g10970.1	OsExo70FX3b
LOC_Os07g10910.1_198_700	OsExo70FX4a
LOC_Os07g10940.1_186_709	OsExo70FX4b
LOC_Os07g10960.1	OsExo70FX4c
LOC_Os02g36619.1	OsExo70FX5a
LOC_Os01g28600.1	OsExo70FX5b
LOC_Os01g67820.1	OsExo70FX6a
LOC_Os01g67810.1	OsExo70FX6b

Identifier	Gene
LOC_Os11g36400.1	OsExo70FX7
LOC_Os08g13270.1	OsExo70FX8a
LOC_Os08g13570.1	OsExo70FX8b
LOC_Os09g17810.1	OsExo70FX8c
LOC_Os05g30660.1	OsExo70FX9a
LOC_Os05g30680.1	OsExo70FX9b
LOC_Os05g30700.1	OsExo70FX9c
LOC_Os05g30640.1	OsExo70FX9d
LOC_Os05g30620.1	OsExo70FX9e
LOC_Os02g05620.1	OsExo70G1
LOC_Os06g48330.1	OsExo70G2
LOC_Os12g01040.1	OsExo70H1a
LOC_Os11g01050.1	OsExo70H1b
LOC_Os11g42989.1	OsExo70H2a
LOC_Os11g43049.1	OsExo70H2b
LOC_Os03g33520.1	OsExo70H2c
LOC_Os08g40840.1	OsExo70I1
Oropetium_20150105_26701A	OtExo70A1
Oropetium_20150105_14997A	OtExo70A3a
Oropetium_20150105_28040A	OtExo70A3b
Oropetium_20150105_10903A_1_562	OtExo70A4
Oropetium_20150105_18752A	OtExo70B1
Oropetium_20150105_03308A	OtExo70B3
Oropetium_20150105_10873A	OtExo70C1
Oropetium_20150105_14956A	OtExo70C2
Oropetium_20150105_05783A	OtExo70D1
Oropetium_20150105_02148A	OtExo70D2
Oropetium_20150105_05787A	OtExo70D3a
Oropetium_20150105_27432A	OtExo70D3b
Oropetium_20150105_12609A	OtExo70E1
Oropetium_20150105_09017A	OtExo70F1
Oropetium_20150105_11249A	OtExo70F2a
Oropetium_20150105_27473A	OtExo70F2b
Oropetium_20150105_08821A	OtExo70F3
Oropetium_20150105_14692A	OtExo70F4a
Oropetium_20150105_14694A	OtExo70F4b
Oropetium_20150105_16002A	OtExo70F5
Oropetium_20150105_17316A	OtExo70FX1
Oropetium_20150105_16422A_1014_1125	OtExo70FX13
Oropetium_20150105_23831A	OtExo70FX2
Oropetium_20150105_24834A	OtExo70FX5a
Oropetium_20150105_26562A_89_686	OtExo70FX5b
Oropetium_20150105_13125A	OtExo70FX6a
Oropetium_20150105_13124A	OtExo70FX6b
Oropetium_20150105_05298A	OtExo70FX9
Oropetium_20150105_14354A	OtExo70G1
Oropetium_20150105_16262A	OtExo70G2
Oropetium_20150105_26824A	OtExo70H1a
Oropetium_20150105_27340A	OtExo70H1b
Oropetium_20150105_28021A	OtExo70H1c
Oropetium_20150105_14767A	OtExo70I1
Sobic.006G274600.1.p	SbExo70A1
Sobic.005G044300.5.p	SbExo70A3
Sobic.008G043600.1.p	SbExo70A4
Sobic.003G341700.2.p	SbExo70B1
Sobic.003G341800.1.p	SbExo70B2
Sobic.009G171000.1.p	SbExo70B3
Sobic.008G048200.1.p	SbExo70C1
Sobic.005G049200.1.p	SbExo70C2

Identifier	Gene
Sobic.002G215100.1.p	SbExo70D1
Sobic.007G148700.1.p	SbExo70D2
Sobic.003G305400.1.p	SbExo70E1
Sobic.003G405700.1.p	SbExo70F1
Sobic.004G153600.1.p	SbExo70F2
Sobic.006G047100.1.p	SbExo70F3
Sobic.007G194400.1.p	SbExo70F4
Sobic.010G271700.1.p	SbExo70FX13a
Sobic.010G272501.1.p	SbExo70FX13b
Sobic.010G271600.1.p	SbExo70FX13c
Sobic.010G272000.2.p	SbExo70FX13d
Sobic.010G272700.1.p	SbExo70FX13e
Sobic.010G271901.1.p	SbExo70FX13f
Sobic.010G271800.1.p	SbExo70FX13g
Sobic.010G272400.2.p	SbExo70FX14a
Sobic.010G272101.1.p	SbExo70FX14b
Sobic.010G272200.1.p	SbExo70FX14c
Sobic.010G271501.1.p	SbExo70FX14d
Sobic.010G269950.1.p	SbExo70FX14e
Sobic.003G155600.1.p	SbExo70FX5
Sobic.003G393400.1.p	SbExo70FX6a
Sobic.003G393500.1.p	SbExo70FX6b
Sobic.010G044700.1.p	SbExo70FX8
Sobic.004G041100.1.p	SbExo70G1
Sobic.010G248100.1.p	SbExo70G2
Sobic.008G000500.1.p	SbExo70H1
Sobic.007G202700.1.p	SbExo70I1
ScExo70	ScExo70
Seita.3G007900.1.p	SiExo70A1
Seita.3G008100.1.p	SiExo70A2
Seita.8G040000.1.p	SiExo70A3
Seita.7G295900.1.p	SiExo70A4
Seita.5G366100.1.p	SiExo70B1
Seita.5G366200.1.p	SiExo70B2
Seita.3G207400.1.p	SiExo70B3
Seita.7G292600.1.p	SiExo70C1
Seita.8G045500.1.p	SiExo70C2
Seita.2G217900.1.p	SiExo70D1
Seita.6G171200.1.p	SiExo70D2
Seita.5G328000.1.p	SiExo70E1
Seita.5G431300.1.p	SiExo70F1
Seita.1G167500.1.p	SiExo70F2
Seita.7G070200.1.p	SiExo70F3
Seita.6G222200.1.p	SiExo70F4
Seita.4G113200.1.p	SiExo70F5
Seita.5G035600.1.p	SiExo70FX13a
Seita.4G232500.1.p	SiExo70FX13b
Seita.4G285400.1.p	SiExo70FX13c
Seita.4G285700.1.p	SiExo70FX14a
Seita.4G285500.1.p	SiExo70FX14b
Seita.4G285800.1.p	SiExo70FX14c
Seita.1G165300.1.p	SiExo70FX14d
Seita.4G050300.1.p	SiExo70FX1a
Seita.4G050500.1.p	SiExo70FX1b
Seita.5G431900.1.p	SiExo70FX3a
Seita.1G130000.1.p	SiExo70FX3b
Seita.5G432000.1.p	SiExo70FX4a
Seita.5G432100.1.p	SiExo70FX4b
Seita.5G432200.1.p_191_611	SiExo70FX4c

Identifier	Gene
Seita.5G175300.1.p	SiExo70FX5
Seita.5G419400.1.p	SiExo70FX6a
Seita.5G419600.1.p	SiExo70FX6b
Seita.4G068100.1.p	SiExo70FX8a
Seita.4G068000.1.p	SiExo70FX8b
Seita.1G088800.1.p	SiExo70G1
Seita.4G244700.1.p	SiExo70G2
Seita.4G117500.1.p	SiExo70H1a
Seita.9G423500.1.p	SiExo70H1b
Seita.6G212800.1.p	SiExo70I1
NM_001196530.1	ZmExo70A1
AC208346.3_FGP004	ZmExo70B1
GRMZM2G141392_P01	ZmExo70B2
GRMZM2G065566_P01	ZmExo70B3a
GRMZM5G869403_P01	ZmExo70B3b
GRMZM2G330361_P01	ZmExo70C1a
GRMZM2G343437_P01	ZmExo70C1b
GRMZM2G066464_P01	ZmExo70C2a
GRMZM2G348151_P01	ZmExo70C2b
GRMZM2G135817_P01	ZmExo70D1a
GRMZM2G143029_P01	ZmExo70D1b
GRMZM2G029527_P01	ZmExo70D2a
GRMZM2G076389_P01	ZmExo70D2b
GRMZM2G390691_P01_1_526	ZmExo70D2c
GRMZM2G111657_P01	ZmExo70E1
GRMZM2G003518_P01	ZmExo70F1a
GRMZM2G022159_P01	ZmExo70F1b
GRMZM2G111782_P02	ZmExo70F2a
GRMZM2G370741_P01_1_107	ZmExo70F2b
AC208418.3_FGP009_1_207	ZmExo70F2c
AC218988.3_FGP003_1_112	ZmExo70F2d
GRMZM2G059965_P01	ZmExo70F3
GRMZM2G165301_P01	ZmExo70F4
GRMZM2G163172_P01	ZmExo70FX1
GRMZM2G436742_P01_306_677	ZmExo70FX4
GRMZM2G437490_P01	ZmExo70FX5a
GRMZM2G353483_P01	ZmExo70FX5b
GRMZM2G177227_P01	ZmExo70FX6
GRMZM5G815077_P01	ZmExo70FX8
GRMZM2G067313_P01	ZmExo70G1a
GRMZM2G146711_P01	ZmExo70G1b
GRMZM2G166032_P01	ZmExo70G1c
GRMZM2G162065_P01	ZmExo70G2
GRMZM2G357443_P01	ZmExo70H1
GRMZM2G149474_P01	ZmExo70I1

Table 7-6. List of Barley accessions.

Accession name	PI/CI Number	Experiment used	Source	*Psh* Field Trial
Baronesse	-	Mo, Bgh, victorin	Oregon State University	Norwich, Oregon, CIMMYT
BCD47	PI 659444	Mo, Bgh, victorin	Oregon State University	Norwich, Oregon, CIMMYT
Nigrate	CIho 2444	Mo, Bgh, victorin	USDA-GRIN	-
Golden Promise	PI 343079	Mo, Bgh, victorin	-	-
SxGP DH47	-	Mo, Bgh, victorin	-	-
Maritime	-	Mo, Bgh, victorin	Wolfgang Spielmeyer	-
Duplex	CIho 12420	Mo, Bgh, victorin	USDA-GRIN	-
Finniss	-	Mo, Bgh, victorin	Wolfgang Spielmeyer	-
HOR 1428	PI 548708	Mo, Bgh, victorin	USDA-GRIN	-
Manchuria	CIho 2330	Mo, Bgh, victorin	USDA-GRIN	-
Bowman	PI 483237	Mo, Bgh, victorin	-	-
Grannenlose Zweizeilige	PI 548740	Mo, Bgh, victorin	USDA-GRIN	-
Siri	-	Mo, Bgh, victorin	John Innes Centre	-
S01	-	Mo, Bgh, victorin	John Innes Centre	-
S02	-	Mo, Bgh, victorin	John Innes Centre	-
S03	-	Mo, Bgh, victorin	John Innes Centre	-
S04	-	Mo, Bgh, victorin	John Innes Centre	-
S06	-	Mo, Bgh, victorin	John Innes Centre	-
S07	-	Mo, Bgh, victorin	John Innes Centre	-
S09	-	Mo, Bgh, victorin	John Innes Centre	-
S10	-	Mo, Bgh, victorin	John Innes Centre	-
S11	-	Mo, Bgh, victorin	John Innes Centre	-
S12	-	Mo, Bgh, victorin	John Innes Centre	-
S13	-	Mo, Bgh, victorin	John Innes Centre	-
S15	-	Mo, Bgh, victorin	John Innes Centre	-
S17	-	Mo, Bgh, victorin	John Innes Centre	-
Siri	-	APR Psh	John Innes Centre	Norwich, Oregon
S01	-	APR Psh	John Innes Centre	Norwich, Oregon
S02	-	APR Psh	John Innes Centre	Norwich, Oregon
S03	-	APR Psh	John Innes Centre	Norwich, Oregon
S04	-	APR Psh	John Innes Centre	Norwich, Oregon
S06	-	APR Psh	John Innes Centre	Norwich, Oregon
S07	-	APR Psh	John Innes Centre	Norwich, Oregon
S09	-	APR Psh	John Innes Centre	Norwich, Oregon
S10	-	APR Psh	John Innes Centre	Norwich, Oregon
S11	-	APR Psh	John Innes Centre	Norwich, Oregon
S12	-	APR Psh	John Innes Centre	Norwich, Oregon
S13	-	APR Psh	John Innes Centre	Norwich, Oregon
S15	-	APR Psh	John Innes Centre	Norwich, Oregon
S17	-	APR Psh	John Innes Centre	Norwich, Oregon
BISON 0-QTL	-	APR Psh	Oregon State University	Norwich, Oregon, CIMMYT
BISON 1H	-	APR Psh	Oregon State University	Norwich, Oregon, CIMMYT
BISON 4H	-	APR Psh	Oregon State University	Norwich, Oregon, CIMMYT
BISON 5H	-	APR Psh	Oregon State University	Norwich, Oregon, CIMMYT
BISON 7H	-	APR Psh	Oregon State University	Norwich, Oregon, CIMMYT
BISON 1H+4H	-	APR Psh	Oregon State University	Norwich, Oregon, CIMMYT
BISON 1H+5H	-	APR Psh	Oregon State University	Norwich, Oregon, CIMMYT
BISON 4H+5H	-	APR Psh	Oregon State University	Norwich, Oregon, CIMMYT
BISON 1H+4H+5H	-	APR Psh	Oregon State University	Norwich, Oregon, CIMMYT
BCD12	-	APR Psh	Oregon State University	Norwich, Oregon, CIMMYT
Manchuria	CIho 2330	APR Psh	USDA-GRIN	Norwich, CIMMYT
HV_14947	LG Diablo	APR Psh	Limagrain Europe	Norwich, CIMMYT
HV_14948	LG Tomahawk	APR Psh	Limagrain Europe	Norwich, CIMMYT
HV_14949	LG Mountain	APR Psh	Limagrain Europe	Norwich, CIMMYT
HV_14950	LG Flynn	APR Psh	Limagrain Europe	Norwich, CIMMYT
HV_14951	LG Casting	APR Psh	Limagrain Europe	Norwich, CIMMYT
HV_05659	rar1-m82 (Sultan 5)	APR Psh	Roger Wise	Norwich, CIMMYT
HV_05660	rar1-m100 (Sultan 5)	APR Psh	Roger Wise	Norwich, CIMMYT
HV_05059	mla 12-m66 (Sultan 5	APR Psh	Roger Wise	Norwich, CIMMYT
HV_07885	Sultan 5	APR Psh	Roger Wise	Norwich, CIMMYT

Table 7-7. Table of Siri panel.

Siri panel line	Historical introgression	*Mla* haplotype
Siri	*Mla8*	*Mla8*
S01	*Mla1*	*Mla1*
S02	*Mla3*	*Mla3*
S03	*Mla6*	*Mla6*
S04	*Mla7 (Nordal)*	*Mla7 (Nordal)*
S06	*Mla7 (Moseman)*	*Mla7 (Moseman)*
S07	*Mla9, Mlk*	*Mla9*
S09	*Mla10, Ml-(Du2)*	*Mla10*
S10	*Mla12*	*Mla12*
S11	*Mla13*	*Mla13*
S12	*Mlc*	*Mla22*
S13	*Ml-(1402)*	*Mla23*
S15	*Ml-(Ru2)*	*Ml-(Ru2)*
S17	*Mlk*	*Mlk*

Table 7-8. List of KASP markers.

Marker name	Source marker name	Purpose	Forward primer allele 1	Forward allele primer 2	Common Reverse primer
K_3_1144	3_1144_60_F	Baronesse x BCD47	GAAGGTCGGAGTCAACGGATTTGACCGGCAAGACCGTCACC	GAAGGTGACCAAGTTCATGCTTGACCGGCAAGACCGTCACT	GCTTGGATCCACCCCCTC
K_1_0419	1_0419_120_F	Baronesse x BCD47	GAAGGTCGGAGTCAACGGATTTGGATGCTCTCAAGGAGACC	GAAGGTGACCAAGTTCATGCTTGATGCTCTCAAGGAGACT	TCTGAGGCAAGCAGCAGC
K_66630	SCRI_RS_66630_159_R	Baronesse x BCD47	GAAGGTCGGAGTCAACGGATTTATCCAGTTCACTGCCCTCC	GAAGGTGACCAAGTTCATGCTTATCCAGTTCACTGCCCTCT	GGCTCCATCCATACACCTCA
K_82277	SCRI_RS_82277_126_F	Baronesse x BCD47	GAAGGTCGGAGTCAACGGATTCATACATCCGCTGGGCATCA	GAAGGTGACCAAGTTCATGCTCATACATCCGCTGGGCATCG	TGGCGGCGAAAAGAAGCA
K_232577	SCRI_RS_232577_124_R	Baronesse x BCD47	GAAGGTCGGAGTCAACGGATTAAGAGCGACCTCCTCCTCAC	GAAGGTGACCAAGTTCATGCTAAGAGCGACCTCCTCCTCAT	TTGTGGATCGAGCACGGGC
K_3_0933	3_0933_60_F	Baronesse x BCD47	GAAGGTCGGAGTCAACGGATTGTAATCTACCTGTATGATTC	GAAGGTGACCAAGTTCATGCTGTAATCTACCTGTATGATTT	TCAGAAGAGTGCAGCATAAACA
-	k08433_26_F	Baronesse x BCD47	GAAGGTCGGAGTCAACGGATTGGGATTTTGTAGCAGCATGCA	GAAGGTGACCAAGTTCATGCTGGGATTTTGTAGCAGCATGCG	CACCAACCCCCAGCCATC
-	k08302_100_R	Baronesse x BCD47	GAAGGTCGGAGTCAACGGATTCTGTAGCAAGTTTGTTCATAC	GAAGGTGACCAAGTTCATGCTCTGTAGCAAGTTTGTTCATAT	TCCAGATGGTCGGGAGGG
K_963924_115	HV5_963924_p1_115_F	Baronesse x BCD47	GAAGGTCGGAGTCAACGGATTAAATTGCACTTCATTGCAGC	GAAGGTGACCAAGTTCATGCTAAATTGCACTTCATTGCAGT	CAGGGATTACGCGAGCACT
K_2_1174	2_1174_120_F	Baronesse x BCD47	GAAGGTCGGAGTCAACGGATTACCGGCGCTCGATTAAGTCA	GAAGGTGACCAAGTTCATGCTACCGGCGCTCGATTAAGTCG	GCATCGCCCGGGTGATACA
-	HV5_963924_p1_378_F	Baronesse x BCD47	GAAGGTCGGAGTCAACGGATTCAACATCAACACTCGTAGCA	GAAGGTGACCAAGTTCATGCTCAACATCAACACTCGTAGCG	CGCCACAACGCTCTTTGAC
-	MLA_186_p1_111_R	Baronesse x BCD47	GAAGGTCGGAGTCAACGGATTTGTATCTAAGTATATACCCC	GAAGGTGACCAAGTTCATGCTTGTATCTAAGTATATACCCT	CCTTCGGCTACCCACTTCC
-	MLA_132_p1_55_F	Baronesse x BCD47	GAAGGTCGGAGTCAACGGATTGGGTTAAACAAAAAATCTCC	GAAGGTGACCAAGTTCATGCTGGGTTAAACAAAAAATCTCT	TGGTTTTGCACTGGCCCT
-	15A08F2_133_R	Baronesse x BCD47	GAAGGTCGGAGTCAACGGATTTCTCCCAACCCCACTAGTC	GAAGGTGACCAAGTTCATGCTTCTCCCAACCCCACTAGTT	GCACAAGGTGGCGTCCAT
-	80H14R1F3_p1_152_F	Baronesse x BCD47	GAAGGTCGGAGTCAACGGATTGACAAGGGTCGGGGATTTTC	GAAGGTGACCAAGTTCATGCTGACAAGGGTCGGGGATTTTT	AGTTTCCTCACACTCACACCA
-	80H14R1F3_p2_128_R	Baronesse x BCD47	GAAGGTCGGAGTCAACGGATTTCCTCTCTCAAACTGTAGC	GAAGGTGACCAAGTTCATGCTTCCTCTCAAACTGTAGT	GGTTGCCCCCAAGGTACCC
-	FWA62F_199_F	Baronesse x BCD47	GAAGGTCGGAGTCAACGGATTTCTTGGGACGGCTTCACTAC	GAAGGTGACCAAGTTCATGCTTCTTGGGACGGCTTCACTAT	CGCCGCGACAACTCTAGT
K_MLA_RGH1_2920	Mla_ORO_2920_R	Baronesse x BCD47	GAAGGTCGGAGTCAACGGATTGGCAGATCCACAATCCAAAC	GAAGGTGACCAAGTTCATGCTGGCAGATCCACAATCCAAAT	CACCCACCAAAACGCAACG
-	MLA_063_p1_73_F	Baronesse x BCD47	GAAGGTCGGAGTCAACGGATTCCTTGCAGATCAGTTGGAGC	GAAGGTGACCAAGTTCATGCTCCTTGCAGATCAGTTGGAGT	GACGATGGAGCTCGGTCG
-	MLA_065_p1_78_F	Baronesse x BCD47	GAAGGTCGGAGTCAACGGATTCTATGGCGACCACCCGTAGC	GAAGGTGACCAAGTTCATGCTCTATGGCGACCACCCGTAGT	CCGTAGGCTGCTCGACAT
-	MLA_079_p1_147_F	Baronesse x BCD47	GAAGGTCGGAGTCAACGGATTTGAAGATGAGTCAAGAGAAA	GAAGGTGACCAAGTTCATGCTTTGAAGATGAGTCAAGAGAAC	ACCTGAGGACATCCGGCT
-	MLA_080_p1_286_F	Baronesse x BCD47	GAAGGTCGGAGTCAACGGATTTCTTTGGGACGGCTTCACTAC	GAAGGTGACCAAGTTCATGCTTCTTTGGGACGGCTTCACTAT	CGCCGCGACAACTCTAGT
-	MLA_118_p1_51_F	Baronesse x BCD47	GAAGGTCGGAGTCAACGGATTTGTGTTGACCAATTTGTTGC	GAAGGTGACCAAGTTCATGCTTGTGTTGACCAATTTGTTGT	TGTCAGTTGCATTTCGACAGG
-	MLA_119_p1_166_R	Baronesse x BCD47	GAAGGTCGGAGTCAACGGATTCCGTTCCCATCCATTGCATA	GAAGGTGACCAAGTTCATGCTCCGTTCCCATCCATTGCATG	GTGAAGCAGTGGATAGCCGA

Marker name	Source marker name	Purpose	Forward primer allele 1	Forward allele primer 2	Common Reverse primer
-	MLA_103_p1_22_F	Baronesse x BCD47	GAAGGTCGGAGTCAACGGATTCTTGGAAGTAAAGGGATAGG	GAAGGTGACCAAGTTCATGCTCTTGGAAGTAAAGGGATAGT	TGGGTGAAGACAACGTCCG
-	MLA_026_p1_38_F	Baronesse x BCD47	GAAGGTCGGAGTCAACGGATTGTTGCATTCTTTAAGCTTCA	GAAGGTGACCAAGTTCATGCTGTTGCATTCTTTAAGCTTCG	TGACAAATCAAGGCAGGGGT
-	MLA_027_p1_282_F	Baronesse x BCD47	GAAGGTCGGAGTCAACGGATTACTTCATGGTTGTCATATGG	GAAGGTGACCAAGTTCATGCTACTTCATGGTTGTCATATGT	TCATTGGTTGTTTGTCCTCCT
-	MLA_028_p1_246_F	Baronesse x BCD47	GAAGGTCGGAGTCAACGGATTATGTCCAAACCAGCATCCGG	GAAGGTGACCAAGTTCATGCTATGTCCAAACCAGCATCCGT	TGGGGCAAACTCACACACA
-	MLA_028_p1_387_R	Baronesse x BCD47	GAAGGTCGGAGTCAACGGATTGCAAGGTAGTGGCCGTTACC	GAAGGTGACCAAGTTCATGCTGCAAGGTAGTGGCCGTTACT	TGAGTTTGCCCCAACGCA
-	MLA_023_p1_28_F	Baronesse x BCD47	GAAGGTCGGAGTCAACGGATTGCTAGTACAAACATGTAAAA	GAAGGTGACCAAGTTCATGCTGCTAGTACAAACATGTAAAG	TGGACAAGGACCAAACTTTGA
K_020_313	MLA_020_p1_313_R	Baronesse x BCD47	GAAGGTCGGAGTCAACGGATTATTCGCTTGGATCATGGGAA	GAAGGTGACCAAGTTCATGCTATTCGCTTGGATCATGGGAG	GGTTAATCAGGAACCTCGGTG
-	MLA_020_p1_446_F	Baronesse x BCD47	GAAGGTCGGAGTCAACGGATTTCACAGTGAGAAGCATGCCA	GAAGGTGACCAAGTTCATGCTTCACAGTGAGAAGCATGCCT	TGTCTTGCTCTTGCGGCT
K_009_53	MLA_009_p1_53_F	Baronesse x BCD47	GAAGGTCGGAGTCAACGGATTGATCAACGAAACAACATCGA	GAAGGTGACCAAGTTCATGCTGATCAACGAAACAACATCGG	GGCTTGGATCCGCCTGAA
K_009_97	MLA_009_p1_97_F	Baronesse x BCD47	GAAGGTCGGAGTCAACGGATTCAACACCATCAACTCCTTCA	GAAGGTGACCAAGTTCATGCTCAACACCATCAACTCCTTCG	GGCTTGGATCCGCCTGAA
K_206D11_281	0206D11_T7_p1_135_F	Baronesse x BCD47	GAAGGTCGGAGTCAACGGATTCTTTTGATCTGATCCGGCGC	GAAGGTGACCAAGTTCATGCTCTTTTGATCTGATCCGGCGG	GCCAACCAAGCAAGTGCC
-	206D11_T7_p1_281_F	Baronesse x BCD47	GAAGGTCGGAGTCAACGGATTCAGGGGGTAGCCCTAAGCAC	GAAGGTGACCAAGTTCATGCTCAGGGGGTAGCCCTAAGCAG	CTCTCGTCGGCGTCTTCC
-	3_0919_60_F	Baronesse x BCD47	GAAGGTCGGAGTCAACGGATTCGCAATAACGAACACAAACA	GAAGGTGACCAAGTTCATGCTCGCAATAACGAACACAAACG	TGCTAGGTGCTGCTGATGT
K_4261	k04261_p1_284_R	Baronesse x BCD47	GAAGGTCGGAGTCAACGGATTGCATCCGAGGTAACATGGAC	GAAGGTGACCAAGTTCATGCTGCATCCGAGGTAACATGGAT	AAACGAGCAATCGGGGCT
-	SCRI_RS_148560_109_F	Baronesse x BCD47	GAAGGTCGGAGTCAACGGATTGAAGCTGGGTTTATGGCCGG	GAAGGTGACCAAGTTCATGCTGAAGCTGGGTTTATGGCCGT	AGGATGTCCTTGCTTCACCA
K_2_0712	2_0712_120_F	Baronesse x BCD47	GAAGGTCGGAGTCAACGGATTGGTGTCGCAATTTCTGGACA	GAAGGTGACCAAGTTCATGCTGGTGTCGCAATTTCTGGACG	ACCCTAGAATGTACACGGTGT
K_2_1354	2_1354_120_F	BISON1H x Baronesse	GAAGGTCGGAGTCAACGGATTGCGGAGAGGACCGCTGGAGC	GAAGGTGACCAAGTTCATGCTGCGGAGAGGACCGCTGGAGG	CATTTCCAGCAGCGACGG
K_3_0933	3_0933_60_F	BISON1H x Baronesse	GAAGGTCGGAGTCAACGGATTGTAATCTACCTGTATGATTC	GAAGGTGACCAAGTTCATGCTGTAATCTACCTGTATGATTT	TCAGAAGAGTGCAGCATAACA
K_2_1226	2_1226_120_F	BISON1H x Baronesse	GAAGGTCGGAGTCAACGGATTCAGTCAGTCTAGTTATACCA	GAAGGTGACCAAGTTCATGCTCAGTCAGTCTAGTTATACCG	TACCTCCGTCCCCTGCTC
K_3_0952	3_0952_60_F	BISON1H x Baronesse	GAAGGTCGGAGTCAACGGATTTCTTGTTATGTTAGAGCATA	GAAGGTGACCAAGTTCATGCTTCTTGTTATGTTAGAGCATT	ACTACACAGCGATGCTTCAC
K_3_0955	3_0955_60_R	BISON1H x Baronesse	GAAGGTCGGAGTCAACGGATTCGGCATTGCTGAACCCTTCA	GAAGGTGACCAAGTTCATGCTCGGCATTGCTGAACCCTTCT	AACTTCAGCGGGGAAGGC
K_2_0749	2_0749_120_F	BISON1H x Baronesse	GAAGGTCGGAGTCAACGGATTCATGAACATGACCGCAGCCC	GAAGGTGACCAAGTTCATGCTCATGAACATGACCGCAGCCT	TGGATTTGGAGGTGCCCG
K_1_0873	1_0873_120_R	BISON1H x Baronesse	GAAGGTCGGAGTCAACGGATTCCACGAACTTGAGGACCTCA	GAAGGTGACCAAGTTCATGCTCCACGAACTTGAGGACCTCG	GGCTCCTGGTGCTCCTTG
K_1_0186	1_0186_120_F	BISON1H x Baronesse	GAAGGTCGGAGTCAACGGATTGGGTCACAAGTGATGGAGTC	GAAGGTGACCAAGTTCATGCTGGGTCACAAGTGATGGAGTT	CGGTGGTGATGGCAAATGG
K_1_0744	1_0744_120_F	BISON1H x Baronesse	GAAGGTCGGAGTCAACGGATTACCCTGAGTTGTTCTTGCGC	GAAGGTGACCAAGTTCATGCTACCCTGAGTTGTTCTTGCGG	ACAGAGCAGCATACTGGACA

Table 7-9. List of oligonucleotides (primers).

Primer ID	Sequence	Manufacturer	Gene construct	Construct ID	Internal ID
RP_Baronesse_225_t1_p1f	GGCGTAGACACCGATCGG	Sigma-Aldrich	RGH2, RGH3	HB_0207	MM067
RP_Baronesse_225_t2_p1f	CTTGGAGTCCGCCGTTGT	Sigma-Aldrich	RGH2, RGH3	HB_0207	MM067
RP_Baronesse_225_t4_p1f	CCCTTTCCTCGTCCGTCG	Sigma-Aldrich	RGH2, RGH3	HB_0207	MM067
RP_Baronesse_225_t5_p1f	CCACCCCAAGCAGGTACG	Sigma-Aldrich	RGH2, RGH3	HB_0207	MM067
RP_Baronesse_225_t6_p1f	TGCTGGTGCTGGTGTTGT	Sigma-Aldrich	RGH2, RGH3	HB_0207	MM067
RP_Baronesse_225_t7_p1f	GTCGTCGTCGGCGTAGAG	Sigma-Aldrich	RGH2, RGH3	HB_0207	MM067
RP_Baronesse_225_t8_p1f	GCCCTCCAAATGGCGGAT	Sigma-Aldrich	RGH2, RGH3	HB_0207	MM067
RP_Baronesse_225_t9_p1f	TCGTGACACTTCGCCCTTC	Sigma-Aldrich	RGH2, RGH3	HB_0207	MM067
RP_Baronesse_225_t10_p1f	GCAAACCCATCGTCCCTCA	Sigma-Aldrich	RGH2, RGH3	HB_0207	MM067
RP_Baronesse_225_t13_p1f	TGCGGAACAGCTTCTCCG	Sigma-Aldrich	RGH2, RGH3	HB_0207	MM067
RP_Baronesse_225_t17_p1f	GCAACTGGCGGAACTCCT	Sigma-Aldrich	RGH2, RGH3	HB_0207	MM067
RP_Baronesse_225_t18_p1f	GTGAGGCCCGTAGTGCAG	Sigma-Aldrich	RGH2, RGH3	HB_0207	MM067
RP_Baronesse_225_t20_p1f	GAGGCCAGTCAGGTGCTC	Sigma-Aldrich	RGH2, RGH3	HB_0207	MM067
RP_Baronesse_225_t21_p1f	GAGCAGTGAGGGAAGGCA	Sigma-Aldrich	RGH2, RGH3	HB_0207	MM067
RP_Baronesse_225_t22_p1f	CGCCGCGACAACTCTAGT	Sigma-Aldrich	RGH2, RGH3	HB_0207	MM067
RP_Baronesse_225_t23_p1f	GGTCAGCTCACCAAGGCA	Sigma-Aldrich	RGH2, RGH3	HB_0207	MM067
RP_Baronesse_225_t27_p1f	TCCTTCCCACCGTTCCCA	Sigma-Aldrich	RGH2, RGH3	HB_0207	MM067
RP_Baronesse_225_t30_p1f	TCCCAGGTTGATGGTGCC	Sigma-Aldrich	RGH2, RGH3	HB_0207	MM067
RP_Baronesse_225_t34_p1f	GAAGGTGGTGCCGTCGAA	Sigma-Aldrich	RGH2, RGH3	HB_0207	MM067
RP_Baronesse_225_t36_p1f	TGTGCCGGTGAATCGCTT	Sigma-Aldrich	RGH2, RGH3	HB_0207	MM067
RP_Baronesse_225_t38_p1f	CTCACCGGTGCCTCCATC	Sigma-Aldrich	RGH2, RGH3	HB_0207	MM067
RP_Baronesse_225_t39_p1f	GAGTGGGCCTGCTCTTGG	Sigma-Aldrich	RGH2, RGH3	HB_0207	MM067
RP_Baronesse_225_t40_p1f	ACCGCTCGTGTTTTTCT	Sigma-Aldrich	RGH2, RGH3	HB_0207	MM067
RP_Baronesse_225_t41_p1f	CAACGACTGCTGGCTCGA	Sigma-Aldrich	RGH2, RGH3	HB_0207	MM067
RP_Baronesse_225_t42_p1f	CCAAGCACAGTCGACCGA	Sigma-Aldrich	RGH2, RGH3	HB_0207	MM067
RP_Baronesse_225_t43_p1f	GAGATCCGCGAGCTGACC	Sigma-Aldrich	RGH2, RGH3	HB_0207	MM067
RP_Baronesse_225_t46_p1f	AGTGGGTATCCAATCAGGCT	Sigma-Aldrich	RGH2, RGH3	HB_0207	MM067
RP_Baronesse_225_t50_p1f	AGTTAGTGCTGGGTGCGG	Sigma-Aldrich	RGH2, RGH3	HB_0207	MM067
RP_Baronesse_225_t54_p1f	TGTCCTGCCAGTGGAAGC	Sigma-Aldrich	RGH2, RGH3	HB_0207	MM067
RP_Baronesse_225_t57_p1f	GACGATGGAGCTCGGTCG	Sigma-Aldrich	RGH2, RGH3	HB_0207	MM067
RP_Baronesse_225_t61_p1f	TTGGGGTATGCTTGCGGT	Sigma-Aldrich	RGH2, RGH3	HB_0207	MM067
RP_Baronesse_225_t62_p1f	GTCGTCCTCCAGCGACAC	Sigma-Aldrich	RGH2, RGH3	HB_0207	MM067
RP_Baronesse_225_t63_p1f	GACAACCTTCCGGTCGCA	Sigma-Aldrich	RGH2, RGH3	HB_0207	MM067
RP_Baronesse_225_t64_p1f	ATCACCGCCGCTGTGAAA	Sigma-Aldrich	RGH2, RGH3	HB_0207	MM067
RP_Baronesse_225_t65_p1f	TGCCTCTGCCGTTTTCGT	Sigma-Aldrich	RGH2, RGH3	HB_0207	MM067
RP_Baronesse_225_t66_p1f	AACCGAGGCCAGGCTAGT	Sigma-Aldrich	RGH2, RGH3	HB_0207	MM067
RP_Baronesse_225_t67_p1f	CAGAACCGACACCAGGGC	Sigma-Aldrich	RGH2, RGH3	HB_0207	MM067
RP_Baronesse_131_t1_p1f	AGCTTCCGCCATCGCTTT	Sigma-Aldrich	RGH1 (Mla3)	HB_0200, HB_0204	MM067
RP_Baronesse_131_t2_p1f	GTCCGCCGGTCTTGTTGA	Sigma-Aldrich	RGH1 (Mla3)	HB_0200, HB_0204	MM067
RP_Baronesse_131_t3_p1f	AGTCCCAGGCCGATCCAT	Sigma-Aldrich	RGH1 (Mla3)	HB_0200, HB_0204	MM067
RP_Baronesse_131_t4_p1f	TGCCGTGCAAAGCCATTT	Sigma-Aldrich	RGH1 (Mla3)	HB_0200, HB_0204	MM067
RP_Baronesse_131_t5_p1f	ACGCATTAAGCACCTATGGT	Sigma-Aldrich	RGH1 (Mla3)	HB_0200, HB_0204	MM067
RP_Baronesse_131_t6_p1f	CTGCCACTCTCGGTGCAA	Sigma-Aldrich	RGH1 (Mla3)	HB_0200, HB_0204	MM067
RP_Baronesse_131_t7_p1f	GCCACCGTCTAGGCAACA	Sigma-Aldrich	RGH1 (Mla3)	HB_0200, HB_0204	MM067
RP_Baronesse_131_t8_p1f	CAGCAAGACCCTGCTGCT	Sigma-Aldrich	RGH1 (Mla3)	HB_0200, HB_0204	MM067
RP_Baronesse_131_t10_p1f	ACCTCCAAATCAGGCGCC	Sigma-Aldrich	RGH1 (Mla3)	HB_0200, HB_0204	MM067
RP_Baronesse_131_t12_p1f	CCGTGCCAACCTAGCCTC	Sigma-Aldrich	RGH1 (Mla3)	HB_0200, HB_0204	MM067
RP_Baronesse_131_t14_p1f	GAGGAGCTCAGGCGAACC	Sigma-Aldrich	RGH1 (Mla3)	HB_0200, HB_0204	MM067
RP_Baronesse_131_t17_p1f	ATTTTCAGGCCTGCCGCT	Sigma-Aldrich	RGH1 (Mla3)	HB_0200, HB_0204	MM067
RP_Baronesse_131_t18_p1f	GCTACTCCCTCCGTCCCA	Sigma-Aldrich	RGH1 (Mla3)	HB_0200, HB_0204	MM067
RP_Baronesse_131_t20_p1f	TCTGACCCCAGTCCCCAG	Sigma-Aldrich	RGH1 (Mla3)	HB_0200, HB_0204	MM067
RP_Baronesse_131_t21_p1f	GGCACCAGTGAAGAGCGT	Sigma-Aldrich	RGH1 (Mla3)	HB_0200, HB_0204	MM067
RP_Baronesse_131_t23_p1f	CAGCTTTCAAGGCACGCC	Sigma-Aldrich	RGH1 (Mla3)	HB_0200, HB_0204	MM067
RP_Baronesse_131_t24_p1f	CCTGCAGGCCCAAATCGA	Sigma-Aldrich	RGH1 (Mla3)	HB_0200, HB_0204	MM067
RP_Baronesse_131_t27_p1f	ACTGTGGACGGCAATTCCT	Sigma-Aldrich	RGH1 (Mla3)	HB_0200, HB_0204	MM067
RP_Baronesse_131_t31_p1f	TGGTCACCAGCCAAAGCA	Sigma-Aldrich	RGH1 (Mla3)	HB_0200, HB_0204	MM067
RP_Baronesse_131_t34_p1f	GGCCCAGGTATAGGTTGGC	Sigma-Aldrich	RGH1 (Mla3)	HB_0200, HB_0204	MM067
RP_Baronesse_131_t36_p1f	GGATTTCTTGGACTGATGCCA	Sigma-Aldrich	RGH1 (Mla3)	HB_0200, HB_0204	MM067

Primer ID	Sequence	Manufacturer	Gene construct	Construct ID	Internal ID
RP_Baronesse_131_t39_p1f	CGCCCTCCATGGAAAGCA	Sigma-Aldrich	RGH1 (Mla3)	HB_0200, HB_0204	MM067
RP_Baronesse_131_t41_p1f	TGACCTCATCGGCCCAGA	Sigma-Aldrich	RGH1 (Mla3)	HB_0200, HB_0204	MM067
RP_Baronesse_131_t42_p1f	TGGAAATGGCACCGGTGA	Sigma-Aldrich	RGH1 (Mla3)	HB_0200, HB_0204	MM067
RP_Baronesse_131_t43_p1f	CGGAGCAGAACACAGCGA	Sigma-Aldrich	RGH1 (Mla3)	HB_0200, HB_0204	MM067
RP_Baronesse_131_t44_p1f	GACAAGCACAGCACGCAC	Sigma-Aldrich	RGH1 (Mla3)	HB_0200, HB_0204	MM067
RP_Baronesse_131_t47_p1f	CAGCCCAGCCCGTAAACA	Sigma-Aldrich	RGH1 (Mla3)	HB_0200, HB_0204	MM067
RP_Baronesse_131_t50_p1f	CAAGCGCTTCGACCCTGA	Sigma-Aldrich	RGH1 (Mla3)	HB_0200, HB_0204	MM067
RP_Baronesse_131_t52_p1f	CACCATCGAAGCTGCCCA	Sigma-Aldrich	RGH1 (Mla3)	HB_0200, HB_0204	MM067
RP_Baronesse_131_t55_p1f	CACCACCTCTGCACCTCG	Sigma-Aldrich	RGH1 (Mla3)	HB_0200, HB_0204	MM067
RP_Baronesse_131_t56_p1f	GACGGTGAGGTGTTGGGG	Sigma-Aldrich	RGH1 (Mla3)	HB_0200, HB_0204	MM067
RP_Baronesse_131_t58_p1f	TCAGCTGGTGCACGTGAG	Sigma-Aldrich	RGH1 (Mla3)	HB_0200, HB_0204	MM067
RP_Baronesse_131_t59_p1f	CCAGGCCAACCGCAACTA	Sigma-Aldrich	RGH1 (Mla3)	HB_0200, HB_0204	MM067
RP_Baronesse_131_t60_p1f	CACACTCCTCGATCGCGG	Sigma-Aldrich	RGH1 (Mla3)	HB_0200, HB_0204	MM067
RP_Baronesse_131_t63_p1f	GGAAGGCAGAGGCAGGTG	Sigma-Aldrich	RGH1 (Mla3)	HB_0200, HB_0204	MM067
RP_Baronesse_131_t66_p1f	AAGGTCCGAAGCAACCCG	Sigma-Aldrich	RGH1 (Mla3)	HB_0200, HB_0204	MM067
RP_Baronesse_131_t69_p1f	TCCGCTCTGCAATCGACG	Sigma-Aldrich	RGH1 (Mla3)	HB_0200, HB_0204	MM067
RP_Baronesse_131_t70_p1f	GTCTCACGACTGCCACGT	Sigma-Aldrich	RGH1 (Mla3)	HB_0200, HB_0204	MM067
RP_Baronesse_131_t71_p1f	GGTGTTCCCGCCATCCTT	Sigma-Aldrich	RGH1 (Mla3)	HB_0200, HB_0204	MM067
RP_Baronesse_131_t72_p1f	CCGTGCTAGGCCAGAAGG	Sigma-Aldrich	RGH1 (Mla3)	HB_0200, HB_0204	MM067
RP_Baronesse_131_t73_p1f	CCGGGGAAGCCTGAATCC	Sigma-Aldrich	RGH1 (Mla3)	HB_0200, HB_0204	MM067
RP_Baronesse_131_t75_p1f	AGCAACCGAGAATGGGCA	Sigma-Aldrich	RGH1 (Mla3)	HB_0200, HB_0204	MM067
RP_Baronesse_225_d17_p1f	TCGTGACACTTCGCCCTTC	Sigma-Aldrich	RGH2, RGH3	HB_0207	MM067
RP_Baronesse_225_d33_p1f	GCAACTGGCGGAACTCCT	Sigma-Aldrich	RGH2, RGH3	HB_0207	MM067
RP_Baronesse_225_d50_p1f	GGGATGTTGCCACTCAGGT	Sigma-Aldrich	RGH2, RGH3	HB_0207	MM067
RP_Baronesse_225_d86_p1f	GGTCCGTTCACGCCATCA	Sigma-Aldrich	RGH2, RGH3	HB_0207	MM067
RP_Baronesse_225_d102_p1f	CAGGCGATGGTTGGCTGA	Sigma-Aldrich	RGH2, RGH3	HB_0207	MM067
RP_Baronesse_225_d121_p1f	TTGGGGTATGCTTGCGGT	Sigma-Aldrich	RGH2, RGH3	HB_0207	MM067
RP_Baronesse_131_d45_p1f	CGTGCGGGTCAGCTTTCA	Sigma-Aldrich	RGH1 (Mla3)	HB_0200, HB_0204	MM067
RP_Baronesse_131_d48_p1f	CAGCCGTTGCGTTTGGTG	Sigma-Aldrich	RGH1 (Mla3)	HB_0200, HB_0204	MM067
RP_Baronesse_131_d51_p1f	GCACCCAGCGTTCCCCNA	Sigma-Aldrich	RGH1 (Mla3)	HB_0200, HB_0204	MM067
RP_Baronesse_131_d54_p1f	ACTGTGGACGGCAATTCCT	Sigma-Aldrich	RGH1 (Mla3)	HB_0200, HB_0204	MM067
RP_Baronesse_131_d57_p1f	AGGGACAAACGGCGACAA	Sigma-Aldrich	RGH1 (Mla3)	HB_0200, HB_0204	MM067
RP_Baronesse_131_d60_p1f	AATCCTTCGGCCACCCAC	Sigma-Aldrich	RGH1 (Mla3)	HB_0200, HB_0204	MM067
RP_Baronesse_131_d63_p1f	GGAGTCATCAACAGAAAGCGG	Sigma-Aldrich	RGH1 (Mla3)	HB_0200, HB_0204	MM067
RP_Baronesse_131_d76_p1f	AGCTGATTGGCATCCAGC	Sigma-Aldrich	RGH1 (Mla3)	HB_0200, HB_0204	MM067
RP_Baronesse_131_d79_p1f	GCTCGAAGGCAAGGGTCA	Sigma-Aldrich	RGH1 (Mla3)	HB_0200, HB_0204	MM067
RP_Baronesse_131_d82_p1f	TGACCTCATCGGCCCAGA	Sigma-Aldrich	RGH1 (Mla3)	HB_0200, HB_0204	MM067
RP_Baronesse_131_d85_p1f	CGGAGCAGAACACAGCGA	Sigma-Aldrich	RGH1 (Mla3)	HB_0200, HB_0204	MM067
RP_Baronesse_225_t1_p1r	ACAACGGCGGACTCCAAG	Sigma-Aldrich	RGH2, RGH3	HB_0207	MM067
RP_Baronesse_225_t2_p1r	CGACGGACGAGGAAAGGG	Sigma-Aldrich	RGH2, RGH3	HB_0207	MM067
RP_Baronesse_225_t4_p1r	CGTACCTGCTTGGGGTGG	Sigma-Aldrich	RGH2, RGH3	HB_0207	MM067
RP_Baronesse_225_t5_p1r	CTCTACGCCGACGACGAC	Sigma-Aldrich	RGH2, RGH3	HB_0207	MM067
RP_Baronesse_225_t6_p1r	GGAGGGCCGTCCGATCTA	Sigma-Aldrich	RGH2, RGH3	HB_0207	MM067
RP_Baronesse_225_t7_p1r	CCATTTGGAGGGCCGTCC	Sigma-Aldrich	RGH2, RGH3	HB_0207	MM067
RP_Baronesse_225_t8_p1r	GGAAGGTACGGAGACCTGC	Sigma-Aldrich	RGH2, RGH3	HB_0207	MM067
RP_Baronesse_225_t9_p1r	AGCGGTCAGATCAGGGCT	Sigma-Aldrich	RGH2, RGH3	HB_0207	MM067
RP_Baronesse_225_t10_p1r	TTGACGGCTGCGAGACTG	Sigma-Aldrich	RGH2, RGH3	HB_0207	MM067
RP_Baronesse_225_t13_p1r	CTGGCTATGCGTCGGAGG	Sigma-Aldrich	RGH2, RGH3	HB_0207	MM067
RP_Baronesse_225_t17_p1r	CTGCACTACGGGCCTCAC	Sigma-Aldrich	RGH2, RGH3	HB_0207	MM067
RP_Baronesse_225_t18_p1r	GAGCACCTGACTGGCCTC	Sigma-Aldrich	RGH2, RGH3	HB_0207	MM067
RP_Baronesse_225_t20_p1r	TGTTCGTCTGGACCGCAC	Sigma-Aldrich	RGH2, RGH3	HB_0207	MM067
RP_Baronesse_225_t21_p1r	GCCTTGGTGAGCTGACCA	Sigma-Aldrich	RGH2, RGH3	HB_0207	MM067
RP_Baronesse_225_t22_p1r	GCCGGGCTTGTTCTTCCT	Sigma-Aldrich	RGH2, RGH3	HB_0207	MM067
RP_Baronesse_225_t23_p1r	TGGAGCTTCCAGCCCAGA	Sigma-Aldrich	RGH2, RGH3	HB_0207	MM067
RP_Baronesse_225_t27_p1r	AGCCGGATGTCCTCAGGT	Sigma-Aldrich	RGH2, RGH3	HB_0207	MM067
RP_Baronesse_225_t30_p1r	CTTCGCCGCAGCATTGTC	Sigma-Aldrich	RGH2, RGH3	HB_0207	MM067
RP_Baronesse_225_t34_p1r	AGCGATTCACCGGCACAA	Sigma-Aldrich	RGH2, RGH3	HB_0207	MM067
RP_Baronesse_225_t36_p1r	AGCTGCGCTTCCTCCAAG	Sigma-Aldrich	RGH2, RGH3	HB_0207	MM067

Primer ID	Sequence	Manufacturer	Gene construct	Construct ID	Internal ID
RP_Baronesse_225_t38_p1r	CCAAGAGCAGGCCCACTC	Sigma-Aldrich	RGH2, RGH3	HB_0207	MM067
RP_Baronesse_225_t39_p1r	TCGTTCGTCACAAGGCCC	Sigma-Aldrich	RGH2, RGH3	HB_0207	MM067
RP_Baronesse_225_t40_p1r	TCGAGCCAGCAGTCGTTG	Sigma-Aldrich	RGH2, RGH3	HB_0207	MM067
RP_Baronesse_225_t41_p1r	GTCAGCTCGCGGATCTCC	Sigma-Aldrich	RGH2, RGH3	HB_0207	MM067
RP_Baronesse_225_t42_p1r	TGATGGCGTGAACGGACC	Sigma-Aldrich	RGH2, RGH3	HB_0207	MM067
RP_Baronesse_225_t43_p1r	GAGCTCCATGACGGCCTC	Sigma-Aldrich	RGH2, RGH3	HB_0207	MM067
RP_Baronesse_225_t46_p1r	CATGTGCTCCCTGGCGAA	Sigma-Aldrich	RGH2, RGH3	HB_0207	MM067
RP_Baronesse_225_t50_p1r	CAGCCAACCATCGCCTGA	Sigma-Aldrich	RGH2, RGH3	HB_0207	MM067
RP_Baronesse_225_t54_p1r	CGGACGTTGTCTTCACCCA	Sigma-Aldrich	RGH2, RGH3	HB_0207	MM067
RP_Baronesse_225_t57_p1r	TGGCTCCACCTGTACCGA	Sigma-Aldrich	RGH2, RGH3	HB_0207	MM067
RP_Baronesse_225_t61_p1r	GTGTCGCTGGAGGACGAC	Sigma-Aldrich	RGH2, RGH3	HB_0207	MM067
RP_Baronesse_225_t62_p1r	TCACAGCGGCGGTGATTT	Sigma-Aldrich	RGH2, RGH3	HB_0207	MM067
RP_Baronesse_225_t63_p1r	CAGACGACGACGACGAGG	Sigma-Aldrich	RGH2, RGH3	HB_0207	MM067
RP_Baronesse_225_t64_p1r	ACGAAAACGGCAGAGGCA	Sigma-Aldrich	RGH2, RGH3	HB_0207	MM067
RP_Baronesse_225_t65_p1r	GCCCTGGTGTCGGTTCTG	Sigma-Aldrich	RGH2, RGH3	HB_0207	MM067
RP_Baronesse_225_t66_p1r	CTCTAGTGAGGTAGGG	Sigma-Aldrich	RGH2, RGH3	HB_0207	MM067
RP_Baronesse_225_t67_p1r	CCTAGCTCTCGCGACTT	Sigma-Aldrich	RGH2, RGH3	HB_0207	MM067
RP_Baronesse_131_t1_p1r	ATGGATCGGCCTGGGACT	Sigma-Aldrich	RGH1 (Mla3)	HB_0200, HB_0204	MM067
RP_Baronesse_131_t2_p1r	GCAGCTGACAGGGGTACA	Sigma-Aldrich	RGH1 (Mla3)	HB_0200, HB_0204	MM067
RP_Baronesse_131_t3_p1r	GCTAGCAACAATGTCTTTGC	Sigma-Aldrich	RGH1 (Mla3)	HB_0200, HB_0204	MM067
RP_Baronesse_131_t4_p1r	CACCGAGAGTGGCAGAGC	Sigma-Aldrich	RGH1 (Mla3)	HB_0200, HB_0204	MM067
RP_Baronesse_131_t5_p1r	TGTTGCCTAGACGGTGGC	Sigma-Aldrich	RGH1 (Mla3)	HB_0200, HB_0204	MM067
RP_Baronesse_131_t6_p1r	CTGTGTACGCCGGACTGG	Sigma-Aldrich	RGH1 (Mla3)	HB_0200, HB_0204	MM067
RP_Baronesse_131_t7_p1r	AGCAGCAGGGTCTTGCTG	Sigma-Aldrich	RGH1 (Mla3)	HB_0200, HB_0204	MM067
RP_Baronesse_131_t8_p1r	GGTTTGCGACTCCAGGCT	Sigma-Aldrich	RGH1 (Mla3)	HB_0200, HB_0204	MM067
RP_Baronesse_131_t10_p1r	GAGGCTAGGTTGGCACGG	Sigma-Aldrich	RGH1 (Mla3)	HB_0200, HB_0204	MM067
RP_Baronesse_131_t12_p1r	GGTTCGCCTGAGCTCCTC	Sigma-Aldrich	RGH1 (Mla3)	HB_0200, HB_0204	MM067
RP_Baronesse_131_t14_p1r	CTACTGGCGGCATCGGAG	Sigma-Aldrich	RGH1 (Mla3)	HB_0200, HB_0204	MM067
RP_Baronesse_131_t17_p1r	TGGGACGGAGGGAGTAGC	Sigma-Aldrich	RGH1 (Mla3)	HB_0200, HB_0204	MM067
RP_Baronesse_131_t18_p1r	TGATGCGGAGGCCTGAGA	Sigma-Aldrich	RGH1 (Mla3)	HB_0200, HB_0204	MM067
RP_Baronesse_131_t20_p1r	ACGCTCTTCACTGGTGCC	Sigma-Aldrich	RGH1 (Mla3)	HB_0200, HB_0204	MM067
RP_Baronesse_131_t21_p1r	AGGCGTGCCTTGAAAGCT	Sigma-Aldrich	RGH1 (Mla3)	HB_0200, HB_0204	MM067
RP_Baronesse_131_t23_p1r	CACCCACCAAACGCAACG	Sigma-Aldrich	RGH1 (Mla3)	HB_0200, HB_0204	MM067
RP_Baronesse_131_t24_p1r	CTCTCTGCACTGCGAGGG	Sigma-Aldrich	RGH1 (Mla3)	HB_0200, HB_0204	MM067
RP_Baronesse_131_t27_p1r	TGTCGCCGTTTGTCCCTT	Sigma-Aldrich	RGH1 (Mla3)	HB_0200, HB_0204	MM067
RP_Baronesse_131_t31_p1r	ACCACAACCCGCATTGTCA	Sigma-Aldrich	RGH1 (Mla3)	HB_0200, HB_0204	MM067
RP_Baronesse_131_t34_p1r	GCAACATGCGCCAAAGGC	Sigma-Aldrich	RGH1 (Mla3)	HB_0200, HB_0204	MM067
RP_Baronesse_131_t36_p1r	TGCGATGCTGGATGCCAA	Sigma-Aldrich	RGH1 (Mla3)	HB_0200, HB_0204	MM067
RP_Baronesse_131_t39_p1r	ACAAGCTCTGGGCCGATG	Sigma-Aldrich	RGH1 (Mla3)	HB_0200, HB_0204	MM067
RP_Baronesse_131_t41_p1r	CTGCTCCGCCGTGAAGAA	Sigma-Aldrich	RGH1 (Mla3)	HB_0200, HB_0204	MM067
RP_Baronesse_131_t42_p1r	TGCGGTGGTAGTGGCATC	Sigma-Aldrich	RGH1 (Mla3)	HB_0200, HB_0204	MM067
RP_Baronesse_131_t43_p1r	CCCGTGGTGCTGGTGAAT	Sigma-Aldrich	RGH1 (Mla3)	HB_0200, HB_0204	MM067
RP_Baronesse_131_t44_p1r	GGGGACGAAGATGCGAGG	Sigma-Aldrich	RGH1 (Mla3)	HB_0200, HB_0204	MM067
RP_Baronesse_131_t47_p1r	GCCTCCCTATGGCTTAGGC	Sigma-Aldrich	RGH1 (Mla3)	HB_0200, HB_0204	MM067
RP_Baronesse_131_t50_p1r	GGCCTCGTTCCATGACCA	Sigma-Aldrich	RGH1 (Mla3)	HB_0200, HB_0204	MM067
RP_Baronesse_131_t52_p1r	CAGGTGGCGCAGGAAAGA	Sigma-Aldrich	RGH1 (Mla3)	HB_0200, HB_0204	MM067
RP_Baronesse_131_t55_p1r	CCCCAACACCTCACCGTC	Sigma-Aldrich	RGH1 (Mla3)	HB_0200, HB_0204	MM067
RP_Baronesse_131_t56_p1r	TTGGTCGCGGTTCACCTC	Sigma-Aldrich	RGH1 (Mla3)	HB_0200, HB_0204	MM067
RP_Baronesse_131_t58_p1r	CGCGATCGAGGAGTGTGG	Sigma-Aldrich	RGH1 (Mla3)	HB_0200, HB_0204	MM067
RP_Baronesse_131_t59_p1r	CCGTAGTGAACTCGCCGG	Sigma-Aldrich	RGH1 (Mla3)	HB_0200, HB_0204	MM067
RP_Baronesse_131_t60_p1r	GCATGAAACCGTGCCGAA	Sigma-Aldrich	RGH1 (Mla3)	HB_0200, HB_0204	MM067
RP_Baronesse_131_t63_p1r	ACCACATCACCTTGGCGG	Sigma-Aldrich	RGH1 (Mla3)	HB_0200, HB_0204	MM067
RP_Baronesse_131_t66_p1r	GGTGATCTGCCTTGCCGT	Sigma-Aldrich	RGH1 (Mla3)	HB_0200, HB_0204	MM067
RP_Baronesse_131_t69_p1r	CAGGAGCCCCCTCAAAGC	Sigma-Aldrich	RGH1 (Mla3)	HB_0200, HB_0204	MM067
RP_Baronesse_131_t70_p1r	CCTTCTGGCCTAGCACGG	Sigma-Aldrich	RGH1 (Mla3)	HB_0200, HB_0204	MM067
RP_Baronesse_131_t71_p1r	CCGCGATCGAGGAAGACC	Sigma-Aldrich	RGH1 (Mla3)	HB_0200, HB_0204	MM067
RP_Baronesse_131_t72_p1r	GATTCAGGCTTCCCCGGG	Sigma-Aldrich	RGH1 (Mla3)	HB_0200, HB_0204	MM067
RP_Baronesse_131_t73_p1r	TGCCCATTCTCGGTTGCT	Sigma-Aldrich	RGH1 (Mla3)	HB_0200, HB_0204	MM067
RP_Baronesse_131_t75_p1r	GGCGCTTTGGATCATCGC	Sigma-Aldrich	RGH1 (Mla3)	HB_0200, HB_0204	MM067

Primer ID	Sequence	Manufacturer	Gene construct	Construct ID	Internal ID
RP_Baronesse_225_d17_p1r	GGAAGGTACGGAGACCTGC	Sigma-Aldrich	RGH2, RGH3	HB_0207	MM067
RP_Baronesse_225_d33_p1r	CAGTGGGACTCAGTGGCG	Sigma-Aldrich	RGH2, RGH3	HB_0207	MM067
RP_Baronesse_225_d50_p1r	ATGCCACACCGCCAATGA	Sigma-Aldrich	RGH2, RGH3	HB_0207	MM067
RP_Baronesse_225_d86_p1r	TCAGCAAGCATGGCAGCA	Sigma-Aldrich	RGH2, RGH3	HB_0207	MM067
RP_Baronesse_225_d102_p1r	GCAACATGAACGCGTGCA	Sigma-Aldrich	RGH2, RGH3	HB_0207	MM067
RP_Baronesse_225_d121_p1r	ATGGTGTCAGCATGCATAGT	Sigma-Aldrich	RGH2, RGH3	HB_0207	MM067
RP_Baronesse_131_d45_p1r	TCGATTTGGGCCTGCAGG	Sigma-Aldrich	RGH2, RGH3	HB_0207	MM067
RP_Baronesse_131_d48_p1r	GGTGCAGCAGGATGACGT	Sigma-Aldrich	RGH2, RGH3	HB_0207	MM067
RP_Baronesse_131_d51_p1r	TGCACAAGAGCTTGGCAAC	Sigma-Aldrich	RGH2, RGH3	HB_0207	MM067
RP_Baronesse_131_d54_p1r	TGGGGAGAATAGCAGCATGC	Sigma-Aldrich	RGH2, RGH3	HB_0207	MM067
RP_Baronesse_131_d57_p1r	TAGCGGCGAGGCATATGC	Sigma-Aldrich	RGH2, RGH3	HB_0207	MM067
RP_Baronesse_131_d60_p1r	TCCTTCGGTCCCTTGGCT	Sigma-Aldrich	RGH2, RGH3	HB_0207	MM067
RP_Baronesse_131_d63_p1r	ACCACAACCCGCATTGTCA	Sigma-Aldrich	RGH2, RGH3	HB_0207	MM067
RP_Baronesse_131_d76_p1r	GGAGGGTTGGGCAAGACC	Sigma-Aldrich	RGH2, RGH3	HB_0207	MM067
RP_Baronesse_131_d79_p1r	AGGGGCTCATGAAGAGGACT	Sigma-Aldrich	RGH2, RGH3	HB_0207	MM067
RP_Baronesse_131_d82_p1r	TCACCGGTGCCATTTCCA	Sigma-Aldrich	RGH2, RGH3	HB_0207	MM067
RP_Baronesse_131_d85_p1r	TGCGGTGGTAGTGGCATC	Sigma-Aldrich	RGH2, RGH3	HB_0207	MM067
Mla3_Baron_t1_p1f	CAGTATCGGCCCCACCAC	Sigma-Aldrich	RGH1 (Mla3)	HB_0200, HB_0204	MM033
Mla3_Baron_t2_p1f	TTACACGGGGGTGGCAAC	Sigma-Aldrich	RGH1 (Mla3)	HB_0200, HB_0204	MM033
Mla3_Baron_t3_p1f	TTACACGGGGGTGGCAAC	Sigma-Aldrich	RGH1 (Mla3)	HB_0200, HB_0204	MM033
Mla3_Baron_t4_p1f	ACAGCAAGCGACTGCCAT	Sigma-Aldrich	RGH1 (Mla3)	HB_0200, HB_0204	MM033
Mla3_Baron_t5_p1f	CTCCGATGCCGCCAGTAG	Sigma-Aldrich	RGH1 (Mla3)	HB_0200, HB_0204	MM033
Mla3_Baron_t6_p1f	AGCGTTCCCCCAGGAGAT	Sigma-Aldrich	RGH1 (Mla3)	HB_0200, HB_0204	MM033
Mla3_Baron_t7_p1f	AGCGTTCCCCCAGGAGAT	Sigma-Aldrich	RGH1 (Mla3)	HB_0200, HB_0204	MM033
Mla3_Baron_t8_p1f	GCATATGCCTCGCCGCTA	Sigma-Aldrich	RGH1 (Mla3)	HB_0200, HB_0204	MM033
Mla3_Baron_t9_p1f	GCATATGCCTCGCCGCTA	Sigma-Aldrich	RGH1 (Mla3)	HB_0200, HB_0204	MM033
Mla3_Baron_t10_p1f	GGTCTTGCCCAACCCTCC	Sigma-Aldrich	RGH1 (Mla3)	HB_0200, HB_0204	MM033
Mla3_Baron_t11_p1f	GGTCTTGCCCAACCCTCC	Sigma-Aldrich	RGH1 (Mla3)	HB_0200, HB_0204	MM033
Mla3_Baron_t1_p1r	GTTGCCACCCCCGTGTAA	Sigma-Aldrich	RGH1 (Mla3)	HB_0200, HB_0204	MM033
Mla3_Baron_t2_p1r	ATGGCAGTCGCTTGCTGT	Sigma-Aldrich	RGH1 (Mla3)	HB_0200, HB_0204	MM033
Mla3_Baron_t3_p1r	ATGGCAGTCGCTTGCTGT	Sigma-Aldrich	RGH1 (Mla3)	HB_0200, HB_0204	MM033
Mla3_Baron_t4_p1r	CACCCACCAAACGCAACG	Sigma-Aldrich	RGH1 (Mla3)	HB_0200, HB_0204	MM033
Mla3_Baron_t5_p1r	ATCTCCTGGGGGAACGCT	Sigma-Aldrich	RGH1 (Mla3)	HB_0200, HB_0204	MM033
Mla3_Baron_t6_p1r	TAGCGGCGAGGCATATGC	Sigma-Aldrich	RGH1 (Mla3)	HB_0200, HB_0204	MM033
Mla3_Baron_t7_p1r	TAGCGGCGAGGCATATGC	Sigma-Aldrich	RGH1 (Mla3)	HB_0200, HB_0204	MM033
Mla3_Baron_t8_p1r	TGCGATGCTGGATGCCAA	Sigma-Aldrich	RGH1 (Mla3)	HB_0200, HB_0204	MM033
Mla3_Baron_t9_p1r	TGCGATGCTGGATGCCAA	Sigma-Aldrich	RGH1 (Mla3)	HB_0200, HB_0204	MM033
Mla3_Baron_t10_p1r	CTGCTCCGCCGTGAAGAA	Sigma-Aldrich	RGH1 (Mla3)	HB_0200, HB_0204	MM033
Mla3_Baron_t11_p1r	CTGCTCCGCCGTGAAGAA	Sigma-Aldrich	RGH1 (Mla3)	HB_0200, HB_0204	MM033
Mla3_p1f	TGCATAGTAGCTCGCTCTGC	IDT	RGH1 (Mla3)	HB_0200, HB_0204	-
Mla3_p1r	CGCCCACCCAAAATGTTTGT	IDT	RGH1 (Mla3)	HB_0200, HB_0204	-
Mla3_p2f	ACCTTTGACACCCGTGGATC	IDT	RGH1 (Mla3)	HB_0200, HB_0204	-
Mla3_p2r	AGGCGAACCCCCATTTCATT	IDT	RGH1 (Mla3)	HB_0200, HB_0204	-
Mla3_p3f	TCGATTGAAGCGACCCTCAC	IDT	RGH1 (Mla3)	HB_0200, HB_0204	-
Mla3_p3r	CCGAGTGCAGTCCTGATACA	IDT	RGH1 (Mla3)	HB_0200, HB_0204	-
RGH2_t1_p1f	AGCTGCGCTTCCTCCAAG	IDT	RGH2	HB_0207	-
RGH2_t1_p1r	GAAGGTGGTGCCGTCGAA	IDT	RGH2	HB_0207	-
RGH2_t2_p1f	AGCGATTCACCGGCACAA	IDT	RGH2	HB_0207	-
RGH2_t2_p1r	ACCTGAGGACATCCGGCT	IDT	RGH2	HB_0207	-
RGH2_t3_p1f	GGCACCATCAACCTGGGA	IDT	RGH2	HB_0207	-
RGH2_t3_p1r	CCAGCCGACGAACCTTGT	IDT	RGH2	HB_0207	-
RGH2_t4_p1f	TGGGAACGGTGGGAAGGA	IDT	RGH2	HB_0207	-
RGH2_t4_p1r	AGGAAGAACAAGCCCGGC	IDT	RGH2	HB_0207	-
RGH2_t5_p1f	ATGCCACACCGCCAATGA	IDT	RGH2	HB_0207	-
RGH2_t5_p1r	CGCCGCGACAACTCTAGT	IDT	RGH2	HB_0207	-
RGH2_t6_p1f	GCCGGGCTTGTTCTTCCT	IDT	RGH2	HB_0207	-
RGH2_t6_p1r	TAGTACCGGCACCCCCAA	IDT	RGH2	HB_0207	-
RGH2_t7_p1f	TGTTCGTCTGGACCGCAC	IDT	RGH2	HB_0207	-
RGH2_t7_p1r	GCAACTGGCGGAACTCCT	IDT	RGH2	HB_0207	-

Primer ID	Sequence	Manufacturer	Gene construct	Construct ID	Internal ID
RGH2_t8_p1f	CAGTGGGACTCAGTGGCG	IDT	RGH2	HB_0207	-
RGH2_t8_p1r	CGACCACCTTGAACGCCT	IDT	RGH2	HB_0207	-
RGH2_t9_p1f	GGAGTTCCGCCAGTTGCT	IDT	RGH2	HB_0207	-
RGH2_t9_p1r	TGCGGAACAGCTTCTCCG	IDT	RGH2	HB_0207	-
RGH2_t10_p1f	CTGGCTATGCGTCGGAGG	IDT	RGH2	HB_0207	-
RGH2_t10_p1r	CAGTCTCGCAGCCGTCAA	IDT	RGH2	HB_0207	-
RGH2_t11_p1f	TTGACGGCTGCGAGACTG	IDT	RGH2	HB_0207	-
RGH2_t11_p1r	TCGTGACACTTCGCCCTTC	IDT	RGH2	HB_0207	-
RGH3_t1_p1f	GAGATCCGCGAGCTGACC	IDT	RGH3	HB_0207	-
RGH3_t1_p1r	CCGGGGATGATTGCAGCA	IDT	RGH3	HB_0207	-
RGH3_t2_p1f	GGTTGATGGGCACTCGCT	IDT	RGH3	HB_0207	-
RGH3_t2_p1r	CAGCCAACCATCGCCTGA	IDT	RGH3	HB_0207	-
RGH3_t3_p1f	GGGGGAAGGGTGTTCTGC	IDT	RGH3	HB_0207	-
RGH3_t3_p1r	GCAACATGAACGCGTGCA	IDT	RGH3	HB_0207	-
RGH3_t4_p1f	CAGGCGATGGTTGGCTGA	IDT	RGH3	HB_0207	-
RGH3_t4_p1r	AACGAATCCCGCAACGGT	IDT	RGH3	HB_0207	-
RGH3_t5_p1f	CACGAGTGCTGGACCTGG	IDT	RGH3	HB_0207	-
RGH3_t5_p1r	TGGCTGGGTTGGAGTTGC	IDT	RGH3	HB_0207	-
RGH3_t6_p1f	GGTTGCCCCAAGGTACCC	IDT	RGH3	HB_0207	-
RGH3_t6_p1r	TGGCTCCACCTGTACCGA	IDT	RGH3	HB_0207	-

8 Bibliography

Abedon, B.G., Tracy, W.F., 1996. Corngrass1 of maize (Zea mays l.) delays development of adult plant resistance to common rust (Puccinia sorghi Schw.) and European corn borer (Ostrinia nubilalis Hubner). J. Hered. 87, 219–223.

Able, A.J., 2003. Role of reactive oxygen species in the response of barley to necrotrophic pathogens. Protoplasma 221, 137–143.

Acevedo-Garcia, J., Kusch, S., Panstruga, R., 2014. Magical mystery tour: MLO proteins in plant immunity and beyond. J. Physiol. 204, 273–281.

Ade, J., DeYoung, B.J., Golstein, C., Innes, R.W., 2007. Indirect activation of a plant nucleotide binding site-leucine-rich repeat protein by a bacterial protease. Proc. Natl. Acad. Sci. U. S. A. 104, 2531–2536.

AHDB, 2019. AHDB Recommended Lists for cereals and oilseeds 2019 / 20.

Allen, R.L., Bittner-Eddy, P.D., Grenville-Briggs, L.J., Meitz, J.C., Rehmany, A.P., Rose, L.E., Beynon, J.L., 2004. Host-parasite coevolutionary conflict between Arabidopsis and downy mildew. Science (80-.). 306, 1957–1960.

Andrews, S., 2010. FastQC: a quality control tool for high throughput sequence data.

Araki, M., Ishii, T., 2015. Towards social acceptance of plant breeding by genome editing. Trends Plant Sci. 20, 145–149.

Arora, D., Gross, T., Brueggeman, R., 2013. Allele characterization of genes required for rpg4-mediated wheat stem rust resistance identifies Rpg5 as the R gene. Phytopathology 103, 1153–1161.

Ashfield, T., Ong, L.E., Nobuta, K., Schneider, C.M., Innes, R.W., 2004. Convergent Evolution of Disease Resistance Gene Specificity in Two Flowering Plant Families. Plant Cell 16, 309–318.

Ashfield, T., Redditt, T., Russell, A., Kessens, R., Rodibaugh, N., Galloway, L., Kang, Q., Podicheti, R., Innes, R.W., 2014. Evolutionary Relationship of Disease Resistance Genes in Soybean and Arabidopsis Specific for the Pseudomonas syringae Effectors AvrB and AvrRpm1. Plant Physiol. 166, 235–251.

Axtell, M.J., Staskawicz, B.J., 2003. Initiation of RPS2-Specified Disease Resistance in Arabidopsis Is Coupled to the AvrRpt2-Directed Elimination of RIN4. Cell 112, 369–377.

Ayliffe, M., Devilla, R., Mago, R., White, R., Talbot, M., Pryor, A., Leung, H., 2011. Nonhost resistance of rice to rust pathogens. Mol. Plant. Microbe. Interact. 24, 1143–1155.

Ayliffe, M., Singh, D., Park, R., Moscou, M., Pryor, T., 2013. Infection of Brachypodium

distachyon with Selected Grass Rust Pathogens. Mol. Plant-Microbe Interact. MPMI 946, 946–957.

Ayliffe, M., Sørensen, C.K., 2019. Plant nonhost resistance: paradigms and new environments. Curr. Opin. Plant Biol. 50, 104–113.

Azevedo, C., Sadanandom, A., Kitagawa, K., Freialdenhoven, A., Shirasu, K., Schulze-Lefert, P., 2002. The RAR1 interactor SGT1, an essential component of R gene-triggered disease resistance. Science 295, 2073–2076.

Bai, J., Pennill, L. a, Ning, J., Lee, S.W., Ramalingam, J., Webb, C. a, Zhao, B., Sun, Q., Nelson, J.C., Leach, J.E., Hulbert, S.H., 2002. Diversity in Nucleotide Binding Site − Leucine-Rich Repeat Genes in Cereals Diversity in Nucleotide Binding Site – Leucine-Rich Repeat Genes in Cereals 1871–1884.

Bai, S., Liu, J., Chang, C., Zhang, L., Maekawa, T., Wang, Q., Xiao, W., Liu, Y., Chai, J., Takken, F.L.W., Schulze-Lefert, P., Shen, Q.H., 2012. Structure-function analysis of barley NLR immune receptor MLA10 reveals its cell compartment specific activity in cell death and disease resistance. PLoS Pathog. 8, 21–25.

Bailey, P.C., Schudoma, C., Jackson, W., Baggs, E., Dagdas, G., Haerty, W., Moscou, M., Krasileva, K. V., 2018. Dominant integration locus drives continuous diversification of plant immune receptors with exogenous domain fusions. Genome Biol. 19, 1–18.

Bailey, T.L., Boden, M., Buske, F.A., Frith, M., Grant, C.E., Clementi, L., Ren, J., Li, W.W., Noble, W.S., 2009. MEME Suite: Tools for motif discovery and searching. Nucleic Acids Res. 37.

Bakker, E.G., Traw, M.B., Toomajian, C., Kreitman, M., Bergelson, J., 2008. Low levels of polymorphism in genes that control the activation of defense response in Arabidopsis thaliana. Genetics 178, 2031–2043.

Ballini, E., Berruyer, R., Morel, J.B., Lebrun, M.H., Nottéghem, J.L., Tharreau, D., 2007. Modern elite rice varieties of the “Green Revolution” have retained a large introgression from wild rice around the Pi33 rice blast resistance locus. New Phytol. 175, 340–350.

Ballini, E., Bordat, A., Vergne, E., Morel, J.-B., Lebrun, M.-H., Nottéghem, J.-L., Tharreau, D., 2006. Cloning of Pi33, the rice resistance gene corresponding to the cloned avirulence gene ACE1 of Magnaporthe grisea.

Barragan, C.A., Wu, R., Kim, S.-T., Xi, W., Habring, A., Hagmann, J., Van de Weyer, A.-L., Zaidem, M., Ho, W.W.H., Wang, G., Bezrukov, I., Weigel, D., Chae, E., 2019. RPW8/HR repeats control NLR activation in Arabidopsis thaliana. PLOS Genet. 15, e1008313.

Belhaj, K., Cano, L.M., Prince, D.C., Kemen, A., Yoshida, K., Dagdas, F.Y., Etherington, G.J., Schoonbeek, H., van Esse, P., Jones, J., Kamoun, S., Schornack, S., 2015.

Arabidopsis late blight: Infection of a nonhost plant by Albugo laibachii enables full colonization by Phytophthora infestans. bioRxiv 1–30.

Belton, J.M., McCord, R.P., Gibcus, J.H., Naumova, N., Zhan, Y., Dekker, J., 2012. Hi-C: A comprehensive technique to capture the conformation of genomes. Methods 58, 268–276.

Bergelson, J., Kreitman, M., Stahl, E.A., Tian, D., 2001. Evolutionary dynamics of plant R-genes. Science (80-.). 292, 2281–2285.

Bernoux, M., Burdett, H., Williams, S.J., Zhang, X., Chen, C., Newell, K., Lawrence, G.J., Kobe, B., Ellis, J.G., Anderson, P.A., Dodds, P.N., 2016. Comparative analysis of the flax immune receptors L6 and L7 suggests an equilibrium-based switch activation model. Plant Cell 28, 146–159.

Bernoux, M., Ellis, J.G., Dodds, P.N., 2011. New insights in plant immunity signaling activation. Curr. Opin. Plant Biol. 14, 512–518.

Berruyer, R., Adreit, H., Milazzo, J., Gaillard, S., Berger, A., Dioh, W., Lebrun, M.H., Tharreau, D., 2003. Identification and fine mapping of Pi33, the rice resistance gene corresponding to the Magnaporthe grisea avirulence gene ACE1. Theor. Appl. Genet. 107, 1139–1147.

Bettgenhaeuser, J., Gilbert, B., Ayliffe, M., Moscou, M.J., 2014. Nonhost resistance to rust pathogens - a continuation of continua. Front. Plant Sci. 5, 664.

Bhattacharjee, S., Garner, C.M., Gassmann, W., 2013. New clues in the nucleus: Transcriptional reprogramming in effector-triggered immunity. Front. Plant Sci. 4, 1–7.

Bhavani, S., Hodson, D.P., Huerta-espino, J., Randhawa, M.S., 2019. Progress in breeding for resistance to Ug99 and other races of the stem rust fungus in CIMMYT wheat germplasm. Front. Agric. Sci. Eng. 0, 0.

Bhullar, N.K., Zhang, Z., Wicker, T., Keller, B., 2010. Wheat gene bank accessions as a source of new alleles of the powdery mildew resistance gene Pm3: A large scale allele mining project. BMC Plant Biol. 10.

Bieri, S., Mauch, S., Shen, Q.H., Peart, J., Devoto, A., Casais, C., Ceron, F., Schulze, S., Steinbiss, H.H., Shirasu, K., Schulze-Lefert, P., 2004. RAR1 positively controls steady state levels of barley MLA resistance proteins and enables sufficient MLA6 accumulation for effective resistance. Plant Cell 16, 3480–3495.

Biffen, R.H., 1905. Mendel's Laws of Inheritance and Wheat Breeding. J. Agric. Sci. 1, 4–48.

Bilgic, H., Steffenson, B.J., Hayes, P.M., 2005. Comprehensive genetic analyses reveal differential expression of spot blotch resistance in four populations of barley. Theor. Appl. Genet. 111, 1238–1250.

Bilgic, H., Steffenson, B.J., Hayes, P.M., 2006. Molecular mapping of loci conferring

resistance to different pathotypes of the spot blotch pathogen in barley. Phytopathology 96, 699–708.

Birkenbihl, R.P., Liu, S., Somssich, I.E., 2017. Transcriptional events defining plant immune responses. Curr. Opin. Plant Biol. 38, 1–9.

Bogdanove, A.J., Schornack, S., Lahaye, T., 2010. TAL effectors: Finding plant genes for disease and defense. Curr. Opin. Plant Biol.

Bolger, A.M., Lohse, M., Usadel, B., 2014. Trimmomatic: A flexible trimmer for Illumina sequence data. Bioinformatics 30, 2114–2120.

Boller, T., Felix, G., 2009. A renaissance of elicitors: perception of microbe-associated molecular patterns and danger signals by pattern-recognition receptors. Annu. Rev. Plant Biol. 60, 379–406.

Bomblies, K., 2009. Too much of a good thing? Hybrid necrosis as a by-product of plant immune system diversification. Botany 87, 1013–1022.

Botella, M.A., Parker, J.E., Frost, L.N., Bittner-Eddy, P.D., Beynon, J.L., Daniels, M.J., Holub, E.B., Jones, J.D.G., 1998. Three genes of the arabidopsis RPP1 complex resistance locus recognize distinct Peronospora parasitica avirulence determinants. Plant Cell 10, 1847–1860.

Bourras, S., Kunz, L., Xue, M., Praz, C.R., Müller, M.C., Kälin, C., Schläfli, M., Ackermann, P., Flückiger, S., Parlange, F., Menardo, F., Schaefer, L.K., Ben-David, R., Roffler, S., Oberhaensli, S., Widrig, V., Lindner, S., Isaksson, J., Wicker, T., Yu, D., Keller, B., 2019. The AvrPm3-Pm3 effector-NLR interactions control both race-specific resistance and host-specificity of cereal mildews on wheat. Nat. Commun. 10, 1–16.

Bourras, S., McNally, K.E., Ben-David, R., Parlange, F., Roffler, S., Praz, C.R., Oberhaensli, S., Menardo, F., Stirnweis, D., Frenkel, Z., Schaefer, L.K., Flückiger, S., Treier, G., Herren, G., Korol, A.B., Wicker, T., Keller, B., 2015. Multiple avirulence loci and allele-specific effector recognition control the Pm3 race-specific resistance of wheat to powdery mildewopen. Plant Cell 27, 2991–3012.

Bourras, S., McNally, K.E., Müller, M.C., Wicker, T., Keller, B., 2016. Avirulence genes in cereal powdery mildews: the gene-for-gene hypothesis 2.0. Front. Plant Sci. 7, 1–7.

Bourras, S., Praz, C.R., Spanu, P.D., Keller, B., 2018. Cereal powdery mildew effectors: a complex toolbox for an obligate pathogen. Curr. Opin. Microbiol. 46, 26–33.

Boyd, L.A., Smith, P.H., Foster, E.M., Brown, J.K.M., 1995. The effects of allelic variation at the Mla resistance locus in barley on the early development of Erysiphe graminis f. sp. hordei and host responses. Plant J. 7, 959–968.

Brabham, H.J., Hernández-Pinzón, I., Holden, S., Lorang, J., Moscou, M.J., 2018. An ancient integration in a plant NLR is maintained as a trans-species polymorphism.

bioRxiv 239541.

Broman, K.W., Wu, H., Sen, Ś., Churchill, G.A., 2003. R/qtl: QTL mapping in experimental crosses. Bioinformatics 19, 889–890.

Brown, A.J., Casselton, L.A., 2001. Mating in mushrooms: Increasing the chances but prolonging the affair. Trends Genet.

Brown, J.K.M., 2015. Durable Resistance of Crops to Disease: A Darwinian Perspective. Annu. Rev. Phytopathol. 53, 513–539.

Brown, J.K.M., Tellier, A., 2011. Plant-Parasite Coevolution: Bridging the Gap between Genetics and Ecology. Annu. Rev. Phytopathol. 49, 345–367.

Brown, N.A., Evans, J., Mead, A., Hammond-Kosack, K.E., 2017. A spatial temporal analysis of the Fusarium graminearum transcriptome during symptomless and symptomatic wheat infection. Mol. Plant Pathol. 18, 1295–1312.

Brown, W.M.J., Hill, J.P., Velasco, V.R., 2001. Barley Yellow Rust in North America. Annu. Rev. Phytopathol. 39, 367–384.

Brueggeman, R., Druka, a, Nirmala, J., Cavileer, T., Drader, T., Rostoks, N., Mirlohi, a, Bennypaul, H., Gill, U., Kudrna, D., Whitelaw, C., Kilian, a, Han, F., Sun, Y., Gill, K., Steffenson, B., Kleinhofs, a, 2008. The stem rust resistance gene Rpg5 encodes a protein with nucleotide-binding-site, leucine-rich, and protein kinase domains. Proc. Natl. Acad. Sci. U. S. A. 105, 14970–5.

Brueggeman, R., Rostoks, N., Kudrna, D., Kilian, a, Han, F., Chen, J., Druka, a, Steffenson, B., Kleinhofs, a, 2002. The barley stem rust-resistance gene Rpg1 is a novel disease-resistance gene with homology to receptor kinases. Proc. Natl. Acad. Sci. U. S. A. 99, 9328–9333.

Bryan, G.T., Wu, K.S., Farrall, L., Jia, Y., Hershey, H.P., McAdams, S.A., Faulk, K.N., Donaldson, G.K., Tarchini, R., Valent, B., 2000. A single amino acid difference distinguishes resistant and susceptible alleles of the rice blast resistance gene Pi-ta. Plant Cell 12, 2033–2045.

Burdon, J.J., Barrett, L.G., Rebetzke, G., Thrall, P.H., 2014. Guiding deployment of resistance in cereals using evolutionary principles. Evol. Appl. 7, 609–624.

Büschges, R., Hollricher, K., Panstruga, R., Simons, G., Wolter, M., Frijters, a, van Daelen, R., van der Lee, T., Diergaarde, P., Groenendijk, J., Töpsch, S., Vos, P., Salamini, F., Schulze-Lefert, P., 1997. The barley Mlo gene: a novel control element of plant pathogen resistance. Cell 88, 695–705.

Caicedo, A.L., Schaal, B.A., Kunkel, B.N., 1999. Diversity and molecular evolution of the RPS2 resistance gene in Arabidopsis thaliana. Proc. Natl. Acad. Sci. U. S. A. 96, 302–306.

Caldo, R. a, Nettleton, D., Peng, J., Wise, R.P., 2006. Stage-specific suppression of basal

defense discriminates barley plants containing fast- and delayed-acting Mla powdery mildew resistance alleles. Mol. Plant. Microbe. Interact. 19, 939–947.

Caldo, R.A., Nettleton, D., Wise, R.P., 2004. Interaction-dependent gene expression in Mla-specified response to barley powdery mildew. Plant Cell 16, 2514–2528.

Camacho, C., Coulouris, G., Avagyan, V., Ma, N., Papadopoulos, J., Bealer, K., Madden, T.L., 2009. BLAST+: Architecture and applications. BMC Bioinformatics 10.

Cao, Y., Liang, Y., Tanaka, K., Nguyen, C.T., Jedrzejczak, R.P., Joachimiak, A., Stacey, G., 2014. The kinase LYK5 is a major chitin receptor in Arabidopsis and forms a chitin-induced complex with related kinase CERK1 3, 3766.

Casey, L.W., Lavrencic, P., Bentham, A.R., Cesari, S., Ericsson, D.J., Croll, T., Turk, D., Anderson, P.A., Mark, A.E., Dodds, P.N., Mobli, M., Kobe, B., Williams, S.J., 2016. The CC domain structure from the wheat stem rust resistance protein Sr33 challenges paradigms for dimerization in plant NLR proteins. Proc. Natl. Acad. Sci. U. S. A. 113, 12856–12861.

Casteel, C.L., Walling, L.L., Paine, T.D., 2006. Behavior and biology of the tomato psyllid, Bactericerca cockerelli, in response to the Mi-1.2 gene. Entomol. Exp. Appl. 121, 67–72.

Castro, A. J., Capettini, F., Corey, A.E., Filichkina, T., Hayes, P.M., Kleinhofs, A., Kudrna, D., Richardson, K., Sandoval-Islas, S., Rossi, C., Vivar, H., 2003. Mapping and pyramiding of qualitative and quantitative resistance to stripe rust in barley. Theor. Appl. Genet. 107, 922–930.

Castro, Ariel J, Chen, X., Hayes, P.M., Johnston, M., 2003. Pyramiding Quantitative Trait Locus (QTL) Alleles Determining Resistance to Barley Stirpe Rust. Effects on Adult Plant Resistence 651–659.

Castro, A.J., Chen, X., Hayes, P.M., Knapp, S.J., Line, R.F., Toojinda, T., Vivar, H., 2002. Coincident QTL which determine seedling and adult plant resistance to stripe rust in barley. Crop Sci. 42, 1701–1708.

Century, K.S., 1995. locus of Arabidopsis thaliana that is required for disease resistance 92, 6597–6601.

Century, K.S., Lagman, R.A., Adkisson, M., Morlan, J., Tobias, R., Schwartz, K., Smith, A., Love, J., Ronald, P.C., Whalen, M.C., 1999. Developmental control of Xa21-mediated disease resistance in rice. Plant J. 20, 231–236.

Cesari, S., 2018. Multiple strategies for pathogen perception by plant immune receptors. New Phytol. 219, 17–24.

Cesari, S., Bernoux, M., Moncuquet, P., Kroj, T., Dodds, P.N., 2014. A novel conserved mechanism for plant NLR protein pairs: the “integrated decoy” hypothesis. Front. Plant Sci. 5, 606.

César, S., Kanzaki, H., Fujiwara, T., Bernoux, M., Chalvon, V., Kawano, Y., Shimamoto, K., Dodds, P., Terauchi, R., Kroj, T., 2014. The NB-LRR proteins RGA4 and RGA5 interact functionally and physically to confer disease resistance. EMBO J. 33, 1–19.

Cesari, S., Kroj, T., 2017. Transposon-Mediated NLR Exile to the Pollen Allows Rice Blast Resistance without Yield Penalty. Mol. Plant 10, 665–667.

Cesari, S., Moore, J., Chen, C., Webb, D., Periyannan, S., Mago, R., Bernoux, M., Lagudah, E.S., Dodds, P.N., 2016. Cytosolic activation of cell death and stem rust resistance by cereal MLA-family CC-NLR proteins. Proc. Natl. Acad. Sci. U. S. A. 113, 10204–10209.

Cesari, S., Thilliez, G., Ribot, C., Chalvon, V., Michel, C., Jauneau, A., Rivas, S., Alaux, L., Kanzaki, H., Okuyama, Y., Morel, J.-B., Fournier, E., Tharreau, D., Terauchi, R., Kroj, T., 2013. The rice resistance protein pair RGA4/RGA5 recognizes the Magnaporthe oryzae effectors AVR-Pia and AVR1-CO39 by direct binding. Plant Cell 25, 1463–81.

Chae, E., Bomblies, K., Kim, S.T., Karelina, D., Zaidem, M., Ossowski, S., Martín-Pizarro, C., Laitinen, R.A.E., Rowan, B.A., Tenenboim, H., Lechner, S., Demar, M., Habring-Müller, A., Lanz, C., Rätsch, G., Weigel, D., 2014. Species-wide genetic incompatibility analysis identifies immune genes as hot spots of deleterious epistasis. Cell 159, 1341–1351.

Chae, E., Tran, D.T.N., Weigel, D., 2016. Cooperation and Conflict in the Plant Immune System. PLoS Pathog. 12, 1–5.

Chang, C., Yu, D., Jiao, J., Jing, S., Schulze-Lefert, P., Shen, Q.-H., 2013. Barley MLA immune receptors directly interfere with antagonistically acting transcription factors to initiate disease resistance signaling. Plant Cell 25, 1158–73.

Charlesworth, D., 2006. Balancing selection and its effects on sequences in nearby genome regions. PLoS Genet. 2, 379–384.

Chauhan, H., Boni, R., Bucher, R., Kuhn, B., Buchmann, G., Sucher, J., Selter, L.L., Hensel, G., Kumlehn, J., Bigler, L., Glauser, G., Wicker, T., Krattinger, S.G., Keller, B., 2015. The wheat resistance gene Lr34 results in the constitutive induction of multiple defense pathways in transgenic barley. Plant J. 84, 202–215.

Chaves, M., Martinelli, J., Wesp, C., Graichen, F., 2008. The cereal rusts: an overview. Pest Technol. 2, 38–55.

Chen, F.Q., Prehn, D., Hayes, P.M., Mulrooney, D., Corey, A., Vivar, H., 1994. Mapping genes for resistance to barley stripe rust (Puccinia striiformis f. sp. hordei). Theor. Appl. Genet. 88, 215–219.

Chen, J., Upadhyaya, N.M., Ortiz, D., Sperschneider, J., Li, F., Bouton, C., Breen, S., Dong, C., Xu, B., Zhang, X., Mago, R., Newell, K., Xia, X., Bernoux, M., Taylor, J.M., Steffenson, B., Jin, Y., Zhang, P., Kanyuka, K., Figueroa, M., Ellis, J.G., Park, R.F.,

Dodds, P.N., 2017. Loss of AvrSr50 by somatic exchange in stem rust leads to virulence for Sr50 resistance in wheat. Science (80-.). 358, 1607–1610.

Chen, X., Line, R.F., 2002. Recessive Genes for Resistance to Puccinia striiformis f. sp. hordei in Barley. Euphytica 129, 127–145.

Chen, X., Moore, M., 2003. High-Temperature, Adult-Plant Resistance in the Barley Cultivar "Bancroft" against Stripe Rust. Barley Newsl.

Chen, X.M., Line, R.F., 1999. Recessive Genes for Resistance to Puccinia-Striiformis F-Sp Hordei in Barley. Phytopathology Vol 89, 226–232.

Cheng, Y.T., Li, X., 2012. Ubiquitination in NB-LRR-mediated immunity. Curr. Opin. Plant Biol. 15, 392–399.

Chinchilla, D., Zipfel, C., Robatzek, S., Kemmerling, B., Nürnberger, T., Jones, J.D.G., Felix, G., Boller, T., 2007. A flagellin-induced complex of the receptor FLS2 and BAK1 initiates plant defence. Nature 448, 497–500.

Chisholm, S.T., Coaker, G., Day, B., Staskawicz, B.J., 2006. Host-microbe interactions: Shaping the evolution of the plant immune response. Cell 124, 803–814.

Chou, S., Krasileva, K. V., Holton, J.M., Steinbrenner, A.D., Alber, T., Staskawicz, B.J., 2011. Hyaloperonospora arabidopsidis ATR1 effector is a repeat protein with distributed recognition surfaces. Proc. Natl. Acad. Sci. U. S. A. 108, 13323–13328.

Chu, C.G., Faris, J.D., Xu, S.S., Friesen, T.L., 2010. Genetic analysis of disease susceptibility contributed by the compatible Tsn1-SnToxA and Snn1-SnTox1 interactions in the wheat-Stagonospora nodorum pathosystem. Theor. Appl. Genet. 120, 1451–1459.

Chuma, I., Zhan, S.-W., Asano, S., Nga, N.T.T., Vy, T.T.P., Shirai, M., Ibaragi, K., Tosa, Y., 2010. PWT1, an avirulence gene of Magnaporthe oryzae tightly linked to the rDNA Locus, is recognized by two staple crops, common wheat and barley. Phytopathology 100, 436–43.

Close, T.J., Bhat, P.R., Lonardi, S., Wu, Y., Rostoks, N., Ramsay, L., Druka, A., Stein, N., Svensson, J.T., Wanamaker, S., Bozdag, S., Roose, M.L., Moscou, M.J., Chao, S., Varshney, R.K., Szucs, P., Sato, K., Hayes, P.M., Matthews, D.E., Kleinhofs, A., Muehlbauer, G.J., DeYoung, J., Marshall, D.F., Madishetty, K., Fenton, R.D., Condamine, P., Graner, A., Waugh, R., 2009. Development and implementation of high-throughput SNP genotyping in barley. BMC Genomics 10, 1–13.

Collemare, J., Pianfetti, M., Houlle, A.E., Morin, D., Camborde, L., Gagey, M.J., Barbisan, C., Fudal, I., Lebrun, M.H., Böhnert, H.U., 2008. Magnaporthe grisea avirulence gene ACE1 belongs to an infection-specific gene cluster involved in secondary metabolism. New Phytol. 179, 196–208.

Collier, S.M., Moffett, P., 2009. NB-LRRs work a "bait and switch" on pathogens. Trends

Plant Sci. 14, 521–529.

Condon, B.J., Leng, Y., Wu, D., Bushley, K.E., Ohm, R.A., Otillar, R., Martin, J., Schackwitz, W., Grimwood, J., MohdZainudin, N.A.I., Xue, C., Wang, R., Manning, V.A., Dhillon, B., Tu, Z.J., Steffenson, B.J., Salamov, A., Sun, H., Lowry, S., LaButti, K., Han, J., Copeland, A., Lindquist, E., Barry, K., Schmutz, J., Baker, S.E., Ciuffetti, L.M., Grigoriev, I. V., Zhong, S., Turgeon, B.G., 2013. Comparative Genome Structure, Secondary Metabolite, and Effector Coding Capacity across Cochliobolus Pathogens. PLoS Genet. 9.

Cook, D.E., Lee, T.G., Guo, X., Melito, S., Wang, K., Bayless, A.M., Wang, J., Hughes, T.J., Willis, D.K., Clemente, T.E., Diers, B.W., Jiang, J., Hudson, M.E., Bent, A.F., 2012. Copy number variation of multiple genes at Rhg1 mediates nematode resistance in soybean. Science 338, 1206–9.

Cook, D.E., Mesarich, C.H., Thomma, B.P.H.J., 2015. Understanding Plant Immunity as a Surveillance System to Detect Invasion. Annu. Rev. Phytopathol. 53, 541–63.

Cooley, M.B., Pathirana, S., Wu, H.J., Kachroo, P., Klessig, D.F., 2000. Members of the Arabidopsis HRT/RPP8 family of resistance genes confer resistance to both viral and oomycete pathogens. Plant Cell 12, 663–676.

Cooper, M.D., Alder, M.N., 2006. The evolution of adaptive immune systems. Cell 124, 815–822.

Costanzo, S., Jia, Y., 2009. Alternatively spliced transcripts of Pi-ta blast resistance gene in Oryza sativa. Plant Sci. 177, 468–478.

Couch, B.C., Kohn, L.M., 2002. A multilocus gene genealogy concordant with host preference indicates segregation of a new species, Magnaporthe oryzae, from M. grisea. Mycologia 94, 683–693.

Cowger, C., Brown, J.K.M., 2019. Durability of Quantitative Resistance in Crops: Greater Than We Know? Annu. Rev. Phytopathol. 57, 253–277.

Cui, H., Tsuda, K., Parker, J.E., 2015. Effector-Triggered Immunity: From Pathogen Perception to Robust Defense. Annu. Rev. Plant Biol. 66, 487–511.

Cvrčková, F., Grunt, M., Bezvoda, R., Hála, M., Kulich, I., Rawat, A., Žárský, V., 2012. Evolution of the land plant exocyst complexes. Front. Plant Sci. 3, 1–13.

da Cunha, L., McFall, A.J., Mackey, D., 2006. Innate immunity in plants: a continuum of layered defenses. Microbes Infect. 8, 1372–1381.

Dangl, J.L., Jones, J.D., 2001. Plant pathogens and integrated defence responses to infection. Nature 411, 826–833.

Dawson, A.M., Ferguson, J.N., Gardiner, M., Green, P., Hubbard, A., Moscou, M.J., 2016. Isolation and fine mapping of Rps6: an intermediate host resistance gene in barley to wheat stripe rust. Theor. Appl. Genet.

de Guillen, K., Ortiz-Vallejo, D., Gracy, J., Fournier, E., Kroj, T., Padilla, A., 2015. Structure Analysis Uncovers a Highly Diverse but Structurally Conserved Effector Family in Phytopathogenic Fungi. PLoS Pathog. 11, 1–27.

De Vries, J.S., Andriotis, V.M.E., Wu, A.J., Rathjen, J.P., 2006. Tomato Pto encodes a functional N-myristoylation motif that is required for signal transduction in Nicotiana benthamiana. Plant J. 45, 31–45.

Dean, R., Van Kan, J.A.L., Pretorius, Z.A., Hammond-Kosack, K.E., Di Pietro, A., Spanu, P.D., Rudd, J.J., Dickman, M., Kahmann, R., Ellis, J., Foster, G.D., 2012. The Top 10 fungal pathogens in molecular plant pathology. Mol. Plant Pathol. 13, 414–430.

Deng, Y., Zhai, K., Xie, Z., Yang, D., Zhu, X., Liu, J., Wang, X., Qin, P., Yang, Y., Zhang, G., Li, Q., Zhang, J., Wu, S., Milazzo, J., Mao, B., Wang, E., Xie, H., Tharreau, D., He, Z., 2017. Epigenetic regulation of antagonistic receptors confers rice blast resistance with yield balance. Science (80-.). 355, 962–965.

Deslandes, L., Olivier, J., Peeters, N., Feng, D.X., Khounlotham, M., Boucher, C., Somssich, I., Genin, S., Marco, Y., 2003. Physical interaction between RRS1-R, a protein conferring resistance to bacterial wilt, and PopP2, a type III effector targeted to the plant nucleus. Proc. Natl. Acad. Sci. U. S. A. 100, 8024–8029.

Develey-Rivière, M.P., Galiana, E., 2007. Resistance to pathogens and host developmental stage: A multifaceted relationship within the plant kingdom. New Phytol. 175, 405–416.

Díaz-Perales, A., Linacero, R., Vázquez, A.M., 2003. Analysis of genetic relationships among 22 European barley varieties based on two PCR markers. Euphytica 129, 53–60.

Ding, J., Cheng, H., Jin, X., Araki, H., Yang, Y., Tian, D., 2007a. Contrasting patterns of evolution between allelic groups at a single locus in Arabidopsis. Genetica 129, 235–242.

Ding, J., Zhang, W., Jing, Z., Chen, J.Q., Tian, D., 2007b. Unique pattern of R-gene variation within populations in Arabidopsis. Mol. Genet. Genomics 277, 619–629.

Dodds, P.N., Lawrence, G.J., Catanzariti, A.-M., Teh, T., Wang, C.-I.A., Ayliffe, M.A., Kobe, B., Ellis, J.G., 2006. Direct protein interaction underlies gene-for-gene specificity and coevolution of the flax resistance genes and flax rust avirulence genes. Proc. Natl. Acad. Sci. U. S. A. 103, 8888–93.

Dodds, P.N., Lawrence, G.J., Catanzariti, A.M., Ayliffe, M.A., Ellis, J.G., 2004. The Melampsora lini AvrL567 avirulence genes are expressed in haustoria and their products are recognized inside plant cells. Plant Cell 16, 755–768.

Dodds, P.N., Lawrence, G.J., Ellis, J.G., 2001. Contrasting modes of evolution acting on the complex N locus for rust resistance in flax. Plant J. 27, 439–453.

Dodds, P.N., Rafiqi, M., Gan, P.H.P., Hardham, A.R., Jones, D.A., Ellis, J.G., 2009. Effectors of biotrophic fungi and oomycetes: Pathogenicity factors and triggers of host resistance. New Phytol. 183, 993–1000.

Dodds, P.N., Rathjen, J.P., 2010. Plant immunity: towards an integrated view of plant–pathogen interactions. Nat. Rev. Genet. 11, 539–548.

Doerge, R.W., Churchill, G.A., 1996. Permutation Tests for Multiple Loci Affecting a Quantitative Character. Genetics 142.

Dreiseitl, A., 2014. The Hordeum vulgare subsp. spontaneum-Blumeria graminis f. sp. hordei pathosystem: Its position in resistance research and breeding applications. Eur. J. Plant Pathol. 138, 561–568.

Edgar, R.C., 2004. MUSCLE: Multiple sequence alignment with high accuracy and high throughput. Nucleic Acids Res. 32, 1792–1797.

Eitas, T.K., Dangl, J.L., 2010. NB-LRR proteins: pairs, pieces, perception, partners, and pathways. Curr. Opin. Plant Biol. 13, 472–477.

El Kasmi, F., Chung, E.H., Anderson, R.G., Li, J., Wan, L., Eitas, T.K., Gao, Z., Dangl, J.L., 2017. Signaling from the plasma-membrane localized plant immune receptor RPM1 requires self-association of the full-length protein. Proc. Natl. Acad. Sci. U. S. A. 114, E7385–E7394.

Ellis, J., Dodds, P., Pryor, T., 2000. Structure, function and evolution of plant disease resistance genes. Curr. Opin. Plant Biol. 3, 278–284.

Ellis, J.G., Dodds, P.N., Lawrence, G.J., 2007. Flax rust resistance gene specificity is based on direct resistance-avirulence protein interactions. Annu. Rev. Phytopathol. 45, 289–306.

Ellis, J.G., Lagudah, E.S., Spielmeyer, W., Dodds, P.N., 2014. The past, present and future of breeding rust resistant wheat. Front. Plant Sci. 5, 641.

Ellis, J.G., Lawrence, G.J., Luck, J.E., Dodds, P.N., 1999. Identification of Regions in Alleles of the Flax Rust Resistance Gene L That Determine Differences in Gene-for-Gene Specificity. Plant Cell 11, 495–506.

Elmore, J.M., Lin, Z.J.D., Coaker, G., 2011. Plant NB-LRR signaling: Upstreams and downstreams. Curr. Opin. Plant Biol. 14, 365–371.

Eriksson, J., 1894. Ueber die Specialisirung des Parasitismus bei den Getreiderostpilzen. Ber. Dtsch. Bot. Ges. 12.

Eulgem, T., Somssich, I.E., 2007. Networks of WRKY transcription factors in defense signaling. Curr. Opin. Plant Biol. 10, 366–371.

Faris, J.D., Zhang, Z., Lu, H., Lu, S., Reddy, L., Cloutier, S., Fellers, J.P., Meinhardt, S.W., Rasmussen, J.B., Xu, S.S., Oliver, R.P., Simons, K.J., Friesen, T.L., 2010. A unique wheat disease resistance-like gene governs effector-triggered susceptibility to

necrotrophic pathogens. Proc. Natl. Acad. Sci. U. S. A. 107, 13544–9.

Ferrier-Cana, E., Macadré, C., Sévignac, M., David, P., Langin, T., Geffroy, V., 2005. Distinct post-transcriptional modifications result into seven alternative transcripts of the CC-NBS-LRR gene JA1tr of Phaseolus vulgaris. Theor. Appl. Genet. 110, 895–905.

Feuillet, C., Travella, S., Stein, N., Albar, L., Nublat, A., Keller, B., 2003. Map-based isolation of the leaf rust disease resistance gene Lr10 from the hexaploid wheat (Triticum aestivum L.) genome. Proc. Natl. Acad. Sci. U. S. A. 100, 15253–8.

Flor, H.H., 1942. Inheritance of pathogenicity in Melampsora lini. Phytopathology 32, 653–669.

Flor, H.H., 1956. The Complementary Genic Systems in Flax and Flax Rust. Adv. Genet. 8, 29–54.

Flor, H.H., 1971. Current status of the gene-fob-gene concept 275–296.

Fox, E.M., Howlett, B.J., 2008. Secondary metabolism: regulation and role in fungal biology. Curr. Opin. Microbiol. 11, 481–487.

Franceschetti, M., Maqbool, A., Jiménez-Dalmaroni, M.J., Pennington, H.G., Kamoun, S., Banfield, M.J., 2017. Effectors of Filamentous Plant Pathogens: Commonalities amid Diversity. Microbiol. Mol. Biol. Rev. 81, 1–17.

Frantzeskakis, L., Kracher, B., Kusch, S., Yoshikawa-Maekawa, M., Bauer, S., Pedersen, C., Spanu, P.D., Maekawa, T., Schulze-Lefert, P., Panstruga, R., 2018. Signatures of host specialization and a recent transposable element burst in the dynamic one-speed genome of the fungal barley powdery mildew pathogen. BMC Genomics 19, 1–23.

Frantzeskakis, L., Kusch, S., Panstruga, R., 2019. The need for speed: compartmentalized genome evolution in filamentous phytopathogens. Mol. Plant Pathol. 20, 3–7.

Freialdenhoven, a, Peterhansel, C., Kurth, J., Kreuzaler, F., Schulze-Lefert, P., 1996. ldentification of Genes Required for the Function of Non-Race-Specific. Plant Cell 8, 5–14.

Freialdenhoven, A., Scherag, B., Hollricher, K., Collinge, D.B., Thordal-Christensen, H., Schulze-Lefert, P., 1994. Nar-1 and Nar-2, Two Loci Required for Mla12-Specified Race-Specific Resistance to Powdery Mildew in Barley. Plant Cell 983–994.

Friesen, T.L., Faris, J.D., Solomon, P.S., Oliver, R.P., 2008. Host-specific toxins: Effectors of necrotrophic pathogenicity. Cell. Microbiol. 10, 1421–1428.

Fudal, I., Collemare, J., Böhnert, H.U., Melayah, D., Lebrun, M.H., 2007. Expression of Magnaporthe grisea avirulence gene ACE1 is connected to the initiation of appressorium-mediated penetration. Eukaryot. Cell 6, 546–554.

Fujisaki, K., Abe, Y., Ito, A., Saitoh, H., Yoshida, K., Kanzaki, H., Kanzaki, E., Utsushi, H., Yamashita, T., Kamoun, S., Terauchi, R., 2015. Rice Exo70 interacts with a fungal

effector, AVR-Pii, and is required for AVR-Pii-triggered immunity. Plant J. 83, 875–887.

Gan, Z.R., 1991. Yeast thioredoxin genes. J. Biol. Chem. 266, 1692–1696.

Gassmann, W., 2008. Alternative splicing in plant defense. Curr. Top. Microbiol. Immunol.

Gibson, D.G., Benders, G. a, Andrews-Pfannkoch, C., Denisova, E. a, Baden-Tillson, H., Zaveri, J., Stockwell, T.B., Brownley, A., Thomas, D.W., Algire, M. a, Merryman, C., Young, L., Noskov, V.N., Glass, J.I., Venter, J.C., Hutchison, C. a, Smith, H.O., 2008. Complete chemical synthesis, assembly, and cloning of a Mycoplasma genitalium genome. Science 319, 1215–1220.

Gilbert, B.M., Wolpert, T.J., 2013. Characterization of the LOV1-mediated, victorin-induced, cell-death response with virus-induced gene silencing. Mol. Plant. Microbe. Interact. 26, 903–17.

Gladieux, P., Condon, B., Ravel, S., Soanes, D., Maciel, J.L.N., Nhani, A., Chen, L., Terauchi, R., Lebrun, M.H., Tharreau, D., Mitchell, T., Pedley, K.F., Valent, B., Talbot, N.J., Farman, M., Fournier, E., 2018. Gene flow between divergent cereal- and grass-specific lineages of the rice blast fungus Magnaporthe oryzae. MBio 9.

Glass, N.L., Kaneko, I., 2003. Fatal attraction: Nonself recognition and heterokaryon incompatibility in filamentous fungi. Eukaryot. Cell.

Glazebrook, J., 2005. Contrasting Mechanisms of Defense Against Biotrophic and Necrotrophic Pathogens. Annu. Rev. Phytopathol. 43, 205–227.

Goggin, F.L., Jia, L., Shah, G., Hebert, S., Williamson, V.M., Ullman, D.E., 2006. Heterologous expression of the Mi-1.2 gene from tomato confers resistance against nematodes but not aphids in eggplant. Mol. Plant-Microbe Interact. 19, 383–388.

Goggin, Fiona L, Shah, G., Williamson, V.M., Ullman, D.E., 2004. Developmental Regulation of Mi -Mediated Aphid Resistance Is Independent of Mi-1 . 2 Transcript Levels 17, 532–536.

Goggin, Fiona L., Shah, G., Williamson, V.M., Ullman, D.E., 2004. Developmental regulation of Mi-mediated aphid resistance is independent of Mi-1.2 transcript levels. Mol. Plant-Microbe Interact. 17, 532–536.

Goritschnig, S., Steinbrenner, A.D., Grunwald, D.J., Staskawicz, B.J., 2016. Structurally distinct Arabidopsis thaliana NLR immune receptors recognize tandem WY domains of an oomycete effector. New Phytol. 210, 984–996.

Grabherr, M.G., Haas, B.J., Yassour, M., Levin, J.Z., Thompson, D.A., Amit, I., Adiconis, X., Fan, L., Raychowdhury, R., Zeng, Q., Chen, Z., Mauceli, E., Hacohen, N., Gnirke, A., Rhind, N., Di Palma, F., Birren, B.W., Nusbaum, C., Lindblad-Toh, K., Friedman, N., Regev, A., 2011. Full-length transcriptome assembly from RNA-Seq data without a reference genome. Nat. Biotechnol. 29, 644–652.

Grant, J.J., Chini, A., Basu, D., Loake, G.J., 2003. Targeted activation tagging of the Arabidopsis NBS-LRR gene, ADR1, conveys resistance to virulent pathogens. Mol. Plant-Microbe Interact. 16, 669–680.

Grant, M.R., Godiard, L., Straube, E., Ashfield, T., Lewald, J., Sattler, A., Innes, R.W., Dangl, J.L., 1995. Structure of the Arabidopsis RPM1 gene enabling dual specificity disease resistance. Science (80-.). 269, 843–846.

Gu, K., Yang, B., Tian, D., Wu, L., Wang, D., Sreekala, C., Yang, F., Chu, Z., Wang, G.L., White, F.F., Yin, Z., 2005. R gene expression induced by a type-III effector triggers disease resistance in rice. Nature 435, 1122–1125.

Gu, Y., Zavaliev, R., Dong, X., 2017. Membrane Trafficking in Plant Immunity. Mol. Plant 10, 1026–1034.

Guo, Huijuan, Huang, L., Sun, Y., Guo, Honggang, Ge, F., 2016. The contrasting effects of elevated CO2 on TYLCV infection of tomato genotypes with and without the resistance gene, Mi-1.2. Front. Plant Sci. 7, 1–14.

Guo, Y.L., Fitz, J., Schneeberger, K., Ossowski, S., Cao, J., Weigel, D., 2011. Genome-wide comparison of nucleotide-binding site-leucine-rich repeat-encoding genes in Arabidopsis. Plant Physiol. 157, 757–769.

Gyawali, S., Verma, R.P.S., Kumar, S., Bhardwaj, S.C., Gangwar, O.P., Selvakumar, R., Shekhawat, P.S., Rehman, S., Sharma-Poudyal, D., 2017. Seedling and adult-plant stage resistance of a world collection of barley genotypes to stripe rust. J. Phytopathol. 166, 18–27.

Haas, B.J., Papanicolaou, A., Yassour, M., Grabherr, M., Blood, P.D., Bowden, J., Couger, M.B., Eccles, D., Li, B., Lieber, M., Macmanes, M.D., Ott, M., Orvis, J., Pochet, N., Strozzi, F., Weeks, N., Westerman, R., William, T., Dewey, C.N., Henschel, R., Leduc, R.D., Friedman, N., Regev, A., 2013. De novo transcript sequence reconstruction from RNA-seq using the Trinity platform for reference generation and analysis. Nat. Protoc. 8, 1494–1512.

Hall, S.A., Allen, R.L., Baumber, R.E., Baxter, L.A., Fisher, K., Bittner-Eddy, P.D., Rose, L.E., Holub, E.B., Beynon, J.L., 2009. Maintenance of genetic variation in plants and pathogens involves complex networks of gene-for-gene interactions. Mol. Plant Pathol. 10, 449–457.

Halterman, D. a, 2003. Powdery Mildew-Induced Mla mRNAs Are Alternatively Spliced and Contain Multiple Upstream Open Reading Frames. Plant Physiol. 131, 558–567.

Halterman, D., Zhou, F., Wei, F., Wise, R.P., Schulze-Lefert, P., 2001. The MLA6 coiled-coil, NBS-LRR protein confers AvrMla6-dependent resistance specificity to Blumeria graminis f. sp. hordei in barley and wheat. Plant J. 25, 335–348.

Halterman, D.A., Wei, F., Wise, R.P., 2003. Powdery mildew-induced Mla mRNAs are

alternatively spliced and contain multiple upstream open reading frames. Plant Physiol. 131, 558–567.

Halterman, D.A., Wise, R.P., 2004. A single-amino acid substitution in the sixth leucine-rich repeat of barley MLA6 and MLA13 alleviates dependence on RAR1 for disease resistance signaling. Plant J. 38, 215–226.

Hao, W., Collier, S.M., Moffett, P., Chai, J., 2013. Structural basis for the interaction between the potato virus X resistance protein (Rx) and its cofactor ran GTPase-activating protein 2 (RanGAP2). J. Biol. Chem. 288, 35868–35876.

Havis, N.D., Brown, J.K.M., Clemente, G., Frei, P., Jedryczka, M., Kaczmarek, J., Kaczmarek, M., Matusinsky, P., McGrann, G.R.D., Pereyra, S., Piotrowska, M., Sghyer, H., Tellier, A., Hess, M., 2015. Ramularia collo-cygni - An emerging pathogen of barley crops. Phytopathology 105, 895–904.

He, B., Xi, F., Zhang, X., Zhang, J., Guo, W., 2007. Exo70 interacts with phospholipids and mediates the targeting of the exocyst to the plasma membrane. EMBO J. 26, 4053–4065.

Heath, M.C., 2000. Nonhost resistance and nonspecific plant defenses. Curr. Opin. Plant Biol. 3, 315–319.

Heese, A., Hann, D.R., Gimenez-Ibanez, S., Jones, A.M.E., He, K., Li, J., Schroeder, J.I., Peck, S.C., Rathjen, J.P., 2007. The receptor-like kinase SERK3/BAK1 is a central regulator of innate immunity in plants. Proc. Natl. Acad. Sci. U. S. A. 104, 12217–12222.

Heider, M.R., Munson, M., 2012. Exorcising the Exocyst Complex. Traffic 13, 898–907.

Heidrich, K., Blanvillain-Baufumé, S., Parker, J.E., 2012. Molecular and spatial constraints on NB-LRR receptor signaling. Curr. Opin. Plant Biol. 15, 385–391.

Hermanns, M., Slusarenko, A.J., Schlaich, N.L., 2003. Organ-specificity in a plant disease is determined independently of R gene signaling. Mol. Plant-Microbe Interact. 16, 752–759.

Herrera-Foessel, S.A., Lagudah, E.S., Huerta-Espino, J., Hayden, M.J., Bariana, H.S., Singh, D., Singh, R.P., 2011. New slow-rusting leaf rust and stripe rust resistance genes Lr67 and Yr46 in wheat are pleiotropic or closely linked. Theor. Appl. Genet. 122, 239–249.

Herrera-Foessel, S.A., Singh, R.P., Lillemo, M., Huerta-Espino, J., Bhavani, S., Singh, S., Lan, C., Calvo-Salazar, V., Lagudah, E.S., 2014. Lr67/Yr46 confers adult plant resistance to stem rust and powdery mildew in wheat. Theor. Appl. Genet. 127, 781–789.

Hiebert, C.W., Thomas, J.B., McCallum, B.D., Humphreys, D.G., DePauw, R.M., Hayden, M.J., Mago, R., Schnippenkoetter, W., Spielmeyer, W., 2010. An introgression on wheat chromosome 4DL in RL6077 (Thatcher*6/PI 250413) confers adult plant

resistance to stripe rust and leaf rust (Lr67). Theor. Appl. Genet. 121, 1083–1091.

Holt, B.F., Belkhadir, Y., Dangl, J.L., 2005. Plant science: Antagonistic control of disease resistance protein stability in the plant immune system. Science (80-.). 309, 929–932.

Horbach, R., Navarro-Quesada, A.R., Knogge, W., Deising, H.B., 2011. When and how to kill a plant cell: Infection strategies of plant pathogenic fungi. J. Plant Physiol. 168, 51–62.

Hovmøller, M.S., 1993. Observed and Predicted Changes in Virulence Gene Frequencies at 11 Loci in a Local Barley Powdery Mildew Population. Phytopathology 83, 253.

Hovmøller, M.S., Sørensen, C.K., Walter, S., Justesen, A.F., 2011. Diversity of Puccinia striiformis on cereals and grasses. Annu. Rev. Phytopathol. 49, 197–217.

Hovmøller, M.S., Walter, S., Bayles, R.A., Hubbard, A., Flath, K., Sommerfeldt, N., Leconte, M., Czembor, P., Rodriguez-Algaba, J., Thach, T., Hansen, J.G., Lassen, P., Justesen, A.F., Ali, S., de Vallavieille-Pope, C., 2016. Replacement of the European wheat yellow rust population by new races from the centre of diversity in the near-Himalayan region. Plant Pathol. 65, 402–411.

Hubbard, A., Lewis, C.M., Yoshida, K., Ramirez-Gonzalez, R.H., de Vallavieille-Pope, C., Thomas, J., Kamoun, S., Bayles, R., Uauy, C., Saunders, D.G.O., 2015. Field pathogenomics reveals the emergence of a diverse wheat yellow rust population. Genome Biol. 16, 1–15.

Hückelhoven, R., Fodor, J., Trujillo, M., Kogel, K.H., 2000. Barley Mla and Rar mutants compromised in the hypersensitive cell death response against Blumeria graminis f.sp. hordei are modified in their ability to accumulate reactive oxygen intermediates at sites of fungal invasion. Planta 212, 16–24.

Hulbert, S.H., Webb, C. a, Smith, S.M., 2001. RESISTANCE GENE COMPLEXES: Evolution and Utilization. Annu. Rev. Phytopathol. 39, 285–312.

Hummel, A.W., Doyle, E.L., Bogdanove, A.J., 2012. Addition of transcription activator-like effector binding sites to a pathogen strain-specific rice bacterial blight resistance gene makes it effective against additional strains and against bacterial leaf streak. New Phytol. 195, 883–893.

Hyon, G.S., Nga, N.T.T., Chuma, I., Inoue, Y., Asano, H., Murata, N., Kusaba, M., Tosa, Y., 2012. Characterization of interactions between barley and various host-specific subgroups of Magnaporthe oryzae and M. grisea. J. Gen. Plant Pathol. 78, 237–246.

IBGSC, Mayer, K.F.X., Waugh, R., Langridge, P., Close, T.J., Wise, R.P., Graner, A., Matsumoto, T., Sato, K., Schulman, A., Muehlbauer, G.J., Stein, N., Ariyadasa, R., Schulte, D., Poursarebani, N., Zhou, R., Steuernagel, B., Mascher, M., Scholz, U., Shi, B., Langridge, P., Madishetty, K., Svensson, J.T., Bhat, P., Moscou, M., Resnik, J., Close, T.J., Muehlbauer, G.J., Hedley, P., Liu, H., Morris, J., Waugh, R., Frenkel, Z.,

Korol, A., Bergès, H., Graner, A., Stein, N., Steuernagel, B., Scholz, U., Taudien, S., Felder, M., Groth, M., Platzer, M., Stein, N., Steuernagel, B., Scholz, U., Himmelbach, A., Taudien, S., Felder, M., Platzer, M., Lonardi, S., Duma, D., Alpert, M., Cordero, F., Beccuti, M., Ciardo, G., Ma, Y., Wanamaker, S., Close, T.J., Stein, N., Cattonaro, F., Vendramin, V., Scalabrin, S., Radovic, S., Wing, R., Schulte, D., Steuernagel, B., Morgante, M., Stein, N., Waugh, R., Nussbaumer, T., Gundlach, H., Martis, M., Ariyadasa, R., Poursarebani, N., Steuernagel, B., Scholz, U., Wise, R.P., Poland, J., Stein, N., Mayer, K.F.X., Spannagl, M., Pfeifer, M., Gundlach, H., Mayer, K.F.X., Gundlach, H., Moisy, C., Tanskanen, J., Scalabrin, S., Zuccolo, A., Vendramin, V., Morgante, M., Mayer, K.F.X., Schulman, A., Pfeifer, M., Spannagl, M., Hedley, P., Morris, J., Russell, J., Druka, A., Marshall, D., Bayer, M., Swarbreck, D., Sampath, D., Ayling, S., Febrer, M., Caccamo, M., Matsumoto, T., Tanaka, T., Sato, K., Wise, R.P., Close, T.J., Wannamaker, S., Muehlbauer, G.J., Stein, N., Mayer, K.F.X., Waugh, R., Steuernagel, B., Schmutzer, T., Mascher, M., Scholz, U., Taudien, S., Platzer, M., Sato, K., Marshall, D., Bayer, M., Waugh, R., Stein, N., Mayer, K.F.X., Waugh, R., Brown, J.W.S., Schulman, A., Langridge, P., Platzer, M., Fincher, G.B., Muehlbauer, G.J., Sato, K., Close, T.J., Wise, R.P., Stein, N., 2012. A physical, genetic and functional sequence assembly of the barley genome. Nature 491, 711–716.

Inoue, Y., Vy, T.T.P., Yoshida, K., Asano, H., Mitsuoka, C., Asuke, S., Anh, V.L., Cumagun, C.J.R., Chuma, I., Terauchi, R., Kato, K., Mitchell, T., Valent, B., Farman, M., Tosa, Y., 2017. Evolution of the wheat blast fungus through functional losses in a host specificity determinant. Science (80-.). 357, 80–83.

Inukai, T., Vales, M.I., Hori, K., Sato, K., Hayes, P.M., 2006. RMo1 confers blast resistance in barley and is located within the complex of resistance genes containing Mla, a powdery mildew resistance gene. Mol. Plant. Microbe. Interact. 19, 1034–1041.

Isidore, E., Scherrer, B., Chalhoub, B., Feuillet, C., Keller, B., 2005. Ancient haplotypes resulting from extensive molecular rearrangements in the wheat A genome have been maintained in species of three different ploidy levels. Genome Res. 15, 526–536.

Islam, M.T., Croll, D., Gladieux, P., Soanes, D.M., Persoons, A., Bhattacharjee, P., Hossain, M.S., Gupta, D.R., Rahman, M.M., Mahboob, M.G., Cook, N., Salam, M.U., Surovy, M.Z., Sancho, V.B., Maciel, J.L.N., NhaniJúnior, A., Castroagudín, V.L., Reges, J.T. d. A., Ceresini, P.C., Ravel, S., Kellner, R., Fournier, E., Tharreau, D., Lebrun, M.H., McDonald, B.A., Stitt, T., Swan, D., Talbot, N.J., Saunders, D.G.O., Win, J., Kamoun, S., 2016. Emergence of wheat blast in Bangladesh was caused by a South American lineage of Magnaporthe oryzae. BMC Biol. 14, 1–11.

Jafary, H., Szabo, L.J., Niks, R.E., 2006. Innate nonhost immunity in barley to different heterologous rust fungi is controlled by sets of resistance genes with different and

overlapping specificities. Mol. Plant. Microbe. Interact. 19, 1270–9.

Jia, Y., Bryan, G.T., Farrall, L., Valent, B., 2003. Natural Variation at the Pi-ta Rice Blast Resistance Locus. Phytopathology 93, 1452–1459.

Jia, Y., McAdams, S.A., Bryan, G.T., Hershey, H.P., Valent, B., 2000. Direct interaction of resistance gene and avirulence gene products confers rice blast resistance. EMBO J. 19, 4004–4014.

Johal, G.S., Briggs, S.P., 1992. Reductase activity encoded by the HM1 disease resistance gene in maize. Science (80-.).

Jones, J.D.G., Dangl, J.L., 2006. The plant immune system. Nature 444, 323–329.

Jones, J.D.G., Vance, R.E., Dangl, J.L., 2016. Intracellular innate immune surveillance devices in plants and animals. Science (80-.). 354.

Jordan, T., Schornack, S., Lahaye, T., 2002. Alternative splicing of transcripts encoding toll-like plant resistance proteins - What's the functional relevance to innate immunity? Trends Plant Sci.

Jordan, T., Seeholzer, S., Schwizer, S., Töller, A., Somssich, I.E., Keller, B., 2011. The wheat Mla homologue TmMla1 exhibits an evolutionarily conserved function against powdery mildew in both wheat and barley. Plant J. 65, 610–621.

Jørgensen, J.H., 1992. Multigene families of powdery mildew resistance genes in locus Mla on Barley chromosome 5. Plant Breed. 108, 53–59.

Jørgensen, J.H., 1994. Genetics of powdery mildew resistance in barley. Critical Reviews in. Plant Sci. 13, 97–119.

Jupe, F., Witek, K., Verweij, W., ??liwka, J., Pritchard, L., Etherington, G.J., Maclean, D., Cock, P.J., Leggett, R.M., Bryan, G.J., Cardle, L., Hein, I., Jones, J.D.G., 2013. Resistance gene enrichment sequencing (RenSeq) enables reannotation of the NB-LRR gene family from sequenced plant genomes and rapid mapping of resistance loci in segregating populations. Plant J. 76, 530–544.

Kang, S., Sweigard, J.A., Valent, B., 1995. The PWL host specificity gene family in the blast fungus Magnaporthe grisea. Mol. Plant. Microbe. Interact.

Kanzaki, H., Yoshida, K., Saitoh, H., Fujisaki, K., Hirabuchi, A., Alaux, L., Fournier, E., Tharreau, D., Terauchi, R., 2012. Arms race co-evolution of Magnaporthe oryzae AVR-Pik and rice Pik genes driven by their physical interactions. Plant J. 72, 894–907.

Karasov, T.L., Kniskern, J.M., Gao, L., Deyoung, B.J., Ding, J., Dubiella, U., Lastra, R.O., Nallu, S., Roux, F., Innes, R.W., Barrett, L.G., Hudson, R.R., Bergelson, J., 2014. The long-term maintenance of a resistance polymorphism through diffuse interactions. Nature 512, 436–440.

Katagiri, F., Tsuda, K., 2010. Understanding the Plant Immune System 23, 1531–1536.

Kawai, T., Kitamura, Y., Ootani, H., Watanabe, K., 1979. Studies on the cultivations of

summer sowing barley, 3: Peculiarity in the occurrence of diseases and insect pests. Kinki Chugoku Agric. Res. 38–41.

Kearse, M., Moir, R., Wilson, A., Stones-Havas, S., Cheung, M., Sturrock, S., Buxton, S., Cooper, A., Markowitz, S., Duran, C., Thierer, T., Ashton, B., Meintjes, P., Drummond, A., 2012. Geneious Basic: An integrated and extendable desktop software platform for the organization and analysis of sequence data. Bioinformatics 28, 1647–1649.

Kettles, G.J., Luna, E., 2019. Food security in 2044: How do we control the fungal threat? Fungal Biol. 123, 558–564.

Kim, H.-S., Desveaux, D., Singer, A.U., Patel, P., Sondek, J., Dangl, J.L., 2005. The Pseudomonas syringae effector AvrRpt2 cleaves its C-terminally acylated target, RIN4, from Arabidopsis membranes to block RPM1 activation. Proc. Natl. Acad. Sci. U. S. A. 102, 6496–501.

Kim, M.G., da Cunha, L., McFall, A.J., Belkhadir, Y., DebRoy, S., Dangl, J.L., Mackey, D., 2005. Two Pseudomonas syringae Type III Effectors Inhibit RIN4-Regulated Basal Defense in Arabidopsis. Cell 121, 749–759.

Kim, M.G., Geng, X., Lee, S.Y., Mackey, D., 2009. The Pseudomonas syringae type III effector AvrRpm1 induces significant defenses by activating the Arabidopsis nucleotide-binding leucine-rich repeat protein RPS2. Plant J. 57, 645–653.

Kim, S.H., Qi, D., Helm, M., 2016. Using decoys to expand the recognition specificity of a plant disease resistance protein. Science (80-.). 351.

Kim, Y.J., Lin, N., Martin, G.B., 2002. Interact with the Pto Kinase and Activate Plant Immunity. Cell 109, 589–598.

Klein, J., Sato, A., Nagl, S., O'Huigín, C., 1998. Molecular trans-species polymorphism. Annu. Rev. Ecol. Syst. 29, 1–21.

Klein, J., Sato, A., Nikolaidis, N., 2007. MHC, TSP, and the Origin of Species: From Immunogenetics to Evolutionary Genetics. Annu. Rev. Genet. 41, 281–304.

Kneeshaw, S., Gelineau, S., Tada, Y., Loake, G.J., Spoel, S.H., 2014. Selective Protein Denitrosylation Activity of Thioredoxin- h5 Modulates Plant Immunity 56, 153–162.

Koenig, D., Hagmann, J., Li, R., Bemm, F., Slotte, T., Nueffer, B., Wright, S.I., Weigel, D., 2019. Long-term balancing selection drives evolution of immunity genes in capsella. Elife 8, 1–27.

Kolmer, J.A., Lagudah, E.S., Lillemo, M., Lin, M., Bai, G., 2015. The Lr46 gene conditions partial adult- plant resistance to stripe rust, stem rust, and powdery mildew in thatcher wheat. Crop Sci. 55, 2557–2565.

Kølster, P., Stølen, O., 1987. Barley Isolines with Genes for Resistance to Erysiphe graminis f. sp. hordei in the Recurrent Parent 'Siri.' Plant Breed. 98, 79–82.

Kong, W., Li, B., Wang, Q., Wang, B., Duan, X., Ding, L., Lu, Y., Liu, L.W., La, H., 2018. Analysis of the DNA methylation patterns and transcriptional regulation of the NB-LRR-encoding gene family in Arabidopsis thaliana. Plant Mol. Biol. 96, 563–575.

Kongprakhon, P., Cuesta-Marcos, A., Hayes, P.M., Richardson, K.L., Sirithunya, P., Sato, K., Steffenson, B., Toojinda, T., 2009. Validation of rice blast resistance genes in barley using a QTL mapping population and near-isolines. Breed. Sci. 59, 341–349.

Kourelis, J., Van Der Hoorn, R.A.L., 2018. Defended to the nines: 25 years of resistance gene cloning identifies nine mechanisms for R protein function. Plant Cell 30, 285–299.

Krasileva, K. V., Dahlbeck, D., Staskawicz, B.J., 2010. Activation of an Arabidopsis resistance protein is specified by the in planta association of its leucine-rich repeat domain with the cognate oomycete effector. Plant Cell 22, 2444–2458.

Krattinger, S.G., Kang, J., Bräunlich, S., Boni, R., Chauhan, H., Selter, L.L., Robinson, M.D., Schmid, M.W., Wiederhold, E., Hensel, G., Kumlehn, J., Sucher, J., Martinoia, E., Keller, B., 2019. Abscisic acid is a substrate of the ABC transporter encoded by the durable wheat disease resistance gene Lr34, New Phytologist.

Krattinger, S.G., Lagudah, E.S., Spielmeyer, W., Singh, R.P., Huerta-Espino, J., McFadden, H., Bossolini, E., Selter, L.L., Keller, B., 2009. A Putative ABC Transporter Confers Durable Resistance to Multiple Fungal Pathogens in Wheat. Science (80-.). 323, 1360–1363.

Krattinger, S.G., Sucher, J., Selter, L.L., Chauhan, H., Zhou, B., Tang, M., Upadhyaya, N.M., Mieulet, D., Guiderdoni, E., Weidenbach, D., Schaffrath, U., Lagudah, E.S., Keller, B., 2015. The wheat durable, multipathogen resistance gene Lr34 confers partial blast resistance in rice. Plant Biotechnol. J. 1–8.

Krenek, P., Samajova, O., Luptovciak, I., Doskocilova, A., Komis, G., Samaj, J., 2015. Transient plant transformation mediated by Agrobacterium tumefaciens: Principles, methods and applications. Biotechnol. Adv. 33, 1024–1042.

Kroj, T., Chanclud, E., Michel-romiti, C., Grand, X., Morel, J., 2016. Integration of decoy domains derived from protein targets of pathogen effectors into plant immune receptors is widespread.

Kruger, W.M., Szabo, L.J., Zeyen, R.J., 2003. Transcription of the defense response genes chitinase IIb, PAL and peroxidase is induced by the barley powdery mildew fungus and is only indirectly modulated by R genes. Physiol. Mol. Plant Pathol. 63, 167–178.

Kuang, H., Caldwell, K.S., Meyers, B.C., Michelmore, R.W., 2008. Frequent sequence exchanges between homologs of RPP8 in Arabidopsis are not necessarily associated with genomic proximity. Plant J. 54, 69–80.

Kusch, S., Panstruga, R., 2017. Mlo-based resistance: An apparently universal “weapon” to

defeat powdery mildew disease. Mol. Plant-Microbe Interact.

Lai, Y., Eulgem, T., 2018. Transcript-level expression control of plant NLR genes. Mol. Plant Pathol. 19, 1267–1281.

Laluk, K., Mengiste, T., 2010. Necrotroph Attacks on Plants: Wanton Destruction or Covert Extortion? Arab. B. 8, e0136.

Le Roux, C., Huet, G., Jauneau, A., Camborde, L., Trémousaygue, D., Kraut, A., Zhou, B., Levaillant, M., Adachi, H., Yoshioka, H., Raffaele, S., Berthomé, R., Couté, Y., Parker, J.E., Deslandes, L., 2015. A receptor pair with an integrated decoy converts pathogen disabling of transcription factors to immunity. Cell 161, 1074–1088.

Leaché, A.D., 2009. The Timetree of Life. S. Blair Hedges and Sudhir Kumar, editors. Integr. Comp. Biol. 50, 141–142.

Lee, H.A., Yeom, S.I., 2015. Plant NB-LRR proteins: Tightly regulated sensors in a complex manner. Brief. Funct. Genomics 14, 233–242.

Lee, T.G., Kumar, I., Diers, B.W., Hudson, M.E., 2015. Evolution and selection of Rhg1, a copy-number variant nematode-resistance locus. Mol. Ecol. 24, 1774–1791.

Leister, D., 2004. Tandem and segmental gene duplication and recombination in the evolution of plant disease resistance genes. Trends Genet. 20, 116–122.

Leng, Y., Zhao, M., Wang, R., Steffenson, B.J., Brueggeman, R.S., Zhong, S., 2018. The gene conferring susceptibility to spot blotch caused by Cochliobolus sativus is located at the Mla locus in barley cultivar Bowman. Theor. Appl. Genet. 131, 1531–1539.

Lewis, D.H., 1973. Cocepts in Fungal Nutrition and the Origin of Biotrophy. Biol. Rev. 48, 261–277.

Lewis, J.D., Lee, A.H.Y., Hassan, J.A., Wana, J., Hurleya, B., Jhingree, J.R., Wang, P.W., Lo, T., Youn, J.Y., Guttman, D.S., Desveaux, D., 2013. The Arabidopsis ZED1 pseudokinase is required for ZAR1-mediated immunity induced by the Pseudomonas syringae type III effector HopZ1a. Proc. Natl. Acad. Sci. U. S. A. 110, 18722–18727.

Li, J., Ding, J., Zhang, W., Zhang, Y., Tang, P., Chen, J.Q., Tian, D., Yang, S., 2010. Unique evolutionary pattern of numbers of gramineous NBS-LRR genes. Mol. Genet. Genomics 283, 427–438.

Li, Y., Li, S., Bi, D., Cheng, Y.T., Li, X., Zhang, Y., 2010. SRFR1 negatively regulates plant NB-LRR resistance protein accumulation to prevent autoimmunity. PLoS Pathog. 6, 1–11.

Li, Z., Huang, J., Wang, Z., Meng, F., Zhang, S., Wu, X., Zhang, Z., Gao, Z., 2019. Overexpression of Arabidopsis nucleotide-binding and leucine-rich repeat genes RPS2 and RPM1(D505v) confers broad-spectrum disease resistance in rice. Front. Plant Sci. 10, 1–16.

Lillemo, M., Asalf, B., Singh, R.P., Huerta-Espino, J., Chen, X.M., He, Z.H., Bjørnstad, Å.,

2008. The adult plant rust resistance loci Lr34/Yr18 and Lr46/Yr29 are important determinants of partial resistance to powdery mildew in bread wheat line Saar. Theor. Appl. Genet. 116, 1155–1166.

Lillemo, M., Singh, R.P., Huerta-Espino, J., Chen, X.M., He, Z.H., Brown, J.K.M., 2007. Leaf Rust Resistance Gene LR34 is Involved in Powdery Mildew Resistance of Cimmyt Bread Wheat Line Saar. In: Wheat Production in Stressed Environments. Springer Netherlands, pp. 97–102.

Ling, H.Q., Wang, Jun, Zhao, S., Liu, D., Wang, Junyi, Sun, H., Zhang, C., Fan, H., Li, D., Dong, L., Tao, Y., Gao, C., Wu, Huilan, Li, Y., Cui, Y., Guo, X., Zheng, S., Wang, B., Yu, K., Liang, Q., Yang, W., Lou, X., Chen, J., Feng, M., Jian, J., Zhang, Xiaofei, Luo, G., Jiang, Y., Liu, J., Wang, Z., Sha, Y., Zhang, B., Wu, Huajun, Tang, D., Shen, Q., Xue, P., Zou, S., Wang, X., Liu, X., Wang, F., Yang, Y., An, X., Dong, Z., Zhang, K., Zhang, Xiangqi, Luo, M.C., Dvorak, J., Tong, Y., Wang, Jian, Yang, H., Li, Z., Wang, D., Zhang, A., 2013. Draft genome of the wheat A-genome progenitor Triticum urartu. Nature 496, 87–90.

Linkert, M., Rueden, C.T., Allan, C., Burel, J.M., Moore, W., Patterson, A., Loranger, B., Moore, J., Neves, C., MacDonald, D., Tarkowska, A., Sticco, C., Hill, E., Rossner, M., Eliceiri, K.W., Swedlow, J.R., 2010. Metadata matters: Access to image data in the real world. J. Cell Biol. 189, 777–782.

Liu, J., Elmore, J.M., Lin, Z.J.D., Coaker, G., 2011. A receptor-like cytoplasmic kinase phosphorylates the host target RIN4, leading to the activation of a plant innate immune receptor. Cell Host Microbe 9, 137–146.

Liu, M., Hambleton, S., 2010. Taxonomic study of stripe rust, Puccinia striiformis sensu lato, based on molecular and morphological evidence. Fungal Biol. 114, 881–899.

Liu, W., Liu, J., Triplett, L., Leach, J.E., Wang, G.-L., 2014. Novel Insights into Rice Innate Immunity against Bacterial and Fungal Pathogens., Annual review of phytopathology.

Liu, Z., Friesen, T.L., Ling, H., Meinhardt, S.W., Oliver, R.P., Rasmussen, J.B., Faris, J.D., 2006. The Tsn1-ToxA interaction in the wheat-Stagonospora nodorum pathosystem parallels that of the wheat-tan spot system. Genome 49, 1265–1273.

Liu, Z., Holmes, D.J., Faris, J.D., Chao, S., Brueggeman, R.S., Edwards, M.C., Friesen, T.L., 2015. Necrotrophic effector-triggered susceptibility (NETS) underlies the barley-Pyrenophora teres f. teres interaction specific to chromosome 6H. Mol. Plant Pathol. 16, 188–200.

Liu, Z., Zurn, J.D., Kariyawasam, G., Faris, J.D., Shi, G., Hansen, J., Rasmussen, J.B., Acevedo, M., 2017. Inverse gene-for-gene interactions contribute additively to tan spot susceptibility in wheat. Theor. Appl. Genet. 130, 1267–1276.

Lorang, J., Cuesta-Marcos, A., Hayes, P.M., Wolpert, T.J., 2010. Identification and mapping

of adult-onset sensitivity to victorin in barley. Mol. Breed. 26, 545–550.

Lorang, J., Kidarsa, T., Bradford, C.S., Gilbert, B., Curtis, M., Tzeng, S.C., Maier, C.S., Wolpert, T.J., 2012. Tricking the guard: Exploiting plant defense for disease susceptibility. Science (80-.). 338, 659–662.

Lorang, J.M., Carkaci-Salli, N., Wolpert, T.J., 2004. Identification and characterization of victorin sensitivity in Arabidopsis thaliana. Mol. Plant. Microbe. Interact. 17, 577–582.

Lorang, J.M., Hagerty, C.H., Lee, R., McClean, P.E., Wolpert, T.J., 2018. Genetic analysis of victorin sensitivity and identification of a causal nucleotide-binding site leucine-rich repeat gene in phaseolus vulgaris. Mol. Plant-Microbe Interact. 31, 1069–1074.

Lorang, J.M., Sweat, T. a, Wolpert, T.J., 2007. Plant disease susceptibility conferred by a "resistance" gene. Proc. Natl. Acad. Sci. U. S. A. 104, 14861–14866.

Losert, D., Maurer, H.P., Leiser, W.L., Würschum, T., 2017. Defeating the Warrior: genetic architecture of triticale resistance against a novel aggressive yellow rust race. Theor. Appl. Genet. 130, 685–696.

Loutre, C., Wicker, T., Travella, S., Galli, P., Scofield, S., Fahima, T., Feuillet, C., Keller, B., 2009. Two different CC-NBS-LRR genes are required for Lr10-mediated leaf rust resistance in tetraploid and hexaploid wheat. Plant J. 60, 1043–1054.

Löytynoja, A., 2014. Phylogeny-aware alignment with PRANK. Methods Mol. Biol. 1079, 155–170.

Lu, X., Kracher, B., Saur, I.M.L., Bauer, S., Ellwood, S.R., Wise, R., Yaeno, T., Maekawa, T., Schulze-Lefert, P., 2016. Allelic barley MLA immune receptors recognize sequence-unrelated avirulence effectors of the powdery mildew pathogen. Proc. Natl. Acad. Sci. U. S. A. 113, E6486–E6495.

Luo, M.C., Gu, Y.Q., Puiu, D., Wang, H., Twardziok, S.O., Deal, K.R., Huo, N., Zhu, T., Wang, L., Wang, Y., McGuire, P.E., Liu, S., Long, H., Ramasamy, R.K., Rodriguez, J.C., Van Sonny, L., Yuan, L., Wang, Z., Xia, Z., Xiao, L., Anderson, O.D., Ouyang, S., Liang, Y., Zimin, A. V., Pertea, G., Qi, P., Bennetzen, J.L., Dai, X., Dawson, M.W., Müller, H.G., Kugler, K., Rivarola-Duarte, L., Spannagl, M., Mayer, K.F.X., Lu, F.H., Bevan, M.W., Leroy, P., Li, P., You, F.M., Sun, Q., Liu, Z., Lyons, E., Wicker, T., Salzberg, S.L., Devos, K.M., Dvoák, J., 2017. Genome sequence of the progenitor of the wheat D genome Aegilops tauschii. Nature 551, 498–502.

Lutz, J., Hsam, S.L.K., Limpert, E., Zeller, F.J., 1995. Chromosomal location of powdery mildew resistance genes in triticum aestivum L. (common wheat). 2. genes pm2 and pm19 from aegi/ops squarrosa L. Heredity (Edinb). 74, 152–156.

Lynch, M., Conery, J.S., 2000. The evolutionary fate and consequences of duplicate genes. Science (80-.). 290, 1151–1155.

Lyngkjær, M.F., Newton, A.C., Atzema, J.L., Baker, S.J., 2000. The Barley mlo-gene: an

important powdery mildew resistance source. Agronomie 20, 745–756.

Ma, Y., Guo, H., Hu, L., Martinez, P.P., Moschou, P.N., Cevik, V., Ding, P., Duxbury, Z., Sarris, P.F., Jones, J.D.G., 2018. Distinct modes of derepression of an Arabidopsis immune receptor complex by two different bacterial effectors. Proc. Natl. Acad. Sci. U. S. A. 115, 10218–10227.

Maciel, J.L.N., Ceresini, P.C., Castroagudin, V.L., Zala, M., Kema, G.H.J., McDonald, B.A., 2014. Population structure and pathotype diversity of the wheat blast pathogen magnaporthe oryzae 25 years after its emergence in Brazil. Phytopathology 104, 95–107.

Mackey, D., Belkhadir, Y., Alonso, J.M., Ecker, J.R., Dangl, J.L., 2003. Arabidopsis RIN4 Is a Target of the Type III Virulence Effector AvrRpt2 and Modulates RPS2-Mediated Resistance. Cell 112, 379–389.

Mackey, D., Holt, B.F., Wiig, A., Dangl, J.L., 2002. RIN4 Interacts with Pseudomonas syringae Type III Effector Molecules and Is Required for RPM1-Mediated Resistance in Arabidopsis. Cell 108, 743–754.

Maekawa, T., Cheng, W., Spiridon, L.N., Töller, A., Lukasik, E., Saijo, Y., Liu, P., Shen, Q.H., Micluta, M.A., Somssich, I.E., Takken, F.L.W., Petrescu, A.J., Chai, J., Schulze-Lefert, P., 2011. Coiled-coil domain-dependent homodimerization of intracellular barley immune receptors defines a minimal functional module for triggering cell death. Cell Host Microbe 9, 187–199.

Maekawa, T., Kracher, B., Vernaldi, S., Van Themaat, E.V.L., Schulze-Lefert, P., 2012. Conservation of NLR-triggered immunity across plant lineages. Proc. Natl. Acad. Sci. U. S. A. 109, 20119–20123.

Mago, R., Zhang, P., Vautrin, S., Šimková, H., Bansal, U., Luo, M.-C., Rouse, M., Karaoglu, H., Periyannan, S., Kolmer, J., Jin, Y., Ayliffe, M.A., Bariana, H., Park, R.F., McIntosh, R., Doležel, J., Bergès, H., Spielmeyer, W., Lagudah, E.S., Ellis, J.G., Dodds, P.N., 2015. The wheat Sr50 gene reveals rich diversity at a cereal disease resistance locus. Nat. Plants 1, 15186.

Manamgoda, D.S., Cai, L., McKenzie, E.H.C., Crous, P.W., Madrid, H., Chukeatirote, E., Shivas, R.G., Tan, Y.P., Hyde, K.D., 2012. A phylogenetic and taxonomic re-evaluation of the Bipolaris - Cochliobolus - Curvularia Complex. Fungal Divers. 56, 131–144.

Maqbool, A., Saitoh, H., Franceschetti, M., Stevenson, C.E.M., Uemura, A., Kanzaki, H., Kamoun, S., Terauchi, R., Banfield, M.J., 2015. Structural basis of pathogen recognition by an integrated HMA domain in a plant NLR immune receptor. Elife 4, 1–24.

Marshall, J.S., Warrington, R., Watson, W., Kim, H.L., 2018. An introduction to

immunology and immunopathology. Allergy, Asthma Clin. Immunol. 14, 1–8.

Martin, G.B., Vicente, M.C., Tanksley, S.D., 1993. High-resolution linkage analysis and physical characterization of the Pto bacterial resistance locus in tomato. Mol. PLANT-MICROBE Interact.

Martinez de Ilarduya, O., Nombela, G., Hwang, C.-F., Williamson, V.M., Muñiz, M., Kaloshian, I., 2004. Rme1 is necessary for Mi-1-mediated resistance and acts early in the resistance pathway. Mol. Plant. Microbe. Interact. 17, 55–61.

Mascher, M., Gundlach, H., Himmelbach, A., Beier, S., Twardziok, S.O., Wicker, T., Radchuk, V., Dockter, C., Hedley, P.E., Russell, J., Bayer, M., Ramsay, L., Liu, H., Haberer, G., Zhang, X.Q., Zhang, Q., Barrero, R.A., Li, L., Taudien, S., Groth, M., Felder, M., Hastie, A., Šimková, H., Stanková, H., Vrána, J., Chan, S., Munõz-Amatriaín, M., Ounit, R., Wanamaker, S., Bolser, D., Colmsee, C., Schmutzer, T., Aliyeva-Schnorr, L., Grasso, S., Tanskanen, J., Chailyan, A., Sampath, D., Heavens, D., Clissold, L., Cao, S., Chapman, B., Dai, F., Han, Y., Li, H., Li, X., Lin, C., McCooke, J.K., Tan, C., Wang, P., Wang, S., Yin, S., Zhou, G., Poland, J.A., Bellgard, M.I., Borisjuk, L., Houben, A., Doleael, J., Ayling, S., Lonardi, S., Kersey, P., Langridge, P., Muehlbauer, G.J., Clark, M.D., Caccamo, M., Schulman, A.H., Mayer, K.F.X., Platzer, M., Close, T.J., Scholz, U., Hansson, M., Zhang, G., Braumann, I., Spannagl, M., Li, C., Waugh, R., Stein, N., 2017. A chromosome conformation capture ordered sequence of the barley genome. Nature 544, 427–433.

Mata-Pérez, C., Spoel, S.H., 2019. Thioredoxin-mediated redox signalling in plant immunity. Plant Sci. 279, 27–33.

Matsumoto, S., Mogi, S., 1979. Ear blast disease of late-summer sown barley. Proc. Assoc. Plant Prot. Kyushu v. 25.

Mayama, S., Bordin, A., Morikawa, T., Tanpo, H., Kato, H., 1995. Association of avenalumin accumulation with co-segregation of victorin sensitivity and crown rust resistance in oat lines carrying the *Pc-2* gene. Physiol. Mol. Plant Pathol.

Mayer, K.F.X., Waugh, R., Langridge, P., Close, T.J., Wise, R.P., Graner, A., Matsumoto, T., Sato, K., Schulman, A., Muehlbauer, G.J., Stein, N., Ariyadasa, R., Schulte, D., Poursarebani, N., Zhou, R., Steuernagel, B., Mascher, M., Scholz, U., Shi, B., Langridge, P., Madishetty, K., Svensson, J.T., Bhat, P., Moscou, M., Resnik, J., Close, T.J., Muehlbauer, G.J., Hedley, P., Liu, H., Morris, J., Waugh, R., Frenkel, Z., Korol, A., Bergès, H., Graner, A., Stein, N., Steuernagel, B., Scholz, U., Taudien, S., Felder, M., Groth, M., Platzer, M., Stein, N., Steuernagel, B., Scholz, U., Himmelbach, A., Taudien, S., Felder, M., Platzer, M., Lonardi, S., Duma, D., Alpert, M., Cordero, F., Beccuti, M., Ciardo, G., Ma, Y., Wanamaker, S., Close, T.J., Stein, N., Cattonaro, F., Vendramin, V., Scalabrin, S., Radovic, S., Wing, R., Schulte, D., Steuernagel, B.,

Morgante, M., Stein, N., Waugh, R., Nussbaumer, T., Gundlach, H., Martis, M., Ariyadasa, R., Poursarebani, N., Steuernagel, B., Scholz, U., Wise, R.P., Poland, J., Stein, N., Mayer, K.F.X., Spannagl, M., Pfeifer, M., Gundlach, H., Mayer, K.F.X., Gundlach, H., Moisy, C., Tanskanen, J., Scalabrin, S., Zuccolo, A., Vendramin, V., Morgante, M., Mayer, K.F.X., Schulman, A., Pfeifer, M., Spannagl, M., Hedley, P., Morris, J., Russell, J., Druka, A., Marshall, D., Bayer, M., Swarbreck, D., Sampath, D., Ayling, S., Febrer, M., Caccamo, M., Matsumoto, T., Tanaka, T., Sato, K., Wise, R.P., Close, T.J., Wannamaker, S., Muehlbauer, G.J., Stein, N., Mayer, K.F.X., Waugh, R., Steuernagel, B., Schmutzer, T., Mascher, M., Scholz, U., Taudien, S., Platzer, M., Sato, K., Marshall, D., Bayer, M., Waugh, R., Stein, N., Mayer, K.F.X., Waugh, R., Brown, J.W.S., Schulman, A., Langridge, P., Platzer, M., Fincher, G.B., Muehlbauer, G.J., Sato, K., Close, T.J., Wise, R.P., Stein, N., 2012. A physical, genetic and functional sequence assembly of the barley genome. Nature 491, 711–716.

McDowell, J.M., 2004. Convergent evolution of disease resistance genes. Trends Plant Sci. 9, 315–317.

McDowell, J.M., Dhandaydham, M., Long, T.A., Aarts, M.G.M., Goff, S., Holub, E.B., Dangl, J.L., 1998. Intragenic recombination and diversifying selection contribute to the evolution of downy mildew resistance at the RPP8 locus of arabidopsis. Plant Cell 10, 1861–1874.

McDowell, J.M., Simon, S.A., 2006. Recent insights into R gene evolution. Mol. Plant Pathol. 7, 437–448.

McIntosh, R.A., 1992. Close genetic linkage of genes conferring adult-plant resistance to leaf rust and stripe rust in wheat. Plant Pathol. 41, 523–527.

McKain, M.R., Tang, H., McNeal, J.R., Ayyampalayam, S., Davis, J.I., Depamphilis, C.W., Givnish, T.J., Chris Pires, J., Stevenson, D.W., Leebens-Mack, J.H., 2016. A phylogenomic assessment of ancient polyploidy and genome evolution across the poales. Genome Biol. Evol. 8, 1150–1164.

Meehan, F., Murphy, H.C., 1946. A New Helminthosporium Blight of Oats. Science (80-.). 413–414.

Meinke, D.W., Cherry, J.M., Dean, C., Rounsley, S.D., Koornneef, M., 1998. Arabidopsis thaliana: A model plant for genome analysis. Science (80-.). 282.

Mengiste, T., 2012. Plant Immunity to Necrotrophs. Annu. Rev. Phytopathol. 50, 267–294.

Meyerowitz, E.M., Somerville, C.R., 1994. Arabidopsis. Cold Spring Harb. Monogr. Ser.

Meyers, B.C., Kozik, A., Griego, A., Kuang, H., Michelmore, R.W., 2003. Genome-wide analysis of NBS-LRR – encoding genes in Arabidopsis. Plant Cell 15, 809–834.

Michelmore, R.W., Meyers, B.C., 1998. Clusters of resistance genes in plants evolve by divergent selection and a birth-and-death process. Genome Res. 8, 1113–1130.

Milligan, S.B., Bodeau, J., Yaghoobi, J., Kaloshian, I., Zabel, P., Williamson, V.M., 1998. The root knot nematode resistance gene Mi from tomato is a member of the leucine zipper, nucleotide binding, leucine-rich repeat family of plant genes. Plant Cell 10, 1307–1319.

Milne, R.J., Dibley, K.E., Schnippenkoetter, W., Mascher, M., Lui, A.C.W., Wang, L., Lo, C., Ashton, A.R., Ryan, P.R., Lagudah, E.S., 2019. The wheat LR67 gene from the sugar transport protein 13 family confers multipathogen resistance in barley. Plant Physiol. 179, 1285–1297.

Miya, A., Albert, P., Shinya, T., Desaki, Y., Ichimura, K., Shirasu, K., Narusaka, Y., Kawakami, N., Kaku, H., Shibuya, N., 2007. CERK1, a LysM receptor kinase, is essential for chitin elicitor signaling in Arabidopsis. Proc. Natl. Acad. Sci. U. S. A. 104, 19613–19618.

Mondragón-Palomino, M., Meyers, B.C., Michelmore, R.W., Gaut, B.S., 2002. Patterns of positive selection in the complete NBS-LRR gene family of Arabidopsis thaliana. Genome Res. 12, 1305–1315.

Monosi, B., Wisser, R.J., Pennill, L., Hulbert, S.H., 2004. Full-genome analysis of resistance gene homologues in rice. Theor. Appl. Genet. 109, 1434–1447.

Monteiro, F., Nishimura, M.T., 2018. Structural, Functional, and Genomic Diversity of Plant NLR Proteins: An Evolved Resource for Rational Engineering of Plant Immunity. Annu. Rev. Phytopathol. 56, 243–267.

Moore, J.W., Herrera-Foessel, S., Lan, C., Schnippenkoetter, W., Ayliffe, M., Huerta-Espino, J., Lillemo, M., Viccars, L., Milne, R., Periyannan, S., Kong, X., Spielmeyer, W., Talbot, M., Bariana, H., Patrick, J.W., Dodds, P., Singh, R., Lagudah, E., 2015. A recently evolved hexose transporter variant confers resistance to multiple pathogens in wheat. Nat. Genet. 47, 1494–1498.

Moscou, M.J., Bogdanove, A.J., 2009. Recognition by TAL Effectors. Science 326, 1501.

Moscou, M.J., Lauter, N., Caldo, R. a, Nettleton, D., Wise, R.P., 2011. Quantitative and temporal definition of the Mla transcriptional regulon during barley-powdery mildew interactions. Mol. Plant. Microbe. Interact. 24, 694–705.

Moseman, J.G., Reid, D.A., 1961. Linkage Relationship of Genes Conditioning Resistance to Leaf Rust and Powdery Mildew in Franger Barley1. Crop Sci. 1, 425.

Muñoz-Amatriaín, M., Eichten, S.R., Wicker, T., Richmond, T.A., Mascher, M., Steuernagel, B., Scholz, U., Ariyadasa, R., Spannagl, M., Nussbaumer, T., Mayer, K.F.X., Taudien, S., Platzer, M., Jeddeloh, J.A., Springer, N.M., Muehlbauer, G.J., Stein, N., 2013. Distribution, functional impact, and origin mechanisms of copy number variation in the barley genome. Genome Biol. 14, 1–17.

Muñoz-Amatriaín, M., Moscou, M.J., Bhat, P.R., Svensson, J.T., Bartoš, J., Suchánková, P.,

Šimková, H., Endo, T.R., Fenton, R.D., Lonardi, S., Castillo, A.M., Chao, S., Cistué, L., Cuesta-Marcos, A., Forrest, K.L., Hayden, M.J., Hayes, P.M., Horsley, R.D., Makoto, K., Moody, D., Sato, K., Vallés, M.P., Wulff, B.B., Muehlbauer, G.J., Doležel, J., Close, T.J., 2011. An Improved Consensus Linkage Map of Barley Based on Flow-Sorted Chromosomes and Single Nucleotide Polymorphism Markers. Plant Genome J. 4, 238.

Nagy, E.D., Bennetzen, J.L., 2008. Pathogen corruption and site-directed recombination at a plant disease resistance gene cluster. Genome Res. 18, 1918–1923.

Nagy, E.D., Lee, T.C., Ramakrishna, W., Xu, Z., Klein, P.E., SanMiguel, P., Cheng, C.P., Li, J., Devos, K.M., Schertz, K., Dunkle, L., Bennetzen, J.L., 2007. Fine mapping of the Pc locus of Sorghum bicolor, a gene controlling the reaction to a fungal pathogen and its host-selective toxin. Theor. Appl. Genet. 114, 961–970.

Narusaka, M., Iuchi, S., Narusaka, Y., 2017. Analyses of natural variation indicates that the absence of RPS4/RRS1 and amino acid change in RPS4 cause loss of their functions and resistance to pathogens. Plant Signal. Behav. 12, 1–8.

Narusaka, M., Kubo, Y., Hatakeyama, K., Imamura, J., Ezura, H., Nanasato, Y., Tabei, Y., Takano, Y., Shirasu, K., Narusaka, Y., 2013. Interfamily Transfer of Dual NB-LRR Genes Confers Resistance to Multiple Pathogens. PLoS One 8, 6–13.

Narusaka, M., Shirasu, K., Noutoshi, Y., Kubo, Y., Shiraishi, T., Iwabuchi, M., Narusaka, Y., 2009. RRS1 and RPS4 provide a dual Resistance-gene system against fungal and bacterial pathogens. Plant J. 60, 218–226.

Nasrallah, J.B., 2002. Recognition and rejection of self in plant reproduction. Science (80-.). 296, 305–308.

Nasrallah, J.B., 2017. Plant mating systems: self-incompatibility and evolutionary transitions to self-fertility in the mustard family. Curr. Opin. Genet. Dev. 47, 54–60.

Newton, A.C., Flavell, A.J., George, T.S., Leat, P., Mullholland, B., Ramsay, L., Revoredo-Giha, C., Russell, J., Steffenson, B.J., Swanston, J.S., Thomas, W.T.B., Waugh, R., White, P.J., Bingham, I.J., 2011. Crops that feed the world 4. Barley: a resilient crop? Strengths and weaknesses in the context of food security. Food Secur. 3, 141–178.

Nga, N.T.T., Inoue, Y., Chuma, I., Hyon, G.-S., Okada, K., Vy, T.T.P., Kusaba, M., Tosa, Y., 2012. Identification of a novel locus Rmo2 conditioning resistance in barley to host-specific subgroups of Magnaporthe oryzae. Phytopathology 102, 674–82.

Nicaise, V., Roux, M., Zipfel, C., 2009. Recent advances in PAMP-triggered immunity against bacteria: pattern recognition receptors watch over and raise the alarm. Plant Physiol. 150, 1638–47.

Nishijima, R., Yoshida, K., Motoi, Y., Sato, K., Takumi, S., 2016. Genome-wide identification of novel genetic markers from RNA sequencing assembly of diverse

Aegilops tauschii accessions. Mol. Genet. Genomics 291, 1681–1694.

Nishimura, M.T., Monteiro, F., Dangl, J.L., 2015. Treasure your exceptions: Unusual domains in immune receptors reveal host virulence targets. Cell 161, 957–960.

Noël, L., Moores, T.L., Van Der Biezen, E.A., Parniske, M., Daniels, M.J., Parker, J.E., Jones, J.D.G., 1999. Pronounced intraspecific haplotype divergence at the RPP5 complex disease resistance locus of Arabidopsis. Plant Cell 11, 2099–2111.

Nombela, G., Williamson, V.M., Muñiz, M., 2003. The root-knot nematode resistance gene Mi-1.2 of tomato is responsible for resistance against the whitefly Bemisia tabaci. Mol. Plant. Microbe. Interact. 16, 645–649.

NordGen, n.d. International Database for Barley Genes and Barley Genetic Stocks [WWW Document]. URL www.nordgen.org

Okuyama, Y., Kanzaki, H., Abe, A., Yoshida, K., Tamiru, M., Saitoh, H., Fujibe, T., Matsumura, H., Shenton, M., Galam, D.C., Undan, J., Ito, A., Sone, T., Terauchi, R., 2011. A multifaceted genomics approach allows the isolation of the rice Pia-blast resistance gene consisting of two adjacent NBS-LRR protein genes. Plant J. 66, 467–479.

Oldroyd, G.E.D., Staskawicz, B.J., 1998. Genetically engineered broad-spectrum disease resistance in tomato. Proc. Natl. Acad. Sci. U. S. A. 95, 10300–10305.

Ostertag, M., Stammler, J., Douchkov, D., Eichmann, R., Hückelhoven, R., 2013. The conserved oligomeric Golgi complex is involved in penetration resistance of barley to the barley powdery mildew fungus. Mol. Plant Pathol. 14, 230–240.

Parker, D., Beckmann, M., Enot, D.P., Overy, D.P., Rios, Z.C., Gilbert, M., Talbot, N., Draper, J., 2008. Rice blast infection of Brachypodium distachyon as a model system to study dynamic host/pathogen interactions. Nat. Protoc. 3, 435–445.

Paulus, J.K., van der Hoorn, R.A.L., 2018. Tricked or trapped—Two decoy mechanisms in host–pathogen interactions. PLoS Pathog. 14, 1–6.

Pedersen, C., van Themaat, E.V.L., McGuffin, L.J., Abbott, J.C., Burgis, T.A., Barton, G., Bindschedler, L. V., Lu, X., Maekawa, T., Weßling, R., Cramer, R., Thordal-Christensen, H., Panstruga, R., Spanu, P.D., 2012. Structure and evolution of barley powdery mildew effector candidates. BMC Genomics 13.

Pedley, K.F., Martin, G.B., 2003. M Olecular B Asis of P To -M Ediated R Esistance To B Acterial S Peck D Isease in T Omato . Annu. Rev. Phytopathol. 41, 215–243.

Pennington, H.G., Jones, R., Kwon, S., Bonciani, G., Thieron, H., Chandler, T., Luong, P., Morgan, S.N., Przydacz, M., Bozkurt, T., Bowden, S., Craze, M., Wallington, E.J., Garnett, J., Kwaaitaal, M., Panstruga, R., Cota, E., Spanu, P.D., 2019. The fungal ribonuclease-like effector protein CSEP0064/BEC1054 represses plant immunity and interferes with degradation of host ribosomal RNA, PLoS Pathogens.

Periyannan, S., Moore, J., Ayliffe, M., Bansal, U., Wang, X., Huang, L., Deal, K., Luo, M., Kong, X., Bariana, H., Mago, R., McIntosh, R., Dodds, P., Dvorak, J., Lagudah, E., 2013. The Gene Sr33, an Ortholog of Barley Mla Genes, Encodes Resistance to Wheat Stem Rust Race Ug99. Science (80-.). 786, 1–5.

Pliego, C., Nowara, D., Bonciani, G., Gheorghe, D.M., Xu, R., Surana, P., Whigham, E., Nettleton, D., Bogdanove, A.J., Wise, R.P., Schweizer, P., Bindschedler, L. V, Spanu, P.D., 2013. Host-induced gene silencing in barley powdery mildew reveals a class of ribonuclease-like effectors. Mol. Plant. Microbe. Interact. 26, 633–42.

Pretorius, Z.A., Singh, R.P., Wagoire, W.W., Payne, T.S., 2000. Detection of Virulence to Wheat Stem Rust Resistance Gene Sr31 in Puccinia graminis. f. sp. tritici in Uganda. Plant Dis. 84, 203.

Puri, K.D., Shrestha, S.M., Khhatri Chhetri, G.B., Joshi, K.D., 2009. Leaf and neck blast resistance reaction in tropical rice lines under green house condition. Euphytica 165, 523–532.

Qi, D., de Young, B.J., Innes, R.W., 2012. Structure-function analysis of the coiled-coil and leucine-rich repeat domains of the RPS5 disease resistance protein. Plant Physiol. 158, 1819–1832.

Ravensdale, M., Nemri, A., Thrall, P.H., Ellis, J.G., Dodds, P.N., 2011. Co-evolutionary interactions between host resistance and pathogen effector genes in flax rust disease. Mol. Plant Pathol.

Rehmany, A.P., Gordon, A., Rose, L.E., Allen, R.L., Armstrong, M.R., Whisson, S.C., Kamoun, S., Tyler, B.M., Birch, P.R.J., Beynon, J.L., 2005. Differential recognition of highly divergent downy mildew avirulence gene alleles by RPP1 resistance genes from two Arabidopsis lines. Plant Cell 17, 1839–1850.

Reichheld, J.P., Mestres-Ortega, D., Laloi, C., Meyer, Y., 2002. The multigenic family of thioredoxin h in Arabidopsis thaliana: Specific expression and stress response. In: Plant Physiology and Biochemistry. pp. 685–690.

Richardson, K.L., Vales, M.I., Kling, J.G., Mundt, C.C., Hayes, P.M., 2006. Pyramiding and dissecting disease resistance QTL to barley stripe rust. Theor. Appl. Genet. 113, 485–495.

Rinaldo, A., Gilbert, B., Boni, R., Krattinger, S.G., Singh, D., Park, R.F., Lagudah, E., Ayliffe, M., 2017. The Lr34 adult plant rust resistance gene provides seedling resistance in durum wheat without senescence. Plant Biotechnol. J. 15, 894–905.

Risk, J.M., Selter, L.L., Chauhan, H., Krattinger, S.G., Kumlehn, J., Hensel, G., Viccars, L.A., Richardson, T.M., Buesing, G., Troller, A., Lagudah, E.S., Keller, B., 2013. The wheat Lr34 gene provides resistance against multiple fungal pathogens in barley. Plant Biotechnol. J. 11, 847–854.

Römer, P., Hahn, S., Jordan, T., Strauß, T., Bonas, U., Lahaye, T., 2007. Plant pathogen recognition mediated by promoter activation of the pepper Bs3 resistance gene. Science (80-.). 318, 645–648.

Römer, P., Recht, S., Lahaye, T., 2009. A single plant resistance gene promoter engineered to recognize multiple TAL effectors from disparate pathogens. Proc. Natl. Acad. Sci. U. S. A. 106, 20526–20531.

Rose, L.E., Bittner-Eddy, P.D., Langley, C.H., Holub, E.B., Michelmore, R.W., Beynon, J.L., 2004. The Maintenance of Extreme Amino Acid Diversity at the Disease Resistance Gene, RPP13, in Arabidopsis thaliana. Genetics 166, 1517–1527.

Rose, L.E., Michelmore, R.W., Langley, C.H., 2007. Natural variation in the Pto disease resistance gene within species of wild tomato (Lycopersicon). II. Population genetics of Pto. Genetics 175, 1307–1319.

Roy, J.K., Smith, K.P., Muehlbauer, G.J., Chao, S., Close, T.J., Steffenson, B.J., 2010. Association mapping of spot blotch resistance in wild barley. Mol. Breed. 26, 243–256.

Russell, A.R., Ashfield, T., Innes, R.W., 2015. Pseudomonas syringae effector AvrPphB suppresses AvrB-induced activation of RPM1 but not AvrRpm1-induced activation. Mol. Plant-Microbe Interact. 28, 727–735.

Rustérucci, C., Aviv, D.H., Holt, B.F., Dangl, J.L., Parker, J.E., 2001. The Disease Resistance Signaling Components *EDS1* and *PAD4* Are Essential Regulators of the Cell Death Pathway Controlled by *LSD1* in Arabidopsis. Plant Cell 13, 2211–2224.

Salas, B., Steffenson, B.J., Casper, H.H., Tacke, B., Prom, L.K., Fetch, T.G., Schwarz, P.B., 1999. Fusarium species pathogenic to barley and their associated mycotoxins. Plant Dis. 83, 667–674.

Sandoval-Islas, J.S., Broers, L.H.M., Mora-Aguilera, G., Parlevliet, J.E., Osada-Kawasoe, S., Vivar, H.E., 2007. Quantitative resistance and its components in 16 barley cultivars to yellow rust, Puccinia striiformis f. sp. hordei. Euphytica 153, 295–308.

Sarris, P.F., Cevik, V., Dagdas, G., Jones, J.D.G., Krasileva, K. V., 2016. Comparative analysis of plant immune receptor architectures uncovers host proteins likely targeted by pathogens. BMC Biol. 14, 8.

Sarris, P.F., Duxbury, Z., Huh, S.U., Ma, Y., Segonzac, C., Sklenar, J., Derbyshire, P., Cevik, V., Rallapalli, G., Saucet, S.B., Wirthmueller, L., Menke, F.L.H., Sohn, K.H., Jones, J.D.G., 2015. A Plant Immune Receptor Detects Pathogen Effectors that Target WRKY Transcription Factors. Cell 161, 1089–1100.

Sato, K., Inukai, T., Hayes, P.M., 2001. QTL analysis of resistance to the rice blast pathogen in barley (Hordeum vulgare). Theor.Appl.Genet. 102, 916–920.

Saucet, S.B., Ma, Y., Sarris, P.F., Furzer, O.J., Sohn, K.H., Jones, J.D.G., 2015. Two linked pairs of Arabidopsis TNL resistance genes independently confer recognition of

bacterial effector AvrRps4. Nat. Commun. 6, 1–12.

Saur, I.M.L., Bauer, S., Kracher, B., Lu, X., Franzeskakis, L., Müller, M.C., Sabelleck, B., Kümmel, F., Panstruga, R., Maekawa, T., Schulze-Lefert, P., 2019. Multiple pairs of allelic MLA immune receptor-powdery mildew AVR a effectors argue for a direct recognition mechanism. Elife 8, 1–31.

Savary, S., Ficke, A., Aubertot, J.N., Hollier, C., 2012. Crop losses due to diseases and their implications for global food production losses and food security. Food Secur.

Savary, S., Willocquet, L., Pethybridge, S.J., Esker, P., McRoberts, N., Nelson, A., 2019. The global burden of pathogens and pests on major food crops. Nat. Ecol. Evol. 3, 430–439.

Schindelin, J., Arganda-Carreras, I., Frise, E., Kaynig, V., Longair, M., Pietzsch, T., Preibisch, S., Rueden, C., Saalfeld, S., Schmid, B., Tinevez, J.Y., White, D.J., Hartenstein, V., Eliceiri, K., Tomancak, P., Cardona, A., 2012. Fiji: An open-source platform for biological-image analysis. Nat. Methods 9, 676–682.

Schornack, S., Meyer, A., Römer, P., Jordan, T., Lahaye, T., 2006. Gene-for-gene-mediated recognition of nuclear-targeted AvrBs3-like bacterial effector proteins. J. Plant Physiol. 163, 256–272.

Schweizer, P., Stein, N., Pflanzengenetik, L., Gatersleben, D.-, 2011. Large-Scale Data Integration Reveals Colocalization of Gene Functional Groups with Meta-QTL for Multiple Disease Resistance in Barley 24, 1492–1501.

Scofield, S.R., Tobias, C.M., Rathjen, J.P., Chang, J.H., Lavelle, D.T., Michelmore, R.W., Staskawicz, B.J., 1996. Molecular basis of gene-for-gene specificity in bacterial speck disease of tomato. Science (80-.). 274, 2063–2065.

Seeholzer, S., Tsuchimatsu, T., Jordan, T., Bieri, S., Pajonk, S., Yang, W., Jahoor, A., Shimizu, K.K., Keller, B., Schulze-Lefert, P., 2010. Diversity at the Mla powdery mildew resistance locus from cultivated barley reveals sites of positive selection. Mol. Plant. Microbe. Interact. 23, 497–509.

Ségurel, L., Thompson, E.E., Flutre, T., Lovstad, J., Venkat, A., Margulis, S.W., Moyse, J., Ross, S., Gamble, K., Sella, G., Ober, C., Przeworski, M., 2013. Erratum: The ABO blood group is a trans-species polymorphism in primates (Proceedings of the National Academy of Sciences of the United States of America (2012) 109 (18493-18498) DOI: 10.1073/pnas.1210603109). Proc. Natl. Acad. Sci. U. S. A. 110, 6607.

Sekereš, J., Pejchar, P., Šantrůček, J., Vukasinovic, N., Žárský, V., Potocký, M., 2017. Analysis of exocyst subunit EXO70 family reveals distinct membrane polar domains in Tobacco pollen tubes. Plant Physiol. 173, 1659–1675.

Sela, H., Loutre, C., Keller, B., Schulman, A., Nevo, E., Korol, A., Fahima, T., 2011. Rapid linkage disequilibrium decay in the Lr10 gene in wild emmer wheat (Triticum

dicoccoides) populations. Theor. Appl. Genet. 122, 175–187.

Sela, H., Spiridon, L.N., Petrescu, A.J., Akerman, M., Mandel-Gutfreund, Y., Nevo, E., Loutre, C., Keller, B., Schulman, A.H., Fahima, T., 2012. Ancient diversity of splicing motifs and protein surfaces in the wild emmer wheat (Triticum dicoccoides) LR10 coiled coil (CC) and leucine-rich repeat (LRR) domains. Mol. Plant Pathol. 13, 276–287.

Shang, J., Tao, Y., Chen, X., Zou, Y., Lei, C., Wang, J., Li, X., Zhao, X., Zhang, M., Lu, Z., Xu, J., Cheng, Z., Wan, J., Zhu, L., 2009. Identification of a new rice blast resistance gene, Pid3, by genomewide comparison of paired nucleotide-binding site-leucine-rich repeat genes and their pseudogene alleles between the two sequenced rice genomes. Genetics 182, 1303–1311.

Sharma, T.R., Rai, a. K., Gupta, S.K., Vijayan, J., Devanna, B.N., Ray, S., 2012. Rice Blast Management Through Host-Plant Resistance: Retrospect and Prospects. Agric. Res. 1, 37–52.

Shen, Q.-H., Zhou, F., Bieri, S., Haizel, T., Shirasu, K., Schulze-Lefert, P., 2003. Recognition Specificity and RAR1/SGT1 Dependence in Barley Mla Disease Resistance Genes to the Powdery Mildew Fungus. Plant Cell 15, 732–744.

Shen, Q., Saijo, Y., Mauch, S., Biskup, C., Bieri, S., Keller, B., Seki, H., Ülker, B., Somssich, I.E., Schulze-lefert, P., 2007. Nuclear Activity of MLA Immune Receptors Links Isolate-Specific and Basal Disease-Resistance Responses. Science (80-.). 315, 1098–1103.

Shirasu, K., Lahaye, T., Tan, M.W., Zhou, F., Azevedo, C., Schulze-Lefert, P., 1999. A novel class of eukaryotic zinc-binding proteins is required for disease resistance signaling in barley and development in C. elegans. Cell 99, 355–366.

Simão, F.A., Waterhouse, R.M., Ioannidis, P., Kriventseva, E. V., Zdobnov, E.M., 2015. BUSCO: Assessing genome assembly and annotation completeness with single-copy orthologs. Bioinformatics 31, 3210–3212.

Singh, R.P., Hodson, D.P., Huerta-Espino, J., Jin, Y., Bhavani, S., Njau, P., Herrera-Foessel, S., Singh, P.K., Singh, S., Govindan, V., 2011. The Emergence of Ug99 Races of the Stem Rust Fungus is a Threat to World Wheat Production. Annu. Rev. Phytopathol. 49, 465–481.

Singh, R.P., Hodson, D.P., Jin, Y., Lagudah, E.S., Ayliffe, M.A., Bhavani, S., Rouse, M.N., Pretorius, Z.A., Szabo, L.J., Huerta-Espino, J., Basnet, B.R., Lan, C., Hovmøller, M.S., 2015. Emergence and spread of new races of wheat stem rust fungus: Continued threat to food security and prospects of genetic control. Phytopathology 105, 872–884.

Singh, R.P., Singh, P.K., Rutkoski, J., Hodson, D.P., He, X., Jørgensen, L.N., Hovmøller, M.S., Huerta-Espino, J., 2016. Disease Impact on Wheat Yield Potential and Prospects

of Genetic Control. Annu. Rev. Phytopathol. 54, 303–322.

Smedley, M.A., Harwood, W.A., 2015. Gateway®-compatible plant transformation vectors. Methods Mol. Biol. 1223, 3–16.

Smit, A.F.A., Hubley, R., Green, P., n.d. RepeatMasker Open-4.0. 2013-2015.

Sohn, K.H., Segonzac, C., Rallapalli, G., Sarris, P.F., Woo, J.Y., Williams, S.J., Newman, T.E., Paek, K.H., Kobe, B., Jones, J.D.G., 2014. The Nuclear Immune Receptor RPS4 Is Required for RRS1SLH1-Dependent Constitutive Defense Activation in Arabidopsis thaliana. PLoS Genet. 10.

Solanki, S., Richards, J., Ameen, G., Wang, X., Khan, A., Ali, H., Stangel, A., Tamang, P., Gross, T., Gross, P., Fetch, T.G., Brueggeman, R.S., 2019. Characterization of genes required for both Rpg1 and rpg4-mediated wheat stem rust resistance in barley. BMC Genomics 20, 1–16.

Song, Z., Bakeer, W., Marshall, J.W., Yakasai, A.A., Khalid, R.M., Collemare, J., Skellam, E., Tharreau, D., Lebrun, M.H., Lazarus, C.M., Bailey, A.M., Simpson, T.J., Cox, R.J., 2015. Heterologous expression of the avirulence gene ACE1 from the fungal rice pathogen Magnaporthe oryzae. Chem. Sci. 6, 4837–4845.

Spanu, P.D., 2017. Cereal immunity against powdery mildews targets RNase-Like Proteins associated with Haustoria (RALPH) effectors evolved from a common ancestral gene. New Phytol. 213, 969–971.

Spanu, P.D., Abbott, J.C., Amselem, J., Burgis, T.A., Soanes, D.M., Stüber, K., Ver Loren van Themaat, E., Brown, J.K.M., Butcher, S. a, Gurr, S.J., Lebrun, M., Ridout, C.J., Schulze-lefert, P., Talbot, N.J., Ahmadinejad, N., Ametz, C., Barton, G.R., Benjdia, M., Bidzinski, P., Bindschedler, L. V, Both, M., Brewer, M.T., Cadle-davidson, L., Cadle-Davidson, M.M., Collemare, J., Cramer, R., Frenkel, O., Godfrey, D., Harriman, J., Hoede, C., King, B.C., Klages, S., Kleemann, J., Knoll, D., Koti, P.S., Kreplak, J., López-Ruiz, F.J., Lu, X., Maekawa, T., Mahanil, S., Micali, C., Milgroom, M.G., Montana, G., Noir, S., O'Connell, R.J., Oberhaensli, S., Parlange, F., Pedersen, C., Quesneville, H., Reinhardt, R., Rott, M., Sacristán, S., Schmidt, S.M., Schön, M., Skamnioti, P., Sommer, H., Stephens, A., Takahara, H., Thordal-Christensen, H., Vigouroux, M., Wessling, R., Wicker, T., Panstruga, R., 2010. Genome Expansion and Gene Loss in. Science (80-.). 330, 1543–1546.

Spielmeyer, W., McIntosh, R.A., Kolmer, J., Lagudah, E.S., 2005. Powdery mildew resistance and Lr34/Yr18 genes for durable resistance to leaf and stripe rust cosegregate at a locus on the short arm of chromosome 7D of wheat. Theor. Appl. Genet. 111, 731–735.

St.Clair, D.A., 2010. Quantitative Disease Resistance and Quantitative Resistance Loci in Breeding. Annu. Rev. Phytopathol. 48, 247–268.

Staal, J., Kaliff, M., Dewaele, E., Persson, M., Dixelius, C., 2008. RLM3, a TIR domain encoding gene involved in broad-range immunity of Arabidopsis to necrotrophic fungal pathogens. Plant J. 55, 188–200.

Stahl, E.A., Dwyer, G., Mauricio, R., Kreitman, M., Bergelson, J., 1999. Dynamics of disease resistance polymorphism at the Rpm1 locus of Arabidopsis. Nature 400, 667–671.

Stamatakis, A., Ludwig, T., Meier, H., 2005. RAxML-III: a fast program for maximum likelihood-based inference of large phylogenetic trees. Bioinformatics 21, 456–463.

Steffenson, B.J., 2003. Fusarium head blight of barley : impact, epidemics, management, and strategies for identifying and utilizing genetic resistance. Fusarium Head Blight Wheat Barley.

Stegmann, M., Anderson, R.G., Westphal, L., Rosahl, S., McDowell, J.M., Trujillo, M., 2014. The exocyst subunit Exo70B1 is involved in the immune response of Arabidopsis thaliana to different pathogens and cell death. Plant Signal. Behav. 8.

Stein, M., Dittgen, J., Sánchez-Rodríguez, C., Hou, B.H., Molina, A., Schulze-Lefert, P., Lipka, V., Somerville, S., 2006. Arabidopsis PEN3/PDR8, an ATP binding cassette transporter, contributes to nonhost resistance to inappropriate pathogens that enter by direct penetration. Plant Cell 18, 731–746.

Stewart, C.N.J., Via, L.E., 1993. A rapid CTAB DNA isolation technique useful for RAPD fingerprinting and other PCR applications. Biotechniques 748–750.

Stirnweis, D., Milani, S.D., Brunner, S., Herren, G., Buchmann, G., Peditto, D., Jordan, T., Keller, B., 2014. Suppression among alleles encoding nucleotide-binding-leucine-rich repeat resistance proteins interferes with resistance in F1 hybrid and allele-pyramided wheat plants. Plant J. 79, 893–903.

Stubbs, R.I.W., Prescott, J.M., Saari, E.E., Dubin, H.J., 1986. Cereal Disease Methodology Manual. International Maize and Wheat Improvement Center (CIMMYT).

Stubbs, R.W., 1985. Stripe Rust. In: Diseases, Distribution, Epidemiology, and Control. Elsevier, pp. 61–101.

Stukenbrock, E.H., McDonald, B.A., 2009. Population genetics of fungal and oomycete effectors involved in gene-for-gene interactions. Mol. Plant-Microbe Interact. 22, 371–380.

Sukarta, O.C.A., Slootweg, E.J., Goverse, A., 2016. Structure-informed insights for NLR functioning in plant immunity. Semin. Cell Dev. Biol. 56, 134–149.

Sweat, T. a, Lorang, J.M., Bakker, E.G., Wolpert, T.J., 2008. Characterization of Natural and Induced Variation in {theLOV1Gene,} a {CC-NB-LRR} Gene Conferring Victorin Sensitivity and Disease Susceptibility {inArabidopsis}. Mol. {Plant-Microbe} Interact. 21, 7–19.

Sweat, T. a, Wolpert, T.J., 2007. Thioredoxin h5 is required for victorin sensitivity mediated by a CC-NBS-LRR gene in Arabidopsis. Plant Cell 19, 673–687.

Sweigard, J.A., Carroll, A.M., Kang, S., Farrall, L., Chumley, F.G., Valent, B., 1995. Identification, Cloning, and Characterization of 7, 1221–1233.

Synek, L., Schlager, N., Eliáš, M., Quentin, M., Hauser, M.T., Žárský, V., 2006. AtEXO70A1, a member of a family of putative exocyst subunits specifically expanded in land plants, is important for polar growth and plant development. Plant J. 48, 54–72.

Takabatake, R., Seo, S., Mitsuhara, I., Tsuda, S., Ohashi, Y., 2006. Accumulation of the two transcripts of the N gene, conferring resistance to tobacco mosaic virus, is probably important for N gene-dependent hypersensitive cell death. Plant Cell Physiol. 47, 254–261.

Takahashi, H., Miller, J., Nozaki, Y., Sukamto, Takeda, M., Shah, J., Hase, S., Ikegami, M., Ehara, Y., Dinesh-Kumar, S.P., 2002. RCY1, an Arabidopsis thaliana RPP8/HRT family resistance gene, conferring resistance to cucumber mosaic virus requires salicylic acid, ethylene and a novel signal transduction mechanism. Plant J. 32, 655–667.

Takken, F.L., Albrecht, M., Tameling, W. IL, 2006. Resistance proteins: molecular switches of plant defence. Curr. Opin. Plant Biol. 9, 383–390.

Takken, F.L.W., Goverse, A., 2012. How to build a pathogen detector: Structural basis of NB-LRR function. Curr. Opin. Plant Biol. 15, 375–384.

Talbot, N.J., 2003. On the trail of a cereal killer: Exploring the biology of Magnaporthe grisea. Annu. Rev. Microbiol. 57, 177–202.

Tameling, W.I.L., Elzinga, S.D.J., Darmin, P.S., Vossen, J.H., Takken, F.L.W., Haring, M.A., Cornelissen, B.J.C., 2002. The tomato R gene products I-2 and MI-1 are functional ATP binding proteins with ATPase activity. Plant Cell 14, 2929–39.

Tan, S., Wu, S., 2012. Genome wide analysis of nucleotide-binding site disease resistance genes in Brachypodium distachyon. Comp. Funct. Genomics 2012.

Tan, X., Meyers, B.C., Kozik, A., West, M. Al, Morgante, M., St Clair, D.A., Bent, A.F., Michelmore, R.W., 2007. Global expression analysis of nucleotide binding site-leucine rich repeat-encoding and related genes in Arabidopsis. BMC Plant Biol. 7, 1–20.

Tanaka, S., Ichikawa, A., Yamada, K., Tsuji, G., Nishiuchi, T., Mori, M., Koga, H., Nishizawa, Y., O'Connell, R., Kubo, Y., 2010. HvCEBiP, a gene homologous to rice chitin receptor CEBiP, contributes to basal resistance of barley to Magnaporthe oryzae. BMC Plant Biol. 10, 288.

Tang, X., Frederick, R.D., Zhou, J., Halterman, D.A., Jia, Y., Martin, G.B., 1996. Initiation of plant disease resistance by physical interaction of AvrPto and Pto kinase. Science (80-.). 274, 2060–2063.

Tarr, D.E.K., Alexander, H.M., 2009. TIR-NBS-LRR genes are rare in monocots: evidence from diverse monocot orders. BMC Res. Notes 2, 197.

Tellier, A., Moreno-Gámez, S., Stephan, W., 2014. Speed of adaptation and genomic footprints of host-parasite coevolution under arms race and trench warfare dynamics. Evolution (N. Y). 68, 2211–2224.

Tena, G., Boudsocq, M., Sheen, J., 2011. Protein kinase signaling networks in plant innate immunity. Curr. Opin. Plant Biol. 14, 519–529.

Thomma, B.P.H.J., Nürnberger, T., Joosten, M.H.A.J., 2011. Of PAMPs and effectors: The blurred PTI-ETI dichotomy. Plant Cell 23, 4–15.

Thordal-Christensen, H., 2003. Fresh insights into processes of nonhost resistance. Curr. Opin. Plant Biol. 6, 351–357.

Tian, D., Traw, M.B., Chen, J.Q., Kreitman, M., Bergelson, J., 2003. Fitness costs of R-gene-mediated resistance in Arabidopsis thaliana. Nature 423, 74–77.

Toojinda, T., Broers, L.H., Chen, X.M., Hayes, P.M., Kleinhofs, A., Korte, J., Kudrna, D., Leung, H., Line, R.F., Powell, W., Ramsay, L., Vivar, H., Waugh, R., 2000. Mapping quantitative and qualitative disease resistance genes in a doubled haploid population of barley (Hordeum vulgare). Theor. Appl. Genet. 101, 580–589.

Torp, J., Jørgensen, J.H., 1986. Modification of barleypowdery mildew resistance gene Mla12 by induced mutation. Can J Genet Cytol 28, 725–731.

Toruño, T.Y., Shen, M., Coaker, G., Mackey, D., 2019. Regulated disorder: Posttranslational modifications control the RIN4 plant immune signaling hub. Mol. Plant-Microbe Interact. 32, 56–64.

Tosa, Y., 1989a. Evidence on wheat for gene-for-gene relationship between formae speciales of Erysiphe graminis and genera of gramineous plants. Genome 32, 918–924.

Tosa, Y., 1989b. Genetic analysis of the avirulence of wheatgrass powdery mildew fungus on common wheat. Genome 32, 913–917.

Tosa, Y., 2009. Genetic analysis of the species-specific parasitism of plant pathogenic fungi. J. Gen. Plant Pathol. 75, 455–457.

Tosa, Y., Matsumura, K., Hosaka, T., 1995. Genetic analysis of interactions between Aegilops species and formae speciales of Erysiphe graminis. Japanese J. Genet. 70, 127–134.

Tosa, Yukio, Osue, J., Eto, Y., Oh, H.-S., Nakayashiki, H., Mayama, S., Leong, S. a, 2005. Evolution of an avirulence gene, AVR1-CO39, concomitant with the evolution and differentiation of Magnaporthe oryzae. Mol. Plant. Microbe. Interact. 18, 1148–60.

Tosa, Y., Sakai, K., 1990. The genetics of resistance of hexaploid wheat to the wheatgrass powdery mildew fungus. Genome 33, 225–230.

Tosa, Y., Tada, S., 1990. Operation of resistance genes in wheat to Erysiphe graminis f.sp.

tritici against E. graminis f.sp. agropyri. Genome 33, 231–234.
Tosa, Y, Tamba, H., Tanaka, K., Mayama, S., 2005. Genetic Analysis of Host Species Specificity of Magnaporthe oryzae Isolates from Rice and Wheat 480–484.
Tsuda, K., Somssich, I.E., 2015. Transcriptional networks in plant immunity. New Phytol. 206, 932–47.
Uchida, N., Igari, K., Bogenschutz, N.L., Torii, K.U., Tasaka, M., 2011. Arabidopsis ERECTA-family receptor kinases mediate morphological alterations stimulated by activation of NB-LRR-Type UNI proteins. Plant Cell Physiol. 52, 804–814.
Ueda, H., Yamaguchi, Y., Sano, H., 2006. Direct interaction between the tobacco mosaic virus helicase domain and the ATP-bound resistance protein, N factor during the hypersensitive response in tobacco plants. Plant Mol. Biol. 61, 31–45.
USDA GRIN, n.d. United States Department of Agriculture (USDA) The Germplasm Resources Information Network (GRIN) [WWW Document]. URL www.ars-grin.gov
Valent, B., Khang, C.H., 2010. Recent advances in rice blast effector research. Curr. Opin. Plant Biol. 13, 434–441.
Vales, M.I., Schön, C.C., Capettini, F., Chen, X.M., Corey, A.E., Mather, D.E., Mundt, C.C., Richardson, K.L., Sandoval-Islas, J.S., Utz, H.F., Hayes, P.M., 2005. Effect of population size on the estimation of QTL: A test using resistance to barley stripe rust. Theor. Appl. Genet. 111, 1260–1270.
Van de Weyer, A.-L., Monteiro, F., Furzer, O.J., Nishimura, M.T., Cevik, V., Witek, K., Jones, J.D.G., Dangl, J.L., Weigel, D., Bemm, F., 2019. A Species-Wide Inventory of NLR Genes and Alleles in Arabidopsis thaliana. Cell 178, 1260-1272.e14.
Van Der Biezen, E.A., Freddie, C.T., Kahn, K., Parker, J.E., Jones, J.D.G., 2002. Arabidopsis RPP4 is a member of the RPP5 multigene family of TIR-NB-LRR genes and confers downy mildew resistance through multiple signalling components. Plant J. 29, 439–451.
Van Der Biezen, E.A., Jones, J.D.G., 1998. Plant disease-resistance proteins and the gene-for-gene concept. Trends Biochem. Sci. 23, 454–456.
Van Der Hoorn, R.A.L., De Wit, P.J.G.M., Joosten, M.H.A.J., 2002. Balancing selection favors guarding resistance proteins. Trends Plant Sci. 7, 67–71.
van der Hoorn, R.A.L., Kamoun, S., 2008. From Guard to Decoy: a new model for perception of plant pathogen effectors. Plant Cell 20, 2009–17.
van Kan, J.A.L., 2006. Licensed to kill: the lifestyle of a necrotrophic plant pathogen. Trends Plant Sci. 11, 247–253.
van Ooijen, J.W., 2006. JoinMap 4 ® Software for the calculation of genetic linkage maps in experimental populations.
van Wersch, S., Li, X., 2019. Stronger When Together: Clustering of Plant NLR Disease

resistance Genes. Trends Plant Sci. 24, 688–699.

Verdier, V., Triplett, L.R., Hummel, A.W., Corral, R., Cernadas, R.A., Schmidt, C.L., Bogdanove, A.J., Leach, J.E., 2012. Transcription activator-like (TAL) effectors targeting OsSWEET genes enhance virulence on diverse rice (Oryza sativa) varieties when expressed individually in a TAL effector-deficient strain of Xanthomonas oryzae. New Phytol. 196, 1197–1207.

Verhoeven, E.C., Bonman, J.M., Bregitzer, P., Brunick, B., Cooper, B., Corey, a. E., Cuesta-Marcos, a., Filichkina, T., Mundt, C.C., Obert, D., Rossnagel, B., Richardson, K., Hayes, P.M., 2011. Registration of the BISON Genetic Stocks in L. J. Plant Regist. 5, 135.

Vos, P., Simons, G., Jesse, T., Wijbrandi, J., Heinen, L., Hogers, R., Frijters, a, Groenendijk, J., Diergaarde, P., Reijans, M., Fierens-Onstenk, J., de Both, M., Peleman, J., Liharska, T., Hontelez, J., Zabeau, M., 1998. The tomato Mi-1 gene confers resistance to both root-knot nematodes and potato aphids. Nat. Biotechnol. 16, 1365–1369.

Walters, D.R., Havis, N.D., Oxley, S.J.P., 2008. Ramularia collo-cygni: The biology of an emerging pathogen of barley. FEMS Microbiol. Lett. 279, 1–7.

Walters, D.R., Havis, N.D., Paterson, L., Taylor, J., Walsh, D.J., Sablou, C., 2014. Control of foliar pathogens of spring barley using a combination of resistance elicitors. Front. Plant Sci. 5, 1–9.

Walton, J.D., 1996. Host-Selective Toxins: Agents of Compatibility. Plant Cell Online 8, 1723–1733.

Wang, G., Roux, B., Feng, F., Guy, E., Li, L., Li, N., Zhang, X., Lautier, M., Jardinaud, M.F., Chabannes, M., Arlat, M., Chen, S., He, C., Noël, L.D., Zhou, J.M., 2015. The Decoy Substrate of a Pathogen Effector and a Pseudokinase Specify Pathogen-Induced Modified-Self Recognition and Immunity in Plants. Cell Host Microbe 18, 285–295.

Wang, Jizong, Hu, M., Wang, Jia, Qi, J., Han, Z., Wang, G., Qi, Y., Wang, H.W., Zhou, J.M., Chai, J., 2019a. Reconstitution and structure of a plant NLR resistosome conferring immunity. Science (80-.). 364.

Wang, Jizong, Wang, Jia, Hu, M., Wu, S., Qi, J., Wang, G., Han, Z., Qi, Y., Gao, N., Wang, H.W., Zhou, J.M., Chai, J., 2019b. Ligand-triggered allosteric ADP release primes a plant NLR complex. Science (80-.). 364.

Wang, X., Jiang, N., Liu, J., Liu, W., Wang, G.L., 2014. The role of effectors and host immunity in plant–necrotrophic fungal interactions. Virulence 5, 722–732.

Wang, X., Richards, J., Gross, T., Druka, a, Kleinhofs, a, Steffenson, B., Acevedo, M., Brueggeman, R., 2013. The rpg4-mediated resistance to wheat stem rust (Puccinia graminis) in barley (Hordeum vulgare) requires Rpg5, a second NBS-LRR gene, and

an actin depolymerization factor. Mol. Plant. Microbe. Interact. 26, 407–18.

Waterhouse, R.M., Seppey, M., Simao, F.A., Manni, M., Ioannidis, P., Klioutchnikov, G., Kriventseva, E. V., Zdobnov, E.M., 2018. BUSCO applications from quality assessments to gene prediction and phylogenomics. Mol. Biol. Evol. 35, 543–548.

Wegulo, S.N., Baenziger, P.S., Hernandez Nopsa, J., Bockus, W.W., Hallen-Adams, H., 2015. Management of Fusarium head blight of wheat and barley. Crop Prot. 73, 100–107.

Wei, F., Gobelman-Werner, K., Morroll, S.M., Kurth, J., Mao, L., Wing, R., Leister, D., Schulze-Lefert, P., Wise, R.P., 1999. The Mla (Powdery Mildew) Resistance Cluster Is Associated With Three NBS-LRR Gene Families and Suppressed Recombination Within a 240-kb DNA Interval on Chromosome 5S (1HS) of Barley. Genetics 153, 1929–1948.

Wei, F., Wing, R. a, Wise, R.P., 2002. Genome dynamics and evolution of the Mla (powdery mildew) resistance locus in barley. Plant Cell 14, 1903–1917.

Wellings, C.R., 2011. Global status of stripe rust: A review of historical and current threats. Euphytica 179, 129–141.

Wellings, C.R., Burdon, J.J., McIntosh, R.A., Wallwork, H., Raman, H., Murray, G.M., 2000. A new variant of Puccinia striiformis causing stripe rust on barley and wild Hordeum species in Australia. Plant Pathol. 49, 803.

Wesenberg, D.M., Burrup, D.E., Brown, W.M.J., Velasco, V.R., Hill, J.P., Whitmore, J.C., 2001. Registration of `Bancroft' Barley. Crop Sci. 41, 265.

Whalen, M.C., 2005. Host defence in a developmental context. Mol. Plant Pathol. 6, 347–360.

Whitham, S., Dinesh-Kumar, S.P., Choi, D., Hehl, R., Corr, C., Baker, B., 1994. The product of the tobacco mosaic virus resistance gene N: Similarity to toll and the interleukin-1 receptor. Cell 78, 1101–1115.

Whitham, S.A., Qi, M., Innes, R.W., Ma, W., Lopes-Caitar, V., Hewezi, T., 2016. Molecular Soybean-Pathogen Interactions. Annu. Rev. Phytopathol. 54, 443–468.

Wickham, H., 2016. ggplot2: Elegant Graphics for Data Analysis Using the Grammar of Graphics. Springer-Verlag New York.

Wiermer, M., Feys, B.J., Parker, J.E., 2005. Plant immunity: The EDS1 regulatory node. Curr. Opin. Plant Biol. 8, 383–389.

Williams, S.J., Sohn, K.H., Wan, L., Bernoux, M., Sarris, P.F., Segonzac, C., Ve, T., Ma, Y., Saucet, S., Ericson, D.J., Casey, L.W., Lonhienne, T., Winzor, D.J., Zhang, X., Coerdt, A., Parker, J.E., Dodds, P.N., Kobe, B., Jones, J.D.G., 2014. Structural Basis for Assembly and Function of a Heterodimeric Plant Immune Receptor. Science (80-.). 344, 299–303.

Wilson, R. a, Talbot, N.J., 2009. Under pressure: investigating the biology of plant infection by Magnaporthe oryzae. Nat. Rev. Microbiol. 7, 185–195.

Wisser, R.J., Sun, Q., Hulbert, S.H., Kresovich, S., Nelson, R.J., 2005. Identification and characterization of regions of the rice genome associated with broad-spectrum, quantitative disease resistance. Genetics 169, 2277–2293.

Witek, K., Jupe, F., Witek, A.I., Baker, D., Clark, M.D., Jones, J.D.G., 2016. Accelerated cloning of a potato late blight-resistance gene using RenSeq and SMRT sequencing. Nat. Biotechnol. 34, 656–660.

Wolpert, T.J., Dunkle, L.D., Ciuffetti, L.M., 2002. HOST-SELECTIVE TOXINS AND AVIRULENCE D ETERMINANTS: What's in a Name? Annu. Rev. Phytopathol. 40, 251–285.

Wolpert, T.J., Lorang, J.M., 2016. Victoria Blight, Defense turned upside Down. Physiol. Mol. Plant Pathol. 1–6.

Wolpert, T.J., Macko, V., 1989. Specific binding of victorin to a 100-kDa protein from oats. Proc. Natl. Acad. Sci. U. S. A. 86, 4092–4096.

Wolpert, T.J., Macko, V., Acklin, W., Jaun, B., Seibl, J., Meili, J., Arigoni, D., 1985. Structure of victorin C, the major host-selective toxin from Cochliobolus victoriae. Experientia 41, 1524–1529.

Wolpert, T.J., Navarre, D. a, Moore, D.L., Macko, V., 1994. Identification of the 100-kD victorin binding protein from oats. Plant Cell 6, 1145–1155.

Wu, A.J., Andriotis, V.M.E., Durrant, M.C., Rathjen, J.P., 2004. A patch of surface-exposed residues mediates negative regulation of immune signaling by tomato Pto kinase. Plant Cell 16, 2809–2821.

Wu, C.H., Abd-El-Haliem, A., Bozkurt, T.O., Belhaj, K., Terauchi, R., Vossen, J.H., Kamoun, S., 2017. NLR network mediates immunity to diverse plant pathogens. Proc. Natl. Acad. Sci. U. S. A. 114, 8113–8118.

Wu, J., Huang, S., Zeng, Q., Liu, S., Wang, Q., Mu, J., Yu, S., Han, D., Kang, Z., 2018. Comparative genome-wide mapping versus extreme pool-genotyping and development of diagnostic SNP markers linked to QTL for adult plant resistance to stripe rust in common wheat. Theor. Appl. Genet. 131, 1777–1792.

Wu, J., Saupe, S.J., Glass, N.L., 1998. Evidence for balancing selection operating at the het-c heterokaryon incompatibility locus in a group of filamentous fungi. Proc. Natl. Acad. Sci. U. S. A. 95, 12398–12403.

Wu, Q., Han, T.S., Chen, X., Chen, J.F., Zou, Y.P., Li, Z.W., Xu, Y.C., Guo, Y.L., 2017. Long-term balancing selection contributes to adaptation in Arabidopsis and its relatives. Genome Biol. 18, 1–15.

Yaegashi, H., 1988. Inheritance of blast resistance in two-rowed barley. Plant Dis.

Yahiaoui, N., Brunner, S., Keller, B., 2006. Rapid generation of new powdery mildew resistance genes after wheat domestication. Plant J. 47, 85–98.

Yan, G., Chen, X., 2008. Identification of a quantitative trait locus for high-temperature adult-plant resistance against Puccinia striiformis f. sp. hordei in “Bancroft” barley. Phytopathology 98, 120–127.

Yang, S., Feng, Z., Zhang, X., Jiang, K., Jin, X., Hang, Y., Chen, J.Q., Tian, D., 2006. Genome-wide investigation on the genetic variations of rice disease resistance genes. Plant Mol. Biol. 62, 181–193.

Yang, S., Li, J., Zhang, X., Zhang, Q., Huang, J., Chen, J., Hartl, D.L., 2013. Rapidly evolving R genes in diverse grass species confer resistance to rice blast disease.

Yang, S., Zhang, X., Yue, J.X., Tian, D., Chen, J.Q., 2008. Recent duplications dominate NBS-encoding gene expansion in two woody species. Mol. Genet. Genomics 280, 187–198.

Yang, Z., 2007. PAML 4: Phylogenetic analysis by maximum likelihood. Mol. Biol. Evol. 24, 1586–1591.

Yin, K., Gao, C., Qiu, J.L., 2017. Progress and prospects in plant genome editing. Nat. Plants 3, 1–6.

Yoshida, K., Schuenemann, V.J., Cano, L.M., Pais, M., Mishra, B., Sharma, R., Lanz, C., Martin, F.N., Kamoun, S., Krause, J., Thines, M., Weigel, D., Burbano, H.A., 2013. The rise and fall of the Phytophthora infestans lineage that triggered the Irish potato famine. Elife 2013, 1–25.

Yoshida, Kentaro, Saitoh, H., Fujisawa, S., Kanzaki, H., Matsumura, H., Yoshida, Kakoto, Tosa, Y., Chuma, I., Takano, Y., Win, J., Kamoun, S., Terauchi, R., 2009. Association genetics reveals three novel avirulence genes from the rice blast fungal pathogen Magnaporthe oryzae. Plant Cell 21, 1573–91.

Yue, J.X., Meyers, B.C., Chen, J.Q., Tian, D., Yang, S., 2012. Tracing the origin and evolutionary history of plant nucleotide-binding site-leucine-rich repeat (NBS-LRR) genes. New Phytol. 193, 1049–1063.

Žárský, V., Cvrčková, F., Potocký, M., Hála, M., 2009. Exocytosis and cell polarity in plants – exocyst and recycling domains. New Phytol. 183, 255–272.

Zeng, X., Tian, D., Gu, K., Zhou, Z., Yang, X., Luo, Y., White, F.F., Yin, Z., 2015. Genetic engineering of the Xa10 promoter for broad-spectrum and durable resistance to Xanthomonas oryzae pv. oryzae. Plant Biotechnol. J. 993–1001.

Zhai, J., Jeong, D.H., de Paoli, E., Park, S., Rosen, B.D., Li, Y., González, A.J., Yan, Z., Kitto, S.L., Grusak, M.A., Jackson, S.A., Stacey, G., Cook, D.R., Green, P.J., Sherrier, D.J., Meyers, B.C., 2011. MicroRNAs as master regulators of the plant NB-LRR defense gene family via the production of phased, trans-acting siRNAs. Genes Dev. 25,

2540–2553.

Zhan, J., Fitt, B.D.L., Pinnschmidt, H.O., Oxley, S.J.P., Newton, A.C., 2008. Resistance, epidemiology and sustainable management of Rhynchosporium secalis populations on barley. Plant Pathol. 57, 1–14.

Zhang, J., Yin, Z., White, F., 2015. TAL effectors and the executor R genes. Front. Plant Sci. 6, 1–9.

Zhang, S., Xu, J.R., 2014. Effectors and Effector Delivery in Magnaporthe oryzae. PLoS Pathog. 10, 1–4.

Zhang, X.C., Gassmann, W., 2003. RPS4-Mediated Disease Resistance Requires the Combined Presence of RPS4 Transcripts with Full-Length and Truncated Open Reading Frames. Plant Cell 15, 2333–2342.

Zhang, Y.M., Shao, Z.Q., Wang, Q., Hang, Y.Y., Xue, J.Y., Wang, B., Chen, J.Q., 2016. Uncovering the dynamic evolution of nucleotide-binding site-leucine-rich repeat (NBS-LRR) genes in Brassicaceae. J. Integr. Plant Biol. 58, 165–177.

Zheng, F., Wu, H., Zhang, R., Li, S., He, W., Wong, F.L., Li, G., Zhao, S., Lam, H.M., 2016. Molecular phylogeny and dynamic evolution of disease resistance genes in the legume family. BMC Genomics 17, 1–13.

Zhou, F., Kurth, J., Wei, F., Elliott, C., Valè, G., Yahiaoui, N., Keller, B., Somerville, S., Wise, R., Schulze-Lefert, P., 2001. Cell-autonomous expression of barley Mla1 confers race-specific resistance to the powdery mildew fungus via a Rar1-independent signaling pathway. Plant Cell 13, 337–350.

Zhou, T., Wang, Y., Chen, J.Q., Araki, H., Jing, Z., Jiang, K., Shen, J., Tian, D., 2004. Genome-wide identification of NBS genes in japonica rice reveals significant expansion of divergent non-TIR NBS-LRR genes. Mol. Genet. Genomics 271, 402–415.

Zipfel, C., 2008. Pattern-recognition receptors in plant innate immunity. Curr. Opin. Immunol. 20, 10–16.

Zipfel, C., Kunze, G., Chinchilla, D., Caniard, A., Jones, J.D.G., Boller, T., Felix, G., 2006. Perception of the Bacterial PAMP EF-Tu by the Receptor EFR Restricts Agrobacterium-Mediated Transformation. Cell 125, 749–760.

Zipfel, C., Robatzek, S., Navarro, L., Oakeley, E.J., Jones, J.D.G., Felix, G., Boller, T., 2004. Bacterial disease resistance in Arabidopsis through flagellin perception. Nature 428, 764–767.

Zuker, M., 2003. Mfold web server for nucleic acid folding and hybridization prediction. Nucleic Acids Res. 31, 3406–3415.